

Thesis reference number:

UNIVERSITY OF SCIENCE AND TECHNOLOGY OF HANOI



DOCTORAL THESIS

INVESTIGATION OF SYNERGISTIC EFFECT OF DIISOPROPYLAMINE DICHLOROACETATE AND FENBENDAZOLE ON LUNG CANCER MODELS

Nguyen Quang Thai

Pharmacological, Medical and Agronomical Biotechnology

9420201

Assoc. Prof. Nguyen Hai Dang, Supervisor

Department of Life Sciences - University of Science and Technology of Hanoi, Vietnam

Academy of Science and Technology, Hanoi, Vietnam

Assist. Prof. Hoang Xuan Ba, Co-supervisor

Department of Surgery, Keck School of Medicine of the University of Southern California,

Los Angeles, CA, USA

Hanoi, 2026

Thesis reference number:

UNIVERSITY OF SCIENCE AND TECHNOLOGY OF HANOI



DOCTORAL THESIS

INVESTIGATION OF SYNERGISTIC EFFECT OF DIISOPROPYLAMINE DICHLOROACETATE AND FENBENDAZOLE ON LUNG CANCER MODELS

Nguyen Quang Thai

Pharmacological, Medical and Agronomical Biotechnology - 9420201

The thesis has been successfully defended on March 19, 2026 in front of a jury composed
of

Assoc.Prof. Nguyen Trung Nam, Institute of Biology, VAST, Chairman
Prof. Jeong- Hyung Lee, Kangwon National University, Korea, Reviewer
Dr. Tran Minh Ngoc, National Institute of Medicinal Materials, Reviewer

Assoc.Prof. Pham The Hai, USTH, Reviewer

Prof. Dong Van Quyen, Institute of Biology, VAST, Member

Dr. Nguyen Phuong Nhung, USTH, Member

Dr. Pham Le Minh, USTH, Member, Secretary

Hanoi, 2026

Approval of supervisor(s) and Co-Supervisor(s)

Assoc.Prof. Nguyen Hai Dang

Assist. Prof. Hoang Xuan Ba

DECLARATION

I, the undersigned, confirm that this thesis is my work, except where stated otherwise. I also affirm that it has not been submitted for any other degree or professional qualification unless noted.

This declaration confirms the authenticity and originality of the thesis.

Parts of this work have been published in the following papers:

1. **Nguyen TQ**, Nguyen DH, Phan UTT, Tran PTT, LE HT, Nguyen SH, Nguyen J, Han BO, Hoang BX. Fenbendazole and Diisopropylamine Dichloroacetate Exert Synergistic Anti-cancer Effects by Inducing Apoptosis and Arresting the Cell Cycle in A549 Lung Cancer Cells. *Anticancer Res.* 2024 Nov;44(11):4761-4772. DOI: 10.21873/anticanres.17302. PMID: 39477286.
2. **Thai Q. Nguyen**, Uyen T. T. Phan Mao V. Can, Bo Han, Dang H. Nguyen and Ba X. Hoang. Synergistic Anti-Tumor Effect of Fenbendazole and Diisopropylamine Dichloroacetate in Immunodeficient BALB/c Nude Mice Transplanted with A549 Lung Cancer Cells- *Translational Lung Cancer Research*, DOI: 10.21037/tlcr-2024-1272
3. Jolie nguyen, Thai Q. Nguyen, Bo Han, Ba X. Hoang. Oral Fenbendazole for Cancer Therapy in Humans and Animals. *Anticancer Research* Sep 2024, 44 (9) 3725- 3735; DOI: 10.21873/anticanres.17197

PhD student

Nguyen Quang Thai

ACKNOWLEDGEMENT

“*What is your dream?*” – This is a question we often hear nowadays, especially for young people. Twenty-four years ago, when I entered the Hanoi University of Pharmacy as a first-year student, no one asked me this question. Yet even if someone had, I would never have thought my answer would be: “*My dream is to develop a novel anticancer drug to help less fortunate patients.*” Despite youthful ambition, I could not imagine that, given the scientific, technological, and economic conditions of Vietnam at the time, such a dream could ever come true.

Ten years ago, while witnessing the cancer treatments carried out by Dr. Hoang Xuan Ba (MD) in both Vietnam and Belarus, I set a goal for my career: to find an effective cancer treatment for Vietnamese patients at a cost of less than 200 USD per month. The convincing results he achieved in his patients – Dr. Ba would later become my secondary supervisor for this research – gave me great confidence that this goal could one day be realized.

But where to start? I discussed with my colleagues at Thai Minh Pharmaceutical JSC – the company I founded and have managed since 2012. Our initial idea was to build a hospital to provide affordable and effective cancer treatment. However, hospital management was not our greatest strength. The better path was to develop one or several effective medicines, take them through full clinical testing, and make them available not just in one hospital, but in many hospitals across the country.

Five years ago, this vision took its first concrete step forward when I was admitted to the PhD program at the University of Science and Technology of Hanoi (USTH) under the Vietnam Academy of Science and Technology (VAST). I am deeply grateful to Associate Professor (Assoc. Prof.) Ha Quy Quynh – Formerly Head of the Department of Application and Technology Transfer, VAST – who introduced me to USTH, where I met my Primary Supervisor, Assoc. Prof. Nguyen Hai Dang. Which was where my journey truly began.

My research focused on investigating the synergistic effect of fenbendazole (FZ) and diisopropylamine dichloroacetate (DADA) on lung cancer models, generating both *in vitro* and *in vivo* data to serve as the foundation for the preclinical development of a potential new drug.

Coming from over a decade in the pharmaceutical business and having been away from research for more than 10 years after graduation, I had to relearn many basic concepts from scratch. Therefore, I am sincerely thankful to Assoc. Prof. Nguyen Hai Dang and all the professors, lecturers, and researchers of the Department of Life Sciences for guiding me from the very fundamentals – such as the principles of MTT assays and cell cycle analysis – to the practical steps that enabled me to conduct my very first experiments.

I discovered that the excitement I felt while waiting for cells to respond to treatment – then measuring absorbance, compiling the results, and analyzing whether the two drugs acted synergistically and at what concentrations – was even greater than the excitement of seeing a business project succeed. I am especially grateful to my research teammates from Thai Minh Pharmaceutical, Nguyen Hoang Son and Phan Thi Tu Uyen (both proud alumni of USTH), who stood by my side throughout these experiments.

In vivo experiments was an entirely new field for me, which led me to how I am grateful to the members of the Biomedical Ethics Committee at the Dinh Tien Hoang Institute for their valuable advice in developing and approving my research proposal. For the first time, I understood the responsibility and respect owed to each laboratory animal: to use the fewest mice possible, and to minimize their pain throughout the experiment. I also wish to thank Assoc. Prof. Can Van Mao and Dr. Ngo Thu Hang at the Military Medical Academy for their important contributions, which enabled me to complete the nude mouse experiments at their facility.

After five years, the results are clear: I have proven my hypothesis correct and identified the optimal dosage ratio *in vitro* and *in vivo*, demonstrating the superior tumor-inhibiting effects – and in some cases complete regression – achieved by this combination. Three international papers have been published, and a patent for this invention is pending by the National Office of Intellectual Property of Vietnam. A strong foundation has now been laid for the dream of creating an affordable anticancer drug for the Vietnamese people.

Beyond the scientific results, my years of study and research at USTH – under the guidance of my supervisors – helped me understand the value of research and its importance to the sustainable growth of a business. This realization had also led me to shift the strategic direction of my company, placing science at first and investing heavily in research on medicinal plants, from cultivation to final product formulation. By the time I had completed my thesis, Thai

Minh Pharmaceutical – the company I founded and chair – had established a Ginseng and Medicinal Plant Research Institute, which is now operational and making its first contributions to Vietnam’s herbal medicine sector. Therefore, I am deeply grateful to USTH, the University’s Board of Rectors, the Department of Life Sciences, the Doctoral School, and all related departments for their continuous support and invaluable contributions throughout my journey.

I truly consider myself fortunate – to have had dedicated supervisors, to have had colleagues who fully supported me and took on much of the company’s operational work so I could focus on research, and to have always had the encouragement and backing of my family.

To end this, I would like to express my heartfelt gratitude to my supervisors, colleagues, family, and friends for helping me complete this thesis. As well as encouraging me to continue pursuing my aspirations and contributing further to the advancement of science.

ABSTRACT

Lung cancer is the leading cause of cancer incidence and mortality worldwide, accounting for approximately 2 million diagnoses and 1.8 million deaths annually. Current treatment options include surgery, radiation therapy, chemotherapy, and targeted therapy. Despite advancements in diagnosis and treatment over the past 25 years, the prognosis for lung cancer patients remains poor. This research aimed to investigate the anti-cancer effects of diisopropylamine dichloroacetate (DADA) and fenbendazole in *in vitro* and *in vivo* level.

Fenbendazole (methyl N-(6-phenylsulfanyl-1H-benzimidazol-2-yl) carbamate) is a broad-spectrum benzimidazole anthelmintic approved for use in various animal species. Recent studies have demonstrated that fenbendazole exhibits cytotoxicity against human cancer cells at micromolar concentrations by mechanisms including mitochondrial translocation of p53 and inhibition of glucose uptake. Diisopropylamine dichloroacetate (DADA), an over-the-counter drug for chronic liver disease, has shown anti-tumor effects as an inhibitor of pyruvate dehydrogenase kinase.

My research indicated a synergistic effect of a 1:5000 ratio of FZ and DADA on the proliferation of A549 lung cancer cells. FZ-DADA combination induced ROS production after 48 hours of treatment. Specifically, the 1:5000 ratio of FZ and DADA induced apoptosis in A549 cells by downregulating Bcl-2 and upregulating BAX at the protein level. On the other hand, FZ-DADA combination activated the caspase-3, caspase-7 at this ratio. This combination activated PARP, further promoting apoptosis in A549 cells. Moreover, the FZ-DADA combination induced cell cycle arrest in A549 cells, as evidenced by the inhibition of Cyclin A and Cyclin E at the protein level. The synergistic effect of FZ and DADA was confirmed through in cell and protein levels. In animal model, the combination of FZ (40 mg/kg) and DADA (100 mg/kg) reduced the tumor volume compared with single treatment and positive control. On the other hand, our treatment showed a significant tumor regression in the combination treatment. The combination of FZ and DADA also did not cause side effect in liver and kidney function.

TÓM TẮT

Ung thư phổi là nguyên nhân hàng đầu gây ra tỷ lệ mắc và tử vong do ung thư trên toàn thế giới, chiếm khoảng 2 triệu ca chẩn đoán và 1,8 triệu ca tử vong hàng năm. Các lựa chọn điều trị hiện tại bao gồm phẫu thuật, xạ trị, hóa trị và liệu pháp nhắm mục tiêu. Bất chấp những tiến bộ trong chẩn đoán và điều trị trong 25 năm qua, tiên lượng cho bệnh nhân ung thư phổi vẫn còn kém. Nghiên cứu này nhằm mục đích đánh giá tác dụng chống ung thư của diisopropylamine dichloroacetate (DADA) và fenbendazole (FZ) trên tế bào ung thư phổi A549.

Fenbendazole (methyl N-(6-phenylsulfanyl-1H-benzimidazol-2-yl) carbamate) là một loại thuốc tẩy giun benzimidazole phổ rộng được phê duyệt để sử dụng cho nhiều loài động vật khác nhau. Các nghiên cứu gần đây đã chứng minh rằng fenbendazole thể hiện độc tính tế bào đối với tế bào ung thư ở người ở nồng độ micromol bằng các cơ chế bao gồm chuyển vị ty thể của p53 và ức chế hấp thu glucose. Diisopropylamine dichloroacetate (DADA), một loại thuốc không kê đơn điều trị bệnh gan mãn tính, đã cho thấy tác dụng chống khối u như một chất ức chế pyruvate dehydrogenase kinase.

Nghiên cứu của tôi chỉ ra tác dụng hiệp đồng của FZ và DADA ở tỷ lệ 1:5000 đối với sự tăng sinh của các tế bào ung thư phổi A549. FZ-DADA gây ra sự sản sinh ROS sau 48 giờ điều trị. Cụ thể, kết hợp FZ và DADA ở tỷ lệ 1:5000 gây ra hiện tượng apoptosis trong các tế bào A549 bằng cách giảm tiết BCL2 và tăng BAX ở mức protein. Mặt khác, kết hợp FZ-DADA đã kích hoạt caspase-3, caspase-7 ở tỷ lệ này. Ngoài ra, sự kết hợp này đã kích hoạt PARP, thúc đẩy hơn nữa quá trình apoptosis trong các tế bào A549. Hơn nữa, kết hợp FZ-DADA gây ra sự bất giữ chu kỳ tế bào trong các tế bào A549, bằng chứng là sự ức chế Cyclin A và Cyclin E ở mức độ protein. Tác dụng hiệp đồng của FZ và DADA đã được xác nhận thông qua mức độ tế bào và protein. Trên mô hình động vật, sự kết hợp của FZ (40mg/kg) và DADA (100mg/kg) làm giảm thể tích khối u so với điều trị đơn lẻ và so với chứng dương. Mặt khác, phương pháp điều trị của chúng tôi ghi nhận thấy tỷ lệ mất khối u hoàn toàn trong phương pháp điều trị kết hợp. Sự kết hợp của FZ và DADA cũng không gây ra tác dụng phụ ở chức năng gan và thận.

KEYWORDS

Lung cancer

Non-small cell lung cancer

Fenbendazole

Diisopropylamine dichloroacetate

Anti-cancer

Drug repurposing

LIST OF ABBREVIATION

Abbreviations	Meanings
%CS	Percentage of Cell Survival
2-DG	2-Deoxyglucose
2-DG6P	2-Deoxyglucose-6-Phosphate
ADP	Adenosine diphosphate
ALK	Anaplastic Lymphoma Kinase
ALT	Alanine Aminotransferase
AST	Aspartate Aminotransferase
ATP	Adenosine Triphosphate
BAX	Bcl-2-Associated X protein
Bcl-2	B-cell Lymphoma 2
CBD	Cannabidiol
CDKs	Cyclin-Dependent Kinase
CDK2	Cyclin-Dependent Kinase 2
CI	Combination Index
CTLA-4	Cytotoxic T-lymphocyte-associated Protein 4
CYP3A4	Cytochrome P450 3A4
DADA	Diisopropylamine Dichloroacetate
DCA	Dichloroacetate
DMEM	Dulbecco's Modified Eagle Medium
DMSO	Dimethyl Sulfoxide
DNA	Deoxyribonucleic Acid
EGFR	Epidermal Growth Factor Receptor
FACS	Fluorescence Activated Cell Sorting
FBS	Fetal Bovine Serum
FMO	Flavin-Monooxygenase
FZ	Fenbendazole
GLUT1	Glucose Transporter protein type 1
HKII	Hexokinase II
HPV	Human Papillomavirus
HSCs	Hepatic Stellate Cells

IC50	Half-maximal Inhibitory Concentration
irAEs	Immune-Related Adverse Events
IRS	Insulin Receptor Substrate
IV	Intravenously
KRPH	Krebs-Ringer Phosphate-Hepes
LDH	Lactate Dehydrogenase
MAPK	Mitogen-Activated Protein Kinase
mTOR	Mammalian Target of Rapamycin
MTT	3-(4,5-Dimethylthiazol-2-yl)-2,5-Diphenyltetrazolium Bromide
NADH	Nicotinamide Adenine Dinucleotide
NADPH	Nicotinamide Adenine Dinucleotide Phosphate
NSCLC	Non-Small Cell Lung Cancer
OSCC	Oral Squamous Cell Carcinoma
PARP	Poly (ADP-Ribose) Polymerase
PBS	Phosphate Buffered Saline
PD-1	Programmed Cell Death Protein 1
PDC	Pyruvate Dehydrogenase Complex
PDH	Pyruvate Dehydrogenase
PDK	Pyruvate Dehydrogenase Kinase
PDK1	Pyruvate Dehydrogenase Kinase 1
PDK2	Pyruvate Dehydrogenase Kinase 2
PDK4	Pyruvate Dehydrogenase Kinase 4
PD-L1	Programmed Cell Death Ligand 1
PET	Positron Emission Tomography
PI	Propidium Iodine
PI3K	Phosphoinositide 3-Kinase
PIP2	Phosphatidylinositol 4,5-Bisphosphate
PIP3	Phosphatidylinositol (3,4,5)-Trisphosphate
PLGA	Poly (Lactic-co-Glycolic Acid)
PS	Penicillin/streptomycin solution
PVDF	Poly (Vinylidene) Fluoride
RIPA	Radio-Immunoprecipitation Assay

RNase	Ribonuclease
ROS	Reactive Oxygen Species
RPMI	Roswell Park Memorial Institute Medium
SCID	Severe Combined Immunodeficiency
SDS-PAGE	Sodium Dodecyl Sulphate Polyacrylamide gel
SH2	Src Homology 2
SMLC	Small Cell Lung Cancer
TCA	Tricarboxylic Acid
TGI	Tumor Growth Inhibition
TME	Tumor Microenvironment
TNBC	Triple-Negative Breast Cancer Cells
TNF- α	Tumor Necrosis Factor alpha
VEGF	Vascular Endothelial Growth Factor
XTT	2,3-Bis-(2-Methoxy-4-Nitro-5-Sulfophenyl)-2H-Tetrazolium-5-Carboxanilide
YAP	Yes-Associated Protein

LIST OF TABLES

Table 1: List of researches of fenbendazole in vitro and in vivo through years.....	7
Table 2: Cell seeding conditional	26
Table 3: The average weight of mice before treatment	58
Table 4: Hematological indices of mice after FZ-DADA treatment	60
Table 5: Urea and creatinine level of mice after FZ-DADA treatment	61
Table 6: The average volume of mice tumors on the first day of treatment.....	65
Table 7: Tumor reduction rate in treated mice	66

LIST OF FIGURES

Figure 1: Chemical structure of Fenbendazole	4
Figure 2: Mechanism of action of Fenbendazole.....	6
Figure 3: Chemical structure of Diisopropylamine dichloroacetate	14
Figure 4: The Warburg effect.	15
Figure 5: Formation of formazan crystals from MTT.	26
Figure 6: Hoechst staining principle	28
Figure 7: Apoptosis pathways are divided into the extrinsic and the intrinsic pathways.....	30
Figure 8: Principle of Annexin V/PI staining	31
Figure 9: Cell cycle arrest and the regulators.	32
Figure 10: Principle of glucose uptake assay.....	33
Figure 11: Cell viability and combination index of FZ and DADA.	41
Figure 12: Hoechst staining	42
Figure 13: FZ-DADA induced apoptosis in A549 cells.	44
Figure 14: FZ-DADA induced apoptosis in via intrinsic pathway.	46
Figure 15: The FZ-DADA combination induced cell cycle arrest in A549 cells.	48
Figure 16: FZ and DADA inhibited the expression of cell cycle checkpoints.	50
Figure 17: FZ-DADA induced ROS level in cells.....	51
Figure 18: FZ and DADA inhibited glucose uptake and lactate production in A549 cells.	52
Figure 19: FZ-DADA inhibited PI3K-AKT pathway in time-dependence.	54
Figure 20: FZ-DADA inhibited PI3K-AKT pathway in concentration-dependence.....	55
Figure 21: Mice's body weight after 60 days	59
Figure 22: Histology sections of kidney of mice after FZ -DADA treatment.	62
Figure 23: Effect of drug formulation on liver function.....	64
Figure 24: Tumor volume results in groups of mice during treatment.	66
Figure 25: Tumor reduction rate in treated mice group.	67
Figure 26: The survival duration and death rate death rate of nude mice.....	70
Figure 27: Mechanism of action of FZ and DADA in lung cancer	72
<i>Figure S1: Cell viability of FZ-DADA in MCF7 cells.....</i>	<i>93</i>
<i>Figure S2: Cell viability of FZ-DADA in PC3 cells</i>	<i>93</i>
<i>Figure S3: Cell viability of FZ-DADA in DU145 cells.....</i>	<i>94</i>
<i>Figure S4: Cell viability of FZ-DADA in Hep G2 cells.....</i>	<i>95</i>

Table of Contents

ABSTRACT	8
KEYWORDS	10
LIST OF ABBREVIATION	11
LIST OF TABLES	14
CHAPTER I: INTRODUCTION	1
CHAPTER II: LITERATURE REVIEW	4
2.1. <i>Fenbendazole</i>	4
2.1.1. Mechanism of action.....	5
2.1.2. Studies on anticancer activities of fenbendazole	6
2.1.3. Research gap	13
2.2. <i>Diisopropylamine dichloroacetate</i>	14
2.2.1. Mechanism of action.....	14
2.2.2. Studies on DADA in anticancer effects	17
2.3. <i>Investigation of synergistic effects</i>	18
2.3.1 <i>In vitro</i> study	19
2.3.2. <i>In vivo</i> study	20
2.4. <i>Lung cancer models</i>	21
2.4.1. Overview of lung cancer therapy	21
2.4.2. A549 lung cancer cell line	23
2.5. Rationale for combining fenbendazole and DADA.....	24
CHAPTER III. MATERIALS AND METHODS	25
3.1. <i>Chemical agents</i>	25
3.2. <i>Cell lines and cell culture</i>	25
3.3. <i>Cell seeding</i>	25
3.4. <i>Cell viability assay</i>	26

<i>Figure 5: Formation of formazan crystals from MTT (99)</i>	26
3.5. <i>Hoestch staining</i>	27
3.6. <i>Apoptosis assay</i>	28
3.7. <i>Cell cycle arrest</i>	31
3.8. <i>ROS assay</i>	32
3.9. <i>Glucose uptake assay</i>	33
3.10. <i>Lactate assay</i>	34
3.11. <i>Total protein extraction and quantification</i>	34
3.12. <i>Western blot</i>	35
3.13. <i>Animal experiments</i>	35
3.13.1 <i>Animal preparation</i>	35
3.13.2 <i>Toxicology study</i>	37
3.13.3 <i>Histopathological imaging</i>	37
3.13.4 <i>Ethical considerations</i>	38
3.14. <i>Statistical analysis</i>	38

CHAPTER IV: SYNERGIC EFFECT OF FZ AND DADA IN A549 NON-SMALL CELL LUNG CANCER CELLS.....40

4.1. <i>Cytotoxic effect of FZ and DADA in A549 lung cancer cells</i>	40
4.2. <i>Hoechst staining</i>	42
4.3. <i>FZ and DADA combination triggers apoptosis</i>	43
4.4. <i>FZ and DADA combination induces cell cycle arrest</i>	47
4.5. <i>FZ-DADA regulate cell cycle in A549 cells</i>	49
4.6. <i>FZ-DADA induced ROS in A549 cells</i>	50
4.7. <i>FZ-DADA combination inhibits glucose uptake and lactate production</i>	52
4.8. <i>FZ and DADA inhibit phosphorylation of PI3K/AKT pathway</i>	53

CHAPTER V: SYNERGIC EFFECT OF FZ AND DADA IN A549 TRANSPLANTED MODEL56

5.1 Hematological function analysis.....	59
5.2. Kidney function of mice after FZ-DADA treatment.....	60
5.3. Liver function of mice after FZ and DADA treatment.....	63
5.4. Synergistic anti-tumor effect of FZ and DADA.....	65
5.5 Tumor Growth Inhibition (TGI) and Evaluation of Synergistic Effects	66
5.6. Tumor reduction rates of FZ and DADA in BALB/c nude mice	67
5.7. Effect of FZ and DADA on the survival duration and death rate of BALB/c nude mice	69
CHAPTER VI: DISCUSSION.....	71
6.1. Synergistic mechanistic insight in vitro	71
6.2. Synergistic effect and safety in vivo	72
6.3. Novelty and significance of the study.....	73
6.4. Bridging the gap: in vitro vs. in vivo dosage discrepancies.....	74
6.5. Limitations of the current study.....	75
6.6. Future research directions.....	76
6.7. Clinical and Social Implications.....	76
CHAPTER VII: CONCLUSION	77
REFERENCES.....	78
SUPPLEMENT INFORMATION	92
LIST OF PUBLICATIONS	96

CHAPTER I: INTRODUCTION

In recent decades, cancer has become one of the biggest health problems in human, with approximately 20 million new cases, and causing 9,7 million deaths each year (1).

The most common type of cancer diagnosed in high-income countries are lung, colon, female breast, cutaneous melanoma, and prostate (2). In 2022, lung cancer was the most frequently diagnosed with 2,5 million new cases accounting for 12,5% of cancer types worldwide (1). As a critical global burden, the incidence and mortality of lung cancer remains high (3). Despite significant scientific advancements in lung cancer prevention, screening, and treatment, substantial inequities remain across racial, economic, and geographic lines globally (4).

In Vietnam, cancer has become a major social problem, with 37,4% of patients unable to afford the treatment (5). Liver, stomach, and lung cancers in men and breast, lung, and colorectal cancers in women are the most common types of cancer in Vietnam (Globocan, 2022). Treatment cost for phase III non-small cell lung cancer fluctuates around 172 million VND to 339 million VND (6). This treatment cost crisis is exacerbated by several factors, including late-stage diagnosis (with over 70% of lung cancer cases detected at advanced stages), limited health insurance coverage for newer targeted therapies and immunotherapies, and significant urban-rural disparities in healthcare access.

While researchers have made progress in developing more accessible diagnostic tools and therapies, low income populations continue to face disproportionate barriers to quality care. These disparities manifest through unequal access to early detection programs, limited availability of targeted therapies in low-resource settings, and systemic healthcare inequalities that disproportionately affect minority and socioeconomically disadvantaged groups. This challenge highlight the necessary of biomedical innovation to reduce the treatment cost and remove barriers to ensure equitable access to lung cancer care globally. In recent years, the concept of drug repurposing has gained growing attention as an innovative approach to accelerate cancer drug discovery.

Drug repurposing, also known as drug repositioning, refers to the strategy of identifying new therapeutic uses for existing drugs that have already been approved for other indications. This approach offers several advantages, including reduced development costs, shorter timelines, and lower safety risks, since the pharmacokinetic and toxicological profiles of these drugs are

already well characterized (7,8). In oncology, drug repurposing has emerged as a particularly promising avenue, as many approved non-oncologic agents have been found to modulate pathways critical for tumor growth, angiogenesis, and metabolism (9).

Several successful examples have demonstrated the potential of this strategy. *Thalidomide*, initially developed as a sedative, was later repurposed for multiple myeloma due to its anti-angiogenic properties (10). *Metformin*, a widely used antidiabetic drug, has shown inhibitory effects on tumor metabolism through the AMPK–mTOR pathway (11). *Disulfiram*, used for alcohol dependence, has exhibited cytotoxicity in various cancers by generating reactive oxygen species through copper chelation (12). Moreover, antiparasitic agents such as *Fenbendazole* and *Ivermectin* have recently attracted attention for their ability to disrupt microtubule polymerization and inhibit oncogenic signaling pathways in preclinical models (13). Collectively, these findings underscore drug repurposing as a cost-effective and innovative strategy for discovering novel anticancer agents and accelerating their clinical translation.

Fenbendazole (FZ), a broad-spectrum benzimidazole anthelmintic used against gastrointestinal parasites in animals, affects cancer cells. In research by Dorga et al., 2018, FZ has been found to cause cancer cell death by modulating multiple cellular pathways, including inhibition of glucose uptake and reduction of lactate level (14). FZ has a very low toxicity, with acute, subacute and long-term toxicity trials in cattle given fenbendazole at dosages of up to 2 g/kg revealed no adverse effects (15) and has been safely used for decades in animal food. While most reported cases of FZ self-administration have noted reductions in tumor size (16,17), in some cases, FZ has been found to cause drug-induced liver injury (18,19) in which patients promptly recover after discontinuation of FZ. To minimize these hepatotoxic effects, co-administration of FZ with a liver-protective agent could represent a promising therapeutic strategy. This combination approach could potentially reduce FZ-induced liver damage, maintain FZ's antitumor efficacy as well as enable safer clinical translation for future pilot trials. Such hepatoprotective combination therapy may be particularly valuable for patients with pre-existing liver conditions or those requiring prolonged FZ treatment, potentially expanding the drug's therapeutic window and clinical applicability in oncology.

Diisopropylamine dichloroacetate (DADA), a derivative of dichloroacetic acid (DCA), yielded better results (20). It has been proven to decrease lactate production in cells. In combination with radiotherapy, DADA showed a significant synergistic effect on esophageal squamous cell

carcinoma (21). Notably, DADA showed superior antitumor efficacy in breast tumor models compared with DCA (22). DADA, is the active component of pangamic acid and has been commercially available for over 50 years for the treatment of chronic liver diseases, with the trade name Vitamin B15 (23) and has low toxicity, with an LD50 oral in mice of 1700 mg/kg (24). There have not been many studies on the mechanism and efficacy of DADA in cancer treatment, especially in preclinical and clinical trials, or their combination to gain maximum synergistic effects. In Vietnam, the treatment of cancer by targeting its metabolic factor has been not received enough attention from both physicians and researchers.

Based on the above knowledge, the hypothesis of this research is the combination of Diisopropylamine dichloroacetate (DADA) and fenbendazole (FZ), at an optimized ratio, could be exhibit synergistic antitumor effects by simultaneously targeting cancer metabolism (via DADA's dichloroacetate moiety) and microtubule disruption (via FZ), while DADA's hepatoprotective properties mitigate FZ-induced liver toxicity. This dual-action approach may enhance therapeutic efficacy, improve treatment tolerability, and preserve quality of life in cancer patients.

This study aimed to investigate the synergistic effects of DADA and FZ in lung cancer treatment *in vitro* using biochemical assays, molecular techniques, and *in vivo* studies. The cancer cells used in the experiments were derived from the human non-small lung cancer cell line A549. The optimal portion of each ingredient in the composition and comparisons with the effects of DADA and fenbendazole alone will be proposed.

The final purpose of this study was to prove that there is a safer and more effective approach to lung cancer treatment. The results of this research will provide evidence for submitting clinical trials to develop new drugs for cancer treatment.

CHAPTER II: LITERATURE REVIEW

2.1. Fenbendazole

Fenbendazole (methyl N-(6-phenylsulfanyl-1H-benzimidazole-2-yl)), is currently used as an antiparasitic therapeutic agent in animals. In human, other benzimidazoles, such as mebendazole and albendazole, are used as antiparasitic agent for years (25). Fenbendazole causes microtubule destabilization and hindering tubulin polymerization in parasites. Having a poorly absorbs by oral administration, fenbendazole is particularly effective for targeting intestinal parasites (26).

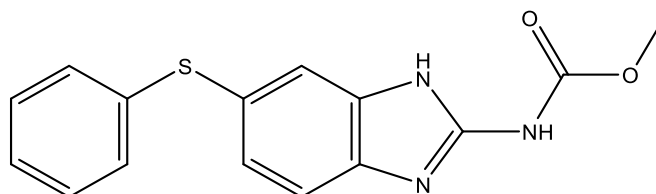


Figure 1: Chemical structure of Fenbendazole

In 2008, Ping Gao et al published a research relating to anti-tumor effect of fenbendazole. They indicated a non-significant effect of fenbendazole in the growth of the P493-6 human lymphoma cell line in SCID mice. In addition, higher inhibition tumor growth was observed in mice that were administered fenbendazole with vitamin-supplemented diet (27). In the years later, two publications on non-small cell lung cancer and breast cancer showed tumor growth inhibition ability of fenbendazole at micromolar concentration (13,28). In 2016, fenbendazole began to attract considerable scientific attention for its potential anticancer effects following a case report in which a patient with small-cell lung cancer self-administered 222 mg of fenbendazole orally, together with vitamin E supplements, CBD oil, and curcumin. Notably, undetectable tumor on a PET scan was confirmed in this patient after three months. Especially, he was the only patient who cured of cancer among the 1100 clinical trial participants (71). Since that event, researchers have made extensive efforts to reveal the mechanisms of action and explore the potential of developing a new safe and affordable anticancer agent from fenbendazole.

2.1.1. Mechanism of action

According to previous studies, FZ has shown multi-target anticancer, involved increasing p53 activation, inhibiting the GLUT1 transporter and reducing glucose uptake in cancer cells (14). As a key tumor suppressor, p53 plays a vital role in combating cancer by repairing DNA damage and triggering programmed cell death (29–31). However, p53 is either inactivated or mutated in many cancers, allowing cancer cells to proliferate (32). Cells expressing wild type p53 are more sensitive to FZ than p53 mutant or null cells. Additionally, FZ has been proved to promote the translocation of p53 into mitochondria (14). By microtubule disruption and p53, p21, p27 activation, FZ directly triggers apoptosis through various pathways. In colorectal cancer, FZ has been shown to arrest cell cycle at G2/M phase by increasing secretion of p21, p27 – cyclin-dependent kinase inhibitors, that can halt cell cycle progression (33). In hepatocellular carcinoma cells, FZ induced apoptosis of actively growing H4IIE via p21-mediated cell-cycle arrest (34). Not only exert this action on parasitic tubulin, FZ but also demonstrates moderate affinity for mammalian tubulin and exerts cytotoxicity to human cancer cells at micromolar concentration. FZ selectively binds to β -tubulin of microtubules to disrupt microtubular polymerization and promote immobilization (35). Microtubules are important for various cellular processes including cell division, intracellular transport, and cell shape maintenance (36). By disrupting microtubule formation, FZ interferes with mitotic spindle assembly, leading to cell cycle arrest and ultimately inducing programmed cell death (apoptosis) in rapidly dividing cancer cells, the same mechanism as that of other conventional chemotherapy drugs such as taxanes and vinca alkaloids (14).

Beside the inducible programmed cell death, FZ leads to an abnormality in energy metabolism of cancer cells. Unlike normal cells, glucose is a primary energy source for tumor cells, which is metabolized through aerobic glycolysis and delivered across the cell membrane *via* the GLUT1 transporter (37). FZ has been shown to interfere with this process by inhibition of GLUT1 transporter. As a result, FZ reduced the uptake of glucose into cancer cells. Moreover, FZ inhibited hexokinase II (HKII) – the first enzyme in the glycolytic pathway and often overexpressed in cancer cells. By that ways, FZ reduced glucose uptake and starved cancer cells of their primary energy source, leading to metabolic stress and cell death (14).

The summary of mechanisms of action of fenbendazole on cancer cells presented in Figure 2.

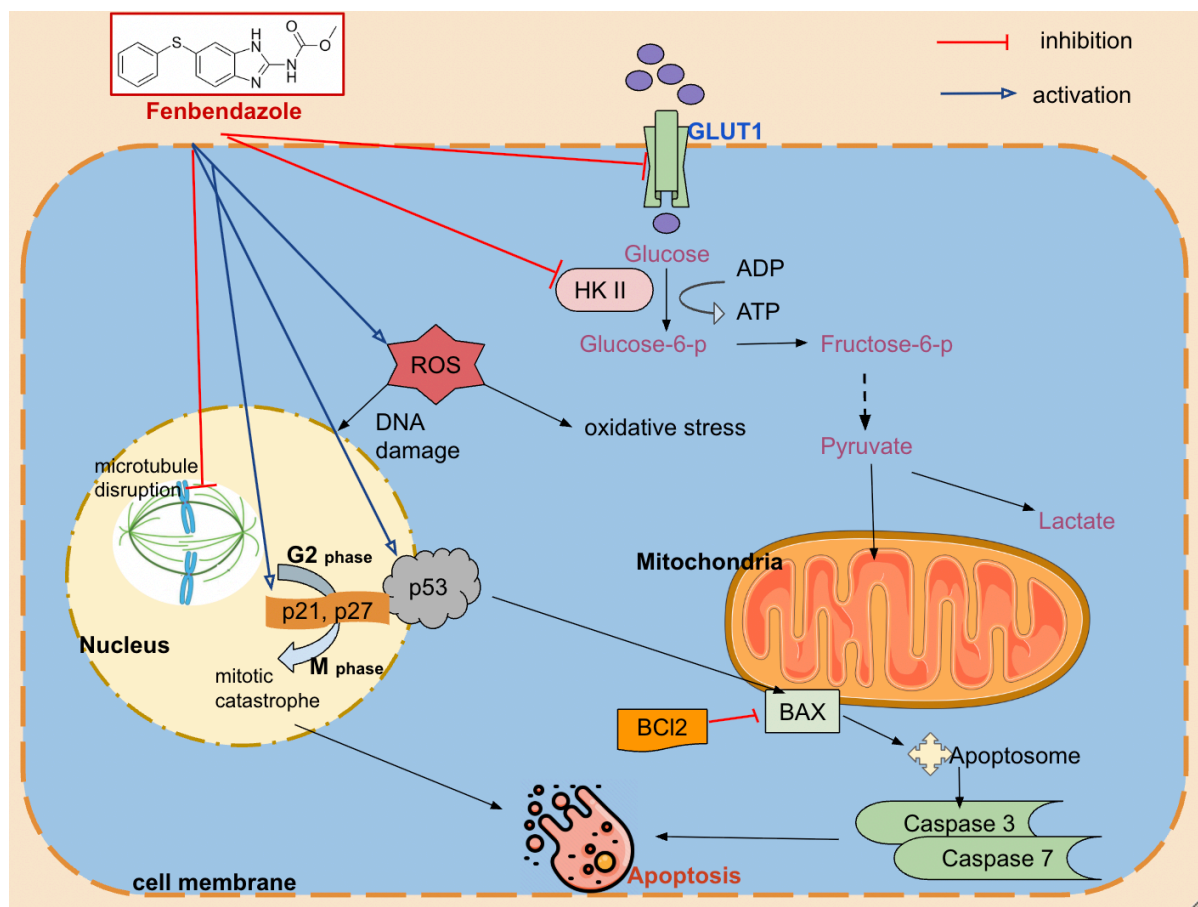


Figure 2: Mechanism of action of Fenbendazole (generated by Google Drawing).

HKII: Hexokinase II, GLUT1: Glucose Transporter protein type 1, ADP: Adenosine Diphosphate, ATP Adenosine triphosphate, ROS Reactive Oxygen Species, Bcl2: B-cell Lymphoma 2, BAX: Bcl-2-Associated X protein.

2.1.2. Studies on anticancer activities of fenbendazole

As shown in the Table 1, since 2018, there were dozens of research on fenbendazole in various cancer models, *in vitro* and *in vivo*, showing its multi-target in numerous types of cells, as well as in its mechanism of action.

Table 1: List of researches of fenbendazole *in vitro* and *in vivo* through years

Cancer type; Cell Lines	Year of publication	Experimental Model	Fenbendazole dose	Results	References
Lymphoma; P493-6B cells in SCID mice	2008	<i>In vivo</i> and <i>in vitro</i>	150 ppm fenbendazole, with diet and/or with vitamins	Observed low anti-cancer effect when fenbendazole was administered alone. Tumor growth inhibition was higher in mice that were administered fenbendazole with vitamin-supplemented diet.	(27)
Non-small cell lung cancer; A549, H460	2012	<i>In vitro</i>	1 μ M for 48 hours	Observed tumor growth inhibition and apoptotic cancer cell death, possibly by inhibiting proteasomal function via the ubiquitin-proteasome pathway. Fenbendazole demonstrated cytotoxicity towards tumor cells but retained non-toxicity to normal cells. Observed p53 induction and up-regulation of p53 target genes.	(28)
Breast cancer; EMT6 mouse mammary	2013	<i>In vitro</i> and <i>in vivo</i>	0.11, 0.33, 1.0, and 3.0 μ M for 8 days <i>in vitro</i>	Higher drug concentrations demonstrated cytotoxicity towards tumors and high tumor inhibition. Tumor appearance also changed, suggested to be due to disruption of tubulin microtubule equilibrium.	(13)

Cancer type; Cell Lines	Year of publication	Experimental Model	Fenbendazole dose	Results	References
tumor cells in female BALB/cRw mice			150 ppm in diet and 50 mg/kg/day, i.p. for 2 days <i>in vivo</i>	No change in tumor growth or metastatic pattern. No change in tumors with radiation.	
Non-small cell lung cancer; H460 and A549 cells in nu/nu mice	2018	<i>In vitro</i> and <i>in vivo</i>	<i>In vitro</i> : 1 μ M for 48 hours <i>In vivo</i> : 1 mg/mouse, p.o., every second day for 12 days	Significant reduction in number of tumor cell colonies. Reduction of tumor size and weight. Confirmation of microtubule disruption, induced cell cycle arrest in G2/M phase.	(14)

Cancer type; Cell Lines	Year of publication	Experimental Model	Fenbendazole dose	Results	References
Skin cancer; A375	2019	<i>In vitro</i>	1,2, and 4 μ M for 24-48 hours	Increased levels of γ H2AX, indicating DNA damage. Confirmation of antiproliferative activity of fenbendazole, microtubule disruption, induced cell cycle arrest at G2/M phase.	(38)
				Increase of p53 activity by downregulating Mdm2 and MdmX expression.	
Breast cancer; MCF- 7	2019	<i>In vitro</i>	1,2, and 4 μ M for 48 hours	Increased levels of γ H2AX, indicating DNA damage. Confirmation of antiproliferative activity of fenbendazole, microtubule disruption, induced cell cycle arrest at G2/M phase. Increase of p53 activity by downregulating Mdm2 and MdmX expression.	(38)
Leukemia; HL60 in mice	2021	<i>In vivo and in vitro</i>	0.1, 0.2, and 0.5 μ M for 1-6 days	Higher concentrations of fenbendazole lead to apoptosis. In as little as 3 days, lower concentrations (0.1 μ M) caused leukemia cells to convert to granulocytes and induced apoptosis.	(39)

Cancer type; Cell Lines	Year of publication	Experimental Model	Fenbendazole dose	Results	References
				At 72 hours, fenbendazole exhibits 14.5-fold selectivity in killing HL60 cells over healthy human bone marrow stem (BMSC) cells.	
Lung cancer; A549, H460, and H1299 cells	2021	<i>In vitro</i>	0.001, 0.01, 0.1, 1, 10, and 100 μ M for 48 hours.	50% tumor inhibition at 1 μ M. Tubulin destabilization activity was observed at 1 and 10 μ M. Induced cell cycle arrest in the G2/M phase.	(40)
Cervical cancer; HeLa, C-33A, CaSki	2022	<i>In vitro</i>	0.1, 1, 10 μ M for 48 hours	Fenbendazole inhibited tumor colony formation and induced cell apoptosis and arrest. It was more toxic to HeLa cells and less toxic to normal cells. Downregulation of MMP2 and MMP9 expression inhibited HeLa cell migration and invasion.	(41)

Cancer type; Cell Lines	Year of publication	Experimental Model	Fenbendazole dose	Results	References
Colorectal cancer; SNU-C5	2022	<i>In vitro</i>	0.50 μ M for 3 days	Triggered cancer cell apoptosis through mitochondrial injury and the caspase 3-PARP pathway. Increased p53 expression, leading to p53-mediated apoptosis.	(33)
Hepatocellular carcinoma; H4IIE cells	2022	<i>In vitro</i>	1.25 μ M for 48 hours	Growth suppression in cancer cells actively growing. Induces p21-mediated apoptosis in tumor cells.	(26)
Epithelial ovarian cancer; HeyA8 and HeyA8-MDR, SKOV3ip1, A2780-CP20 and SKOV3-TR	2023	<i>in vitro</i>	0.32 μ M to 1.01 μ M from 24 hours to 72 hours	Significant reduction of cell viability in all EOC cell lines after 48 hours. Decreases the activation of mTOR and several MAPK members. Causing apoptosis cell death	(42)

Cancer type; Cell Lines	Year of publication	Experimental Model	Fenbendazole dose	Results	References
HeyA8 and HeyA8-MDR		<i>In vivo</i>	1mg/mouse and 10mg/mouse	Fenbendazole did not reduce the tumor weight in either HeyA8 or HeyA8-MDR model	
epithelial ovarian cancer; A2780, SKOV3	2024	<i>in vitro</i>	0.38 μ M to 1.3 μ M from 24 hours to 72 hours	Fenbendazole inhibited the proliferation and promoted the apoptosis of ovarian cancer cells in a dose-dependent manner, mechanism of action through promoting apoptosis via mitotic catastrophe	(43)
		<i>In vivo</i>	50mg/kg in 21 days	Fenbendazole inhibited the growth of ovarian cancer tumors in vivo (reduce tumor weight)	

In vitro, FZ inhibited proliferation of multiple cancer cell lines, with MDA-MB-231 breast cancer cells being most sensitive ($IC_{50} < 10 \mu M$), suggesting selective cytotoxicity (44). In addition, it induces oxidative stress on triple-negative breast cancer cells (MDA-MB-231) and selectively reduces viability while sparing normal breast epithelial cells, indicating a redox-mediated, cancer-targeting mechanism (45).

In ovarian cancer models, fenbendazole-incorporated PLGA nanoparticles (FZ-PLGA-NPs) demonstrated strong antiproliferative effects both *in vitro* and *in vivo*, including in patient-derived xenograft models, especially when administered intravenously, overcoming limitations in bioavailability (42). Additionally, a co-encapsulation of FZ with rapamycin in polymeric micelles significantly enhanced cytotoxicity *in vitro* and suppressed tumor growth *in vivo* without observable toxicity (46). In H4IIE hepatocellular carcinoma cells, FZ induced p21-mediated cell cycle arrest and apoptosis selectively in actively growing cells, without affecting quiescent cells, and independent of glycolysis, ROS, and MAPKs (34). Fenbendazole was particularly effective in 5-fluorouracil-resistant colorectal cancer cells, promoting apoptosis, G2/M arrest, increased ferroptosis, and apoptosis independent of p53, making it a candidate for overcoming drug resistance (33). In HeLa cervical cancer cells, both FZ and its analog (analog 6) impaired proliferation via ROS accumulation, p38-MAPK activation, apoptosis, and energy metabolism disruption. Analog 6 showed reduced toxicity to normal cells (41).

In canine melanoma cells, FZ caused G2/M arrest, disrupted microtubules, and triggered mitotic catastrophe, suggesting potent cytotoxicity via anti-tubulin activity (47). In mouse lymphoma models, FZ caused G2/M arrest and apoptosis *in vitro*, but showed no significant tumor suppression *in vivo* due to immunosuppressive microenvironment modulation (48). A combination of FZ and rapamycin showed increased bioavailability, stability, and antitumor activity in A549 lung cancer cells, which confirming the enhanced pharmacokinetic profile and therapeutic potential of this combination (49).

2.1.3. Research gap

Showing multitarget inhibition of cancer cell growth across various types of cancer models, even at very small doses, fenbendazole is a potential candidate for developing a new, safe and reasonable anticancer agent. However up to now, fenbendazole has not been applied to clinical trial for cancer treatment. Some cases have been reported with positive results in patients (17) but it is not enough for such a serious problem as cancer. Currently, all available

pharmacokinetic data-including absorption, distribution, metabolism, and excretion profiles-are derived exclusively from animal studies, primarily in animals (50–52). This creates significant knowledge gaps regarding its behavior in humans, such as oral bioavailability, plasma half-life, tissue penetration, and potential drug-drug interactions.

On the other hand, despite having many beneficial bioactivities, especially anticancer, prolonged administration of FZ led to an increase in liver cytochrome enzyme activity (53), which may impact the metabolism of fenbendazole and co-administered drugs, such as aflatoxins (54). As a clear result, self-medication with fenbendazole led to drug-induced liver injury in cancer patients, in which patients promptly recover after discontinuation of fenbendazole (18,19), raising safety concerns of self-administering fenbendazole.

Therefore, a combination of fenbendazole with another hepatoprotective drug such as dichloroacetate or its derivative may reduce dose of both two agents and help to prevent hepatotoxic side effect of fenbendazole *in vivo* and in further clinical trial.

2.2. Diisopropylamine dichloroacetate

Diisopropylamine dichloroacetate (DADA), a derivative of dichloroacetic acid (DCA), is a small molecule, which has been commercially available for over 50 years for the treatment of chronic liver diseases with the trade name Vitamin B15. DADA its own has low toxicity, with an LD50 oral in mice of 1700 mg/kg (24). In recent years, DADA was reported to show significant anticancer effects, especially in lung, breast, colorectal, and esophageal cancer.

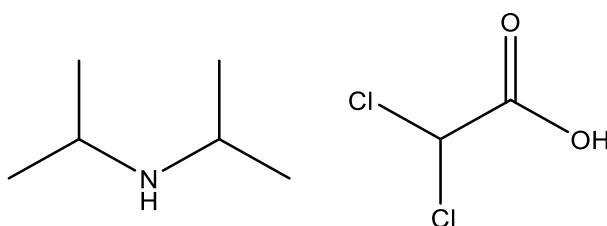


Figure 3: Chemical structure of Diisopropylamine dichloroacetate

2.2.1. Mechanism of action

In general, normal cells generate needed energy by mitochondrial oxidative phosphorylation, whereby a pyruvate molecule enters Krebs' cycle to be metabolized. In contrast, cancer cells use pyruvate in the process of aerobic glycolysis - a phenomenon termed “the Warburg effect” (37).

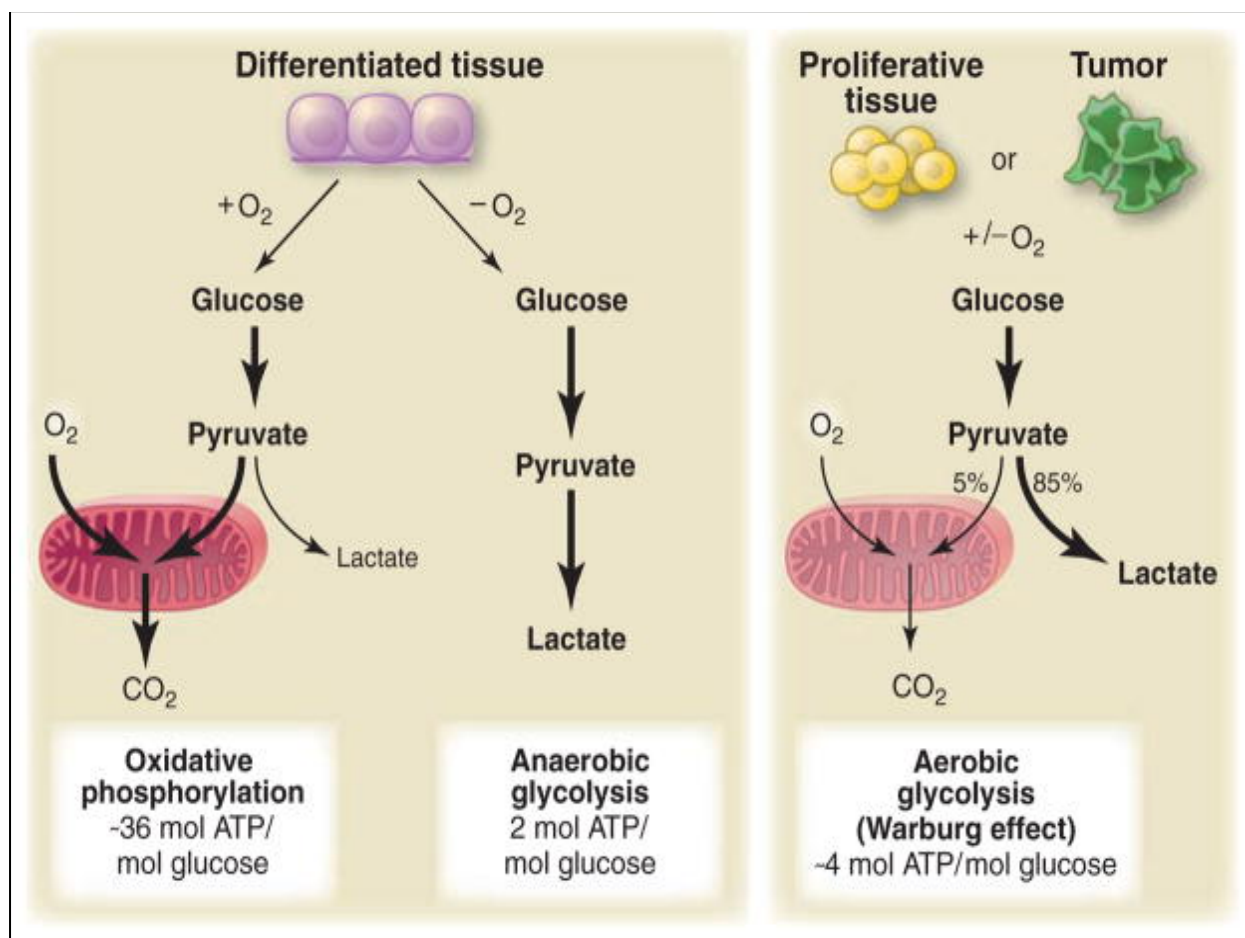


Figure 4: The Warburg effect.

Oxidative phosphorylation fully oxidizes glucose to CO₂ in mitochondria when oxygen is available, generating approximately 36 ATP per glucose molecule. Under oxygen-limited conditions, anaerobic glycolysis converts glucose to lactate to regenerate NAD⁺, producing only 2 ATP per glucose. The Warburg effect (aerobic glycolysis) is observed in cancer and proliferating cells, which preferentially produce lactate even in the presence of oxygen. This metabolic reprogramming allows proliferating cells to divert glucose carbons into biosynthetic pathways for nucleotides, lipids, and other macromolecules needed for rapid cell division (55)

As shown in Figure 4, glycolysis starts when a glucose molecule enters the liquid part of the intracellular environment (cytosol). After phosphorylation, glucose is converted into two molecules of pyruvate. In normal metabolism, pyruvate, catalyzed by the enzyme pyruvate dehydrogenase (PDH), is converted to acetyl-CoA and enters the Krebs cycle within mitochondria. Pyruvate dehydrogenase kinase (PDK) inhibits PDH and may affect this process. Alternatively, pyruvate may enter a process called lactic acid fermentation, in which pyruvate converts into lactate (base conjunction of lactic acid), especially in the absence of oxygen. It

often occurs in hypoxic conditions, for example, in overworked muscles that are starved of oxygen or in tumor organs, as explored by Warburg. This anaerobic fermentation produces only 2 ATP per glucose molecule compared to up to 32 ATP from complete oxidative phosphorylation, which contributes to the fatigue and cachexia often experienced by cancer patients (55).

DADA has been shown to inhibit PDK4 – the main protein in PDK group, thereby liberating PDH. This reactivation of PDH facilitates the entry of pyruvate into the mitochondria, thereby shifting glucose metabolism from glycolysis to mitochondrial oxidative phosphorylation. As a PDK blocker, DADA inhibited proliferation of cancer cells *in vitro* and *in vivo* by shifting metabolism of cancer cells and induced autophagy and cell death in a breast cancer model (22). By blocking PDK, DADA allows pyruvate to enter the mitochondria, which promotes mitochondrial oxidation and leads to an increased reactive oxygen species (ROS) (21). Under normal conditions, ROS may not be harmful; however, increasing ROS levels may cause cellular damage and trigger apoptosis (56). Interestingly, DADA has shown synergistic effect in combination with conventional cancer treatments. DADA acts as a radiosensitizer, rendering cancer cells more sensitive to radiation. This may be explained by increased ROS production and DNA damage. Recently, a study demonstrated the improved effect of DADA in NSCLC either alone or in combination with radiotherapy in both *in vitro* and *in vivo* (21). Furthermore, the combination combination of DADA, radiotherapy and anti-PD-1 antibody exhibited superior tumor inhibition to the combination of radiotherapy and anti-PD-1 antibody in NSCLC model (57). In a chemotherapy study, the combination of DADA and pemetrexed displayed a significant inhibition of the proliferation of NSCLC cells *in vitro* compared to single-agent treatment (57). Furthermore, lactic acid produced by tumors may help cancer cells to overcome immune surveillance (21,58,59). In a condition of low tumor lactate level, DCA increases T-cell proliferation and cytokine production (60).

DADA, on the other hand, has been used as a hepatoprotective over-the-counter drug for years, with some key mechanisms such as restoration of pyruvate dehydrogenase (PDH) activity and ATP levels in some conditions like inflammation, liver damage in which mitochondrial function and ATP production were reduced (61). DADA, by inhibiting PDK (especially PDK4, which is often upregulated in stressed or damaged liver cells), reactivates PDH (20). This promotes the flow of pyruvate into the Krebs cycle (TCA cycle), thus restoring ATP production and improving cellular energy homeostasis in the liver. Moreover, DCA has antifibrotic effects

by inhibiting hepatic stellate cells (HSCs) activation and proliferation (62). Liver fibrosis is a common outcome of chronic liver injury, with hepatic stellate cells play a central role in the process of accumulation of matrix proteins: when activated, they become fibrogenic (63).

2.2.2. Studies on DADA in anticancer effects

In recent years, DADA has been a focus for finding new candidates for novel anticancer therapy. Before discussing DADA, it is important to revisit DCA — a precursor of DADA — which has demonstrated clear anticancer effects and has been extensively studied over the past years.

There have been several studies on DCA's mechanism of anticancer activity, in which DCA reduced circulating lactate, preserved mitochondrial function, and maintained physical performance in late-stage cancer (64). In hepatocellular carcinoma, DCA reduces the stemness of carcinoma cells by promoting the nucleus-cytoplasm translocation of YAP and activating the Hippo pathway, implicating it as a stemness inhibitor (65). In glioblastoma, the antitumor effectiveness of DCA varies based on the ionic formulation and tumor model, suggesting cell-specific response variability (66,67). Sodium and magnesium DCA suppress glioblastoma growth and neoangiogenesis in pediatric tumor models, indicating dose- and ion-dependent effects (68). DCA inhibited proliferation, induced apoptosis, and slowed tumor growth in a mouse model of HPV-positive head and neck cancer, especially when combined with quercetin, partly through mTOR inhibition and immune modulation (69). Additionally, in a Phase II trial, DCA combined with chemoradiotherapy for head and neck cancer increased complete response rates without increasing severe toxicity (70). In colorectal cancer stem cells, DCA triggers ferroptosis by sequestering iron in lysosomes, leading to reduced stemness and migration (71). In lung cancer, DCA reduced cell viability, inhibited tumor growth *in vivo*, and enhanced the effects of cisplatin, gefitinib, and erlotinib (72). Moreover, DCA shifted the metabolism of breast tumor-educated macrophages toward a pro-inflammatory antitumor phenotype, increasing TNF- α and reducing VEGF levels (73). In oral squamous cell carcinoma (OSCC), DCA combined with arsenite and chloroquine suppressed tumor development, improved survival, and reduced dysplasia *in vivo* by modulating glycolysis, autophagy, and ROS pathways (74). DCA alters glucose metabolism in pancreatic cancer cells by activating oxidative phosphorylation and inhibiting glycolysis, particularly affecting amino acid biosynthesis (75).

Interestingly, it has been shown that DADA has a superior antitumor effect compared to DCA in MDA-MB-231 a triple -negative breast cancer cells (TNBC) (22). The IC₅₀ of DADA and DCA in MDA-MB-231 was 7.1 ± 1.1 mmol/L and 15.6 ± 2.0 mmol/L, respectively. In a subcutaneous breast tumor xenograft model, at the same dosage (100 mg/kg) DADA demonstrated better efficacy than DCA in suppressing tumor growth.

In non-small cell lung cancer (NSCLC), DADA induces apoptosis and inhibits lactate production, thereby altering the tumor microenvironment and enhancing antitumor immune responses when combined with chemotherapy, radiotherapy, or immune checkpoint inhibitors (57). For colorectal cancer, *in situ* administration of DADA-loaded mats suppresses tumor growth up to 95% without recurrence, by targeting tumor-specific metabolism (76). DADA also enhances radiosensitization in esophageal squamous cell carcinoma by increasing mitochondrial ROS and DNA damage while promoting G2/M arrest and apoptosis (21).

2.3. Investigation of synergistic effects

Drug synergy occurs when two drugs, when used together, produce a combined effect that is greater than the sum of their individual effects. This phenomenon is particularly significant in cancer therapy, where combination treatments can overcome drug resistance and enhance therapeutic efficacy.

There are several quantitative methods for assessing the synergistic effect: Loewe Additivity, Bliss Independence, and Combination Index. When Loewe Additivity assumes that two drugs act through the same mechanism, synergy is detected when the combine effect is greater than predicted by the sum of individual effect (77). Bliss Independence method assumes that drug act independently (78). Synergy is detected when the combined effect is greater than the product of individual effects. Because of the efficacy of DADA in combinations with other therapies and their efficacy in protecting liver function in this study, we used the Combination Index as the main method to determine whether fenbendazole and DADA are synergistic *in vitro*.

2.3.1 *In vitro* study

The Combination Index (CI) was introduced by Chou and Talalay in the 1980s to enable the rigorous analysis of drug combinations. CI is a quantitative measurement used to determine the interaction between two or more drugs – whether synergistic, additive, or antagonistic (79).

Mathematical basis:

The median-effect equation is:

$$\frac{Fa}{Fu} = \left(\frac{D}{Dm} \right)^m$$

Where:

- Fa = fraction affected (e.g., % inhibition/100)
- $Fu = 1 - Fa$ = fraction unaffected
- D = dose of drug
- Dm = median-effect dose (analogous to IC50)
- m = slope of the dose – response curve

Using this, the Combination Index (CI) for two drugs (Drug 1 and Drug 2) is calculated as:

$$CI = \frac{D1}{D1x} + \frac{D2}{D2x}$$

Where:

- $D1$ and $D2$ are the dose of Drug 1 and Drug 2 in combination required to achieve a certain effect level (e.g./ 50% inhibition)
- $D1x$ and $D2x$ are the dose of each drug alone that produce the same effect.

With:

- $CI < 1$: synergism
- $CI = 1$: additive effect
- $CI > 1$: antagonism

To capture subtle differences, the Chou-Talalay method also provides graded CI values:

- $CI < 0.1$: Very strong synergism
- $0.1 \leq CI < 0.3$: Strong synergism
- $0.3 \leq CI < 0.7$: Synergism

- $0.7 \leq CI < 0.85$: Moderate synergism
- $0.85 \leq CI \leq 1.1$: Nearly additive
- $1.1 < CI \leq 1.45$: Moderate antagonism
- $1.45 < CI \leq 3.3$: Antagonism
- $CI > 3.3$: Strong antagonism

Experimental implementation (80)

Generating dose-response curves on data of cell-based assays: using common assays, such as cell viability assays (MTT, XTT, trypan blue), apoptosis assays, cell cycle analysis or other specific pathway reporter assays for single drugs and fixed-ratio combinations.

- Data fitting: using software such as: CompuSyn by Chou and Martin (we used CompuSyn in this thesis); Calcu Syn or SynergyFinder
- Counting CI values at various effect levels (e.g. 25%, 50%, 75% or 90% inhibition)

Advantages of CI Method:

- Provided a mechanistically grounded, quantitative evaluation of drug interactions
- Allow assessment across multiple effect level, not just a single IC_{50}
- Generates isobolograms and Fa-CI plots for visualization of synergy

Limitations:

- Assumes accurate curve fitting and requires a well-characterized dose-response for each drug
- Works best when drugs act on related or complementary pathways: may misrepresent interaction between drugs with unrelated mechanisms
- Sensitive to experimental variability, particularly in high-dose or low-effect ranges.

2.3.2. *In vivo* study

In vivo systems are biologically complex, and drug concentrations may not follow linear kinetics. Therefore, empirical models based on actual tumor volume measurements are the most practical. The most widely used *in vivo* approach is the Tumor Growth Inhibition (TGI) method combined with a synergy assessment index. Moreover, xenograft mouse models and syngeneic tumor models have been used to assess tumor growth inhibition, survival, and histopathological changes. These studies provide insights into systemic effects, bioavailability,

and immune-related interactions to compare the effectiveness of a single agent with a combination at the same doses.

Tumor Growth Inhibition (TGI)

$$TGI = \left(1 - \frac{TV_{treatment}}{TV_{control}}\right) \times 100\%$$

Where:

- TV = tumor volume at endpoint (e.g., Day 21)
- TGI is calculated for each group (monotherapy and combination)

Then we use a Modification of Expected Additivity for *in vivo* synergy:

$$Expected\ TGI_{combo} = TG_1 + TG_2 - \left(\frac{TG_1 \times TG_2}{100}\right)$$

After that, we compare with Observed TGI of the combination:

- If Observed TGI > Expected TGI → Synergy
- If Observed TGI ≈ Expected TGI → Additivity
- If Observed TGI < Expected TGI → Antagonism

Another option is using two-way ANOVA to assess if the interaction term (Drug A × Drug B) is statistically significant for tumor size or survival. If the result is statistically significant, we can confirm about synergy between agents.

2.4. Lung cancer models

2.4.1. Overview of lung cancer therapy

Lung cancer is the most frequently diagnosed cancer in 2022, with 2,5 million new cases (12,4% of cancer types) worldwide (1). Based on report of WHO lung cancer is the leading cause of cancer-related death (1,8 million deaths, 18,7% of total cancer deaths). The number of death from lung cancer nearly 2.5 times higher than that from colorectal cancer, which ranks second. In Vietnam, lung cancer is the second most common type of cancer in both sexes (81). Lung cancer arises from the progressive accumulation of genetic and epigenetic alterations within cellular nuclei over extended periods (82). This malignant transformation begins when a cell escapes normal regulatory mechanisms that govern division and spatial organization. The

development and advancement of lung cancer are driven by the following molecular and cellular disruptions, namely dysregulated cell cycle control, oncogenic mutations, impaired DNA repair mechanisms, sustained angiogenesis, apoptosis evasion, telomerase reactivation, metastatic competence. It is broadly categorized into small cell lung cancer (SMLC) and non-small cell lung cancer (NSCLC), in which NSCLC accounting for 85% of all cases (83). NSCLC arise from the epithelial cells of the lung of the central bronchi to the terminal alveoli. Squamous cell carcinomas usually begin near the central bronchus.

The main treatment modalities used for NSCLC include surgery, radiation therapy, chemotherapy, immunotherapy, and the combination treatments. Surgery is often the primary and most effective treatment option for early-stage NSCLC (Stage I, II, and some Stage IIIA) when the tumor is localized and can be fully removed (84). Radiation therapy, on the other hand, uses high-energy rays to kill cancer cells or shrink tumor. Radiation therapy is used in various setting to curative intent for early-stage NSCLC in patients who cannot undergo surgery or for locally advanced NSCLC combined with chemotherapy (85). Chemotherapy, a key therapy for cancer treatment is used typically given intravenously (IV), to eliminate cancer cells throughout the body. Chemotherapy usually involves a combination of two drugs, often including a platinum-based drug (cisplatin or carboplatin) combined with another agent, such as pemetrexed, paclitaxel, vinorelbine, gemcitabine or etoposide (86). Chemotherapy can cause significant side effects (fatigue, nausea, hair loss, bone marrow suppression) due to its impact on fast-growing healthy cells. Recent years, targeted therapy in which drugs that specifically attack cancer cells by targeting specific molecular pathways or genetic mutations that drive their growth and survival pays attention in various type of cancer (87). In lung cancer, targeted therapy are used in the treatment of advanced NSCLC (88). To determine whether targeted therapy is an option, molecular testing (biomarker testing) of the tumor tissue is crucial to identify specific "driver mutations". Small-molecule drugs with small structure, which enter cells easily, are used as targets inside cells, and monoclonal antibodies – proteins produced in the lab–designed to attach to specific targets found on cancer cells (89). However, targeted therapy can also cause side effects, such as diarrhea, liver problems, fatigue, and high blood pressure. In addition, the cost of this type of therapy is not affordable for everyone (90). In contrast with previous therapies, immunotherapy uses drugs that harness the body's own immune system to recognize and attack cancer cells, like PD-1 inhibitors (Pembrolizumab, Nivolumab), PD-L1 inhibitors (Atezolimumab, Durvalumab), CTLA-4 inhibitors (ipilimumab, tremelimumab...) (86). Immunotherapy, therefore, can cause unique side effects known as "immune-related adverse events" (irAEs), where the activated immune system attacks healthy

organs (91,92). Nowadays, combination therapy is applying in NSCLC treatments to improve efficacy, overcome resistance, and target cancer cells through multiple pathways, such as: chemotherapy + immunotherapy; chemotherapy + radiation; targeted therapy + chemotherapy; targeted therapy + immunotherapy. Despite the development of new drugs and technologies for cancer treatment, lung cancer remains one of the hardest obstacles owing to late prognosis, the effectiveness and side effects of current therapies. Therefore, alternative treatment strategies are required.

Combining drugs is one of the most important strategies to overcome resistance, achieve higher efficacy with lower individual drug doses, and target multiple pathways. Thus, to confirm my hypothesis regarding the synergistic effect, I chose to conduct further experiments on lung cancer models, despite the fact that this combination may work effectively in various types of cancer.

2.4.2. A549 lung cancer cell line

A549 is a human non-small cell lung carcinoma cell line derived from a patient with lung adenocarcinoma (93). First isolated in 1972 from the lung cancer tissue of a 58-year-old Caucasian male, the A549 cancer cell line was established by D. J. Giard and associates. They are characterized by an adherent growth pattern, forming monolayers with an epithelial-like morphology reminiscent of squamous lung tissue cells. A549 is frequently used in lung cancer models because of its high reproductivity (stable growth characteristics allow for reproducible *in vitro* and *in vivo* experiments), strong experimental design with extensive literature exists on this cell line, and it is relevant to the most common subtype of lung cancer (93). In addition, there are some limitations of A549 as a sole model: A549 does not represent the vast heterogeneity of lung cancer patients, and monolayer A549 cultures lack a complex tumor microenvironment. In xenografts, the lack of the human immune system in mice is a significant limitation for assessing immunomodulatory drug effects of immune-mediated synergy in A549 derived cancer cells (94).

There was a huge number of literature on A549 line, including investigations the synergistic effect of drugs, such as: combination of herbal extracts (*Phyllanthus emblica* and *Terminalia bellerica* extract) (95), chemotherapy combination (cisplatin + doxorubicin), targeted therapy combination (EGFR inhibitors + ALK inhibitors) (96) or natural products/repurposed drugs (curcumin + gemcitabine (93), metformin + cisplatin (97)).

2.5. Rationale for combining fenbendazole and DADA

Both fenbendazole and DADA have shown successful case studies when combined with other agents for cancer therapy (21,42,58). Based on the previously described mechanism of action of fenbendazole and DADA, the combination of fenbendazole and DADA may exert some important effects in cancer models. Both DADA and fenbendazole strongly affect glucose metabolism in cancer cells by reducing their main source of energy and starving (14). Consequently, cancer cells may shift their metabolism to normal oxidative phosphorylation or starvation, and the process of rapid growth is stopped. Both agents have been found to induceable ROS levels (21,34) which may cause cellular damage and trigger apoptosis, in addition to other effects of fenbendazole in the activation of apoptosis, as shown above in the mechanism of action. As a hepatoprotector, DADA may help prevent side effects of fenbendazole in the liver (18,19). Moreover, decreasing the dose of fenbendazole in cases of synergy with DADA has a lot of meaning in long-term treatment of patients.

CHAPTER III. MATERIALS AND METHODS

3.1. Chemical agents

FZ (Thermo Fisher, USA), DADA (TCI, Japan), camptothecin (Thermo Fisher, USA) and paclitaxel (Thermo Fisher, USA) were dissolved in dimethyl sulfoxide (DMSO) and then diluted to the required working concentrations in complete medium.

Camptothecin was used as positive control for screening the IC₅₀ and optimal doses on A549 and other cell lines in MTT experiments at the first steps. For further experiments for exploring mechanism of action, paclitaxel was selected as a comparative control because it shares a similar pharmacological profile with FZ. Both agents target the microtubule system—leading to cell cycle arrest and subsequent apoptosis—thereby providing a more relevant basis for evaluating the anti-tumor efficacy of our combination.

In vivo experiments, cisplatin (Ewebe pharma, Austria) for injection was used for positive control because of animal research center's (Medical Military Academy) availability.

3.2. Cell lines and cell culture

A549 cells were purchased from ATCC. PC-3, DU145, MCF-7, HepG2 were provided by Professor Lee Jeong Hyung, Kangwon National University, Gangwo-do, Korea. A549, MCF-7 cells were cultivated in a complete culture medium Roswell Park Memorial Institute medium (RPMI) (Sigma-Aldrich Solution, Merck, Germany) composed of 10% Fetal bovine serum (FBS) (Gibco, Invitrogen, USA), and 1% penicillin/streptomycin solution - penicillin 10000 units/mL, streptomycin 10000 (g/mL) (PS) (Gibco, Invitrogen, USA). PC-3, DU145 and HepG2 were maintained in complete medium Dulbecco's Modified Eagle Medium (DMEM) (Gibco, Invitrogen, USA), composed of 10% FBS and 1% PS. The cells were incubated in an Eppendorf CellXpert C170 humidified incubator at 37°C with 5% CO₂. The cells were passed every 2 - 3 days depending on their confluence, and after 3 passages, they were considered stable for further experiments.

3.3. Cell seeding

A549 cells were seeded with different density based on the requirement of each experiment. The table belows display the seeding and treating process.

Table 2: Cell seeding conditional

Experiment	Plate	Density
MTT	96-wells plate cells/well	2.5×10^4 cells/well
ROS	96-wells plate	2.5×10^4 cells/well
Cell cycle	6-wells plate	1×10^5 cells/well
Apoptosis	6-wells plate	1×10^5 cells/well
Glucose uptake	96-wells plate	5×10^4 cells/well
Lactate	96-wells plate	5×10^4 cells/well
Hoechst staining	6 cm plate	5×10^5 cells/plate
Western blot	6 cm plate	5×10^5 cells/plate

3.4. Cell viability assay

A549 cells were cultured in the 96 wells plate (2.5×10^4 cells/well) and incubated in the CO₂ 5% incubator 37°C overnight. Cells were treated with various concentrations of FZ alone, DADA alone and FZ-DADA combination for 24, 48 and 72 hours. Cell viability of A549 cells under effect of FZ and DADA was measured by MTT method (98). MTT is reduced by NADH enzyme in the mitochondria of a cell to formazan (Figure 5).

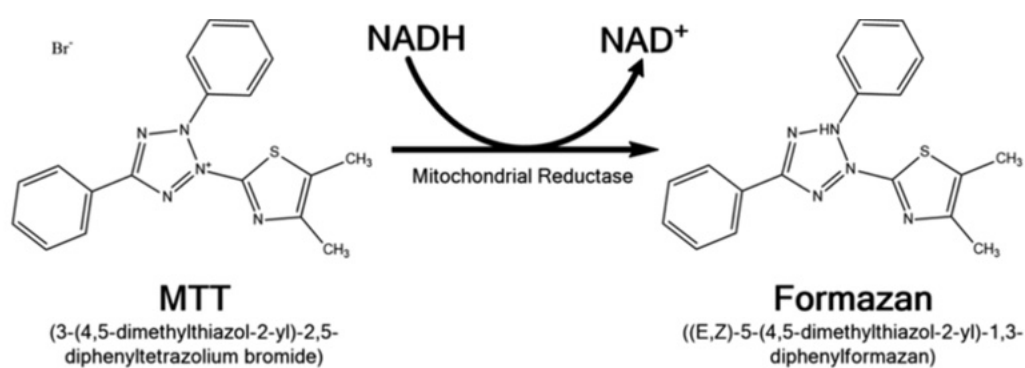


Figure 5: Formation of formazan crystals from MTT (99).

Cells was incubated with MTT working solution (5mg/mL) at least 4 hours at 37°C, 5% CO₂. Supernatant after that was removes, formazan was solvented by isopropanol, the absorbance was measured with a spectrophotometer at 570 nm by using the SpectraMax ID5 microplate

reader. Experiment was triplicated for statistic analysis. The percentage of cell survival (% CS) was calculated by following formula:

$$CS\% = \frac{OD_{sample}}{OD_{control}} \times 100\%$$

3.5. Hoestch staining

Apoptosis, or programmed cell death, plays an important role in normal development, homeostasis, even pathogenic processes. Apoptosis is a form of cell death characterized by chromatin condensation, cell shrinkage, membrane blebbing, and finally loss of membrane integrity (119,120) . To assess the effects of FZ and DADA combination on nuclear material, cells were stained with Hoechst 33342. Hoechst 33342 is a nuclear dye that emits fluorescence at wave length of 461 nm, making it a valuable tool for visualizing DNA in cells. Cells are stained with Hoechst 33342 and observed under a fluorescence microscope, differences in nuclear morphology and fluorescence patterns can help distinguish between healthy, necrotic, and apoptotic cells. Healthy cells display round, uniformly stained nuclei with evenly distributed chromatin, producing a strong and consistent fluorescent signal. Apoptotic cells, on the other hand, usually show a weaker fluorescent signal due to chromatin condensation or nuclear fragmentation. In some cases, the apoptotic cells may lack fragmentation but can still be identified by condensed chromatin. In contrast, the necrotic cells have less condensed DNA and a poorly defined nuclear envelope, resulting in a weaker and more diffuse fluorescent signal (Figure 6).

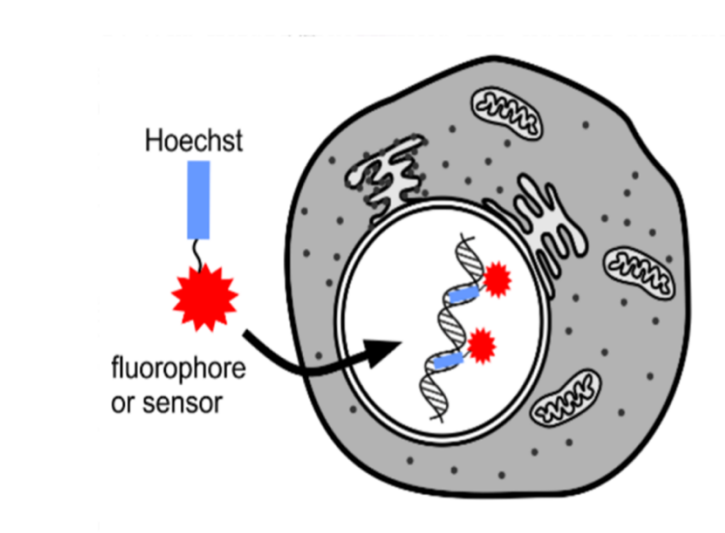


Figure 6: Hoechst staining principle

Cells were seeded in 6 cm plate in 24 hours and treated with FZ and DADA in 48 hours. Hoechst 33342 (Thermo Scientific, Germany) stock solution with concentration of 20 mM were diluted with PBS (Phosphate buffered saline) 1X (Gibco, Invitrogen, USA,) to final concentration of 10 μ M. 1 mL of 10 μ M Hoechst 33342 was added into each plate and incubated in the incubator in 30 minutes. Dye solution was removed from the well and cells were washed with 1 mL of PBS 1X. The morphology of cells under the effect of drug treatment was observed with Nikon Eclipse Ni-U microscope (Nikon, Japan) cooperated with a DS-Ri2/DS-Qi2 camera (Nikon, Japan), x20. Apoptosis cells were counted by manually.

3.6. Apoptosis assay

Apoptosis, or programmed cell death, plays a critical role in maintaining cellular homeostasis and eliminating damaged or abnormal cells (105). In cancer treatment, inducing apoptosis in malignant cells is a key therapeutic strategy. Many chemotherapeutic agents and targeted therapies aim to restore apoptotic pathways that are often dysregulated in cancer, thereby inhibiting tumor growth and promoting cell death. Studying apoptosis provides valuable insights into the efficacy and mechanisms of potential anti-cancer agents. The two main pathways of apoptosis are the extrinsic (death receptor) and the intrinsic (mitochondrial) pathways (Figure 7). The death receptor pathway is initiated when extracellular death ligands bind to cell surface death receptors, triggering the formation of the death-inducing signaling complex (DISC) and subsequent activation of caspase-8. This caspase then directly cleaves and activates executioner caspases like caspase-3 and caspase-7, leading to apoptotic cell death.

In contrast, the intrinsic pathway is activated by intracellular stress signals such as DNA damage, oxidative stress, or growth factor deprivation, which cause mitochondrial outer membrane permeabilization (MOMP) through the action of pro-apoptotic Bcl-2 family proteins. This releases cytochrome C into the cytosol, where it binds Apaf-1 to form the apoptosome and activate caspase-9, which then activates the same downstream executioner caspases as the extrinsic pathway. Importantly, these pathways can intersect through Bid, a pro-apoptotic protein cleaved by caspase-8 to generate tBid, which amplifies the apoptotic signal by activating the intrinsic pathway. Both pathways are tightly regulated by anti-apoptotic proteins like Bcl-2 and Bcl-xL, which inhibit MOMP, and their dysregulation is a hallmark of cancer, making them important targets for therapeutic intervention (106).

Under physiological conditions, healthy cells maintain a distinct distribution of phospholipids across their lipid bilayers. Choline-containing phospholipids, such as phosphatidylcholine and sphingomyelin, are predominantly located on the extracellular side, while aminophospholipids, including phosphatidylserine and phosphatidylethanolamine, are confined to the cytoplasmic side. However, during apoptosis, phosphatidylserine translocates to the extracellular side of the lipid bilayer, serving as an early marker of programmed cell death.

Phosphatidylserine exposure can be detected using Annexin V, a 36-kDa protein tagged with a fluorochrome (108). This probe binds reversibly to phosphatidylserine residues in a calcium dependent manner. In the later stages of apoptosis, the integrity of the cell membrane is compromised, allowing propidium iodide (PI), a nuclear-staining fluorochrome dye, to penetrate the cell and bind to nuclear DNA, thus distinguishing late apoptotic or necrotic cells (Figure 8).

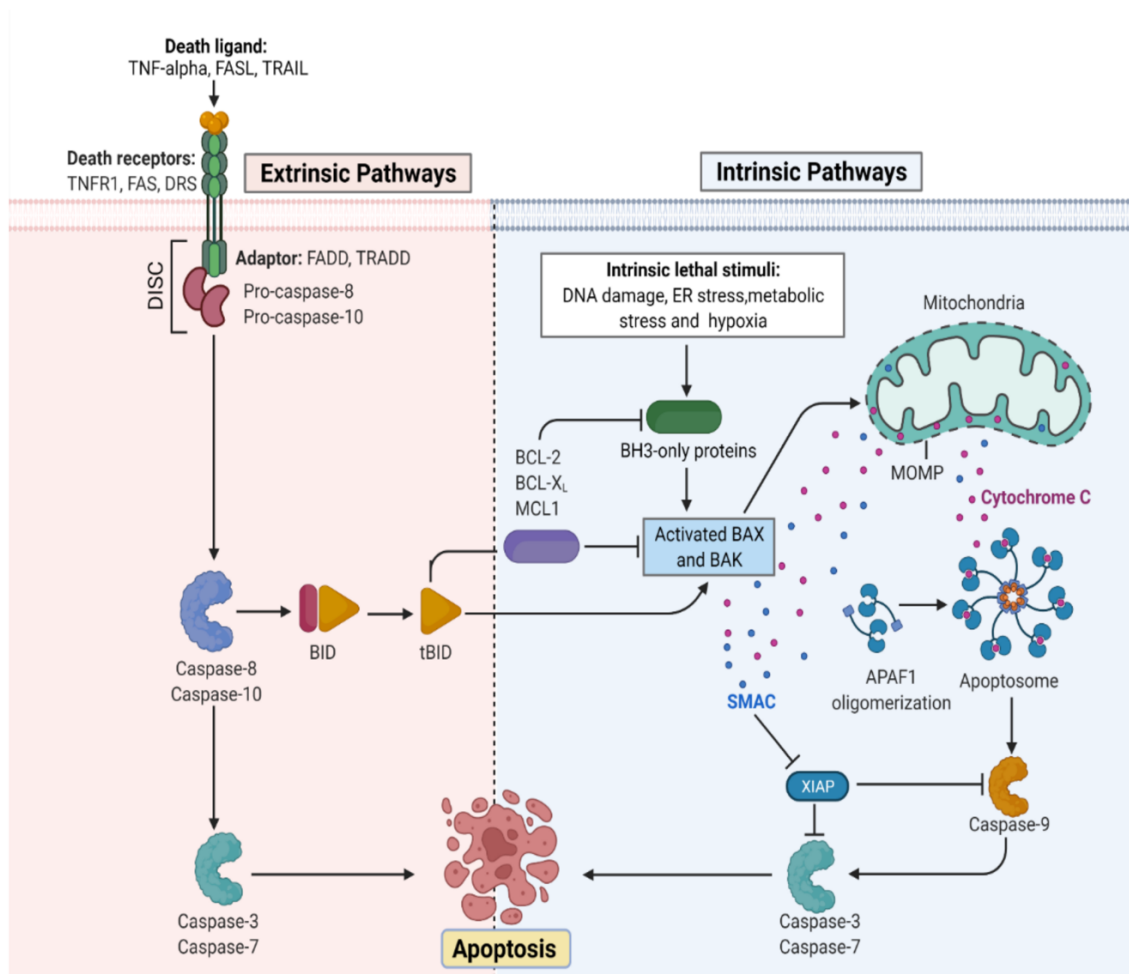


Figure 7: Apoptosis pathways are divided into the extrinsic and the intrinsic pathways

Extrinsic pathway is initiated when extracellular death ligands bind to cell surface death receptors, triggering the formation of tDISC) and subsequent activation of caspase-8. This caspase then directly cleaves and like caspase-3 and caspase-7, leading to apoptotic cell death. DISCL:death-inducing signaling complex, BID, tBID FADD, TRADD. Intrinsic pathway is activated by intracellular stress signals. The permeability of mitochondria was altered and cytochrome C was released through the atc of Bcl family. Cytochrome C activate caspase-9 and then caspase-3, caspase-7 resulting in apoptosis. ER, MOMP, BAX, BAK, APAF1 (107).

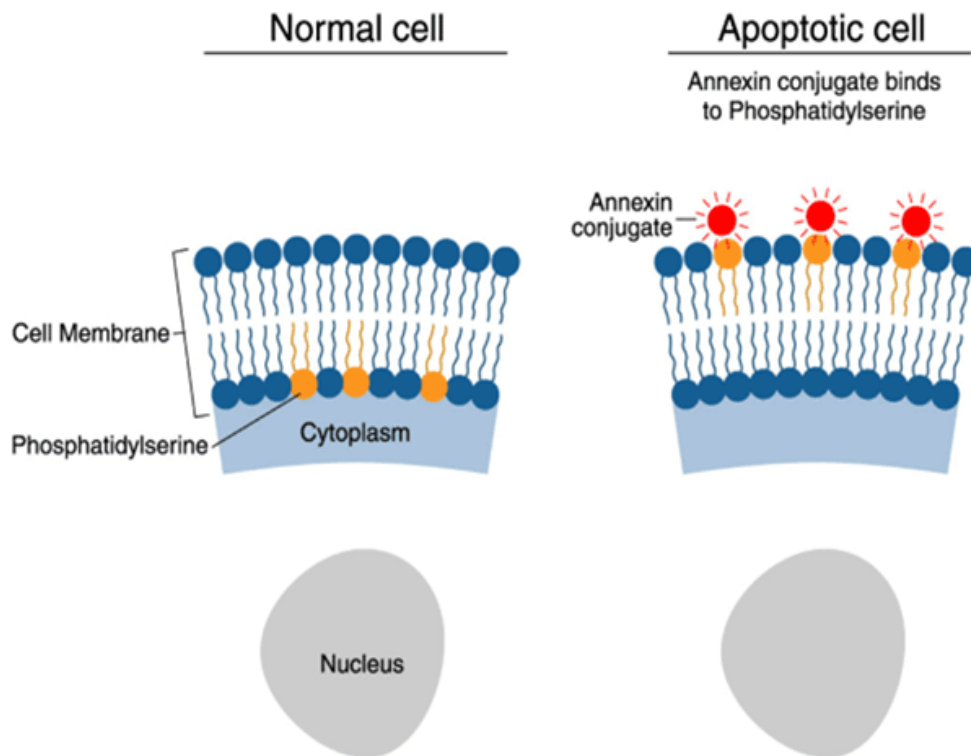


Figure 8: Principle of Annexin V/PI staining (109)

A549 cells were seeded in 6-well plates for 24 hours before being treated with or without FZ, DADA, a FZ-DADA combination in 48 hours in concentration dependent experiment and treat with or without a FZ-DADA combination in 24, 48 and 72 hours for time dependant experiment. The supernatant and death cells were washed with PBS and adhering cells were collected and washed in PBS twice. Apoptotic cells were stained with annexin-V (1 mg/mL) and PI (1 mg/mL) following annexin-V/PI staining kit. Apoptosis analysis was performed using a Novocyte 2000 flow cytometer (ACEA Biosciences Inc, USA) and NovoExpress software.

3.7. Cell cycle arrest

The cell cycle plays an important role in the growth and proliferation of cells (100). Cyclin-dependent kinases (CDKs) are a critical proteins in controlling the cell cycle progression. The activated of CDKs provide a means for the cell to move from one phase of the cell cycle to the next ones. Furthermore, the CDKs are regulated positively by cyclins and regulated negatively by naturally occurring CDK inhibitors (CDKIs) (100). The cell cycle is also a key target in cancer treatment, as dysregulation of cell cycle is a hallmark of cancer. Many cancer therapies aim to inhibit CDKs or modulate cyclins to prevent the unchecked proliferation of cancer cells

(100–103). Targeting the cell cycle machinery allows for a more precise approach in disrupting cancer cell growth while sparing normal cells (Figure 9).

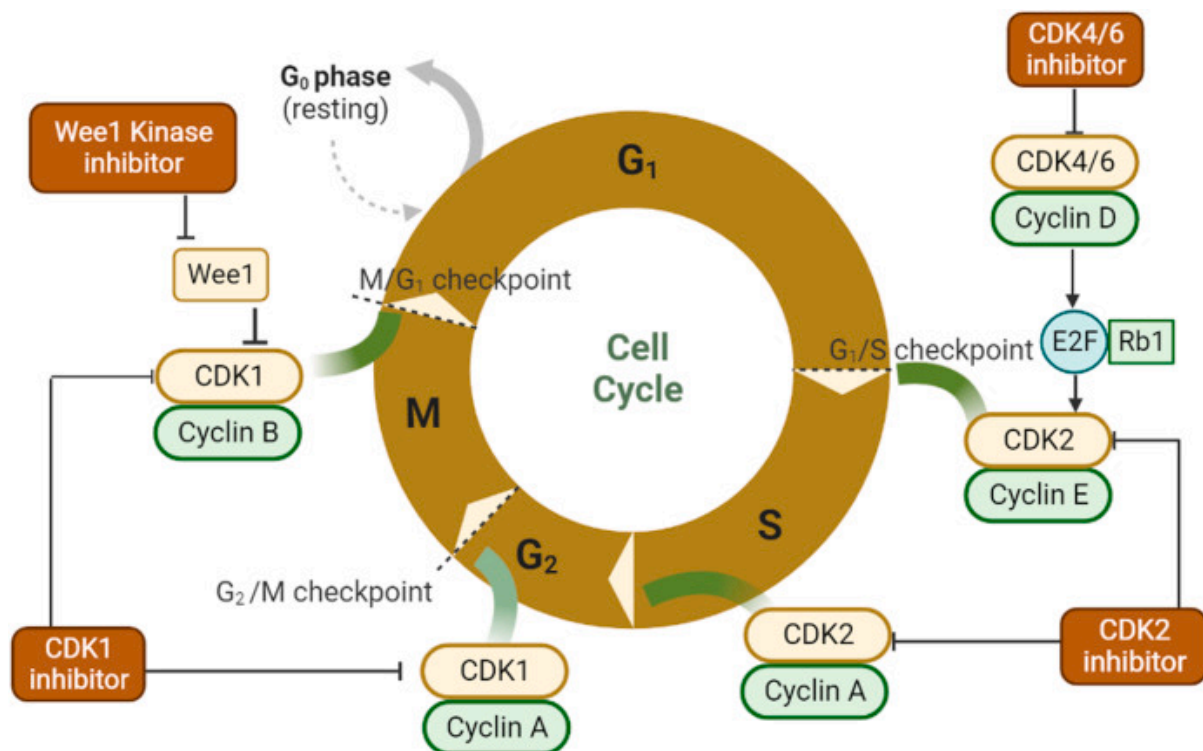


Figure 9: Cell cycle arrest and the regulators.

Various agents can be targeted to induce cell cycle arrest: CDK4/6 inhibitors target G₁/S checkpoint while CDK2 and CDK1 inhibitors target S/G₂ and G₂/M checkpoint respectively. CDK: Cyclin-Dependent Kinase, CDK1: Cyclin-Dependent Kinase 1, CDK2: Cyclin-Dependent Kinase 2, CDK4/6: Cyclin-Dependent Kinase 4-6 (104)

A549 cells were seeded in 6-well plates for 24 hours before being treated with or without FZ, DADA, or a FZ-DADA combination for 48 hours. Adhering cells were collected and washed in PBS twice. After fixing with ice-cold 70% ethanol, at -20°C for 2 hours, cells were washed with PBS and treated in PBS for 30 minutes with 1 mg/mL propidium iodide (PI) (Thermos, USA) and 20 µg/mL RNase (Thermos, USA). Cell cycle analysis was performed using a Novocyte 2000 flow cytometer (ACEA Biosciences Inc, USA) and NovoExpress software.

3.8. ROS assay

A549 cells were cultured in the 96 wells plate (2.5x10⁴ cells/well) with RPMI 10% FBS 1% PS and incubated in the CO₂ 5% incubator 37°C overnight. Cells were treated with various

concentrations of FZ alone, DADA alone and FZ-DADA combination in 48 hours. Supernatant was removed. ROS level in were measured by Reactive Oxygen Species (ROS) Detection Assay Kit (ab287839) in which cells were washed with ROS washing buffer and then incubated with 100 μ L ROS label in 45 minutes (light protected). ROS label was removed, 100 μ L was added into each well. ROS levels were measured at Ex/Em= 495/529 nm in an end point mode using SpectraMax ID5 microplate reader.

3.9. Glucose uptake assay

Glucose uptake assay was conducted using 2-deoxyglucose (2-DG), which is structurally similar to glucose, according to the manufacturer's instruction (glucose uptake kit AbCam, UK). 2-DG is taken by glucose transporters and converted to 2-DG-6-phosphate (2-DG6P) (110). 2-DG6P cannot be processed further and consequently accumulates inside cells. The accumulation of 2-DG6P is proportional to the absorption of 2-DG (or glucose) by cells. In this assay, 2-DG6P is oxidized to produce NADPH, the concentration of which is measured using an enzymatic recycling amplification reaction (Figure 10).

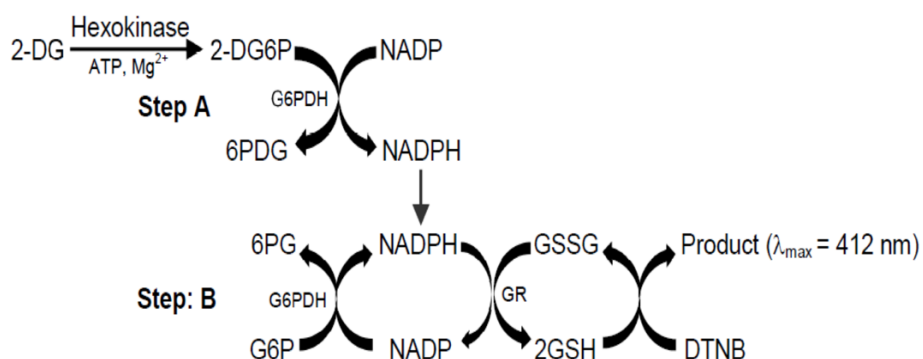


Figure 10: Principle of glucose uptake assay (111)

A549 were seeded in a 96-well plate (5x10⁴ cells/well) for one day and then starved with DMEM high glucose without FBS overnight. Cells were then treated with FZ, DADA, FZ and DADA with various combination in 24 hours. Cells were incubated with Krebs-Ringer Phosphate-Hepes (KRPH) buffer for 40 minutes and insulin 1 μ M for 20 minutes. Then, 10 mM 2-DG was added and incubated for an additional 20 minutes. Cells were lysed with an extraction buffer; frozen in -80°C in 10 minutes and heated at 85°C for 40 minutes. The lysates were neutralized by adding a neutralization buffer and centrifuged to collect the supernatant samples containing NADPH. The products were amplified following the glucose uptake kit

15 minutes. The supernatant containing proteins was collected and stored at -80°C for further experiments. Before carrying out western blot analysis, the amount of total protein was measured using the Bradford method based on protocol provided by the manufacturer (iNtRON Biotechnology, USA).

3.12. Western blot

Protein was loaded onto sodium dodecyl sulphate polyacrylamide gel (SDS-PAGE) with a similar amount (30 µg/well). After running electrophoresis (90 V-30 minutes and 120 V - 80 minutes), the separating protein in the gel was transferred onto a polyvinylidene fluoride (PVDF) blotting membrane (GE Healthcare, Amersham, UK). Afterwards, the PVDF membrane was blocked in 5% BSA in TBS-T 1X (50 mmol/L Tris-HCL pH 7.6, 150 mmol/L NaCl containing 0.1% Tween-20) in one hour. Membranes were incubated with different targeted primary antibodies (anti-β-tubulin, anti-p-PI3K, anti-PI3K, anti-p-Akt, and anti-Akt, anti-BAX, anti-Bcl2 (Cell signalling, USA), anti-Cyclin A, anti-Cyclin E (Abcam, UK) at 4°C overnight. Membranes were washed in TBS-T 1X (3 times, 15 minutes each) and subsequently labelled with secondary antibodies (anti-rabbit or anti-mouse) for 1.5 hours at room temperature. After washing with TBS-T 1X (3 times, 15 minutes each) protein blots were visualised using Cytiva Amersham™ ECL™ Prime Western Blotting Detection Reagent (UK) in accordance with the manufacturer's instructions. The signals of proteins expression were detected and captured by ImageQuant™ LAS 500 (Cytiva, USA). Finally, the band intensities were densitometrically quantified by the ImageJ software.

3.13. Animal experiments

3.13.1 Animal preparation

In order to evaluate the anti-cancer activity of FZ and DADA, the immunodeficient BALB/c nude mice (Foxn1nu), 6-8 week, weight from 18 to 22 grams from BioLASCO (Taiwan) were utilized for the *in vivo* assessment. Mice were housed in a sterile environment following the standard operating procedures for nude mouse care provided by the Dinh Tien Hoang Institute of Medicine. All animals were acclimated to the facility's conditions for one week before the initiation of the experiment, with ad libitum access to food and water. Room temperature and humidity were carefully controlled, and a 12-hour light/dark cycle was maintained. Human

lung cancer cells (A549) were grown on cell culture flasks in RPMI 1640 culture media supplemented with 10% FBS, 1% penicillin and streptomycin at 37°C and CO₂. Cells were checked 2 to 3 times per week. Cell were washed twice with 1X PBS before being detached from the culture flask using 1X Trypsin-EDTA solution. Subsequently, the viable cell density was determined using an Invitrogen Countess® II FL cell counter and analyzer. The cell solution was then diluted in fresh culture media to achieve a final concentration of 2 x 10⁷ cells/mL. The prepared cell solution was aspirated into a 1 mL syringe and injected into the right flank's subcutaneous site of immobilized, immunodeficient mice (2 x10⁶ cells /0.1 mL/ mouse) into the right flank's subcutaneous site. The manipulation is done in a sterile environment.

When the tumor reached 50 mm³ after 3 weeks of injection, the mice were randomized into eight groups:

Group 1: Healthy control - 6 mice

Group 2: Tumor control - 9 mice

Group 3: Positive control - Cisplatin – 8 mice

Group 4: FZ 40 mg/kg - 9 mice

Group 5: DADA 20 mg/kg - 10 mice

Group 6: DADA 100 mg/kg – 10 mice

Group 7: FZ 40 mg/kg + DADA 20 mg/kg - 10 mice

Group 8: FZ 40 mg/kg + DADA 100 mg/kg - 10 mice

Animals in the treatment groups (group 4, 5, 6, 7, 8) received a daily oral treatment, while mice in positive control group received 5 mg/kg cisplatin daily by injection subcutaneously near the tumor. The tumor control group received daily oral administration of purified water instead of any treatment.

Following tumor transplantation, these indices were monitored: Overall health, weight, appearance, tumor growth, and time to death in groups of mice.

Tumor length and width was measured weekly by NSK 150mm vernier caliper (NSK, Japan).

The tumor volume was calculated using following formulation:

$$V = \frac{(D \times R^2)}{2}$$

While:

V: tumor volume (mm³).

D: tumor length as measured (mm).

R: tumor width as measured (mm).

3.13.2 Toxicology study

After 60 days of treatment, mice were anesthetized with isoflurane and euthanized by cervical dislocation. Serum, lung, and tumor samples were collected for assays. Post tumor inoculation, the following parameters were monitored to assess overall health and treatment effects, including body weight, appearance, tumor growth, and survival time. The health condition of the mice was assessed based on the following criteria:

Weight: recorded twice weekly using an electronic scale TE3102S Sartorius (Germany) to track mice's weight changes before and after treatment.

Movement: Observations were made on movement patterns (normal, hyperactive, hypoactive, or immobile).

Response to stimuli: Response to tactile and environmental stimuli was categorized as normal, heightened, reduced, or absent.

Skin color: Evaluated for changes, including standard color, purple, and bleeding.

Mice feces: Monitored for consistency and appearance (normal, loose, bloody stool)

Aspartate aminotransferase (AST) and Alanine aminotransferase (ALT) are liver enzymes measured in blood, which represent the liver function (117). To evaluate the impacts of FZ and DADA treatment on function and structure of mouse liver by measuring AST, ALT level in blood by AU480 chemistry analyzer (Beckman Coulter, Japan) and histopathology images.

Serum urea and creatinine levels are well-established parameters for assessing renal status (118). By evaluating serum urea and creatinine levels by AU480 chemistry analyzer (Beckman Coulter, Japan). Alongside histopathological images, the renal function and structure of animals undergoing treatment with FZ and DADA were assessed.

The complete blood count, including the numbers of red blood cells and white blood cells, was measured at the end of the study using MEK 7300 analyzing machine (Nihon Kohden, Japan), prior to the euthanasia of the mice

3.13.3 Histopathological imaging

After 60 days, the mice were euthanized, and blood samples and tissue specimens were collected for further analysis.

Tissue samples were collected and immediately fixed in a formaldehyde:alcohol:acetic acid solution (10%:50%:5%) under vacuum for 3 hours, with fresh fixative supplied every hour.

After fixation, the tissues were processed through a graded ethanol series (30%, 50%, 70%, 90%, and 100%), with each solution replaced hourly. The samples were then incubated in an ethanol–butanol mixture with gradually increasing concentrations of butanol until reaching 100%, followed by overnight incubation in 100% butanol to facilitate paraffin infiltration.

Subsequently, the tissues were transferred through a series of solutions in which butanol was progressively replaced by xylene to ensure its complete removal. Paraffin infiltration was performed at 60 °C, during which the xylene was continuously exchanged with molten paraffin. After 48–72 hours of solidification, the samples were embedded in paraffin using a Myr EC350 modular tissue embedding center (Thermo Scientific, USA). Paraffin blocks were sectioned into 10- μ m thick slices using an HM 340E rotary microtome (Thermo Scientific, USA). The sections were mounted on glass slides and dried at 50 °C for 2 hours. Before staining, the slides were deparaffinized in 100% xylene (Merck, USA) and rehydrated through a graded ethanol series (100%, 95%, 80%, 70%) followed by rinsing in distilled water. Hematoxylin and eosin (H&E) staining was then performed. After staining, the slides were dehydrated through increasing concentrations of ethanol (70% \rightarrow 80% \rightarrow 95% \rightarrow 100%) and cleared twice in 100% xylene. Finally, coverslips were applied using a xylene-based mounting medium, and the slides were allowed to dry completely before imaging.

3.13.4 Ethical considerations

All experimental procedures involving animals followed ethical guidelines for laboratory animal use, and the protocol was approved by the Dinh Tien Hoang Institute of Medicine’s review board (approval number IRB-A-2200 on March 25th, 2022).

3.14. Statistical analysis

Data were analyzed using SPSS software version 22.0 (IBM Corp) and GraphPad Prism 10 (GraphPad Software, USA). The Chi-square test (χ^2 test) was used to compare two observed proportions. In comparison, a one-way analysis of variance (ANOVA) is used to compare the means among three or more groups, with a Dunnett test used to determine which differences are significant. A two-way ANOVA compares the means among three or more groups at different time points. Comparison of medians between two independent groups was performed using the Mann-Whitney U test, with the significance determined based on the p value ($p >$

0.05: no statistically significant difference and $p < 0.05$: statistically significant difference). The Log-rank test was applied to compare the cumulative survival time between different treatment methods.

CHAPTER IV: SYNERGIC EFFECT OF FZ AND DADA IN A549 NON-SMALL CELL LUNG CANCER CELLS

4.1. Cytotoxic effect of FZ and DADA in A549 lung cancer cells

FZ and DADA not only affect viability of A549 lung cancer cells (Figure 11.A) but also reduce the cell survival in other cancer cell lines. Viability of MCF-7 breast cancer cell (Figure S1), PC3 prostate cancer cells (Figure S2), DU145 (Figure S3) and Hep G2 liver cancer cells (Figure S4), after treatment of FZ and DADA was measured by MTT assay. Camptothecin was used as a positive control to validate the reliability of the results. The cytotoxic activities of FZ and DADA were different among these cancer cells with the highest effect observed in A549 lung cancer cells. Therefore this research focused on the mechanism of action of FZ and DADA in A549 lung cancer cell model.

A549 cells were treated with a serial concentration of FZ and DADA in 48 hours. Camptothecin was used as a positive control for all experiment. IC_{50} values of FZ and DADA were determined approximately 1 μ M and 5 mM, respectively (Figure 11.A). The cell death rate was dose-dependent with approximately 30% of cells dead after treatment with the FZ alone, or FZ and DADA combination. My results demonstrated that the FZ-DADA combination ratio [1:5000] significantly reduced cell viability compared to FZ or DADA alone (Figure 11.B). Hence, this combination ratio was chosen for further cytotoxic experiments. The synergistic effects of FZ and DADA were investigated through evaluating the capacity to inhibit the growth of A549 cells. A computational model was applied to investigate the synergistic effect of FZ-DADA combination at ratio [1:5000]. The combination index (CI) value was calculated (Figure 11.C). The results revealed that at the ratio [1:5000], FZ together with DADA had synergistic effects after 48 hours, with the efficacy increasing in a dose-dependent manner. This was proved by the CI value below one across all tested doses, with the maximal fraction affected index (Fa) reaching approximately 0.8.

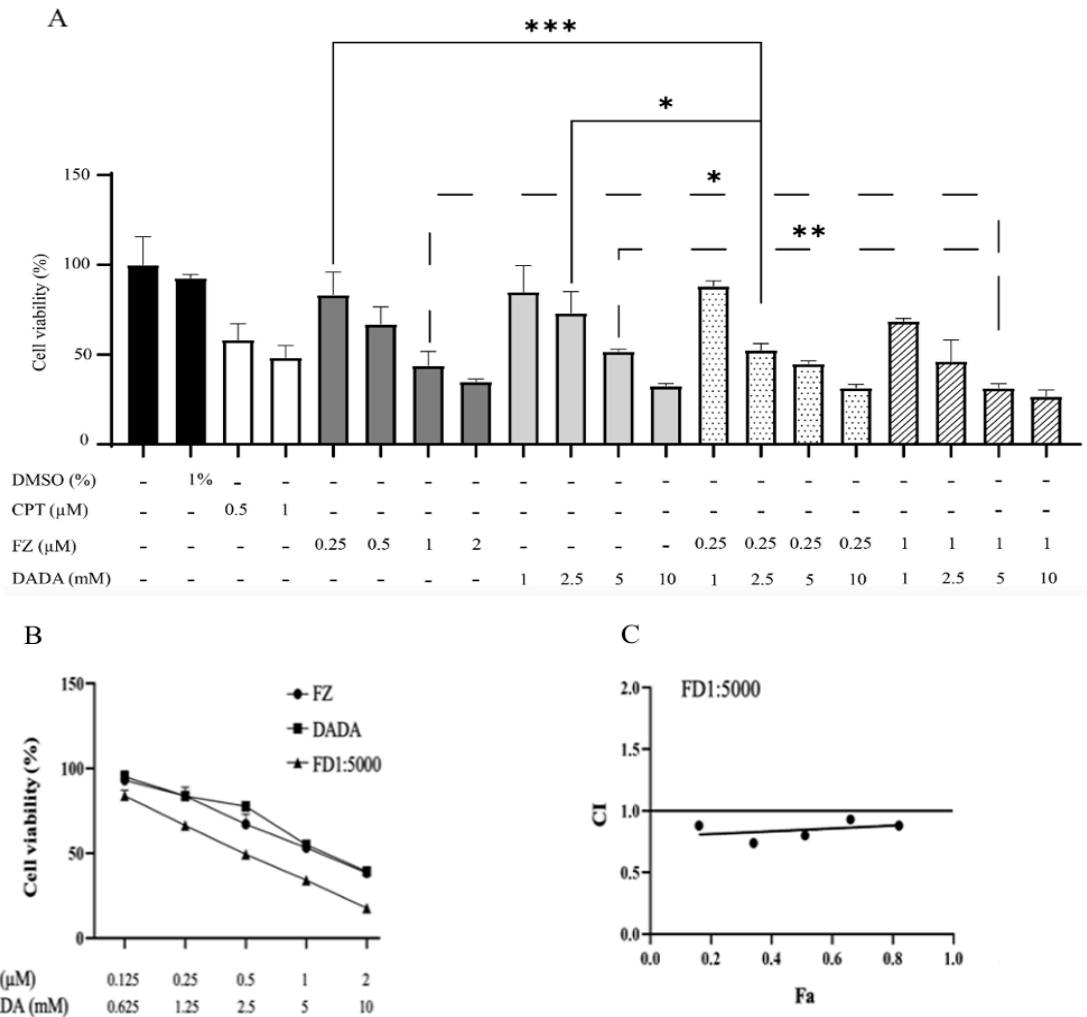


Figure 11: Cell viability and combination index of FZ and DADA.

A,B – Cells were treated with FZ, DADA and its combination at various dosages for 48 h, cell viability was determined by formazan crystal formation of MTT assay. The colorimetric was identified using microplate reader at 570 nm. The results were analyzed by ANOVA, with a Dunnett test used to determine which differences are significant. * Correspond to $p < 0.05$, ** $p < 0.01$, *** $p < 0.001$. All treatments were performed in triplicate.

C - The combination index (CI) and fraction affected (Fa) were calculated using compusyn software. The $CI < 1$ is synergism and the $CI > 1$ is antagonism.

4.2. Hoechst staining

The Hoechst staining assay performed on the DMSO control, the positive control paclitaxel (1 μM), and the individual as well as combined treatments of FZ and DADA at a [1:5000] ratio demonstrated that the combination induced apoptosis. The percentage of apoptotic cells in the combination group reached 20%, which was significantly higher than that of FZ and DADA alone, at 14% and 3%, respectively (Figure 12).

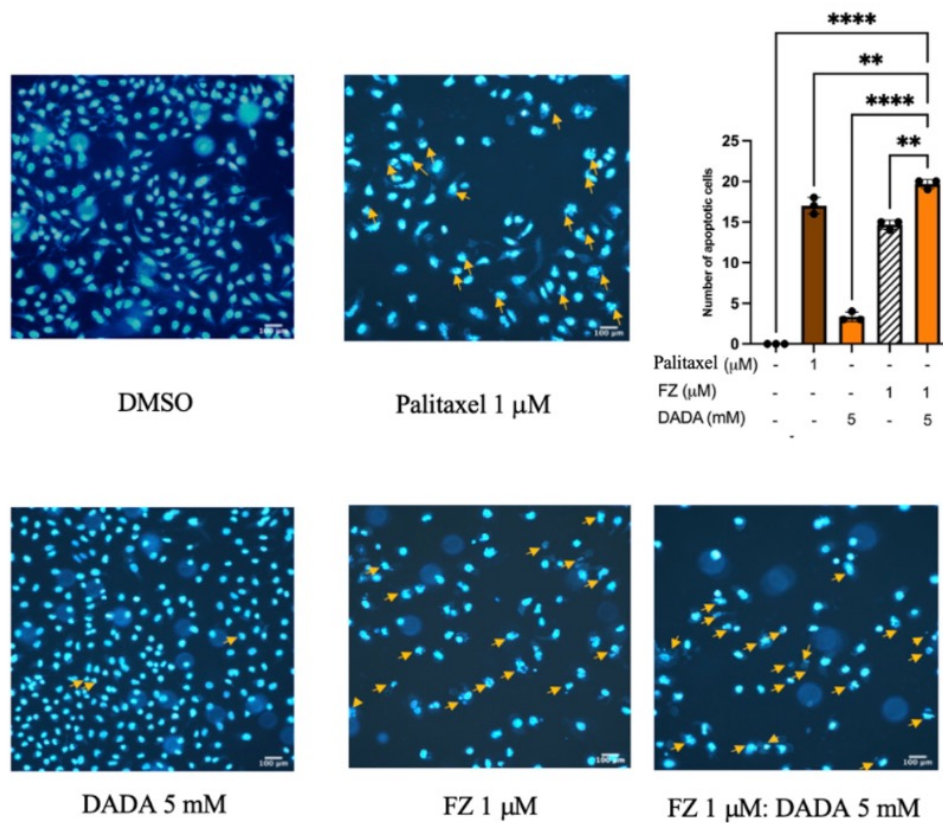


Figure 12: Hoechst staining

Cells were treated with DADA, FZ alone as well as the combination of DADA and FZ at ration 1:5000 in 48 h, nuclear of cells were stained by Hoechst dyes and observed under fluorescence microscopy at objective 20x . Number apoptotic cells was recorded in differencnt point of each sample. The yellow arrows indicated the apoptotic cells. The results were analyzed by ANOVA, with a Dunnett test used to determine which differences are significant. ** $p < 0.01$, **** $p < 0.0001$.

4.3. FZ and DADA combination triggers apoptosis

To measure the effect of FZ and DADA in the cell death programming, fluorescence activated cell sorting (FACS) analysis employing Annexin-V-FITC and propidium iodide staining was used. The flow cytometry results after 48h treatments revealed that FZ and DADA alone substantially triggered apoptosis at their IC₅₀, with apoptotic rates of 38.83% (14.62% early apoptosis and 24.01% late apoptosis) and 38.48% (16% early apoptosis and 22.48% late apoptosis), respectively. However, in FZ-DADA combination at ratio 1:5000 the rate of apoptosis increased considerably at 71.54% (13.1% early apoptosis and 58.44% late apoptosis) (Figure 13). This combination significantly increased the proportion of late apoptotic cells compared with FZ and DADA alone.

To elucidate the mechanism of action of FZ and DADA in programmed cell death in A549 cells, we checked the impacts of this combination on the expression of the proteins regulating apoptosis. FZ-DADA increased the expression of BAX 17 times fold while it reduced 4 times the expression of Bcl-2. In apoptotic cell death, Bcl-2 family proteins play an important role. The high expression of Bcl-2 in many cancers mediates the resistance of cancers to a wide range of chemotherapeutic drugs and γ -irradiation, which acts by inducing apoptosis in tumor cells. Blocking Bcl-2 activity thus can restore the apoptotic process in tumor cells (121). Conversely, BAX, a pro-apoptotic protein of Bcl-2 family, promotes cell death. The upregulation of BAX results in the elimination of cancer cells via the apoptotic pathway (122). During apoptosis, the morphological changes are primarily dependent on the caspase family (123). In human, caspase family contains 12 fate-determining cysteine proteases which drive cell death (both of apoptosis and pyroptosis) (124). Caspases are divided into three main groups based on their function and mechanism of action. Group I include caspase-1, caspase-4 and caspase-5 (or caspase-11 in mouse) comprises the inflammatory caspases. Group II is formed by the apoptotic effector caspases-3, caspase-6, and caspase-7, which are described as the “executors of apoptosis”.

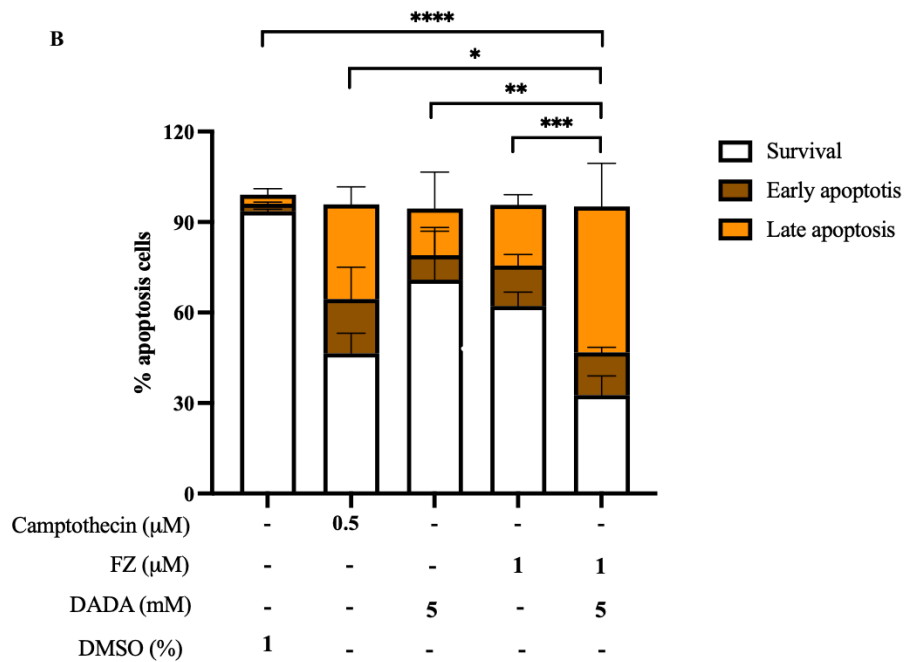
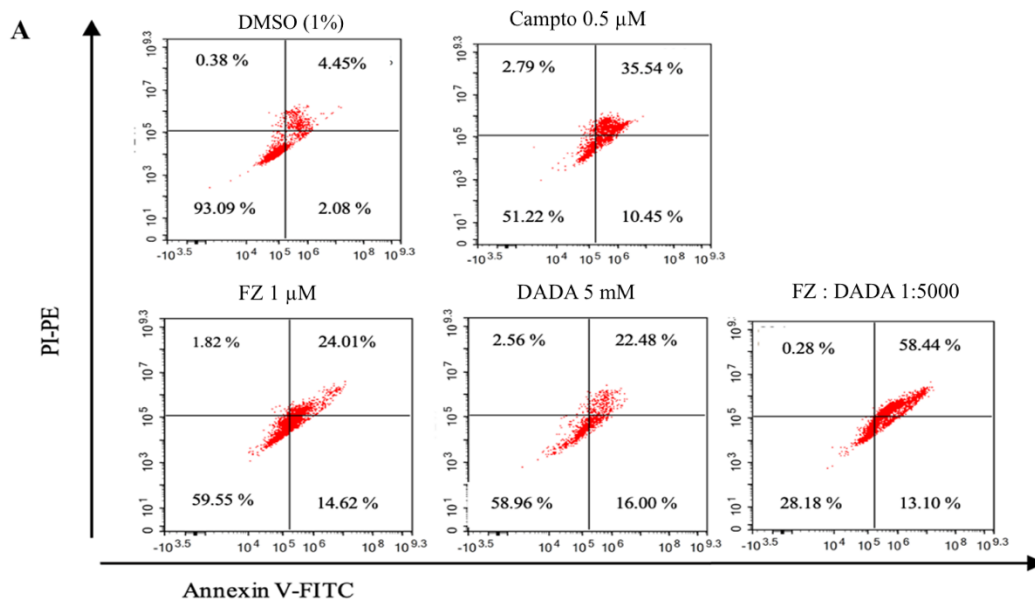


Figure 13: FZ-DADA induced apoptosis in A549 cells.

(A,B) Cells were treated with FZ, DADA, and their combinations for 48 hours before being incubated with Annexin V and propidium iodine to detect the apoptotic stage. B. The bar graph represented the cells at the combination of FZ-DADA at the ratio 1:5000 compared with their separate treatment. The results were analysed by one-way ANOVA, with a Dunnett test used to determine which differences are significant. * $p < 0.05$, ** $p < 0.01$, *** $p < 0.001$, **** $p < 0.0001$.

The last group, caspase-8, caspase-9, and caspase-10, comprises initiator caspases that contain a long pro-domain preferentially cleave substrates with a leucine or valine at the P4 position (124). Caspase-3 is an apoptosis-inducing protease enzyme, which plays a pivotal role in cell death by cleaving key proteins involved in the cell repair process. In the apoptotic cells, caspase 3 is cleaved at an aspartate residue, producing p12 and p17 subunits that together form the active cleaved caspase 3. This enzyme is crucial for the morphological and biochemical characteristic alteration during apoptosis (125–128). In my research, at protein level, both FZ 1 μ M, DADA 5 mM treatment induced an increase in cleaved caspase 3 level at approximately 3,3 times fold. The combination of FZ and DADA at ratio 1:5000 exhibited a 4-times higher of cleaved caspase-3 level compared to the control. Similar to caspase 3 activity, caspase-7 are universally activated during apoptosis. Interestingly, the combination of FZ and DADA at the 1:5000 ratio increased the expression of cleaved caspase 7, which is 3 times and 12 times higher than the levels induced by FZ and DADA alone, respectively. Caspase family, especially caspase-3 and caspase-7 cleave the 116 kDa form of PARP into 85 kDa and 24 kDa fragments (129). PARP was suggested to contribute to cell death by depleting the cellular NAD and ATP (130). PARP-1 cleavage is a switch point that directs death receptor signaling toward either apoptosis or necrosis (130). My results indicated that the combination treatment significantly increased cleaved PARP expression—by approximately 8-fold—compared to control. In contrast, FZ at 1 μ M induced about a 3-fold increase, while DADA at 5 mM did not alter cleaved PARP levels. These findings strongly support the synergistic effect of the FZ (1 μ M) and DADA (5 mM) combination. My results (Figure 14) provided valuable evidence to demonstrate the activity of FZ DADA as well as their synergistic effect in the apoptosis of A549 lung cancer cells.

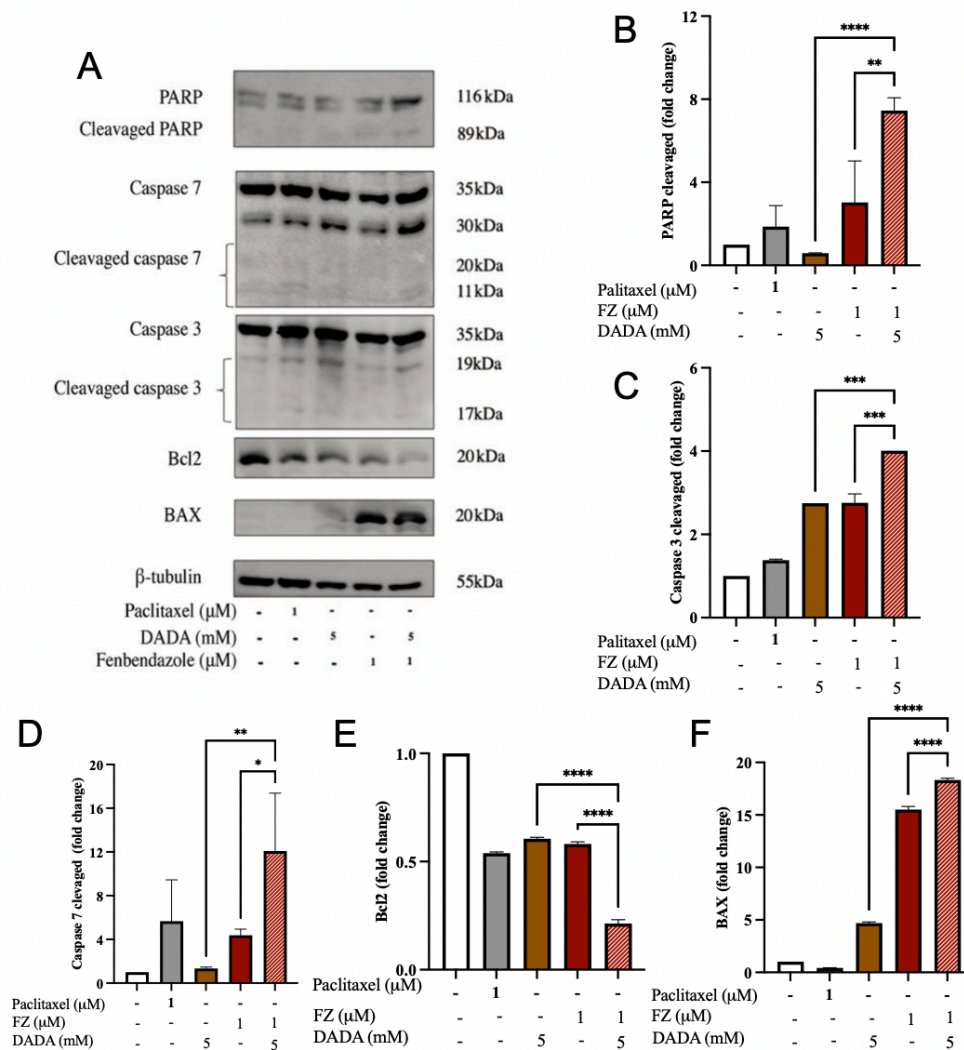


Figure 14: FZ-DADA induced apoptosis in via intrinsic pathway.

A - Photos of bands of protein in Western Blot experiment; B - PARP-cleaved expression; C - Caspase-3 cleaved expression; D - Expression of Caspase-7 cleaved; E - Expression of Bcl-2; F - Expression of BAX. A549 cells were seeded in 6-cm plates in 24h. Cells were treated with DADA, FZ alone as well as the combination of DADA and FZ at the ratio 1:5000 in 48h and then harvested to extract protein for Western Blot with indicated antibodies. The expression of PARP, Cleaved PARP, Bcl-2, BAX, caspase 3, cleaved caspase 3, caspase 7 and cleaved caspase 7 were normalized with the housekeeping α -tubulin, data are mean \pm SD (n = 3). The results were analysed by one-way ANOVA, with a Dunnett test used to determine which differences are significant * $p < 0.05$, ** $p < 0.01$, *** $p < 0.001$, **** $p < 0.0001$

4.4. FZ and DADA combination induces cell cycle arrest

Cell cycle is a mammalian cell replication process that is closely related to apoptosis. Cell cycle arrest modulates apoptosis induction via the activation of numerous signaling molecules and regulatory proteins. FZ treatment alone at IC_{50} for 48 hours substantially enhanced G2/M and sub G1 population compared to control (Figure 15). The combination treatment at a ratio of 1:5000 further enhanced the accumulation of cells in G2/M and sub-G1 phases while G1 population significantly decreased. This shift was statistically significant. Furthermore, a marked redistribution of cells from the G1 and S phases to the G2/M phase was observed at ratio 1:5000. These findings, together with earlier apoptosis data, suggest that the FZ-DADA combination synergistically induces apoptosis through G2/M phase cell cycle arrest. Cyclins interact with their catalytic partners, cyclin-dependent kinases (CDKs), to regulate cell cycle progression by managing the transitions between different phases of the cell cycle (131,132).

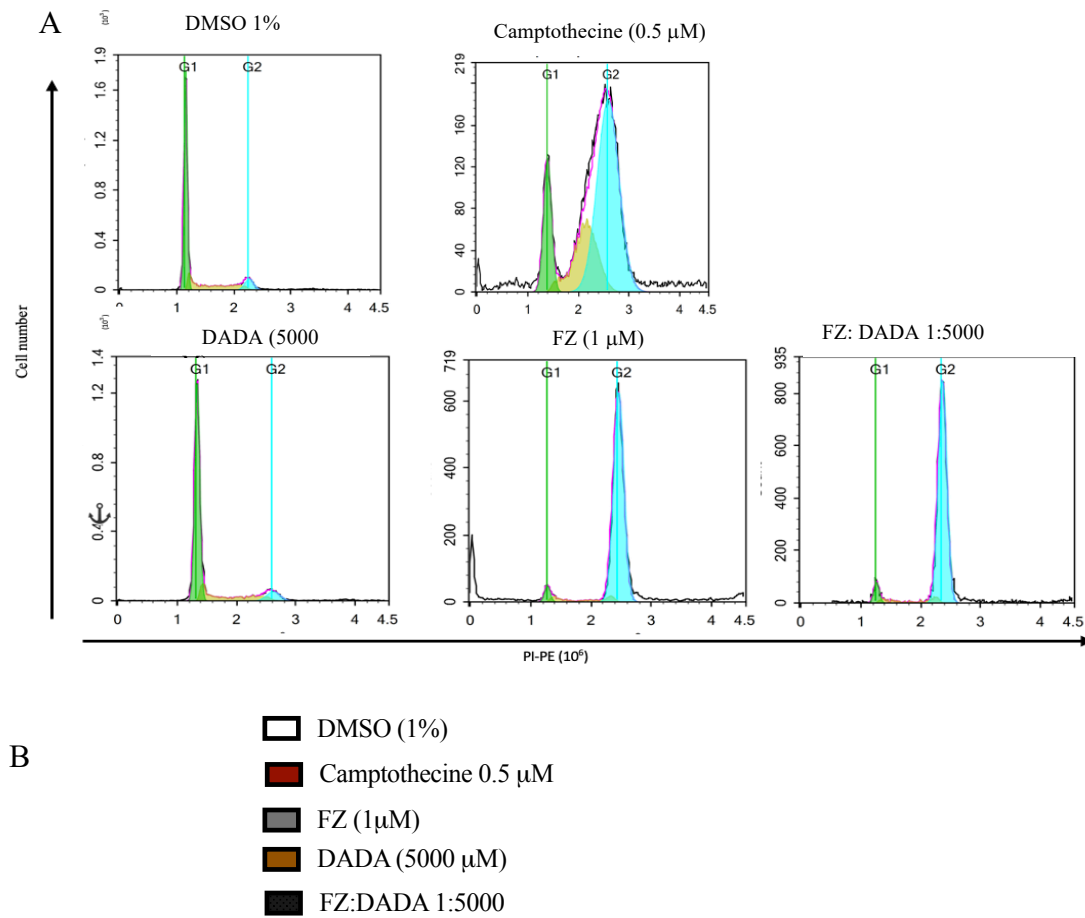


Figure 15: The FZ-DADA combination induced cell cycle arrest in A549 cells.

A - Measurement of various cell cycle stages in untreated and treated A549 cells. B - The bar graph represented the cell cycle results at the combination of FZ and DADA at the ratio 1:5000 compared with their separate treatment. The results were analysed by one-way ANOVA, with a Dunnett test used to determine which differences are significant. *** $p < 0.001$. Error bars represent the standard deviation of three experiments.

4.5. FZ-DADA regulate cell cycle in A549 cells

In order to elucidate the regulation cell cycle of FZ and DADA, we evaluated the expression of several cell cycle checkpoints under the influence of FZ and DADA. At the protein level, FZ-DADA combination decreased the expression of Cyclin A and Cyclin E by approximately 3.5 and 6.6 times fold, respectively (Figure 16). Given that cyclins interact with (CDKs) to regulate cell cycle progression (131,132), the observed reduction in Cyclin A and Cyclin E expression suggests that the FZ-DADA combination effectively disrupts cell cycle progression, particularly at the G2/M checkpoint. In contrast, separate treatments of DADA and FZ resulted in cell cycle arrest at the G2 phase and the G1/S transition, respectively. Cyclin E, in complex with CDK2, is essential for the G1-to-S phase transition, while Cyclin A plays a critical role in both S phase progression and the G2/M transition (133,134). A significant downregulation of these proteins suggests cell cycle arrest, which could lead to reduced proliferation or increased apoptosis. These findings, together with the cell cycle distribution patterns observed via flow cytometry, strongly support the synergistic activity of FZ and DADA in disrupting cell cycle control in A549 lung cancer cells.

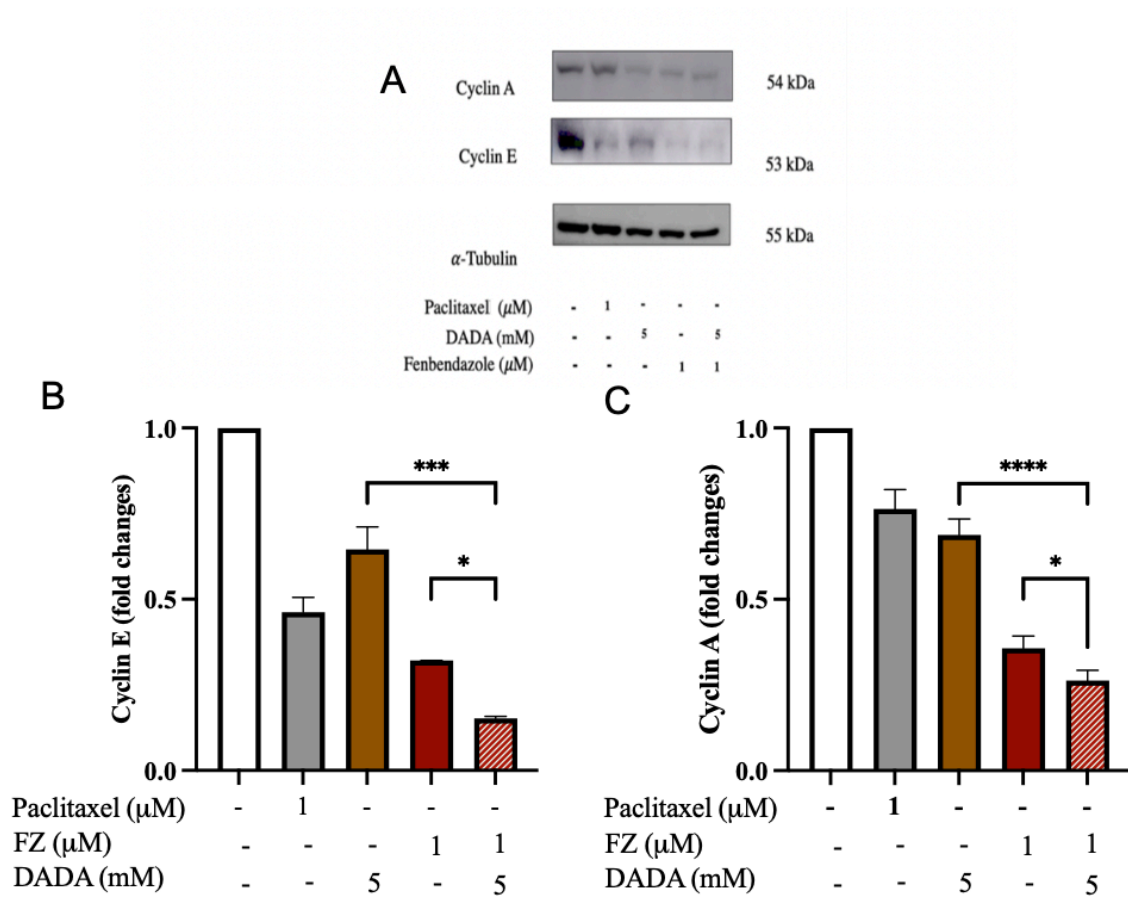


Figure 16: FZ and DADA inhibited the expression of cell cycle checkpoints. A – photo of band of cyclin A and cyclin E in Western Blot

B - Expression of Cyclin E C – Expression of Cyclin A
 A549 cells treated with FZ, DADA alone and a combination at the ratio 1:5000 in 48 hours. Cells were harvested and extracted protein for Western Blot with indicated antibodies. The expression of cyclin A and cyclin E were normalized with α -tubulin, the house-keeping protein. Data was presented in mean \pm SD (n = 3). The results were analysed by one-way ANOVA, with a Dunnett test used to determine which differences are significant., * $p < 0.05$, *** $p < 0.001$, **** $p < 0.0001$.

4.6. FZ-DADA induced ROS in A549 cells

Reactive oxygen species (ROS) are chemically reactive chemicals containing oxygen (135). ROS are formed as a natural by-product of normal oxygen metabolism and have crucial roles in cell signaling and homeostasis (136). A high level of ROS may lead to an increase of cell

damage through oxidative stress of genetic materials, carbohydrates, lipids and proteins that results in cell death (137). In order to evaluate the effect of FZ and DADA in the ROS production, A549 cells were treated with FZ, DADA and various ratios of this combination. The levels of ROS in cells were measured after 48 hours. The results indicated that FZ-DADA was able to induce ROS generation in A549 cells in both of monotherapy and combination treatment (Figure 17).

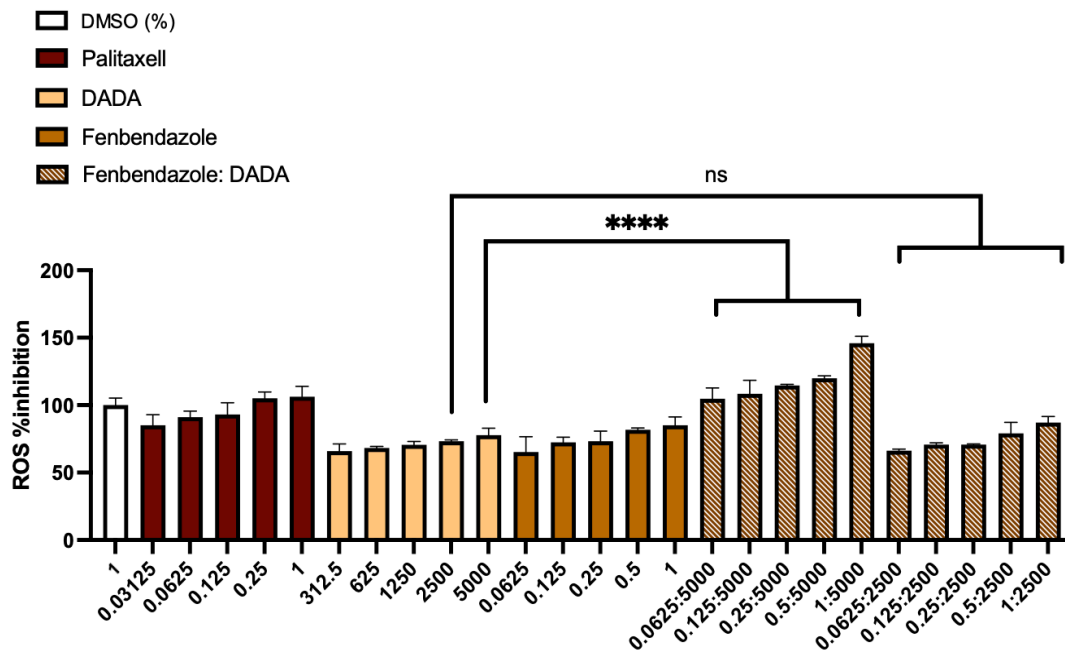


Figure 17: FZ-DADA induced ROS level in cells.

A549 cells were treated with different concentrations of FZ, DADA and the combination of FZ-DADA in 48h in 96-wells plate. ROS level was evaluated by Reactive Oxygen Species (ROS) Detection Assay Kit. Data were presented in mean \pm SD ($n = 3$). The results were analysed by one-way ANOVA, with a Dunnett test used to determine which differences are significant., **** $p < 0.0001$, ns: non significant. All data were obtained from three independent experiments performed in triplicate.

Different concentrations of FZ and DADA were tested individually and in combination. The ratio that consistently exhibited a synergistic effect on ROS levels was [1:5000]. These findings further confirm that the ratio of [1:5000] represents the most appropriate in vitro combination of the two compounds, as evidenced by multiple independent experiments.

4.7. FZ-DADA combination inhibits glucose uptake and lactate production

Dorga et al indicated the anticancer effect of FZ was linked to the inhibition of glucose uptake, resulting in changes in glucose metabolism (14). DADA, on the other hand, was discovered to be a PDK-4 inhibitor, which reduces lactate generation (20,22). Based on previous results, my research focuses on the synergistic effect of the FZ-DADA combination of [1:5000] in the glucose metabolism study. Cancer cells often exhibit increased glucose uptake and metabolism, a phenomenon known as the Warburg effect, where they preferentially convert glucose into lactate even in the presence of oxygen. Targeting glucose metabolism in cancer treatment, thus, is a promising strategy, as inhibiting glucose uptake or glycolysis can disrupt the energy supply needed for tumor growth and survival.

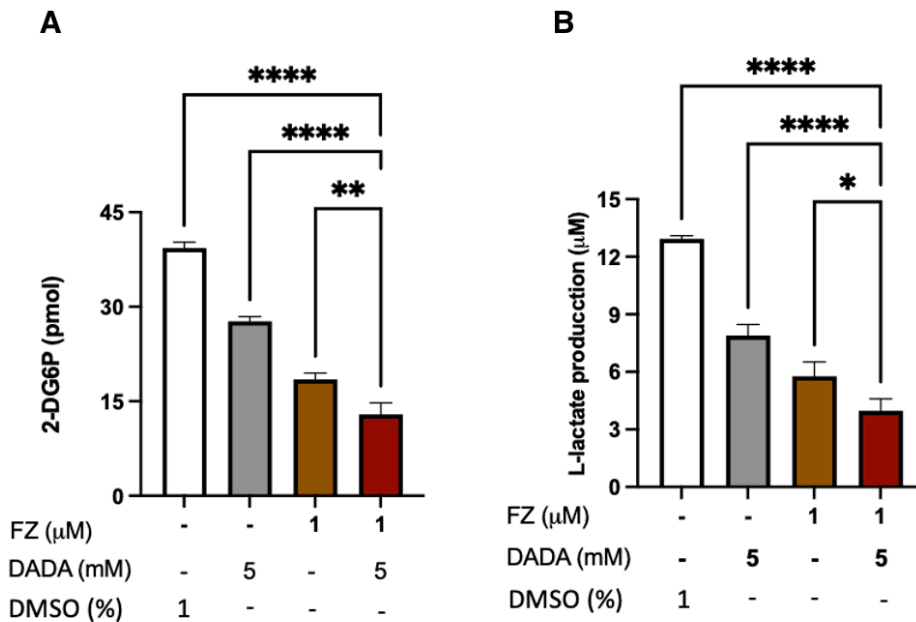


Figure 18: FZ and DADA inhibited glucose uptake and lactate production in A549 cells.

A549 cells were treated with FZ 1 µM, DADA 5 mM alone and their combination in 24h. (A) The uptake of 2-deoxyglucose (2-DG) was examined following glucose uptake assay. (B) The level of L-lactate in culture medium was measured by L-lactate assay kit. Each bar shows the mean ± SD, results were analysed by one-way ANOVA, with a Dunnett test used to determine which differences are significant. * $p < 0.05$, ** $p < 0.01$, *** $p < 0.001$, **** $p < 0.0001$ compared with combination treatment. All data were obtained from three independent experiments performed in triplicate.

Similar to earlier findings, in this research, FZ and high dose DADA alone dramatically inhibited glucose uptake in A549 cells after 24 hours of treatment (Figure 18.A). When compared to the separate treatment therapy, the absorption of 2-deoxyglucose was dramatically reduced after treatment with the combination. Expectedly, FZ, DADA alone treatment reduced lactate generation after 48 hours, and when both drugs were combined, the effect was enhanced (Figure 18.B). Hence, the FZ-DADA combination had the synergistic effect on inhibiting glucose uptake and lactate production.

4.8. FZ and DADA inhibit phosphorylation of PI3K/AKT pathway

Glucose uptake is a critical physiological process regulated by several mechanisms, with insulin playing the most prominent role. This powerful anabolic hormone facilitates the transport of glucose into cells, primarily in metabolically active tissues such as skeletal muscles, adipose tissue, and the liver, through a specialized transporter known as GLUT4. The process involves a complex sequence of events, primarily mediated by the PI3K/AKT signaling pathway (138). Insulin binds to its receptors, causing them to dimerize and autophosphorylate their tyrosine residues, creating binding sites for IRS proteins. These IRS proteins are also phosphorylated and interact with PI3K through their SH2 domains. Activated PI3K converts PIP2 to PIP3, leading to the activation of PDK1 and PDK2. These kinases then phosphorylate and activate AKT, which in turn phosphorylates AS160. This phosphorylation event is crucial for the translocation of GLUT4 to the cell membrane, facilitating glucose entry into the cell (138,139). My results indicated the role of FZ and DADA in both of time and concentration-dependent manner. In time-dependent experiment, the combination of FZ-DADA at ratio 1:5000 reduced the phosphorylation of both AKT and PI3K (Figure 19). After 5 hours and 7 hours of treatment, FZ-DADA reached the strongest effect in the inhibition of the phosphorylation of AKT and PI3K, respectively. Therefore, in concentration-dependent experiments, A549 cells were treated with FZ, DADA alone and combination for 7 hours. At protein level, FZ and DADA inhibited the phosphorylation of AKT and PI3K (Figure 20). The combination treatment exhibited a more significant reduction in phosphorylation of AKT and PI3K compared with separate ones. These results proposed that the combination FZ and DADA inhibited of glucose uptake and lactate production of through PI3K/AKT pathway.

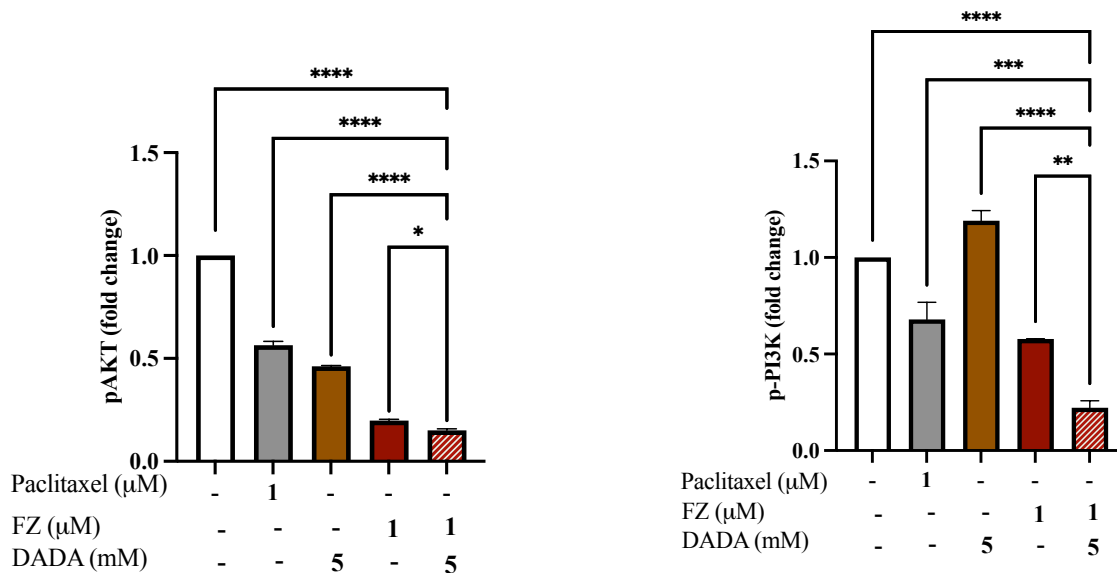
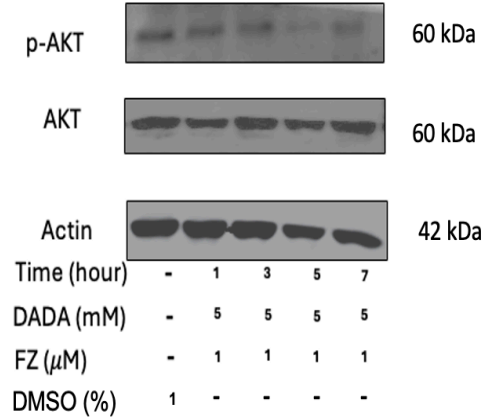
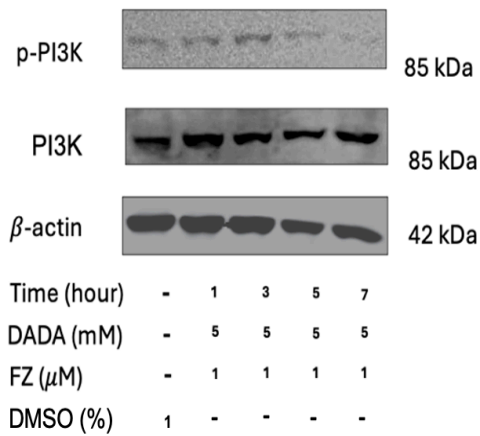


Figure 19: FZ-DADA inhibited PI3K-AKT pathway in time-dependence.

A549 cells were treated with FZ-DADA (1:5000) in 1,3,5,7 hours. Cells were harvested and protein were extracted for Western Blot with AKT, pAKT, PI3K, p-PI3K antibody. The expression of these proteins were normalized with the housekeeping protein β -actin, the expression of, p-PI3K then was normalized with PI3K, p-AKT was normalized with AKT. The results were analysed by one-way ANOVA, with a Dunnett test used to determine which differences are significant. data shows mean \pm SD (n=3) * $p < 0.05$, **** $p < 0.0001$, ns: non significant.

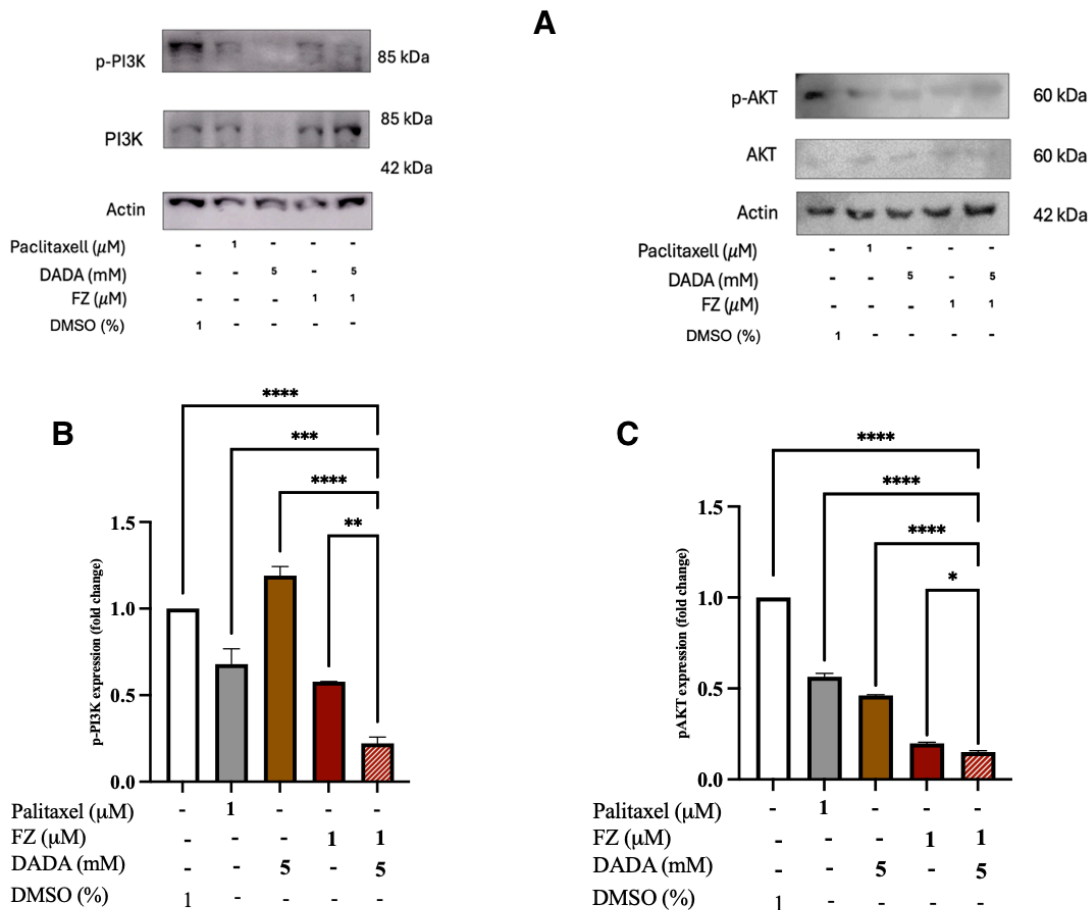


Figure 20: FZ-DADA inhibited PI3K-AKT pathway in concentration-dependance

A – photo of bands in Western Blot. B – Expression of p-PI3K. C – Expression of pAKT. A549 cells were treated with FZ, DADA and FZ-DADA [1:5000] in 7 hours. Cells were harvested and extracted protein for Western Blot. The expression of these proteins were normalized with the housekeeping protein β -actin, the expression of, p-PI3K then was normalized with PI3K, p-AKT was normalized with AKT. The results were analysed by one-way ANOVA, with a Dunnett test used to determine which differences are significant., data shows mean \pm SD ($n = 3$) * $p < 0.05$, ** $p < 0.01$, *** $p < 0.001$, **** $p < 0.0001$ compared with untreated group.

CHAPTER V: SYNERGIC EFFECT OF FZ AND DADA IN A549 TRANSPLANTED MODEL

To further investigate the effects of FZ and DADA in an *in vivo* model, we conducted a study using immunodeficient BALB/c nude mice transplanted with A549 lung cancer cells. The mice were treated with FZ and DADA as monotherapies and in combination to evaluate their impact on tumor progression.

Reported cases described a case of self-administered oral fenbendazole (FZ) at 222 mg/day, demonstrating potential anti-tumor activity in a human patient (140). Using FDA body surface area normalization, this dose converts to ~45.6 mg/kg in mice. A publication in ovarian cancer showed that 50 mg/kg FZ inhibited the epithelial ovarian cancer *in vivo* (43). In addition, mice receiving a diet supplement with 150 ppm fenbendazole (~ 30 mg/kg) showed no anti-tumor effect in models using lymphoma cells (27) and breast cancer (EMT6) cells (141). Therefore, a dose of 40 mg/kg of FZ was selected as a lower-than-standard dose compared with the commonly used 45–50 mg/kg *in vivo*, in order to evaluate whether a reduced dosage could still exert antitumor activity and maintain safety.

In vivo studies with DADA alone for anticancer action showed that a dose of 100 mg/kg DADA suppressed the growth of tumor in BALB/c mice transplanted with MDA-MB-231 cells (22). Therefore, we chose this dose of DADA for this *in vivo* study. A lower dose of DADA (20 mg/kg) was used to investigate the range of effects.

Cisplatin, a medication for solid cancer treatment was used as a positive control in which 5 mg/kg of cisplatin was injected once a week (142,143).

Immunodeficient BALB/c nude mice (Foxn1nu) were housed in a sterile environment following the standard operating procedures for nude mouse care. A549 cells were grown on cell culture flasks in RPMI 1640 culture media supplemented with 10% FBS, 1% Penicillin and Streptomycin at 37°C and CO₂. After one week housing, A549 cells were injected into mice with 2 x 10⁶ cells/0.1 mL/mouse into the right flank's subcutaneous site. The manipulation is done in a sterile environment. When the tumor reached 50 mm³, the mice were randomized into seven groups: Healthy control, tumor control, Cisplatin, FZ 40 mg/kg - 9 mice, DADA 20 mg/kg, DADA 100 mg/kg, FZ 40 mg/kg + DADA 20 mg/kg, FZ 40 mg/kg + DADA 100 mg/kg.

In total, mice were divided into eight groups for investigation:

- Group 1: Healthy control - 6 mice
- Group 2: Tumor control - 9 mice
- Group 3: Positive control - Cisplatin – 8 mice
- Group 4: FZ 40 mg/kg - 9 mice
- Group 5: DADA 20 mg/kg - 10 mice
- Group 6: DADA 100 mg/kg – 10 mice
- Group 7: FZ 40 mg/kg + DADA 20 mg/kg - 10 mice
- Group 8: FZ 40 mg/kg + DADA 100 mg/kg - 10 mice

Initially, our experimental design intended for 10 mice per group to ensure robust statistical power. However, during the tumor induction phase, a few mice failed to develop tumors of a sufficient and uniform size required for baseline consistency at the start of the treatment. To maintain the integrity of the study, we excluded these mice and prioritized the remaining subjects for the treatment groups (Groups 5–8), which required 10 mice each to evaluate the combination therapy's efficacy thoroughly. While Groups 1 through 4 have slightly lower numbers (6 to 9 mice), these sizes still meet the minimum requirements for statistical significance in this model. All statistical analyses were adjusted to account for these differences in group size.

In these first steps, the safety profile of FZ and DADA in animals was measured in nude mice transplanted with A549 small lung cancer cells. Following A549 cell transplantation, the mice exhibited normal behavior, including consistent food consumption, weight gain, mobility, and appropriate responses to stimuli. No signs of diarrhea were observed, and the anal region remained dry. Additionally, the injection site was normal, with no sign of bleeding and infection. Prior to treatment, the average body weight across all seven groups was comparable, with no statistically significant differences ($p > 0.05$) (Table 3).

Table 3: The average weight of mice before treatment (g). *The results were analysed by one-way ANOVA, with a Dunnett test used to determine which differences are significant.*

Parameters Groups	n	$\bar{X} \pm SD$	p
Non-treatment tumor control (2)	9	20.10 ± 1.97	> 0.05
Positive control – Cisplatin 5 mg/kg (3)	8	19.11 ± 1.24	
FZ 40 mg/kg (4)	10	18.80 ± 1.65	
DADA 20 mg/kg (5)	10	19.11 ± 1.82	
DADA 100 mg/kg (6)	10	18.81 ± 1.68	
FZ 40mg/kg + DADA 20 mg/kg (7)	10	19.47 ± 1.69	
FZ 40mg/kg + DADA 100 mg/kg (8)	10	19.48 ± 1.45	

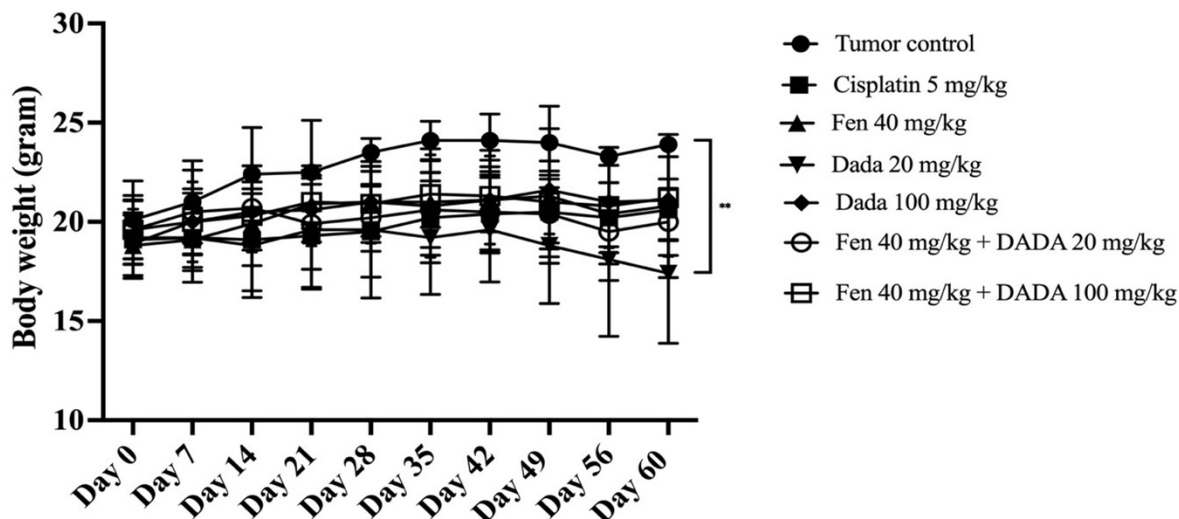


Figure 21: Mice's body weight after 60 days (g)

Body weight of seven groups of mice was recorded twice a week by electronic scale TE3102S Sartorius. Data present mean \pm SD. The results were analysed by one-way ANOVA, with a Dunnett test used to determine which differences are significant, ** $p < 0.01$.

During the treatment period, body weight was monitored twice per week. After treatment, the body weight of seven groups was weighed twice a week. The body weight tended to increase compared to the baseline. After 60 days of treatment, there was no significant different in the body weigh of treatment groups, excepted group DADA 20 mg/kg (Figure 21).

5.1 Hematological function analysis

Hematological indices of mice play a vital role in evaluating the effect of FZ and DADA in BALB/c mice. In order to validate further effects of my treatment in the safety of animal, we examined the alteration of hematological indices under FZ and DADA treatment. My results indicated that after 60 days of FZ and DADA in both of single and combination treatment, the number of red blood cells, white blood cells and hemoglobin content, of animal did not significantly change in eight groups of mice (Table 4).

Table 4: Hematological indices of mice after FZ-DADA treatment

Groups	n	Hematological indices		
		Red blood cell count (T/L)	Hemoglobin content (g/L)	White blood cell count (g/L)
1 - Healthy control	6	9.70 ± 0.42	142.33 ± 6.31	4.93 ± 1.63
2 - Non-treatment tumor control	2	9.66 ± 0.53	144.00 ± 5.66	4.29 ± 0.95
3 - Positive control- Cisplatin 5 mg/kg	7	9.79 ± 0.50	143.71 ± 5.65	4.73 ± 1.21
4 - FZ 40 mg/kg	8	9.66 ± 0.60	140.50 ± 6.87	6.62 ± 2.34
5 - DADA 20 mg/kg	7	9.42 ± 0.75	137.29 ± 10.53	3.30 ± 1.51
6 - DADA100 mg/kg	9	9.32 ± 0.60	135.78 ± 11.65	5.02 ± 3.75
7 - FZ 40 mg/kg + DADA 20 mg/kg	10	9.23 ± 0.89	135.40 ± 11.06	3.65 ± 2.04
8 - FZ 40 mg/kg + DADA 100 mg/kg	10	9.49 ± 0.66	138.90 ± 9.00	5.87 ± 4.29
p		> 0.05	> 0.05	> 0.05

The results were analysed by one-way ANOVA, with a Dunnett test used to determine which differences are significant.

5.2. Kidney function of mice after FZ-DADA treatment

To evaluate effects of FZ and DADA in kidney function, levels of urea and creatinine in mice's blood were measured. Interestingly, there was no significant difference between treatment groups and the tumor non-treatment control group ($p > 0.05$) (Table 5).

Table 5: Urea and creatinine level of mice after FZ-DADA treatment

Groups	n	Urea (mg/dL)	Creatinine (mg/dL)
1 - Healthy control	6	7.49 ± 1.88	26.85 ± 3.19
2 - Non-treatment tumor control	2	7.23 ± 1.61	28.84 ± 2.43
3 - Positive control- Cisplatin 5 mg/kg	7	6.36 ± 1.14	25.49 ± 1.37
4 - FZ 40 mg/kg	8	6.26 ± 1.30	26.84 ± 2.18
5 - DADA 20 mg/kg	7	6.91 ± 0.75	25.81 ± 2.16
6 - DADA100 mg/kg	9	6.94 ± 1.64	25.60 ± 2.11
7 - FZ 40 mg/kg + DADA 20 mg/kg	10	6.77 ± 0.65	26.32 ± 1.61
8 - FZ 40 mg/kg + DADA 100 mg/kg	10	6.84 ± 1.94	26.79 ± 1.77
p		> 0.05	> 0.05

The results were analysed by one-way ANOVA, with a Dunnett test used to determine which differences are significant.

Moverover, histological analysis of the kidney tissues once again confirmed that FZ and DADA treatment did not adversely affect kidney function (Figure 22).

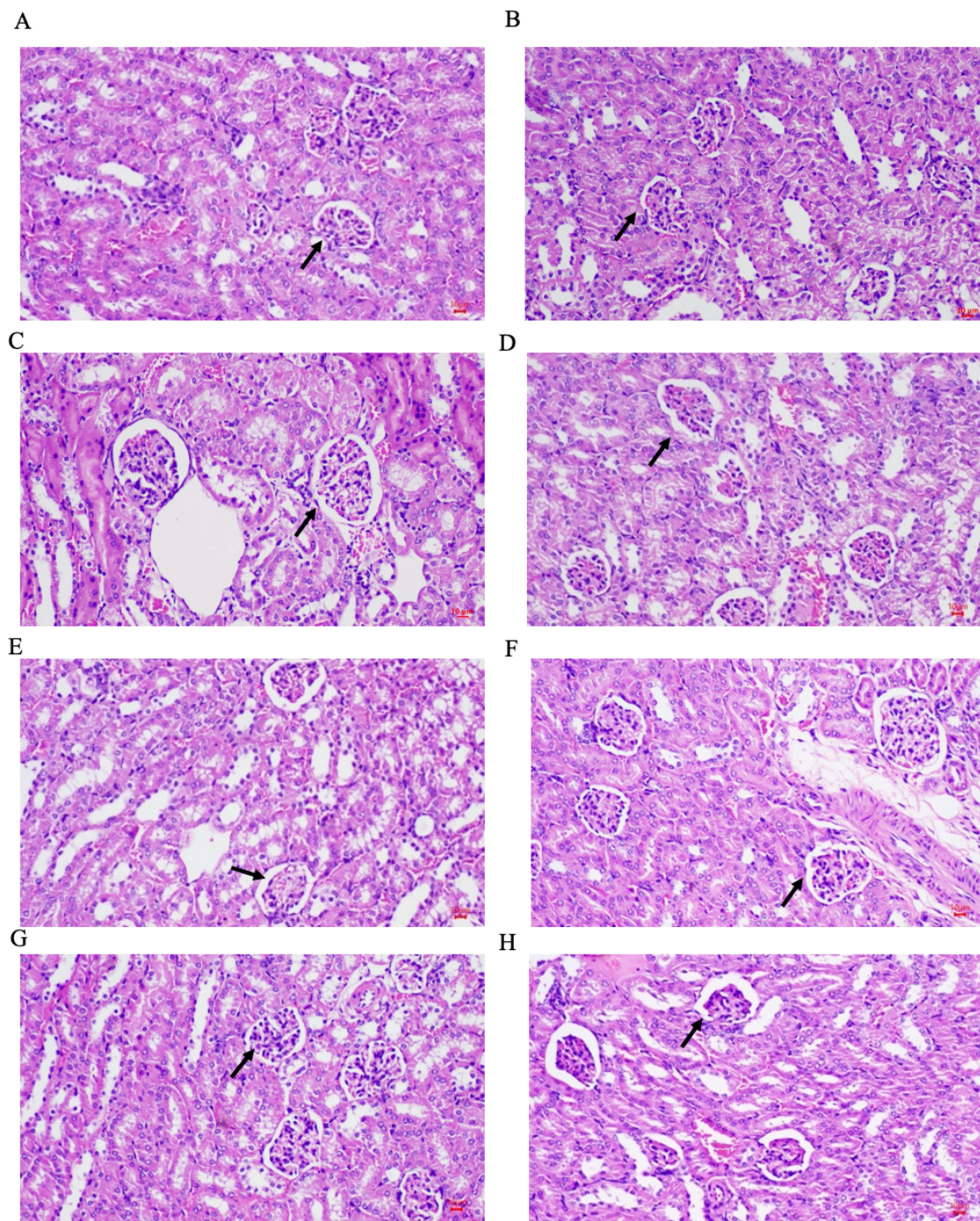
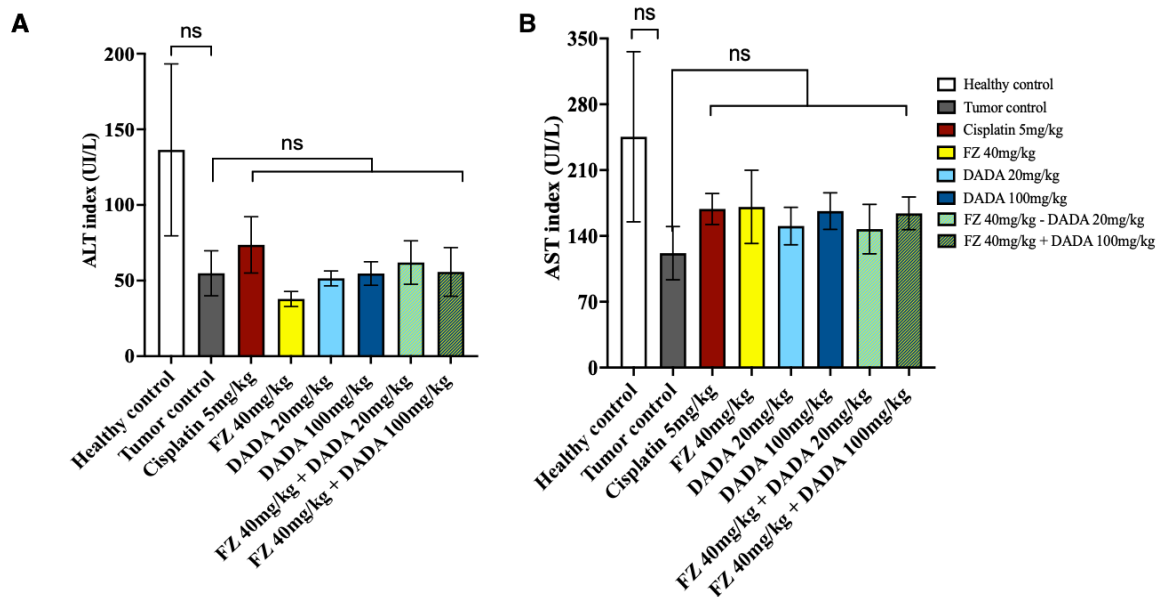


Figure 22: Histology sections of kidney of mice after FZ -DADA treatment.

Hematoxylin and Eosin staining were applied on liver and kidney tissues after harvesting. Magnification 40×, A. Group 1 (n=6), B. Group 2 (n=2), C. Group 3 (n=7), D. Group 4 (n=8), E. Group 5 (n=7), F. Group 6 (n=9), G. Group 7 (n=10), H. Group 8 (n=10). The arrows represent for the glomerulus.

5.3. Liver function of mice after FZ and DADA treatment

Fenbendazole undergoes partial absorption in the liver, where it is rapidly metabolized by flavin-monooxygenase (FMO) and CYP3A4 enzymes into its sulfoxide derivative, oxfendazole (fenbendazole sulfoxide) (144,145). Otherwise, Kaufman et al indicated that high doses of dicloroacetate lead to the alteration of liver function in patient with mitochondrial myopathy, encephalopathy, lactic acidosis and stroke-like episodes (146). Therefore, the liver function of mice was measured via the ALT and AST levels as well as histological examination of liver tissue after 60 days of treatment (Figure 23). From the results, it is clearly that there was no significant hepatocellular damage in treatment groups.



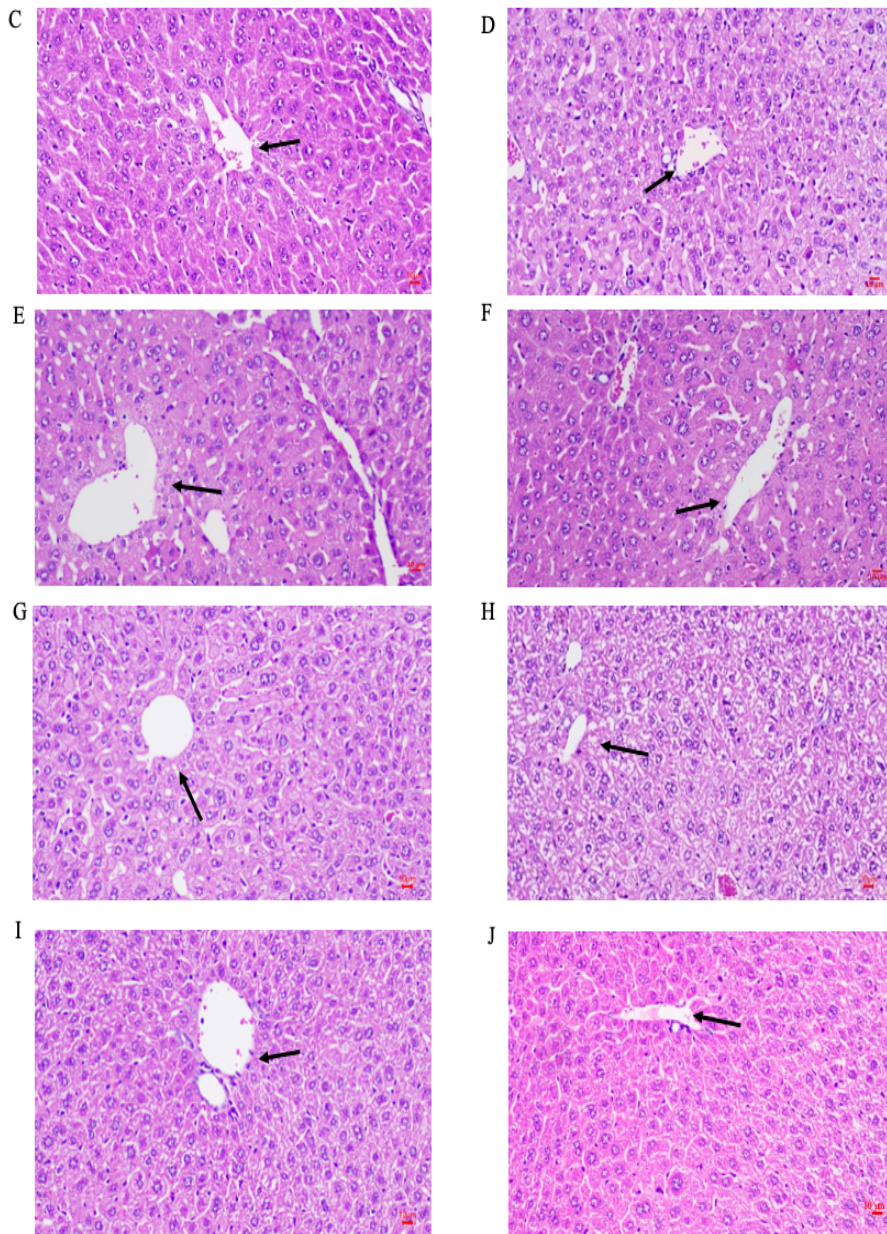


Figure 23: Effect of drug formulation on liver function

A,B: The AST and ALT index in eight group were measured at day 60 after of the treatment. Data presents mean \pm SD. One-way ANOVA, with a Dunnett test used to determine which differences are significant among untreat and the others groups, ns: non significant. C-J: Hematoxylin and Eosin staining were applied on liver tissues after harvesting. Magnification 40 \times , C. Group 1 (n=6), D. Group 2 (n=2), E. Group 3 (n=7), F. Group 4 (n=8), G. Group 5 (n=7), H. Group 6 (n=9), I. Group 7 (n=10), J. Group 8 (n=10). The arrows represent for the central lobule vein.

5.4. Synergistic anti-tumor effect of FZ and DADA

In the *in vivo* model, at the beginning of treatment, there was no significant difference in the tumor volume across the groups ($p > 0.05$) (Table 6).

Table 6: The average volume of mice tumors on the first day of treatment

Indexes Groups	n	Tumor volume (mm ³)		p
		$\bar{X} \pm SD$	Median [25%;75%]	
Tumor control (2)	9	50.67± 14.69	48.00 (34.00; 60.88)	> 0.05
Positive control – Cisplatin 5 mg/kg (3)	8	58.04 ± 17.02	50.40 (39.00; 75.00)	
FZ 40 mg/kg (4)	10	58.73 ± 16.58	62.50 (44.00; 75.00)	
DaDa 20 mg/kg (5)	10	64.54 ± 39.92	50.60 (45.60; 126.00)	
DaDa 100 mg/kg (6)	10	50.38 ± 27.97	49.30 (34.00; 68.80)	
FZ 40 mg/kg + DADA 20 mg/kg (7)	10	66.52 ± 21.31	65.35 (44.20; 95.10)	
FZ 40 mg/kg + DADA 100 mg/kg (8)	10	54.35 ± 12.30	50.60 (49.30; 75.00)	

One-way ANOVA, with a Dunnett test used to determine which differences are significant among untreated and the others groups

It is clear that, in the combination treatment group the growth of tumor was slower than their counterpart untreated group. Interestingly, the combination of FZ and DADA in a ratio of 40:100 resulted in a greater reduction in tumor volume than in single-dose groups across all time points. Especially, from day 14, group 8 (FZ 40 mg/kg + DADA 100 mg/kg) significantly decreased tumor volume comparing with control group, while the others did not show any statistically significant difference. At the end of experiment, there was a significant difference in the tumor volume in the combination treatment group and their separate treatment (Figure

24), indicating the synergistic anti-tumor effect of FZ and DADA at 40:100 mg/kg ratio.

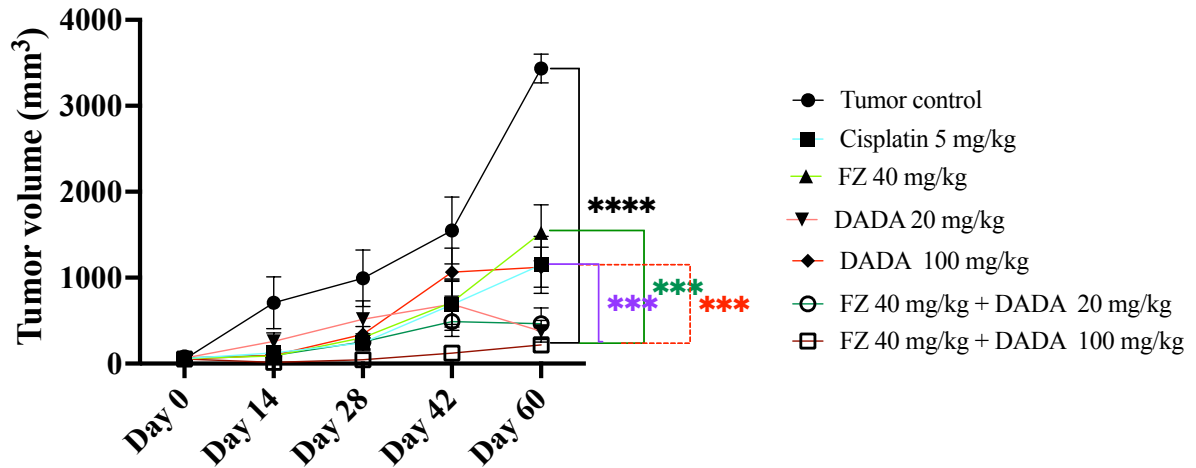


Figure 24: Tumor volume results in groups of mice during treatment.

The tumor volume was calculated using follow formula: $V = (D \times R^2) \times 0,5$ with V : tumor volume (mm^3), D : tumor length as measured (mm), R : tumor width as measured (mm). Data present mean \pm SEM, One-way ANOVA, with a Dunnett test used to determine which differences are significant among untreat and the others groups, *** $p < 0.001$, **** $p < 0.0001$

5.5 Tumor Growth Inhibition (TGI) and Evaluation of Synergistic Effects

The tumor growth inhibition (TGI) for each treatment group was calculated using the following formula:

$$TGI = \left(1 - \frac{TV_{treatment}}{TV_{control}}\right) \times 100\%$$

where $TV_{treatment}$ and $TV_{control}$ represent the mean tumor volumes of the treated and control groups, respectively.

Based on the experimental data, the observed TGI values were as follows:

- DADA 20 mg/kg: 60.17%
- DADA 100 mg/kg: 71.19%
- Fenbendazole (FZ) 40 mg/kg: 63.90%
- FZ 40 mg/kg + DADA 20 mg/kg: 87.83%
- FZ 40 mg/kg + DADA 100 mg/kg: 93.62%

To assess the interaction between FZ and DADA *in vivo*, the **Modified Expected Additivity model** was applied, as defined by the equation:

$$Expected\ TGI_{combo} = TG_1 + TG_2 - \left(\frac{TG_1 \times TG_2}{100} \right)$$

The calculated expected TGI values were **85.62%** for the combination of FZ 40 mg/kg + DADA 20 mg/kg and **89.60%** for FZ 40 mg/kg + DADA 100 mg/kg. Both observed values (87.83% and 93.62%, respectively) exceeded their corresponding expected values, indicating a **synergistic effect** between FZ and DADA in the lung cancer xenograft model.

These findings support the hypothesis that the combination of FZ and DADA enhances tumor growth inhibition beyond the expected additive effect, suggesting potential therapeutic synergy *in vivo*.

5.6. Tumor reduction rates of FZ and DADA in BALB/c nude mice

Besides the decrease of the development of tumor, the regression of tumor was occurring from day 7 following treatment in mice of groups 6, 7, and 8. Following the duration of treatment, the number of mice losing tumors in the treatment groups increased. In contrast, no mice in the tumor untreated group lost tumor at any stage throughout the trial, whereas the number of dead mice progressively grew (Table 7).

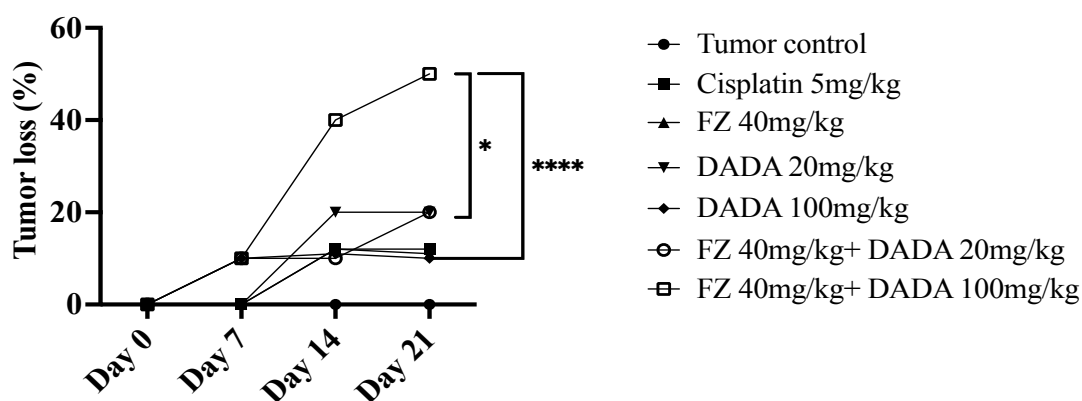


Figure 25: Tumor reduction rate in treated mice group.

The number of tumor loss mice in seven groups was recorded during 60 days. Chi-square test for was used for comparison of two percentages, * $p < 0.05$, **** $p < 0.0001$

Table 7: Tumor reduction rate in treated mice

Days	Tumor reduction rate	Groups							p
		2	3	4	5	6	7	8	
Day 7	n	0	0	0	0	1	1	1	> 0.05
	%	0.0%	0.0%	0.0%	0.0%	10.0%	10.0%	10.0%	
Day 14	n	0	1	1	2	1	1	4	p2-8 = 0.054
	%	0.0%	12.5%	12.5%	20.0%	11.1%	10.0%	40.0%	
Day 21	n	0	1	1	2	1	2	5	P2-8 <0.0001, P4-8 = 0.0135 P6-8 <0.0001
	%	0.0%	12.5%	11.1%	20.0%	10.0%	20.0%	50.0%	
Day 28	n	0	0	1	2	1	2	5	P2-8 <0.0001, P4-8 = 0.0135 P6-8 <0.0001
	%	0.0%	0.0%	11.1%	20.0%	10.0%	20.0%	50.0%	
Day 35	n	0	0	1	1	1	2	5	P2-8 <0.0001, P4-8 = 0.0135 P6-8 <0.0001
	%	0.0%	0.0%	11.1%	10.0%	10.0%	20.0%	50.0%	
Day 42	n	0	0	1	1	1	2	5	P2-8 <0.0001, P4-8 = 0.0135 P6-8 <0.0001
	%	0.0%	0.0%	11.1%	10.0%	10.0%	20.0%	50.0%	
Day 49	n	0	0	1	1	1	2	5	P2-8 <0.0001, P4-8 = 0.0135 P6-8 <0.0001
	%	0.0%	0.0%	11.1%	10.0%	10.0%	20.0%	50.0%	
Day 56	n	0	0	1	1	0	2	5	P2-8 <0.0001, P4-8 = 0.0135 P6-8 <0.0001
	%	0.0%	0.0%	11.1%	10.0%	0.0%	20.0%	50.0%	
Day 60	n	0	0	1	1	0	2	5	P2-8 <0.0001, P4-8 = 0.0135 P6-8 <0.0001
	%	0.0%	0.0%	11.1%	11.1%	0.0%	20.0%	50.0%	

Group 2- Tumor control, 3-Cisplatin 5mg/kg, 4-FZ 40 mg/kg, 5- DADA 20 mg/kg, 6-DADA 100 mg/kg, 7- FZ 40 mg/kg + DADA 20 mg/kg, 8- FZ 40 mg/kg + DADA 100 mg/kg. Chi-square test was used for comparison of two percentages.

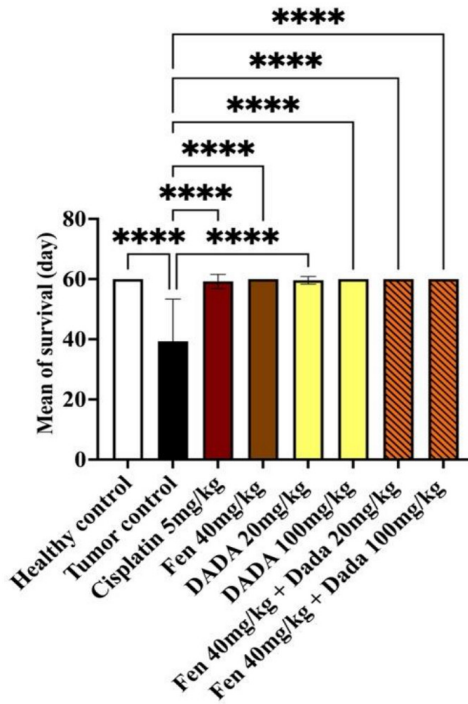
From day 21, the proportion of tumor-free mice in group 8 was significantly higher than that of the untreated group ($p < 0.0001$). In day 60, the tumor reduction rate in the tumor control group, cisplatin, and group 6 was 0 (0%) while group 4 and 5 was 1 (11.1%).

In the combination group, 20% mice in receiving 40 mg/kg of FZ and 20 mg/kg of DADA were tumor-free, compared with 50% of mice with 40mg/kg FZ and 100 mg/kg of DADA. Totally, the number of mice with tumor loss was 9, accounting for 15% of the total. Interestingly, from day 21 to day 60, the proportion of tumor-losing mice in group 8 was significantly higher than that of group 4 and group 6 (Table 7, Figure 24). My results indicated the synergic effect of FZ and DADA at a ratio of 40:100 mg/kg in promoting tumor regression in BALB/c nude mice.

5.7. Effect of FZ and DADA on the survival duration and death rate of BALB/c nude mice

For further evaluation of the anti-cancer effect of FZ and DADA, survival time was used as a criterion to assess the effectiveness of FZ and DADA treatment in A549 lung cancer-bearing nude mice. As demonstrated in Figure 25, all treated groups showed significantly extended survival compared to untreated controls. In addition, survival rates were further analyzed to confirm treatment effectiveness. In the untreated group, the first death occurred on day 21, with mortality increasing steadily throughout the time. Notably, the tumor control group consistently showed higher mortality rates than the six treatment groups at all observed time points. However, statistically significant differences in survival between the control and treatment groups were only evident from day 49 onward, with the most pronounced effects observed by the end of the experiment (day 60). These findings suggest that FZ and DADA treatments delay tumor progression and improve survival, though their full therapeutic impact becomes most apparent in later stages.

A



B

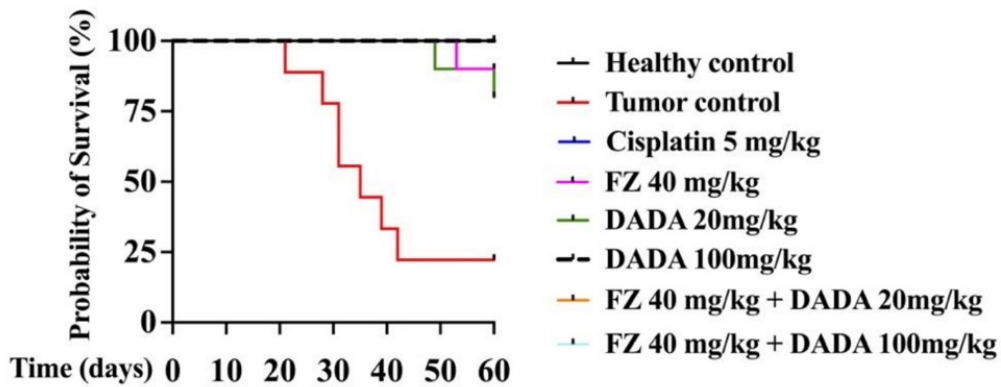


Figure 26: The survival duration and death rate death rate of nude mice.

The number of survival mice in eight groups was recorded during 60 days of experiment. A. Mean of survival (day) data present mean \pm SD, One-way ANOVA was used to compare mean of treatment groups and untreat group . B. Survival rate (%), the Log-rank test was applied to compare the cumulative survival time between different treatment methods, **** $p < 0.0001$

CHAPTER VI: DISCUSSION

Lung cancer remains the most prevalent and deadly malignancy worldwide, with 1.8 million deaths (18.7% of all cancer-related mortality) reported in 2022 alone. Current epidemiological models project a concerning 67% increase in global lung cancer incidence by 2040, underscoring the urgent need for more effective prevention, diagnostic, and therapeutic strategies (147). Despite decades of research and advancements in treatment modalities including surgery, chemotherapy, radiation, and targeted therapies the 5-year survival rate for lung cancer patients remains disappointingly low at approximately 10-20% (148) due to the pervasive challenge of late-stage diagnosis, the rapid evolution of treatment resistance as well as the metabolic adaptability of tumor cells enabling evasion of conventional treatments. Given these challenges, combination therapies that target multiple oncogenic pathways simultaneously represent a promising approach to enhance treatment efficacy by overcoming resistance mechanisms and reducing toxicity through synergistic lower-dose combinations. This research successfully investigated a novel synergistic combination of Fenbendazole (FZ) and Diisopropylamine Dichloroacetate (DADA) as a potential repurposing strategy to enhance treatment efficacy while maintaining a high safety profile.

6.1. Synergistic mechanistic insight *in vitro*

The FZ-DADA combination in this thesis demonstrates remarkable synergistic activity in promoting apoptotic cell death in A549 lung cancer cells. Mechanistic investigations reveal this effect is mediated through substantial alterations in critical apoptotic regulators, particularly the upregulation of pro-apoptotic BAX and concurrent downregulation of anti-apoptotic Bcl2 (121), (123), (149). These opposing changes create a decisive shift in the mitochondrial apoptotic pathway, where BAX facilitates mitochondrial outer membrane permeabilization (MOMP) and subsequent cytochrome C release (121), (122) while Bcl2 normally functions to maintain mitochondrial integrity and prevent apoptosis initiation. The observed imbalance in these counteracting forces establishes a permissive environment for programmed cell death (121), (123), (149).

Furthermore, my results demonstrate significant activation of downstream executioner caspases-3 / caspase-7 which serve as the terminal effectors of apoptosis through proteolytic cleavage of essential cellular components (123),(125-128). The coordinated upregulation of

these caspases confirms that the FZ-DADA combination successfully engages the complete apoptotic cascade, from initial mitochondrial signaling to final cellular demolition.

In summary, the synergistic effect of combination FZ-DADA on A549 cells is illustrated in the graphic below:

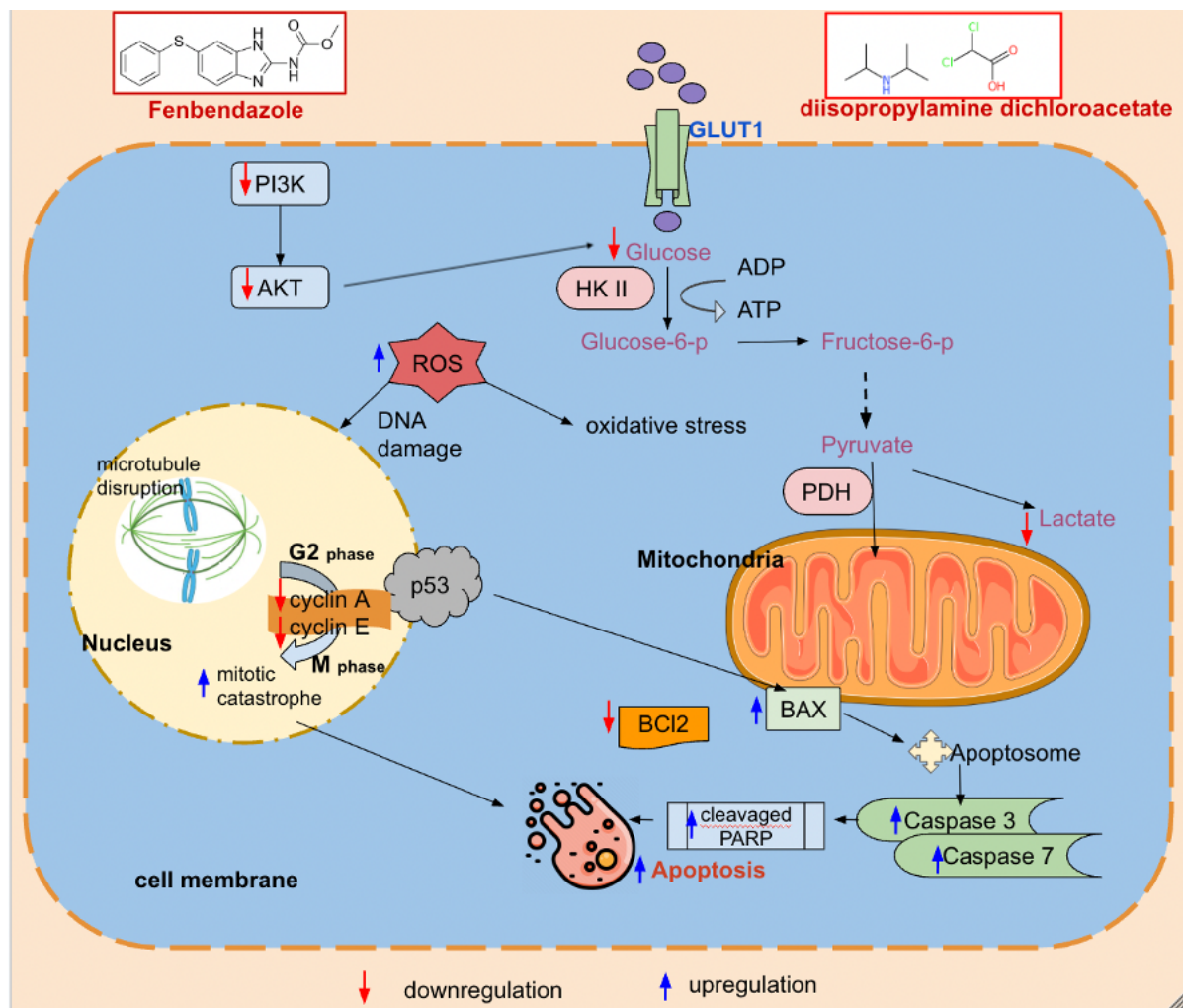


Figure 27: Mechanism of action of FZ and DADA in lung cancer (generated by Google Drawing).

6.2. Synergistic effect and safety *in vivo*

In vivo experiments further confirmed that FZ (40 mg/kg), DADA (100 mg/kg), and their combination were well tolerated in BALB/c mice. There was no significant alteration in body weight, blood sugar levels, or liver and kidney function of mice after 60 days of treatment. My data contributed valuable results of safety profiling of FZ and DADA for preclinical research. The safety profiling of FZ and DADA in animal was measured in 60 days of treatment provided the strong evidence for long-time treatment of FZ and DADA. Results demonstrated the

combination of FZ (40 mg/kg) and DADA (100 mg/kg) produced significant anti-tumor effects in an A549 xenograft model using BALB/c nude mice. The combined treatment showed markedly enhanced therapeutic outcomes compared to either agent administered alone. Importantly, the combination therapy conferred a significant survival advantage, improving 60-day survival rates in the combination treatment group compared with tumor control group. These *in vivo* findings corroborate my previous *in vitro* results and strongly support the therapeutic potential of this drug combination for NSCLC treatment. The enhanced efficacy observed with the FZ-DADA combination suggests synergistic interactions. The combination of FZ (40 mg/kg) and DADA (100 mg/kg) markedly showed tumor regression in 50% of animals from day 21 after treatment.

6.3. Novelty and significance of the study

Previous studies have established FZ as a broad-spectrum anticancer agent, demonstrating efficacy across multiple malignancies including breast, colorectal and hepatocellular carcinomas. Parallel investigations have characterized DADA as a dual-function compound, acting both as a pyruvate dehydrogenase kinase (PDK) inhibitor that disrupts cancer metabolism and as a hepatoprotective agent that mitigates treatment-related toxicity. Building upon these foundations, my study reveals for the first time that oral co-administration of FZ and DADA produces synergistic antitumor effects in NSCLC models. This combination strategy capitalizes on complementary mechanisms of action: FZ's established antiproliferative properties combined with DADA's metabolic modulation and hepatoprotective effects, potentially offering both enhanced efficacy and reduced toxicity - a critical advantage for long-term cancer management. The observed synergy suggests this regimen may represent a novel paradigm in NSCLC treatment, particularly for patients with metabolic vulnerabilities or those requiring chronic therapy. Previous studies on the combination of FZ and DADA with other agents have indicated the anticancer effects of FZ and DADA in various cancer types. Dogra et al reported synergistic interactions between FZ and metabolic modulators (DCA, 2DG) or chemotherapeutics (in a range of taxol) using the CI method (14). However, the study lacks cellular-level validation of these proposed synergies. Otherwise, the combination of FZ with multivitamins demonstrated enhanced anti-tumor effects compared to monotherapy in SCID mice xenografted with human Burkitt lymphoma cells (P493-6 B cells) (27). However, two key limitations temper interpretation of these results: the mechanistic basis for this synergy remains unknown, and the small cohort size ($n = 4-5$ per group) limits statistical power and

generalizability. Another research failed to delay the development of tumor using the combination of FZ and X-ray in EMT6 mouse mammary tumors growing in BALB/cRw mice (141). My research for the first time identified a combination that synergistically inhibited the development of NSCLC in both *in vitro* and *in vivo* models.

Futhermore, FZ and DADA not only inhibited the proliferation of A549 lung cancer cells, but also reduced the viability of other common cancer cells, such as MCF7 breast cancer cells, Hep G2 liver cancer cells, DU145 and PC3 prostate cancer cells. These features indicated the potential of FZ and DADA in a wide-range of cancer types: breast cancer, liver cancer, prostate cancer ...

Fenbendazole has been found to cause drug-induced liver injury. In my study, there was no liver injury observed in both monotherapy and combination treatment of FZ. In this case, a reasonable hypothesis is that a certain subgroup of patients might be inherently more sensitive to FZ, thereby experiencing greater hepatotoxic effects. Indeed, the number of toxicity of FZ in liver in human is quite limited.

6.4. Bridging the gap: *in vitro* vs. *in vivo* dosage discrepancies

A significant observation in this study is the marked difference between the optimal drug ratios identified *in vitro* (1:5000) and those applied *in vivo* (1:2.5). Specifically, a molar ratio of 1:5000 was required in cell culture to observe significant synergy, whereas a dose of 40 mg/kg FZ and 100 mg/kg DADA yielded superior results in the BALB/c nude mouse model.

This discrepancy is primarily attributed to the distinct physicochemical and pharmacokinetic profiles of the two compounds. Fenbendazole is characterized by extremely low water solubility (~0.05 µg/mL) and poor oral bioavailability, estimated at only 10-20% in rodent models (150–152). In the controlled environment of an *in vitro* assay, FZ is typically dissolved in organic solvents like DMSO, ensuring immediate and uniform exposure to the cells. However, in a living system, FZ must navigate the gastrointestinal tract, undergo hepatic metabolism, and reach the tumor site through systemic circulation. The limited absorption necessitates a significantly higher mass dose *in vivo* to achieve effective concentrations within the tumor microenvironment.

In contrast, DADA is a highly soluble small molecule with efficient systemic distribution (24). The selection of the 40 mg/kg FZ and 100 mg/kg DADA doses was not arbitrary but

strategically informed by established literature. Previous studies indicated that 50 mg/kg FZ could inhibit epithelial ovarian cancer *in vivo* (43), while doses below 30 mg/kg often failed to suppress lymphoma or breast cancer growth (27). Similarly, DADA at 100 mg/kg has been documented to effectively suppress MDA-MB-231 xenograft growth (22). By utilizing these doses, we successfully achieved a synergic anti-tumor effect that resulted in a striking 50% complete tumor loss rate in Group 8. When converted using FDA body surface area normalization, these dosages suggest a human equivalent dose (HED) of approximately 194 mg/day of FZ and 487 mg/day of DADA. This range is conveniently close to the empirical doses (~222 mg/day) used off-label by patients such as Joe Tippens, supporting the feasibility of oral clinical translation (153).

6.5. Limitations of the current study

While this research provides a strong foundation for the FZ-DADA combination, several limitations must be acknowledged:

Lack of normal cell line controls: A critical shortcoming is that the current thesis does not include experiments on normal (non-cancerous) cell lines to evaluate the treatment's selectivity. Although our *in vivo* data showed no significant toxicity to liver and kidney functions, confirming a differential response between healthy lung epithelial cells and A549 cells *in vitro* would provide essential evidence of a wide therapeutic window.

Breadth of cell line testing: The mechanistic depth of this study was focused primarily on the A549 lung cancer model. While supplementary data on MCF7, PC3, and HepG2 lines suggest broad potential, a more comprehensive investigation into different histologic subtypes of lung cancer (e.g., small cell lung cancer or squamous cell carcinoma) is necessary to determine the regimen's universality.

Absence of post-study tumor sampling: Due to the initial focus on tumor volume and survival metrics, tumor tissues from the mice were not preserved for further molecular analysis. The inability to perform immunohistochemistry or transcriptomic analysis on the excised tumors limits our understanding of whether the *in vitro* mechanisms (such as p-PI3K/AKT inhibition and BAX upregulation) are replicated identically within the complex tumor microenvironment.

6.6. Future research directions

Moving forward, the translational development of the FZ-DADA combination should focus on several key pillars:

Comprehensive selectivity assays: Future phases must include comparative toxicity studies on normal human bronchial epithelial cells to definitively prove the safety of the 1:5000 ratio.

Pharmacokinetic (PK) and ADME profiling: To optimize human dosing, detailed studies on the absorption, distribution, metabolism, and excretion (ADME) of the co-administered drugs are essential.

In-depth in vivo mechanistic validation: Replicating the animal studies with a focus on collecting tumor tissue will allow for the analysis of markers for angiogenesis, immune infiltration, and intra-tumoral metabolic shifts.

6.7. Clinical and Social Implications

The findings of this thesis have significant implications for cancer care in Vietnam. With treatment costs for advanced NSCLC reaching up to 339 million VND (6), many patients face financial catastrophe. Both FZ and DADA are off-patent, low-cost, and easy to manufacture. The pending patent for this synergistic formulation represents a major step toward providing a safe, effective, and affordable metabolic therapy for lung cancer patients.

CHAPTER VII: CONCLUSION

My study presents a new discovery in cancer drug repurposing, demonstrating for the first time the synergistic combination of FZ with DADA to develop a novel anticancer therapy in non-small cell lung cancer. The research successfully identified the optimal *in vitro* and *in vivo* concentrations, maximizing therapeutic efficacy while ensuring safety. Mechanistic studies confirmed multiple anticancer pathways of FZ and DADA, including ROS induction, apoptosis activation, and caspase modulation. My results indicated the anti-cancer effect of FZ and DADA via inducing apoptosis and arresting the cell cycle through ROS induction was confirmed in A549 cells with the ratio 1:5000 of FZ and DADA. This combination inhibited the proliferation of not only A549 but also many common cancer cells, namely MCF7 breast cancer cells, HepG2 liver cancer cells, PC3 and DU145 prostate cancer cells. These investigations supported its potential as a non-selective therapy. Furthermore, the combination of 100 mg/kg DADA with 40 mg/kg FZ demonstrated significant synergistic antitumor activity in an A549 xenograft model using immunocompromised BALB/c nude mice compared to monotherapies. Notably, *in vivo* experiments showed 50% of treated mice achieving complete tumor regression and remaining tumor-free for two months post-treatment, alongside good safety profiles in biochemical and hematological analyses. My study is under patent pending by the Vietnam Intellectual Property Office, highlighting its innovation. Given that both drugs are low-cost, easily accessible, and simple to manufacture, this combination offers a promising, affordable treatment option with high translational potential. These findings pave the way for future clinical trials and deeper investigations into dose optimization and mechanistic pathways for specific cancer types.

To further advance this promising drug combination toward clinical application, additional pharmacokinetic studies and *in vivo* mechanistic investigations are essential. A deep understanding of the absorption, distribution, metabolism, and excretion (ADME) profiles of both FZ and DADA will be critical to optimize dosing regimens and predict potential drug interactions in humans. Furthermore, detailed *in vivo* studies should elucidate the precise molecular mechanisms underlying their synergistic anticancer effects, including potential effects on tumor microenvironment, immune modulation, and resistance pathways. These preclinical validations will provide crucial data to support subsequent phase I clinical trials in larger populations, ensuring both efficacy and safety before broader clinical implementation. Such foundational research will strengthen the translational potential of this cost-effective therapeutic strategy while minimizing risks in human trial.

REFERENCES

1. Bray F, Laversanne M, Sung H, Ferlay J, Siegel RL, Soerjomataram I, et al. Global cancer statistics 2022: GLOBOCAN estimates of incidence and mortality worldwide for 36 cancers in 185 countries. *CA Cancer J Clin*. 2024 May-Jun;74(3):229–63.
2. Schwartz SM. Epidemiology of Cancer. *Clin Chem*. 2024 Jan 4;70(1):140–9.
3. Leiter A, Veluswamy RR, Wisnivesky JP. The global burden of lung cancer: current status and future trends. *Nat Rev Clin Oncol*. 2023 Sep;20(9):624–39.
4. Zhou J, Xu Y, Liu J, Feng L, Yu J, Chen D. Global burden of lung cancer in 2022 and projections to 2050: Incidence and mortality estimates from GLOBOCAN. *Cancer Epidemiol*. 2024 Dec;93:102693.
5. Hoang VM, Pham CP, Vu QM, Ngo TT, Tran DH, Bui D, et al. Household Financial Burden and Poverty Impacts of Cancer Treatment in Vietnam. *Biomed Res Int*. 2017;2017:1–8.
6. Dinh HT, Nguyen TTT. Cost of Non Small Cell Lung Cancer by Vietnamese and European Treatment Standards in Vietnam. *Value Health*. 2014 Nov;17(7):A625.
7. Pushpakom S, Iorio F, Eyers PA, Escott KJ, Hopper S, Wells A, et al. Drug repurposing: progress, challenges and recommendations. *Nat Rev Drug Discov*. 2019 Jan;18(1):41–58.
8. Ashburn TT, Thor KB. Drug repositioning: identifying and developing new uses for existing drugs. *Nat Rev Drug Discov*. 2004 Aug;3(8):673–83.
9. Pantziarka P, Bouche G, Meheus L, Sukhatme V, Sukhatme VP, Vikas P. The Repurposing Drugs in Oncology (ReDO) Project. *Ecancermedicalsecience*. 2014 Jul 10;8:442.
10. Singhal S, Mehta J, Desikan R, Ayers D, Roberson P, Eddlemon P, et al. Antitumor activity of thalidomide in refractory multiple myeloma. *N Engl J Med*. 1999 Nov 18;341(21):1565–71.
11. Pollak M. Metformin and Other Biguanides in Oncology: Advancing the Research Agenda. *Cancer Prev Res (Phila)*. 2010 Sep;3(9):1060–5.
12. Cen D, Gonzalez RI, Buckmeier JA, Kahlon RS, Tohidian NB, Meyskens FL. Disulfiram induces apoptosis in human melanoma cells: a redox-related process. *Mol Cancer Ther*. 2002 Jan;1(3):197–204.

13. Duan Q, Liu Y, Rockwell S. Fenbendazole as a potential anticancer drug. *Anticancer Res.* 2013 Feb;33(2):355–62.
14. Dogra N, Kumar A, Mukhopadhyay T. Fenbendazole acts as a moderate microtubule destabilizing agent and causes cancer cell death by modulating multiple cellular pathways. *Sci Rep.* 2018 Aug 9;8(1):11926.
15. Udhavrao BA. Successful Therapeutic Management of Ivermectin Toxicity in Deoni Calf. *J Dairy Vet Sci.* 2017 May 5;2(4):555592.
16. Abughanimeh O, Evans T, Kallam A. Fenbendazole as a Treatment for Diffuse Large B-Cell Lymphoma. *Ann Hematol Oncol.* 2020;7(2):1284.
17. Chiang RS, Syed AB, Wright JL, Montgomery B, Srinivas S. Case Report: Fenbendazole Enhancing Anti-Tumor Effect: A Case Series. *IDCases.* 2021 Mar 18;24:e01130.
18. Thakurdesai A, Rivera-Matos L, Nagra N, Busch B, Mais DD, Cave MC. Severe Drug-Induced Liver Injury Due to Self-administration of the Veterinary Anthelmintic Medication, Fenbendazole. *ACG Case Rep J.* 2024 May 13;11(5):e01354.
19. Yamaguchi T, Shimizu J, Oya Y, Horio Y, Hida T. Drug-Induced Liver Injury in a Patient with Nonsmall Cell Lung Cancer after the Self-Administration of Fenbendazole Based on Social Media Information. *Case Rep Oncol.* 2021 Jun 17;14(2):886–91.
20. Yamane K, Indalao IL, Chida J, Yamamoto Y, Hanawa M, Kido H. Diisopropylamine Dichloroacetate, a Novel Pyruvate Dehydrogenase Kinase 4 Inhibitor, as a Potential Therapeutic Agent for Metabolic Disorders and Multiorgan Failure in Severe Influenza. *PLoS One.* 2014 May 27;9(5):e98032.
21. Dong G, Chen Q, Jiang F, Yu D, Mao Q, Xia W, et al. Diisopropylamine dichloroacetate enhances radiosensitization in esophageal squamous cell carcinoma by increasing mitochondria-derived reactive oxygen species levels. *Oncotarget.* 2016 Oct 18;7(42):68170–8.
22. Su L, Zhang H, Yan C, Chen A, Meng G, Wei J, et al. Superior anti-tumor efficacy of diisopropylamine dichloroacetate compared with dichloroacetate in a subcutaneous transplantation breast tumor model. *Oncotarget.* 2016 Oct 4;7(40):65721–31.
23. Herbert V. Pangamic acid (“vitamin B15”). *Am J Clin Nutr.* 1979 Jul;32(7):1534–40.
24. Kraushaar AE, Schunk RW, Thym HF. [On the pharmacology of diisopropylamines]. *Arzneimittelforschung.* 1963 Feb;13:109–17. German.

25. Moser W, Schindler C, Keiser J. Drug Combinations Against Soil-Transmitted Helminth Infections. *Adv Parasitol.* 2019;103:91–115.
26. Jasmer DP, Yao C, Rehman A, Johnson S. Multiple lethal effects induced by a benzimidazole anthelmintic in the anterior intestine of the nematode *Haemonchus contortus*. *Mol Biochem Parasitol.* 2000 Jan 5;105(1):81–90.
27. Gao P, Watson J. Unexpected Antitumorigenic Effect of Fenbendazole when Combined with Supplementary Vitamins. *J Am Assoc Lab Anim Sci.* 2008 Nov;47(6):37-40.
28. Dogra N, Mukhopadhyay T. Impairment of the Ubiquitin-Proteasome Pathway by Methyl N-(6-Phenylsulfanyl-1H-benzimidazol-2-yl)carbamate Leads to a Potent Cytotoxic Effect in Tumor Cells. *J Biol Chem.* 2012 Aug 31;287(36):30625–40.
29. Abuetabh Y, Wu HH, Chai C, Al Yousef H, Persad S, Sergi CM, et al. DNA damage response revisited: the p53 family and its regulators provide endless cancer therapy opportunities. *Exp Mol Med.* 2022 Oct;54(10):1658–69.
30. Williams AB, Schumacher B. p53 in the DNA-Damage-Repair Process. *Cold Spring Harb Perspect Med.* 2016 May 2;6(5):a026070.
31. Rodriguez-Pastrana I, Birli E, Coutts AS. p53-dependent DNA repair during the DNA damage response requires actin nucleation by JMY. *Cell Death Differ.* 2023 Jul;30(7):1636–47.
32. Herrero A, Rojas E, Misiewicz-Krzeminska I, Krzeminski P, Gutiérrez N. Molecular Mechanisms of p53 Deregulation in Cancer: An Overview in Multiple Myeloma. *Int J Mol Sci.* 2016 Nov 30;17(12):2003.
33. Park D, Lee JH, Yoon SP. Anti-cancer effects of fenbendazole on 5-fluorouracil-resistant colorectal cancer cells. *Korean J Physiol Pharmacol.* 2022 Sep 1;26(5):377–87.
34. Park D. Fenbendazole Suppresses Growth and Induces Apoptosis of Actively Growing H4IIE Hepatocellular Carcinoma Cells via p21-Mediated Cell-Cycle Arrest. *Biol Pharm Bull.* 2022 Feb 1;45(2):242–5.
35. Sultana T, Jan U, Lee H, Lee H, Lee JI. Exceptional Repositioning of Dog Dewormer: Fenbendazole Fever. *Curr Issues Mol Biol.* 2022 Oct 17;44(10):4977–86.
36. Cooper GM. *The Cell: A Molecular Approach.* 2nd ed. Sunderland (MA): Sinauer Associates; 2000.
37. Warburg O. The Metabolism of Carcinoma Cells. *J Cancer Res.* 1925 Mar;9(1):148–63.

38. Mrkvová Z, Uldrijan S, Pombinho A, Bartůněk P, Slaninová I. Benzimidazoles Downregulate Mdm2 and MdmX and Activate p53 in MdmX Overexpressing Tumor Cells. *Molecules*. 2019 Jun 7;24(11):2152.
39. KalantarMotamedi Y, Ejeian F, Sabouhi F, Bahmani L, Nejati AS, Bhagwat AM, et al. Transcriptional drug repositioning and cheminformatics approach for differentiation therapy of leukaemia cells. *Sci Rep*. 2021 Jun 15;11(1):12537.
40. Jang J, Lee K, Koh B. Investigation of benzimidazole anthelmintics as oral anticancer agents. *Bull Korean Chem Soc*. 2022 May;43(5):750–6.
41. Peng Y, Pan J, Ou F, Wang W, Hu H, Chen L, et al. Fenbendazole and its synthetic analog interfere with HeLa cells' proliferation and energy metabolism via inducing oxidative stress and modulating MEK3/6-p38-MAPK pathway. *Chem Biol Interact*. 2022 Jul 1;361:109983.
42. Chang CS, Ryu JY, Choi JK, Cho YJ, Choi JJ, Hwang JR, et al. Anti-cancer effect of fenbendazole-incorporated PLGA nanoparticles in ovarian cancer. *J Gynecol Oncol*. 2023 Sep;34(5):e71.
43. Wang X, Tian W, Wang N, Yang X, Liu Z, Li L, et al. Transcriptome analysis reveals the anticancer effects of fenbendazole on ovarian cancer: an in vitro and in vivo study. *BMC Cancer*. 2024 Dec 30;24(1):1593.
44. Vlachou I, Parsonidis P, Mamagkaki A, Bouris I, Papatotiriou I. Teaching an old dog new tricks: The case of Fenbendazole. *Cancer Treat Res Commun*. 2022;32:100601.
45. Semkova S, Nikolova B, Tsoneva I, Antov G, Ivanova D, Angelov A, et al. Redox-mediated Anticancer Activity of Anti-parasitic Drug Fenbendazole in Triple-negative Breast Cancer Cells. *Anticancer Res*. 2023 Mar;43(3):1207–12.
46. Shin YB, Choi JY, Shin DH, Lee JW. Anticancer Evaluation of Methoxy Poly(Ethylene Glycol)-b-Poly(Caprolactone) Polymeric Micelles Encapsulating Fenbendazole and Rapamycin in Ovarian Cancer. *Int J Nanomedicine*. 2023 May 10;18:2209–23.
47. Kim S, Perera SK, Choi S, Rebhun RB, Seo K. G2/M arrest and mitotic slippage induced by fenbendazole in canine melanoma cells. *Vet Med Sci*. 2022 May;8(3):966–81.
48. Jung H, Kim SY, Joo HG. Fenbendazole Exhibits Differential Anticancer Effects In Vitro and In Vivo in Models of Mouse Lymphoma. *Curr Issues Mol Biol*. 2023 Nov 8;45(11):8925–38.

49. Shin HJ, Jo MJ, Jin IS, Park CW, Kim JS, Shin DH. Optimization and Pharmacokinetic Evaluation of Synergistic Fenbendazole and Rapamycin Co-Encapsulated in Methoxy Poly(Ethylene Glycol)-b-Poly(Caprolactone) Polymeric Micelles. *Int J Nanomedicine*. 2021 Jul 20;16:4873–89.
50. McKellar QA, Gokbulut C, Muzandu K, Benchaoui H. Fenbendazole Pharmacokinetics, Metabolism, and Potentiation in Horses. *Drug Metab Dispos*. 2002 Nov;30(11):1230–9.
51. Youssefi MR, Khabbazian FG, Navidi N, Rostam MMY, Giorgi M, Abouhosseini Tabari M. Pharmacokinetics and therapeutic efficacies of fenbendazole in comparison with levamisole in helminth-infected Caspian turtles (*Mauremys caspica*). *J Vet Pharmacol Ther*. 2023 May;46(3):170–6.
52. Petersen MB, Friis C. Pharmacokinetics of fenbendazole following intravenous and oral administration to pigs. *Am J Vet Res*. 2000 May;61(5):573–6.
53. Ichinose P, Miró MV, Larsen K, Lanusse C, Lifschitz A, Virkel G. Medication with fenbendazole in feed: plasma concentrations and effects on hepatic xenobiotic metabolizing enzymes in swine. *Vet Res Commun*. 2023 Jun;47(2):803–15.
54. Ichinose P, Miró MV, Larsen K, Lifschitz A, Virkel G. Unravelling drug-drug interactions in pigs: Induction of hepatic cytochrome P450 1A (CYP1A) metabolism after the in-feed medication with the anthelmintic fenbendazole. *Res Vet Sci*. 2024 Feb;167:105113.
55. Vander Heiden MG, Cantley LC, Thompson CB. Understanding the Warburg Effect: The Metabolic Requirements of Cell Proliferation. *Science*. 2009 May 22;324(5930):1029–33.
56. Arfin S, Jha NK, Jha SK, Kesari KK, Ruokolainen J, Roychoudhury S, et al. Oxidative Stress in Cancer Cell Metabolism. *Antioxidants (Basel)*. 2021 Apr 22;10(5):642.
57. Wei M, Shen X, Liu Y, Chen X, Su S, Lv X, et al. The antitumor effect of diisopropylamine dichloroacetate on non-small cell lung cancer and its influence on the tumor immune microenvironment. *Front Oncol*. 2024 Aug 29;14:1447072.
58. Brand A, Singer K, Koehl GE, Kolitzus M, Schoenhammer G, Thiel A, et al. LDHA-Associated Lactic Acid Production Blunts Tumor Immunosurveillance by T and NK Cells. *Cell Metab*. 2016 Nov 8;24(5):657–71.
59. Fischer K, Hoffmann P, Voelkl S, Meidenbauer N, Ammer J, Edinger M, et al. Inhibitory effect of tumor cell-derived lactic acid on human T cells. *Blood*. 2007 May 1;109(9):3812–9.

60. Rostamian H, Khakpoor-Koosheh M, Jafarzadeh L, Masoumi E, Fallah-Mehrjardi K, Tavassolifar MJ, et al. Restricting tumor lactic acid metabolism using dichloroacetate improves T cell functions. *BMC Cancer*. 2022 Jan 6;22(1):39.
61. Zhang IW, López-Vicario C, Duran-Güell M, Clària J. Mitochondrial Dysfunction in Advanced Liver Disease: Emerging Concepts. *Front Mol Biosci*. 2021 Nov 23;8:773343.
62. Koltai T, Fliegel L. Dichloroacetate for Cancer Treatment: Some Facts and Many Doubts. *Pharmaceuticals (Basel)*. 2024 Jun 6;17(6):744.
63. Wells RG. Cellular Sources of Extracellular Matrix in Hepatic Fibrosis. *Clin Liver Dis*. 2008 Nov;12(4):759–68.
64. Zhang X, Lee WD, Leitner BP, Zhu W, Fosam A, Li Z, et al. Dichloroacetate as a novel pharmaceutical treatment for cancer-related fatigue in melanoma. *Am J Physiol Endocrinol Metab*. 2023 Oct 1;325(4):E363–75.
65. Su D, Lin Z. Dichloroacetate attenuates the stemness of hepatocellular carcinoma cells via promoting nucleus-cytoplasm translocation of YAP. *Environ Toxicol*. 2021 May;36(5):975–83.
66. Stakišaitis D, Damanskienė E, Curkūnavičiūtė R, Juknevičienė M, Alonso MM, Valančiūtė A, et al. The Effectiveness of Dichloroacetate on Human Glioblastoma Xenograft Growth Depends on Na⁺ and Mg²⁺ Cations. Dose Response. 2021 Jan-Mar;19(1):1559325821995641.
67. Tataranni T, Piccoli C. Dichloroacetate (DCA) and Cancer: An Overview towards Clinical Applications. *Oxid Med Cell Longev*. 2019 Nov 14;2019:8201079.
68. Damanskienė E, Balnytė I, Valančiūtė A, Lesauskaitė V, Alonso MM, Stakišaitis D. The Comparative Experimental Study of Sodium and Magnesium Dichloroacetate Effects on Pediatric PBT24 and SF8628 Cell Glioblastoma Tumors Using a Chicken Embryo Chorioallantoic Membrane Model and on Cells In Vitro. *Int J Mol Sci*. 2022 Sep 9;23(18):10455.
69. Zhuang Y, Coppock JD, Haugrud AB, Lee JH, Messerli SM, Miskimins WK. Dichloroacetate and Quercetin Prevent Cell Proliferation, Induce Cell Death and Slow Tumor Growth in a Mouse Model of HPV-Positive Head and Neck Cancer. *Cancers (Basel)*. 2024 Apr 17;16(8):1525.
70. Powell SF, Mazurczak M, Dib EG, Bleeker JS, Geeraerts LH, Tinguely M, et al. Phase II study of dichloroacetate, an inhibitor of pyruvate dehydrogenase, in combination

- with chemoradiotherapy for unresected, locally advanced head and neck squamous cell carcinoma. *Invest New Drugs*. 2022 Jun;40(3):622–33.
71. Sun J, Cheng X, Pan S, Wang L, Dou W, Liu J, et al. Dichloroacetate attenuates the stemness of colorectal cancer cells via triggering ferroptosis through sequestering iron in lysosomes. *Environ Toxicol*. 2021 Apr;36(4):520–9.
 72. Al-Azawi A, Sulaiman S, Arafat K, Yasin J, Nemmar A, Attoub S. Impact of Sodium Dichloroacetate Alone and in Combination Therapies on Lung Tumor Growth and Metastasis. *Int J Mol Sci*. 2021 Nov 21;22(22):12553.
 73. Dias AS, Almeida CR, Helguero L, Duarte IF. Antitumoral Activity and Metabolic Signatures of Dichloroacetate, 6-Aminonicotinamide and Etomoxir in Breast-Tumor-Educated Macrophages. *J Proteome Res*. 2024 Dec 6;23(12):5498–510.
 74. Benbelkacem M, Moulai N, Chader H, Ouahioune W, Bourouba M. Dichloroacetate and chloroquine in combination with arsenite suppress ROS-induced oral squamous cell carcinoma (OSCC) development and improve BALB/c mice survival. *Free Radic Biol Med*. 2025 Feb;227:593–607.
 75. Feuerecker B, Biechl P, Veltkamp C, Saur D, Eisenreich W. Metabolic Response of Pancreatic Carcinoma Cells under Treatment with Dichloroacetate. *Metabolites*. 2021 May 30;11(6):350.
 76. Liu D, Wang F, Yue J, Jing X, Huang Y. Metabolism targeting therapy of dichloroacetate-loaded electrospun mats on colorectal cancer. *Drug Deliv*. 2015 Jan;22(1):136–43.
 77. Loewe S. Antagonisms and antagonists. *Pharmacol Rev*. 1957 Jun;9(2):237–42.
 78. Bliss CI. The toxicity of poisons applied jointly. *Ann Appl Biol*. 1939 Aug;26(3):585–615.
 79. Chou TC. The combination index ($CI < 1$) as the definition of synergism and of synergy claims. *Synergy*. 2018 Dec;7:49–50.
 80. Chou TC. Theoretical Basis, Experimental Design, and Computerized Simulation of Synergism and Antagonism in Drug Combination Studies. *Pharmacol Rev*. 2006 Sep;58(3):621–81.
 81. Statistics at a glance, 2022. Top 5 most frequent cancers. Number of new cases 180 480. [cited 2025 Aug 6].
 82. Massion PP, Carbone DP. The molecular basis of lung cancer: molecular abnormalities and therapeutic implications. *Respir Res*. 2003 Oct 7;4(1):12.

83. Brennan S, et al. Temporal trends in small cell lung cancer: analysis of the U.S. surveillance, epidemiology, and end results. *J Thorac Oncol.* 2023;18:S124-S125.
84. Van Schil PE, Balduyck B, De Waele M, Hendriks JM, Hertoghs M, Lauwers P. Surgical treatment of early-stage non-small-cell lung cancer. *Eur J Cancer Suppl.* 2013 Sep;11(2):110–22.
85. American Cancer Society. Treating Non-Small Cell Lung Cancer [Internet]. [cited 2025 Aug 6]. Available from:
86. Ashrafi A, Akter Z, Modareszadeh P, Berisha E, Alemi PS, et al. Current Landscape of Therapeutic Resistance in Lung Cancer and Promising Strategies to Overcome Resistance. *Cancers (Basel).* 2022 Sep 20;14(19):4562.
87. Min HY, Lee HY. Molecular targeted therapy for anticancer treatment. *Exp Mol Med.* 2022 Oct;54(10):1670–94.
88. Bowen Jones S, Chan C, Filippi AR, Harada K, Louie AV, Lindsay CR, et al. Emerging Role of Targeted Therapies Combined With Radiotherapy in Inoperable Stages I to III NSCLC: A Review From the IASLC ART Subcommittee. *J Thorac Oncol.* 2025 May;20(5):610-625.
89. Li Q, Kang C. Mechanisms of Action for Small Molecules Revealed by Structural Biology in Drug Discovery. *Int J Mol Sci.* 2020 Jul 24;21(15):5262.
90. Shih YCT, Smieliauskas F, Geynisman DM, Kelly RJ, Smith TJ. Trends in the Cost and Use of Targeted Cancer Therapies for the Privately Insured Nonelderly: 2001 to 2011. *J Clin Oncol.* 2015 Jul 1;33(19):2190–6.
91. Kichloo A, Albosta M, Dahiya D, Guidi JC, Aljadah M, Singh J, et al. Systemic adverse effects and toxicities associated with immunotherapy: A review. *World J Clin Oncol.* 2021 Mar 24;12(3):150–63.
92. Mahalingam P, Newsom-Davis T. Cancer immunotherapy and the management of side effects. *Clin Med (Lond).* 2023 Jan;23(1):56–60.
93. Foster KA, Oster CG, Mayer MM, Avery ML, Audus KL. Characterization of the A549 Cell Line as a Type II Pulmonary Epithelial Cell Model for Drug Metabolism. *Exp Cell Res.* 1998 Sep;243(2):359–66.
94. Junttila MR, de Sauvage FJ. Influence of tumour micro-environment heterogeneity on therapeutic response. *Nature.* 2013 Sep 19;501(7467):346–54.
95. Pinmai K, Chunlaratthanabhorn S, Ngamkitidechakul C, Soonthornchareon N, Hahnvajanawong C. Synergistic growth inhibitory effects of *Phyllanthus emblica* and *Terminalia bellerica* extracts with conventional cytotoxic agents: Doxorubicin and

- cisplatin against human hepatocellular carcinoma and lung cancer cells. *World J Gastroenterol.* 2008 Mar 14;14(10):1491–503.
96. Katayama Y, Yamada T, Tanimura K, Tokuda S, Morimoto K, Hirai S, et al. Adaptive resistance to lorlatinib via EGFR signaling in ALK-rearranged lung cancer. *NPJ Precis Oncol.* 2023 Jan 26;7(1):12.
 97. Morelli A, Tortelli Jr T, Pavan I, Silva F, Granato D, Peruca G, et al. Metformin impairs cisplatin resistance effects in A549 lung cancer cells through mTOR signaling and other metabolic pathways. *Int J Oncol.* 2021 Apr 8;58(6):28.
 98. Riss TL, Moravec RA, Niles AL, Duellman S, Benink HA, Worzella TJ, et al. Cell Viability Assays. In: Sittampalam GS, et al, editors. *Assay Guidance Manual* [Internet]. Bethesda (MD): Eli Lilly & Company and the National Center for Advancing Translational Sciences; 2004.
 99. Kamiloglu S, Sari G, Ozdal T, Capanoglu E. Guidelines for cell viability assays. *Food Front.* 2020 Sep 16;1(3):332–49.
 100. Schwartz GK. Development of cell cycle active drugs for the treatment of gastrointestinal cancers: a new approach to cancer therapy. *J Clin Oncol.* 2005 Jul 10;23(20):4499–508.
 101. Malumbres M. Cyclins and related kinases in cancer cells. *J BUON.* 2007;12 Suppl 1:S45-52.
 102. Sherr CJ, Roberts JM. CDK inhibitors: positive and negative regulators of G1-phase progression. *Genes Dev.* 1999 Jun 15;13(12):1501–12.
 103. Waldman T, Zhang Y, Dillehay L, Yu J, Kinzler K, Vogelstein B, et al. Cell-cycle arrest versus cell death in cancer therapy. *Nat Med.* 1997 Sep;3(9):1034–6.
 104. Iwaloye O, Ottu PO, Olawale F, Babalola OO, Elekofehinti OO, Kikiowo B, et al. Computer-aided drug design in anti-cancer drug discovery: What have we learnt and what is the way forward? *Inform Med Unlocked.* 2023;41:101332.
 105. Elmore S. Apoptosis: a review of programmed cell death. *Toxicol Pathol.* 2007 Jun;35(4):495–516.
 106. Guerin MB, Mckernan DP, O'brien CJ, Cotter TG. Retinal ganglion cells: dying to survive. *Int J Dev Biol.* 2006;50(8):665–74.
 107. Wani AK, Akhtar N, Mir Tul G, Singh R, Jha PK, Mallik SK, et al. Targeting Apoptotic Pathway of Cancer Cells with Phytochemicals and Plant-Based Nanomaterials. *Biomolecules.* 2023 Jan 18;13(2):194.

108. Bossy-Wetzel E, Green DR. Detection of Apoptosis by Annexin V Labeling. *Methods Enzymol.* 2000;322:15–8.
109. van Engeland M, Nieland LJ, Ramaekers FC, Schutte B, Reutelingsperger CP. Annexin V-affinity assay: a review on an apoptosis detection system based on phosphatidylserine exposure. *Cytometry.* 1998 Jan 1;31(1):1–9.
110. Pajak B, Siwiak E, Sołtyka M, Priebe A, Zieliński R, Fokt I, et al. 2-Deoxy-d-Glucose and Its Analogs: From Diagnostic to Therapeutic Agents. *Int J Mol Sci.* 2019 Dec 29;21(1):234.
111. Abcam. ab136955 Glucose Uptake Assay Kit (Colorimetric). Version 16. Last updated 10 January 2018.
112. Lee TY. Lactate: a multifunctional signaling molecule. *Yeungnam Univ J Med.* 2021 Jul;38(3):183–93.
113. Walenta S, Schroeder T, Mueller-Klieser W. Lactate in Solid Malignant Tumors: Potential Basis of a Metabolic Classification in Clinical Oncology. *Curr Med Chem.* 2004 Aug;11(16):2195–204.
114. Hirschhaeuser F, Sattler UGA, Mueller-Klieser W. Lactate: A Metabolic Key Player in Cancer. *Cancer Res.* 2011 Nov 15;71(22):6921–5.
115. Walenta S, Mueller-Klieser WF. Lactate: mirror and motor of tumor malignancy. *Semin Radiat Oncol.* 2004 Jul;14(3):267–74.
116. Gatenby RA, Gillies RJ. Why do cancers have high aerobic glycolysis? *Nat Rev Cancer.* 2004 Nov;4(11):891–9.
117. Hall P, Cash J. What is the real function of the liver “function” tests? *Ulster Med J.* 2012 Jan;81(1):30–6.
118. Pandya D, Nagrajappa AK, Ravi KS. Assessment and Correlation of Urea and Creatinine Levels in Saliva and Serum of Patients with Chronic Kidney Disease, Diabetes and Hypertension- A Research Study. *J Clin Diagn Res.* 2016 Oct;10(10):ZC58–62.
119. Raff MC, Barres BA, Burne JF, Coles HS, Ishizaki Y, Jacobson MD. Programmed Cell Death and the Control of Cell Survival: Lessons from the Nervous System. *Science.* 1993 Oct 29;262(5134):695–700.
120. Vaux DL, Strasser A. The molecular biology of apoptosis. *Proc Natl Acad Sci U S A.* 1996 Mar 19;93(6):2239–44.

121. Naseri MH, Mahdavi M, Davoodi J, Tackallou SH, Goudarzvand M, Neishabouri SH. Up regulation of Bax and down regulation of Bcl2 during 3-NC mediated apoptosis in human cancer cells. *Cancer Cell Int.* 2015 May 28;15:55.
122. Wei MC, Zong WX, Cheng EHY, Lindsten T, Panoutsakopoulou V, Ross AJ, et al. Proapoptotic BAX and BAK: A Requisite Gateway to Mitochondrial Dysfunction and Death. *Science.* 2001 Apr 27;292(5517):727–30.
123. Golstein P. Controlling Cell Death. *Science.* 1997 Feb 21;275(5303):1081–2.
124. Julien O, Wells JA. Caspases and their substrates. *Cell Death Differ.* 2017 Aug;24(8):1380–9.
125. Beroske L, Van den Wyngaert T, Stroobants S, Van der Veken P, Elvas F. Molecular Imaging of Apoptosis: The Case of Caspase-3 Radiotracers. *Int J Mol Sci.* 2021 Apr 11;22(8):3948.
126. Huang JS, Yang CM, Wang JS, Liou HH, Hsieh IC, Li GC, et al. Caspase-3 expression in tumorigenesis and prognosis of buccal mucosa squamous cell carcinoma. *Oncotarget.* 2017 Oct 13;8(48):84237–47.
127. Gao H, et al. A caspase-3 activatable photoacoustic probe for in vivo imaging of tumor apoptosis. In: *Apoptosis - Healing and Disease.* IntechOpen; 2021. p. 21–57.
128. Wang Y, Yin B, Li D, Wang G, Han X, Sun X. GSDME mediates caspase-3-dependent pyroptosis in gastric cancer. *Biochem Biophys Res Commun.* 2018 Jan 1;495(1):1418–25.
129. Los M, Mozoluk M, Ferrari D, Stepczynska A, Stroh C, Renz A, et al. Activation and caspase-mediated inhibition of PARP: a molecular switch between fibroblast necrosis and apoptosis in death receptor signaling. *Mol Biol Cell.* 2002 Mar;13(3):978–88.
130. Chaitanya GV, Steven AJ, Babu PP. PARP-1 cleavage fragments: signatures of cell-death proteases in neurodegeneration. *Cell Commun Signal.* 2010 Dec 22;8:31.
131. Sherr CJ, Roberts JM. Inhibitors of mammalian G1 cyclin-dependent kinases. *Genes Dev.* 1995 May 15;9(10):1149–63.
132. Sherr CJ. The Pezcoller lecture: cancer cell cycles revisited. *Cancer Res.* 2000 Jul 15;60(14):3689–95.
133. Nevzorova YA, Trautwein C. Regulation of Cell Cycle During Liver Regeneration. In: *Liver Regeneration.* Elsevier; 2015. p. 153–66.
134. Oakes V, Wang W, Harrington B, Lee WJ, Beamish H, Chia KM, et al. Cyclin A/Cdk2 regulates Cdh1 and claspin during late S/G2 phase of the cell cycle. *Cell Cycle.* 2014;13(20):3302–11.

135. Collin F. Chemical Basis of Reactive Oxygen Species Reactivity and Involvement in Neurodegenerative Diseases. *Int J Mol Sci.* 2019 May 15;20(10):2407.
136. Lennicke C, Cochemé HM. Redox metabolism: ROS as specific molecular regulators of cell signaling and function. *Mol Cell.* 2021 Sep 16;81(18):3691–707.
137. Patel P, Chatterjee S. Innate and Adaptive Immunity. In: *Immunity and Inflammation in Health and Disease.* Elsevier; 2018. p. 3–13.
138. Świdarska E, Strycharz J, Wróblewski A, Szemraj J, Drzewoski J, Śliwińska A. Role of PI3K/AKT Pathway in Insulin-Mediated Glucose Uptake. In: *Blood Glucose Levels.* London: IntechOpen; 2020.
139. Manna P, Jain SK. PIP3 but not PIP2 increases GLUT4 surface expression and glucose metabolism mediated by AKT/PKC ζ / λ phosphorylation in 3T3L1 adipocytes. *Mol Cell Biochem.* 2013 Sep;381(1–2):291–9.
140. Makis W, Baghli I, Martinez P. Fenbendazole as an Anticancer Agent? A Case Series of Self-Administration in Three Patients. *Case Rep Oncol.* 2025 May 26;18(1):856–63.
141. Duan Q, Liu Y, Booth CJ, Rockwell S. Use of fenbendazole-containing therapeutic diets for mice in experimental cancer therapy studies. *J Am Assoc Lab Anim Sci.* 2012 Mar;51(2):224–30.
142. Xiong F, Jiang M, Chen M, Wang X, Zhang S, Zhou J, et al. Study on inhibitory effect of MaiMenDong Decoction and WeiJing Decoction combination with cisplatin on NCI-A549 Xenograft in nude mice and its mechanism. *J Cancer.* 2017;8(13):2449–55.
143. Li T, Yang XH, Shao MJ, Dong YX, Li LY, Lin CZ. Effectiveness and mechanism of cisplatin combined with PDT on human lung adenocarcinoma A549 cells transplanted tumor in nude mice. *Sci Rep.* 2025 Dec 1;15(1):15420.
144. Virkel G, Lifschitz A, Sallovitz J, Pis A, Lanusse C. Comparative hepatic and extrahepatic enantioselective sulfoxidation of albendazole and fenbendazole in sheep and cattle. *Drug Metab Dispos.* 2004 May;32(5):536–44.
145. Capece BPS, Virkel GL, Lanusse CE. Enantiomeric behaviour of albendazole and fenbendazole sulfoxides in domestic animals: Pharmacological implications. *Vet J.* 2009 Sep;181(3):241–50.
146. Kaufmann P, Engelstad K, Wei Y, Jhung S, Sano MC, Shungu DC, et al. Dichloroacetate causes toxic neuropathy in MELAS: a randomized, controlled clinical trial. *Neurology.* 2006 Feb 14;66(3):324–30.

147. Bray F, Ferlay J, Soerjomataram I, Siegel RL, Torre LA, Jemal A. Global cancer statistics 2018: GLOBOCAN estimates of incidence and mortality worldwide for 36 cancers in 185 countries. *CA Cancer J Clin*. 2018 Nov;68(6):394–424.
148. Lu T, Yang X, Huang Y, Zhao M, Li M, Ma K, et al. Trends in the incidence, treatment, and survival of patients with lung cancer in the last four decades. *Cancer Manag Res*. 2019 Jan 15;11:943–53.
149. Raisova M, Hossini AM, Eberle J, Riebeling C, Orfanos CE, Geilen CC, et al. The Bax/Bcl-2 Ratio Determines the Susceptibility of Human Melanoma Cells to CD95/Fas-Mediated Apoptosis. *J Invest Dermatol*. 2001 Aug;117(2):333–40.
150. McKellar QA, Harrison P, Galbraith EA, Inglis H. Pharmacokinetics of fenbendazole in dogs. *J Vet Pharmacol Ther*. 1990 Dec;13(4):386–92.
151. Petersen MB, Friis C. Pharmacokinetics of fenbendazole following intravenous and oral administration to pigs. *Am J Vet Res*. 2000 May;61(5):573–6.
152. Melian ME, Ibarra M, Ceballos L, Paredes AJ, Munguía B, Faccio R, et al. Improving the in vitro dissolution rate and pharmacokinetic performance of fenbendazole in sheep using drug nanocrystals. *Res Vet Sci*. 2022 Jan;142:110–6.
153. Song B, Kim KJ, Ki SH. Experience with and perceptions of non-prescription anthelmintics for cancer treatments among cancer patients in South Korea: A cross-sectional survey. *PLoS One*. 2022 Oct 20;17(10):e0275620.

Số: 84320/QĐ-SHTT.17

Hà Nội, ngày 22 tháng 05 năm 2025

QUYẾT ĐỊNH
Về việc chấp nhận đơn hợp lệ

CỤC SỞ HỮU TRÍ TUỆ

Căn cứ Quyết định số 156/QĐ-BKHCN ngày 03/3/2025 của Bộ trưởng Bộ Khoa học và Công nghệ quy định chức năng, nhiệm vụ, quyền hạn và cơ cấu tổ chức của Cục Sở hữu trí tuệ;

Căn cứ khoản 4 Điều 109 của Luật Sở hữu trí tuệ ngày 29/11/2005, được sửa đổi, bổ sung theo Luật sửa đổi, bổ sung một số điều của Luật Sở hữu trí tuệ ngày 19/6/2009, Luật sửa đổi, bổ sung một số điều của Luật kinh doanh bảo hiểm, Luật Sở hữu trí tuệ ngày 14/6/2019 và Luật sửa đổi, bổ sung một số điều của Luật Sở hữu trí tuệ ngày 16/6/2022 (sau đây gọi tắt là Luật Sở hữu trí tuệ);

Căn cứ kết quả thẩm định hình thức đơn đăng ký sáng chế:

Số đơn: 1-2025-02697;

Theo đề nghị của Giám đốc Trung tâm Thẩm định Sáng chế.

QUYẾT ĐỊNH:



Điều 1. Chấp nhận đơn hợp lệ về hình thức với những ghi nhận sau đây:

Số đơn: 1-2025-02697

Ngày nộp đơn: 22/04/2025

Người nộp đơn(*): Công ty Cổ phần Dược phẩm Thái Minh (VN)

Địa chỉ: số 3, ngõ 2, phố Thọ Tháp, phường Dịch Vọng, quận Cầu Giấy, thành phố Hà Nội

Tên sáng chế: Chế phẩm dược chứa Fenbendazole và Diisopropylamin dicloaxetat trong điều trị ung thư

Điều 2. Công bố đơn trên Công báo Sở hữu công nghiệp theo quy định tại khoản 2 Điều 110 và thẩm định nội dung để đánh giá khả năng cấp văn bằng bảo hộ trong trường hợp có yêu cầu theo quy định tại điểm a khoản 1 Điều 114 của Luật Sở hữu trí tuệ.

Điều 3. Quyết định này có hiệu lực kể từ ngày ký. Chánh Văn phòng Cục, Trưởng phòng Đăng ký, Giám đốc Trung tâm Thẩm định Sáng chế và Giám đốc Trung tâm Thông tin sở hữu công nghiệp chịu trách nhiệm thi hành Quyết định này./.

Nơi nhận:

- Như Điều 3;
- Người nộp đơn;
- Lưu: VT, HS.

KT. CỤC TRƯỞNG

PHÓ CỤC TRƯỞNG



Lê Huy Anh

SUPPLEMENT INFORMATION

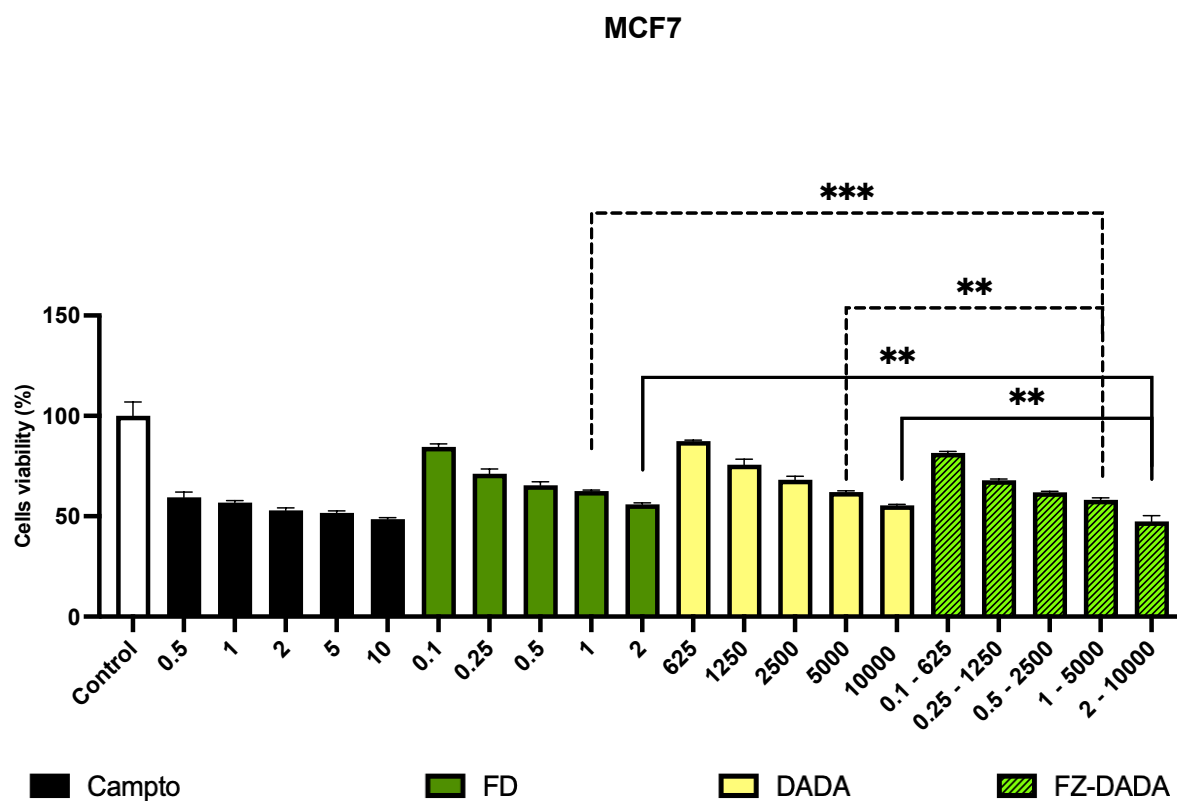


Figure S1: Cell viability of FZ-DADA in MCF7 cells. MCF7 cells were seeded at 20 000 cells/well and incubated in 37°C in 24h. FZ, DADA and its combination at various dosages were treated for 48 h, cell viability was determined by formazan crystal formation of MTT assay. The colorimetric was identified using microplate reader at 570 nm. The result was analyzed by ANOVA. * Correspond to $p < 0.05$, ** $p < 0.01$, *** $p < 0.001$. All treatments were performed in triplicate. Concentration in μM .

PC3

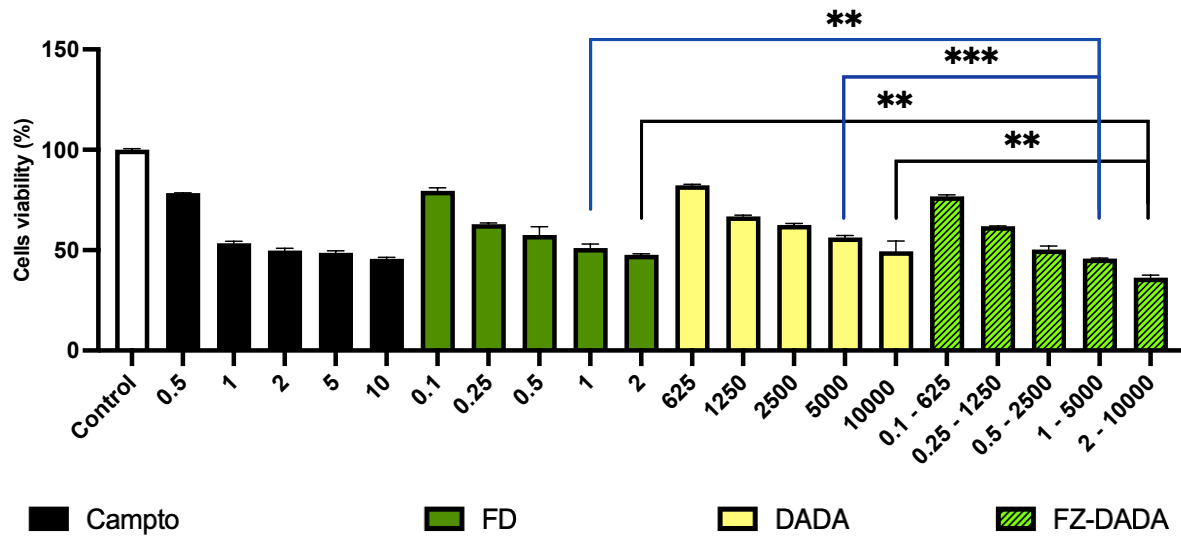


Figure S2: Cells viability of FZ-DADA in PC3 cells. PC3 cells were seed at 20 000 cells/well and incubate in 37oC in 24h . FZ, DADA and its combination at various dosages were treated for 48 h, cell viability was determined by formazan crystal formation of MTT assay. The colorimetric was identified using microplate reader at 570 nm. The result was analyzed by ANOVA. * Correspond to $p < 0.05$, ** $p < 0.01$, *** $p < 0.001$. All treatments were performed in triplicate. Concentration in μM .

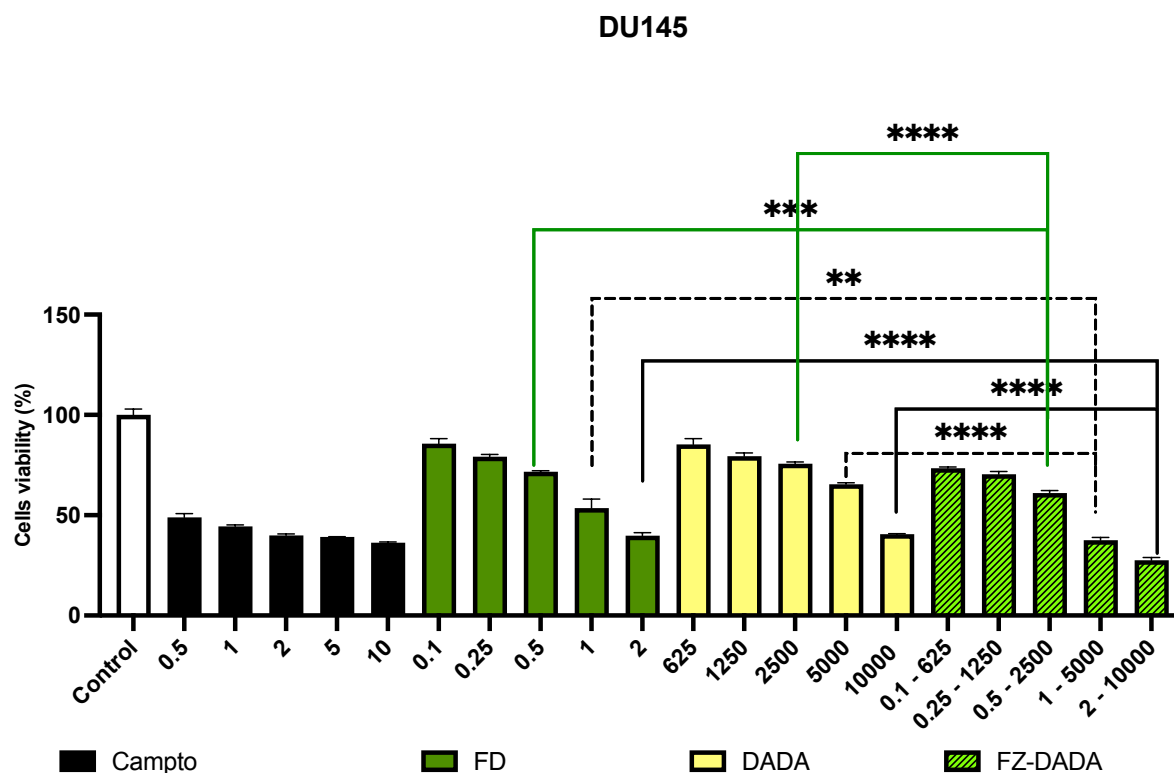


Figure S3: Cells viability of FZ-DADA in DU145 cells. DU145 cells were seed at 20 000 cells/well and incubate in 37oC in 24h . FZ, DADA and its combination at various dosages were treated for 48 h, cell viability was determined by formazan crystal formation of MTT assay. The colorimetric was identified using microplate reader at 570 nm. The result was analyzed by ANOVA. * Correspond to $p < 0.05$, ** $p < 0.01$, *** $p < 0.001$. All treatments were performed in triplicate. Concentration in μM .

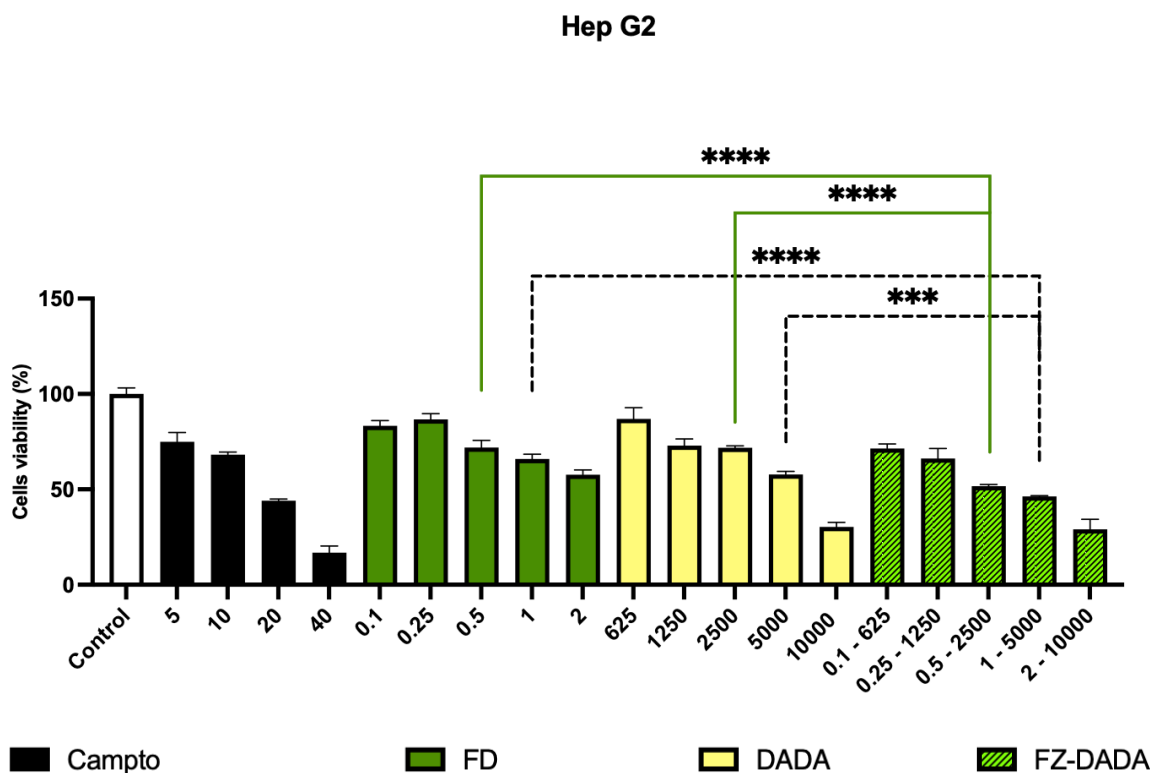


Figure S4: Cells viability of FZ-DADA in Hep G2 cells. Hep G2 cells were seed at 20 000 cells/well and incubate in 37oC in 24h . FZ, DADA and its combination at various dosages were treated for 48 h, cell viability was determined by formazan crystal formation of MTT assay. The colorimetric was identified using microplate reader at 570 nm. The result was analyzed by ANOVA. * Correspond to $p < 0.05$, ** $p < 0.01$, *** $p < 0.001$. All treatments were performed in triplicate. Concentration in μM .

LIST OF PUBLICATIONS

1. Nguyen TQ, Nguyen DH, Phan UTT, Tran PTT, LE HT, Nguyen SH, Nguyen J, Han BO, Hoang BX. Fenbendazole and Diisopropylamine Dichloroacetate Exert Synergistic Anti-cancer Effects by Inducing Apoptosis and Arresting the Cell Cycle in A549 Lung Cancer Cells. *Anticancer Res.* 2024 Nov;44(11):4761-4772. DOI: 10.21873/anticancerres.17302. PMID: 39477286.
2. Jolie nguyen, Thai Q. Nguyen, Bo Han, Ba X. Hoang. Oral Fenbendazole for Cancer Therapy in Humans and Animals. *Anticancer Research* Sep 2024, 44 (9) 3725-3735; DOI: 10.21873/anticancerres.17197
3. Thai Q. Nguyen, Uyen T. T. Phan, Mao V. Can, Bo Han, Dang H. Nguyen and Ba X. Hoang. Synergistic Anti-Tumor Effect of Fenbendazole and Diisopropylamine Dichloroacetate in Immunodeficient BALB/c Nude Mice Transplanted with A549 Lung Cancer Cells- *Translational Lung Cancer Research*, DOI: 10.21037/tlcr-2024-1272

Review

Oral Fenbendazole for Cancer Therapy in Humans and Animals

JOLIE NGUYEN¹, THAI Q. NGUYEN², BO HAN³ and BA X. HOANG³

¹School of Pharmacy, University of Pittsburgh, Pittsburgh, PA, U.S.A.;

²Life Science Department, University of Science and Technology of Hanoi, Hanoi, Vietnam;

³Nimni-Cordoba Tissue Engineering and Drug Discovery Lab, Department of Surgery, Keck School of Medicine of University of Southern California, Los Angeles, CA, U.S.A.

Abstract. Fenbendazole is a benzimidazole anthelmintic agent commonly used to treat animal parasitic infections. In humans, other benzimidazoles, such as mebendazole and albendazole, are used as antiparasitic agents. Since fenbendazole is not currently approved by the FDA or EMA, its pharmacokinetics and safety in humans have yet to be well-documented in medical literature. Despite this, insights can be drawn from existing *in vitro* and *in vivo* animal studies on its pharmacokinetics. Given the low cost of fenbendazole, its high safety profile, accessibility, and unique anti-proliferative activities, fenbendazole would be the preferred benzimidazole compound to treat cancer. To ensure patient safety in the repurposing use of fenbendazole, it is crucial to perform clinical trials to assess its potential anticancer effects, optimal doses, therapeutic regimen, and tolerance profiles. This review focuses on the pharmacokinetics of orally administered fenbendazole and its promising anticancer biological activities, such as inhibiting glycolysis, down-regulating glucose uptake, inducing oxidative stress, and enhancing apoptosis in published experimental studies. Additionally, we evaluated the toxicity profile of fenbendazole and discussed possibilities for improving the bioavailability of the drug, enhancing its efficacy, and reducing potential toxicity.

Fenbendazole, also known as methyl N-(6-phenylsulfanyl-1H-benzimidazole-2-yl), is currently used as an antiparasitic

Correspondence to: Ba X. Hoang, MD, Ph.D., Nimni-Cordoba Tissue Engineering and Drug Discovery Lab, Department of Surgery, Keck School of Medicine of University of Southern California, 1333 San Pablo Street, BMT-302, Los Angeles, CA, U.S.A. E-mail: baxuanho@usc.edu

Key Words: Fenbendazole, fenbendazole pharmacokinetics, cancer treatment, repurposed drugs, glycolysis inhibitors, review.



This article is an open access article distributed under the terms and conditions of the Creative Commons Attribution (CC BY-NC-ND) 4.0 international license (<https://creativecommons.org/licenses/by-nc-nd/4.0>).

therapeutic agent in dogs and other animals. In humans, other benzimidazoles, such as mebendazole and albendazole, are used as antiparasitic agents (1). Fenbendazole exerts its antiparasitic effects primarily in the anterior intestine by depolymerizing microtubules, inhibiting intestinal secretory vesicle transport. Fenbendazole binds to beta-tubulin in parasites, causing microtubule destabilization and hindering tubulin polymerization. This destabilization disrupts cellular function, such as glucose uptake, thereby affecting the energy management of parasites. Due to its poor absorption by oral administration, fenbendazole is particularly effective for targeting intestinal parasites (2).

In August 2016, fenbendazole garnered global attention as a potential anti-cancer therapy following the complete recovery success story of Joe Tippens, who was diagnosed with small-cell lung cancer. At the time, Tippens was undergoing a clinical trial for a novel anti-cancer drug. Meanwhile, under the guidance of a veterinarian, Tippens began self-administering 222 mg fenbendazole orally, along with vitamin E supplements, CBD oil, and bioavailable curcumin. After three months of self-administration, a PET scan revealed no detectable cancer cells in his body. Notably, Tippens was the only patient cured of cancer among the 1,100 clinical trial participants (3). While the Joe Tippens case is compelling, it remains an anecdotal report. It underscores the need for rigorous clinical trials to validate the efficacy and safety of fenbendazole as an anti-cancer therapy.

The anti-cancer activity of fenbendazole has been studied across many cell lines, demonstrating anti-tumor effects against multiple cancer types (Table I) (4-7). Additionally, fenbendazole has shown efficacy against 5-FU, paclitaxel, and docetaxel-resistant cancer cells (5, 8, 9). Compared to albendazole, fenbendazole was more effective against 5-FU-resistant colorectal cells, likely due to its intervention in glycolysis (5).

Although fenbendazole exhibits promising anti-cancer effects, experimental studies indicated its poor water solubility has hindered its therapeutic performance. When

Table I. Studies of fenbendazole in vivo and in vitro cell lines.

Cancer type; Cell lines	Experimental model	Fenbendazole dose	Results	References
Skin cancer; A375	<i>In vitro</i>	1.2, and 4 μM for 24-48 hours	Increased levels of γH2AX , indicating DNA damage. Confirmation of antiproliferative activity of fenbendazole, microtubule disruption, induced cell cycle arrest at G_2/M phase. Increase of p53 activity by down-regulating Mdm2 and MdmX expression.	(35)
Lung cancer; A549, H460, and H1299 cells	<i>In vitro</i>	0.001, 0.01, 0.1, 1, 10, and 100 μM for 48 hours.	50% tumor inhibition at 1 μM . Tubulin destabilization activity was observed at 1 and 10 μM . Induced cell cycle arrest in the G_2/M phase.	(10)
Non-small cell lung cancer; H460 and A549 cells in <i>nu/nu</i> mice	<i>In vitro</i> and <i>in vivo</i>	<i>In vitro</i> : 1 μM for 48 hours <i>In vivo</i> : 1 mg/ mouse, <i>p.o.</i> , every second day for 12 days	Significant reduction in number of tumor cell colonies. Reduction of tumor size and weight. Confirmation of microtubule disruption, induced cell cycle arrest in G_2/M phase.	(4)
Non-small cell lung cancer; A549, H460	<i>In vitro</i>	1 μM for 48 hours	Observed tumor growth inhibition and apoptotic cancer cell death, possibly by inhibiting proteasomal function. Fenbendazole demonstrated cytotoxicity towards tumor cells but retained non-toxicity to normal cells. Observed p53 induction and up-regulation of p53 target genes.	(58)
Cervical cancer; HeLa, C-33A, CaSki	<i>In vitro</i>	0.1, 1, 10 μM for 48 hours	Fenbendazole inhibited tumor colony formation and induced cell apoptosis and arrest. It was more toxic to HeLa cells and less toxic to normal cells. Down-regulation of MMP2 and MMP9 expression inhibited HeLa cell migration and invasion.	(37)
Colorectal cancer; SNU-C5	<i>In vitro</i>	0.50 μM for 3 days	Triggered cancer cell apoptosis through mitochondrial injury and the caspase 3-PARP pathway. Increased p53 expression, leading to p53-mediated apoptosis.	(5)
Colorectal cancer; SNU-C5/5-FU resistant cells	<i>In vitro</i>	4.09 μM for 3 days	Triggered cancer cell apoptosis without affecting p53 expression. Enhanced p53-independent apoptosis and ferroptosis-augmented apoptosis.	(5)
Lymphoma; P493-6B cells in SCID mice	<i>In vivo</i> and <i>in vitro</i>	150 ppm fenbendazole, with diet and/or with vitamins	Observed low anti-cancer effect when fenbendazole was administered alone. Tumor growth inhibition was higher in mice administered fenbendazole with a vitamin-supplemented diet.	(59)
Leukemia; HL60 in mice	<i>In vivo</i> and <i>in vitro</i>	0.1, 0.2, and 0.5 μM for 1-6 days	Higher concentrations of fenbendazole led to apoptosis. In as little as 3 days, lower concentrations (0.1 μM) caused leukemia cells to convert to granulocytes and induced apoptosis. At 72 hours, fenbendazole exhibited 14.5-fold selectivity in killing HL60 cells over healthy human bone marrow stem (BMSC) cells.	(6)
Hepatocellular carcinoma; H4IIE cells	<i>In vitro</i>	1.25 μM for 48 hours	Growth suppression in cancer cells actively growing. Induced p21-mediated apoptosis in tumor cells.	(7)
Breast cancer; MCF-7	<i>In vitro</i>	1.2, and 4 μM for 48 hours	Increased levels of γH2AX , indicating DNA damage. Confirmation of antiproliferative activity of fenbendazole, microtubule disruption, induced cell cycle arrest at G_2/M phase. Increase of p53 activity by down-regulating Mdm2 and MdmX expression.	(35)

Table I. Continued

Table I. *Continued*

Cancer type; Cell lines	Experimental model	Fenbendazole dose	Results	References
Breast cancer; EMT6 mouse mammary tumor cells in female BALB/cRw mice	<i>In vitro</i> and <i>in vivo</i>	0.11, 0.33, 1.0, and 3.0 μ M for 8 days <i>in vitro</i> 150 ppm in diet and 50 mg/kg/day, <i>i.p.</i> for 2 days <i>in vivo</i>	Higher drug concentrations demonstrated cytotoxicity towards tumors and high tumor inhibition. Tumor appearance also changed, suggested to be due to disruption of tubulin microtubule equilibrium. No change in tumor growth or metastatic pattern. No change in tumors with radiation.	(27)

administered orally, fenbendazole struggles to reach systemic circulation and, subsequently, the therapeutic levels necessary to impact tumors (10-12). Addressing pharmacokinetic limitations is crucial to repurposing fenbendazole for cancer treatment.

This review focuses on the pharmacokinetics of fenbendazole when administered orally and its promising anticancer biological activities, such as inhibiting glycolysis, down-regulating glucose uptake, inducing oxidative stress, and enhancing apoptosis. In addition, we evaluate the toxicity profile of fenbendazole and discuss possibilities for improving the bioavailability of the drug, enhancing its efficacy, and reducing potential toxicity. This comprehensive review aims to provide a detailed understanding of fenbendazole's potential as a repurposed anti-cancer agent and outline the necessary steps for its clinical application.

Anti-cancer Mechanisms and Targets of Fenbendazole

Studies attribute the anti-cancer mechanisms of fenbendazole to increasing p53 activation, inhibiting the GLUT1 transporter and hexokinase, and reducing glucose uptake in cancer cells (4). Enhanced glycolysis is a crucial signal of tumor progression (13-15). Under anaerobic conditions, glycolysis produces lactate, which increases acidification in the tumor microenvironment and leads to drug resistance (16). Metabolic disturbances, such as glutamine overuse, further enhance glycolysis, creating a feedback loop for tumor growth (15, 17). Fenbendazole has been found to inhibit glucose uptake, resulting in reduced lactate levels (4). Thus, fenbendazole can serve as a viable treatment for drug-resistant cancer cells.

Fenbendazole exhibits several other mechanisms contributing to its anti-cancer effects, primarily by disrupting energy metabolism. It functions as a microtubule destabilizing agent, impairs proteasomal function, and inhibits glucose metabolism. Glucose, a primary energy source for tumor cells, is metabolized through aerobic

glycolysis and delivered across the cell membrane *via* the GLUT1 transporter (18). Unlike normal cells, cancer cells perform glycolysis to metabolize glucose to lactate even under aerobic conditions (13, 16, 19). Although aerobic glycolysis is not an efficient method of supplying energy and appears to produce less ATP than oxidative phosphorylation, it provides essential materials for tumor cell growth, such as nucleotides, amino acids, and lipids (20, 21). Additionally, the ATP/ADP and NADH/NAD⁺ ratios in tumor cells remain high, indicating sufficient ATP supply through glycolytic tumor metabolism (22).

The GLUT1 transporter has been highly expressed in 99% of patients with squamous cell carcinoma and 50% of patients with adenocarcinoma (23-25), leading to being proposed as a promising therapeutic target in cancer therapy (26). Fenbendazole induces mitochondrial translocation of p53, indicating activation of the p53-p21 pathway, which inhibits GLUT transporter expression and prevents glucose uptake in cancer cells (4). Through p53 activation, fenbendazole is believed to impede hexokinase II (HKII) (4, 7), the first glycolytic pathway enzyme critical for cancer cell growth. However, another study did not observe inhibition of HKII activity at 1 and 10 μ M fenbendazole (10). As a primary enzyme in glucose metabolism, the inhibition of HKII would prevent tumor development (4, 27, 28). Therefore, fenbendazole's actions on HKII warrant further exploration. Thus, through targeting GLUT1, HKII, and glycolysis, fenbendazole can lead to cancer cell starvation and reverse drug resistance, aiding cancer treatment.

In addition to glycolysis inhibition, fenbendazole induces apoptosis in cancer cells (4-7). In colorectal cancer (CRC) cells, fenbendazole triggers apoptosis through mitochondrial injury and the caspase 3-PARP pathway. In wild-type CRC, fenbendazole activates p53-mediated apoptosis by increasing p53 expression. Additionally, it induces necrosis, autophagy, and ferroptosis. In 5-FU-resistant CRC, fenbendazole triggers apoptosis without affecting p53 expression, likely enhancing p53-independent ferroptosis-augmented apoptosis (5).

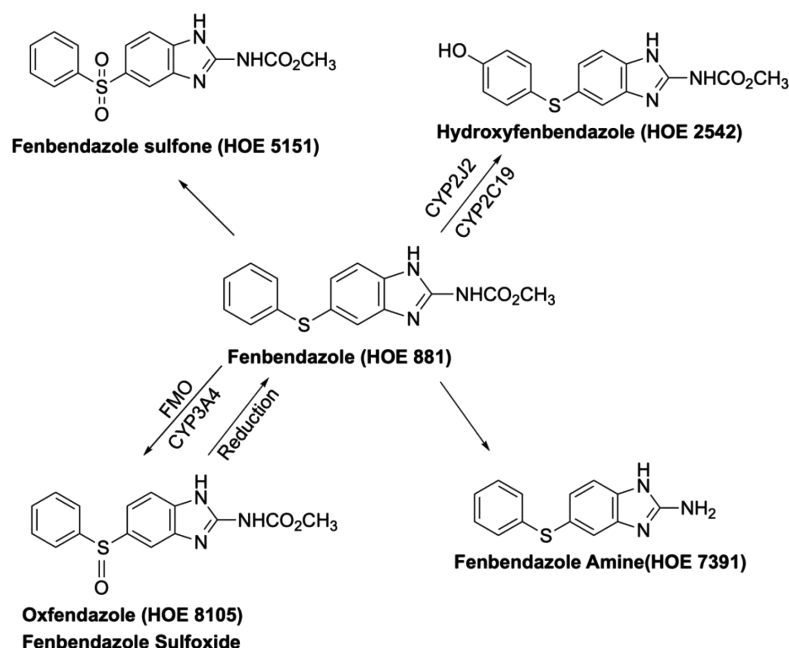


Figure 1. The metabolites of fenbendazole. Structures based on the metabolic scheme shown in the Fenbendazole UN FAO document (42).

Fenbendazole also acts as a microtubule destabilizing agent. Microtubule-targeting agents are promising cancer treatments due to the microtubules' roles in mitosis, cell structure maintenance, and other cellular events (29-33). Some cancer therapy drugs inhibit microtubule polymerization (vincristine, vinblastine), while others stabilize microtubules (paclitaxel, docetaxel), leading to apoptosis and metaphase arrest (34). Fenbendazole shows microtubule depolymerizing activity in human cancer cell lines and demonstrates anticancer effects *in vitro* and *in vivo* (4, 10, 35). Fenbendazole induces cell cycle arrest in the G₂/M phase (4, 36) and demonstrates tubulin destabilization activity at concentrations of 1 and 10 μ M, with more cell cycle arrest demonstrated at higher concentrations (10 μ M) (10).

When administered orally at micromolar concentrations, fenbendazole induces cytotoxicity and effectively blocks cancer cell growth. Fenbendazole also causes oxidative stress and activates the MEK3/6-p38MAPK pathway, inhibiting cancer cell proliferation and enhancing apoptosis. Fenbendazole reduces toxicity to normal cells while maintaining its anti-cancer effects of impairing energy metabolism and restraining cancer cell migration and invasion (37). Beyond oncology, fenbendazole shows potential in treating pulmonary fibrosis by inhibiting the progression of bleomycin-induced lung fibrosis (36).

Pharmacokinetics of Fenbendazole

Given that fenbendazole has not been approved for regulatory use in humans, pharmacokinetic data for this drug is limited. While no clinical trials have tested fenbendazole in humans, insights can be drawn from *in vitro* and *in vivo* animal studies. The FDA recently granted a fast-track designation for developing oxfendazole, a major metabolite of fenbendazole, to treat human trichuriasis. Pharmacological studies of oxfendazole can help supplement the understanding of fenbendazole's pharmacokinetics in humans.

Fenbendazole undergoes partial absorption in the liver, where it is rapidly metabolized by flavin-monooxygenase (FMO) and CYP3A4 enzymes to become its sulfoxide derivative, oxfendazole (fenbendazole sulfoxide) (38, 39). Additionally, CYP2J2 and CYP2C19 enzymes metabolize fenbendazole into hydroxyfenbendazole (40). Another metabolic pathway converts fenbendazole into fenbendazole sulfone (41, 42) by pre-systemic and systemic metabolism (43). Although fenbendazole sulfone predominates in the plasma following administration (41), oxfendazole is the primary metabolite responsible for the biological activity of fenbendazole (44). Through systemic metabolism (43), oxfendazole is reduced back to fenbendazole (44) rather than first-pass metabolism (Figure 1) (45).

Table II. Pharmacokinetic profile of fenbendazole when administered orally to male rats at a dose of 10 mg/kg. After the peak concentration, the drug concentration remained lower than 0.1 µg/ml (10).

Parameter	Oral Fenbendazole (10 mg/kg)
T _{max} (h)	0.25±0.00
T _{1/2}	8.23±2.49
C _{max} (µg/ml)	0.32±0.24
AUC _{last} (µg·h/ml)	0.73±0.05
AUC _∞ (µg·h/ml)	0.88±0.17

In male rats, the maximum concentration of fenbendazole was observed to be 0.32 µg/ml (Table II) (10). After hepatic metabolism, fenbendazole and its metabolites are excreted via the feces and urine. A study performed in cattle found that 36% of orally administered fenbendazole was recovered in the feces, with none in urine. When administered

intravenously, over 50% of the fenbendazole dose was excreted as hydroxyfenbendazole (46).

Due to its low water solubility and permeability of 0.3 µg/ml (11), fenbendazole struggles to reach systemic circulation at levels sufficient to affect tumors. Its drug release rate is 5% within 15 min and 81% within an hour (12).

Safety and Toxicity

In animals, fenbendazole demonstrated a high safety margin and low toxicity. A safety profile study of fenbendazole administered to cattle found that fenbendazole was well-tolerated, even when administered at six times the prescribed dose and three times the recommended duration (47). In rodents, its lethal dose (LD₅₀) exceeded 10 g/kg, which is 1,000 times the therapeutic level. Lifetime studies in rats indicated no maternal or reproductive toxicity and no carcinogenesis. However, morphologic changes in hepatocellular hypertrophy and hyperplasia were observed (48).

Table III. Studies exploring various vehicles to improve the solubility of fenbendazole.

Vehicle	Description & Study Results	Reference
PLGA nanoparticles (FZ-PLGA-NPs)	Fenbendazole-encapsulated poly(D,L-lactide-co-glycolide) acid (PLGA) nanoparticles (FZ-PLGA-NPs) have shown increased anti-cancer effects of fenbendazole on epithelial ovarian cancer (EOC) cells both <i>in vitro</i> and <i>in vivo</i> . In xenograft mouse models, <i>i.v.</i> injections of FZ-PLGA-NPs significantly reduced tumor weight compared to the control group. FZ-PLGA-NPs decreased cancer cell proliferation in patient-derived xenograft models as well.	(8)
DMSO (100% DMSO) or DNTC (DMSO, NMP, Tween-80 and Cremophor mix in 1:3:2:2 ratio)	Fenbendazole-DNTC and Fenbendazole-DMSO demonstrated significantly higher cytotoxicity than control groups of DNTC and DMSO alone. DNTC and DMSO can be vehicles to improve the solubility of fenbendazole. Fenbendazole alone significantly inhibited tumor growth more than paclitaxel. Moreover, Fenbendazole-DNTC was found to be significantly more cytotoxic than paclitaxel. Fenbendazole itself was the only drug more significantly cytotoxic and apoptotic in both paclitaxel-resistant prostate cancer cell lines compared to paclitaxel, clofazimine, fluspirilene, suloctidil, and niclosamide.	(41, 53)
Methyl-β-cyclodextrin	Fenbendazole complexed with methyl-β-cyclodextrin at a 1:1 ratio. Methyl-β-cyclodextrin, when complexed with fenbendazole, can increase the water solubility of fenbendazole to 20.21 mg/ml.	(11)
Fenbendazole-loaded Soluplus [®] micelles	Fenbendazole was encapsulated in low-toxicity Soluplus [®] micelles for injection. <i>In vitro</i> pharmacokinetic studies showed that fenbendazole-loaded Soluplus [®] micelles had lower total clearance and volume of distribution, along with higher AUC and plasma concentration at T ₀ . Fenbendazole-loaded Soluplus [®] micelles released fenbendazole more gradually than the Fen-25% Cremophor El [®] /EtOH solution. At ≤72 h, the release rate for Fenbendazole-loaded Soluplus [®] micelles was 50.4% and 75.1% for the Fen-25% Cremophor El [®] /EtOH solution. An <i>in vivo</i> toxicity assay revealed that Fen-loaded Soluplus [®] micelles did not induce severe toxicity to normal cells.	(60)
Supplementary vitamins (A/Retinol, D3/Cholecalciferol, E, K3, B1, B2, B6, B12, folate, niacin, pantothenic acid, biotin)	Twenty-four-week-old SCID (human lymphoma cell line) mice were divided into four treatment groups: standard diet only, diet with fenbendazole, vitamin-supplemented diet, and vitamin-supplemented diet with fenbendazole. The group of SCID mice treated with a vitamin-supplemented diet with fenbendazole exhibited significant inhibition of tumor growth. This is believed to be due to the antimicrotubular activity of fenbendazole. Additionally, taking fenbendazole with food may have increased its absorption.	(59)
Cocrystals (cinnamic, benzoic, and salicylic acids)	Among the tested cocrystals, fenbendazole-salicylic acid exhibited the highest cumulative drug release of 38% in 15 min. In under 1 h, fenbendazole-salicylic showed a 100% drug release, while pure fenbendazole had a drug release of 81% at 1 h.	(12)

Oxfendazole, a major metabolite of fenbendazole, is well tolerated in humans. A randomized, double-blind, placebo-controlled, phase I study conducted in 70 healthy participants evaluated multiple ascending oral doses of oxfendazole, from 0.5 to 60 mg/kg. The dose study found acceptable safety and tolerability profiles, even after 5 repeated daily doses of up to 15 mg/kg. This clinical trial also characterized the disposition of fenbendazole, describing the drug as a one-compartment model with formation rate-limited elimination (43).

Although studies of the pharmacokinetics of oxfendazole can give insight into the safety of fenbendazole, it should be noted that the solubility of oxfendazole is 44.12 µg/ml (49), demonstrating much higher pharmacokinetic exposure than the solubility of fenbendazole at 0.3 µg/ml (11), even after the same oral dose (50). Further clinical studies using fenbendazole are needed to accurately assess its safety, toxicity, and therapeutic dose in humans.

Increasing Fenbendazole Solubility and Absorption

A significant challenge in using fenbendazole is its low water solubility and bioavailability. Improving the water solubility is essential, as it would reduce the amount of drug needed to reach the same therapeutic effect. With this increase in solubility, fenbendazole can also meet the requirements for use as a systemic anticancer drug. Several studies have investigated various vehicles to overcome this low solubility limit (Table III).

Among the discussed vehicles for increasing the bioavailability of oral fenbendazole, it would be worthwhile to focus on dimethyl sulfoxide (DMSO), Salicylic acid, and methyl-β-cyclodextrin. DMSO and DNTC (DMSO, NMP, Tween-80, and Cremophor mix in a 1:3:2:2 ratio) are highly promising solvents that warrant further exploration. DMSO inhibits several cytochrome P450 subtypes (2C9, 2C19, 2E1, and 3A4) in a concentration-dependent manner (51, 52). Since 2C19 and 3A4 are known CYP450 subtypes that metabolize fenbendazole, inhibiting these enzymes would allow fenbendazole to stay in circulation at higher concentrations for longer periods. Through this increase in bioavailability, fenbendazole can prolong its effects on cancer cells. Fen-DMSO and Fen-DNTC have also been found to be cytotoxic and induce apoptosis in paclitaxel-resistant cells (53). Due to their enhanced cytotoxicity, DMSO or DNTC formulations could be beneficial in treating drug-resistant cancer types.

Another method to improve the solubility of fenbendazole would be to complex it with methyl-β-cyclodextrin at a 1:1 ratio. When fenbendazole is complexed with methyl-β-cyclodextrin, the complex can significantly increase the drug's water solubility to 20.21 mg/ml, which is 60,000 times better than the average solubility of fenbendazole. With this complex, fenbendazole can meet the water solubility

requirements (5-10 mg/ml) and could be tested in future clinical trials as a potential anti-cancer drug. Additionally, methyl-β-cyclodextrin increases the drug release rate of fenbendazole to 75% in 15 min, compared to 5% for pure fenbendazole (11).

Salicylic acid would also be an excellent vehicle to improve the drug release rate of fenbendazole. Fenbendazole-salicylic acid performed exceptionally well, achieving a 100% drug release rate in under 1 hour and a 1.052 mg/ml solubility. This significant drug release rate improvement could offer immediate therapeutic action. The enhancement in solubility is suggested to be due to intermolecular interactions such as carboxylic-carboxylic or carboxylic-amino groups forming hydrogen bonds (12).

Fenbendazole as a Cancer Therapy in Humans

Despite the lack of regulatory approval and extensive clinical trials for fenbendazole as a cancer treatment in humans, some cancer patients have self-administered the drug, as documented in case studies. Table IV discusses four case reports where fenbendazole has led to a reduction in tumor size (54, 55) and two cases (56, 57) where patients experienced drug-related hepatic dysfunction (Table IV). In both cases, despite the hepatotoxicity, patients' liver function recovered rapidly upon discontinuing fenbendazole.

Due to its accessibility over the counter at a relatively low price, patients have turned to fenbendazole as an at-home treatment for cancer. As the published case reports observed, the most common self-administered regimen involves taking 1 gram of fenbendazole orally once daily for three consecutive days, followed by four days off treatment (54-57). However, the use of fenbendazole for cancer therapy in humans requires further pilot and extensive clinical trials to establish effective doses and regimens. Patients with compromised liver function, liver cirrhosis, or liver cancer should use fenbendazole with caution. Additionally, combining fenbendazole with glycolysis inhibitors and hepatoprotective pharmaceutical or nutraceutical agents can lead to synergistic therapeutic activity while reducing potential liver toxicity.

Conclusion and Perspectives

Fenbendazole's disruptive effects on energy metabolism are fascinating areas of study that could lead to significant advancements in cancer treatment. Various studies in cell lines and animals have demonstrated the efficacy of fenbendazole in inhibiting tumors and targeting drug-resistant cancer cells through glycolysis inhibition. By increasing p53 expression and impacting multiple cellular pathways that act on GLUT and HKII, fenbendazole down-

Table IV. Summarized patient case reports on the self-administration of fenbendazole for cancer.

Patient case; Cancer type	Treatment	Results	Evaluation of findings	Reference
83-year-old male patient; Stage IVa diffuse large B-cell lymphoma (DLBCL)	First 6 months: 1g fenbendazole, administered orally once per day (based on self-research). He adjusted his doses between 1 and 6 tablets/day depending on his symptoms. Months 7 and 8: Due to peripheral neuropathy, the patient reduced doses to 1-three tablets of fenbendazole, taken orally once daily. Repeated PET/CT scans revealed smaller mediastinal lymph nodes. Month 9: Followed up with oncology and had a repeated PET/CT scan, which showed improved lymphadenopathy. Months 10, 11, 12: The patient continued tapering down fenbendazole, reducing to three tablets per week. Another PET/CT scan revealed further improvement with no new lesions observed.	Repeated PET/CT scans over 12 months revealed that the patient's lymphadenopathy improved compared to previous scans. In addition, no new lesions were observed.	Physicians speculated that the regression of the patient's stage IVa DLBCL might be due to fenbendazole. However, whether this improvement is directly related to fenbendazole or other factors remains uncertain.	(54)
63-year-old Caucasian male; high-grade clear cell renal cell carcinoma (mRCC)	800 mg pazopanib was initiated; the patient had intolerable side effects and required discontinuation. Cabozantinib was initiated next, but it had limited effectiveness and intolerable side effects, requiring discontinuation. Nivolumab was initiated (three treatments of 240 mg, over one month); the patient had intolerable side effects and required discontinuation. Patient initiated 1g fenbendazole, administered orally once/day for three days/week.	Due to the side effects of immunotherapies, fenbendazole was taken as an alternative treatment. Interval MRI imaging revealed near complete resolution of left renal mass and a decrease in pancreatic head/body and right posterior iliac spine lesions.	Fenbendazole significantly reduced tumor size and had no reported side effects. At the time of the report, the patient had been taking fenbendazole with no new lesions observed for about 10 months without further continuing immune checkpoint inhibitor therapy (nivolumab).	(55)
72-year-old Caucasian male; high-grade urothelial carcinoma (HGUC)	Gamma knife radiotherapy, carboplatin, paclitaxel, and pembrolizumab combination treatments. Gemcitabine and cisplatin for six cycles over four months. Alternative therapy of 1g fenbendazole administered orally once/day for three days/week, 800 mg vitamin E orally once/day, 600 mg curcumin orally once/day, and CBD oil.	Initial combination therapies addressed the patient's brain and pulmonary metastases. However, while on pembrolizumab maintenance, the patient developed progressive retroperitoneal disease. Gem/cisplatin therapy was initially effective, leading to a near complete response. However, interval CT revealed an increase in aortocaval node size. After initiation of alternative therapy with 1g fenbendazole, serial CTs from the past nine months showed a decrease in tumor size.	Alternative therapy with fenbendazole resulted in a decrease in tumor size, achieving a complete radiographic response.	(55)

Table IV. Continued

Table IV. *Continued*

Patient case; Cancer type	Treatment	Results	Evaluation of findings	Reference
63-year-old Caucasian female; urothelial carcinoma of the bladder	Transurethral resection of bladder tumor (TURBT). Accelerated Methotrexate, Vinblastine, Doxorubicin, and Cisplatin (AMVAC) for six cycles over four months, along with concurrent 1 g fenbendazole administered orally once/day for three days/week.	Follow-up CT revealed no evidence of disease and minimal residual thickening.	Follow-up CT showed that AMVAC/Fenbendazole therapy effectively decreased disease size. The patient remains on surveillance with no disease progression.	(55)
80-year-old female with advanced non-small-cell lung cancer (NSCLC) with brain metastases	Pembrolizumab monotherapy was initiated for nine months. 1g fenbendazole was administered once/day orally for three days, followed by four days off. The patient self-administered fenbendazole for one month. After fenbendazole was discontinued, pembrolizumab therapy recommenced.	The patient's liver function tests indicated severe hepatic dysfunction, with a Naranjo Adverse Drug Reaction Probability score of 6, suggesting that fenbendazole was the probable cause. A chest CT showed no antitumor effects on the patient's lung cancer before and after 1 month of fenbendazole administration. Due to increased tumor size in her lung, pembrolizumab monotherapy was terminated.	After discontinuation of fenbendazole, the patient's liver dysfunction was resolved. No hepatic disorder relapse was observed; therefore, fenbendazole was likely responsible for the liver dysfunction. However, it is possible that pembrolizumab, in combination with fenbendazole, enhanced hepatotoxicity.	(56)
67-year-old female; history of colon cancer post-resection.	Fenbendazole is administered orally three days/week for one year to cure a precancerous skin lesion. Drug strength unknown.	A liver biopsy revealed severe drug-induced liver injury (DILI) with a RUCAM score of 9, suggesting a high probability that fenbendazole was the cause. Consequently, fenbendazole was discontinued.	Histology confirmed that fenbendazole was likely responsible for the patient's severe DILI. After discontinuation of fenbendazole, the patient's hepatocellular injury pattern improved.	(57)

regulates glucose uptake, causing cancer cell starvation and enhancing apoptosis. Through this mechanism, fenbendazole effectively eliminates cancer cells while exhibiting no or acceptable minimal toxicity to normal cells.

Improving the solubility of fenbendazole is crucial for enhancing its bioavailability and reducing the drug needed to reach therapeutic effects. Future studies could compare these vehicles and test various concentrations to optimize fenbendazole's solubility and drug release. Additionally, combining fenbendazole with hepatoprotective pharmaceutical, nutraceutical, and glycolysis inhibitors can be a promising approach to improving the drug's effectiveness while reducing its potential reversible liver toxicity.

With its high safety profile, affordability, and minimal side effects, fenbendazole stands out as a potential option for

cancer therapy. Moreover, fenbendazole is easy to acquire and can be administered orally, offering a less invasive treatment that can increase patient adherence. Furthermore, by inhibiting glycolysis in cancer cells and preventing lactate buildup, fenbendazole surpasses albendazole and mebendazole in treating drug-resistant cells, making it the benzimidazole of choice for cancer therapy.

Despite numerous success stories using fenbendazole and the extensive research performed *in vitro* and *in vivo*, repurposing fenbendazole for cancer treatment remains non-suggested by conventional medical institutions and oncologists. Clinical trials should be funded and performed to promote the possible application of fenbendazole as an inexpensive, well-characterized, and widely available anticancer therapeutic in animals and humans.

Conflicts of Interest

All Authors declare no conflicts of interest in writing and publishing the manuscript.

Authors' Contributions

JN: Conceptualization, Visualization, Writing – original draft, Writing – review & editing; TQN: Conceptualization, Writing – review & editing; BH: Prepared the references, Writing – review & editing; BXH: Conceptualization, Supervision, Writing – review & editing. All Authors read the manuscript before submission.

Funding

The manuscript writing and submission are author-initiated with no funding.

References

- Moser W, Schindler C, Keiser J: Drug combinations against soil-transmitted helminth infections. *In: Advances in parasitology*. Academic Press, pp. 91-115, 2019.
- Jasmer DP, Yao C, Rehman A, Johnson S: Multiple lethal effects induced by a benzimidazole anthelmintic in the anterior intestine of the nematode *Haemonchus contortus*. *Mol Biochem Parasitol* 105(1): 81-90, 2000. DOI: 10.1016/S0166-6851(99)00169-3
- Edmond Man Says Cheap Drug for Dogs Cured His Cancer. Oklahoma, USA, Koco News, 2019. Available at: <https://www.koco.com/article/edmond-man-says-cheap-drug-for-dogs-cured-his-cancer/2726538> [Last accessed on June 29, 2024]
- Dogra N, Kumar A, Mukhopadhyay T: Fenbendazole acts as a moderate microtubule destabilizing agent and causes cancer cell death by modulating multiple cellular pathways. *Sci Rep* 8(1): 11926, 2018. DOI: 10.1038/s41598-018-30158-6
- Park D, Lee JH, Yoon SP: Anti-cancer effects of fenbendazole on 5-fluorouracil-resistant colorectal cancer cells. *Korean J Physiol Pharmacol* 26(5): 377-387, 2022. DOI: 10.4196/kjpp.2022.26.5.377
- KalantarMotamedi Y, Ejeian F, Sabouhi F, Bahmani L, Nejati AS, Bhagwat AM, Ahadi AM, Tafreshi AP, Nasr-Esfahani MH, Bender A: Transcriptional drug repositioning and cheminformatics approach for differentiation therapy of leukaemia cells. *Sci Rep* 11(1): 12537, 2021. DOI: 10.1038/s41598-021-91629-x
- Park D: Fenbendazole suppresses growth and induces apoptosis of actively growing H4IIE hepatocellular carcinoma cells *via* p21-mediated cell-cycle arrest. *Biol Pharm Bull* 45(2): 184-193, 2022. DOI: 10.1248/bpb.b21-00697
- Chang CS, Ryu JY, Choi JK, Cho YJ, Choi JJ, Hwang JR, Choi JY, Noh JJ, Lee CM, Won JE, Han HD, Lee JW: Anti-cancer effect of fenbendazole-incorporated PLGA nanoparticles in ovarian cancer. *J Gynecol Oncol* 34(5): e58, 2023. DOI: 10.3802/jgo.2023.34.e58
- Duan Q, Liu Y, Booth CJ, Rockwell S: Use of fenbendazole-containing therapeutic diets for mice in experimental cancer therapy studies. *J Am Assoc Lab Anim Sci* 51(2): 224-230, 2012.
- Jang J, Lee K, Koh B: Investigation of benzimidazole anthelmintics as oral anticancer agents. *Bull Korean Chem Soc* 43(5): 750-756, 2022. DOI: 10.1002/bkcs.12519
- Ding Y, Zhang Z, Ding C, Xu S, Xu Z: Preparation and evaluation of fenbendazole methyl- β -cyclodextrin inclusion complexes. *BMC Vet Res* 20(1): 214, 2024. DOI: 10.1186/s12917-024-04056-1
- Priyanka KB, Ramya TS, Swarnalatha K, Sushmitha G, Ara A, Srujana TS, Swapna B: Cocrystals of fenbendazole with enhanced *in vitro* dissolution performance. *Eur Chem Bull* 12(8): 9056-9061, 2023. DOI: 10.31838/ecb/2023.12.Si8.826
- Phan LM, Yeung SC, Lee MH: Cancer metabolic reprogramming: importance, main features, and potentials for precise targeted anti-cancer therapies. *Cancer Biol Med* 11(1): 1-19, 2014. DOI: 10.7497/j.issn.2095-3941.2014.01.001
- Seyfried TN, Flores RE, Poff AM, D'Agostino DP: Cancer as a metabolic disease: implications for novel therapeutics. *Carcinogenesis* 35(3): 515-527, 2014. DOI: 10.1093/carcin/bgt480
- Reinfeld BI, Madden MZ, Wolf MM, Chytil A, Bader JE, Patterson AR, Sugiura A, Cohen AS, Ali A, Do BT, Muir A, Lewis CA, Hongo RA, Young KL, Brown RE, Todd VM, Huffstater T, Abraham A, O'Neil RT, Wilson MH, Xin F, Tantawy MN, Merryman WD, Johnson RW, Williams CS, Mason EF, Mason FM, Beckermann KE, Vander Heiden MG, Manning HC, Rathmell JC, Rathmell WK: Cell-programmed nutrient partitioning in the tumour microenvironment. *Nature* 593(7858): 282-288, 2021. DOI: 10.1038/s41586-021-03442-1
- Bose S, Le A: Glucose metabolism in cancer. *In: The heterogeneity of cancer metabolism*. Cham, Switzerland, Springer, pp. 3-12, 2018.
- Damiani C, Colombo R, Gaglio D, Mastroianni F, Pescini D, Westerhoff HV, Mauri G, Vanoni M, Alberghina L: A metabolic core model elucidates how enhanced utilization of glucose and glutamine, with enhanced glutamine-dependent lactate production, promotes cancer cell growth: The WarburQ effect. *PLoS Comput Biol* 13(9): e1005758, 2017. DOI: 10.1371/journal.pcbi.1005758
- Lunt SY, Vander Heiden MG: Aerobic glycolysis: Meeting the metabolic requirements of cell proliferation. *Ann Rev Cell Dev Biol* 27(1): 441-464, 2011. DOI: 10.1146/annurev-cellbio-092910-154237
- Vander Heiden MG, Cantley LC, Thompson CB: Understanding the Warburg effect: the metabolic requirements of cell proliferation. *Science* 324(5930): 1029-1033, 2009. DOI:10.1126/science.1160809
- Pavlova NN, Thompson CB: The emerging hallmarks of cancer metabolism. *Cell Metab* 23(1): 27-47, 2016. DOI: 10.1016/j.cmet.2015.12.006
- Schiliro C, Firestein BL: Mechanisms of metabolic reprogramming in cancer cells supporting enhanced growth and proliferation. *Cells* 10(5): 1056, 2021. DOI: 10.3390/cells10051056
- Martinez-Reyes I, Chandel NS: Cancer metabolism: looking forward. *Nat Rev Cancer* 21(10): 669-680, 2021. DOI: 10.1038/s41568-021-00378-6
- Koh YW, Lee SJ, Park SY: Differential expression and prognostic significance of GLUT1 according to histologic type of non-small-cell lung cancer and its association with volume-dependent parameters. *Lung Cancer* 104: 31-37, 2017. DOI: 10.1016/j.lungcan.2016.12.003
- Goodwin J, Neugent ML, Lee SY, Choe JH, Choi H, Jenkins DMR, Ruthenborg RJ, Robinson MW, Jeong JY, Wake M, Abe H, Takeda N, Endo H, Inoue M, Xuan Z, Yoo H, Chen M, Ahn JM, Minna JD, Helke KL, Singh PK, Shackelford DB, Kim JW: The distinct metabolic phenotype of lung squamous cell carcinoma defines selective vulnerability to glycolytic inhibition. *Nat Commun* 8: 15503, 2017. DOI: 10.1038/ncomms15503

- 25 Smolle E, Leko P, Stacher-Priehse E, Brcic L, El-Heliebi A, Hofmann L, Quehenberger F, Hrzjenjak A, Popper HH, Olschewski H, Leithner K: Distribution and prognostic significance of gluconeogenesis and glycolysis in lung cancer. *Mol Oncol* 14(11): 2853-2867, 2020. DOI: 10.1002/1878-0261.12780
- 26 Sizemore ST, Zhang M, Cho JH, Sizemore GM, Hurwitz B, Kaur B, Lehman NL, Ostrowski MC, Robe PA, Miao W, Wang Y, Chakravarti A, Xia F: Pyruvate kinase M2 regulates homologous recombination-mediated DNA double-strand break repair. *Cell Res* 28(11): 1090-1102, 2018. DOI: 10.1038/s41422-018-0086-7
- 27 Duan Q, Liu Y, Rockwell S: Fenbendazole as a potential anticancer drug. *Anticancer Res* 33(2): 355-362, 2013.
- 28 Patra KC, Wang Q, Bhaskar PT, Miller L, Wang Z, Wheaton W, Chandel N, Laakso M, Muller WJ, Allen EL, Jha AK, Smolen GA, Clasquin MF, Robey B, Hay N: Hexokinase 2 is required for tumor initiation and maintenance and its systemic deletion is therapeutic in mouse models of cancer. *Cancer Cell* 24(2): 213-228, 2013. DOI: 10.1016/j.ccr.2013.06.014
- 29 Čermák V, Dostál V, Jelínek M, Libusová L, Kovář J, Rösel D, Brábek J: Microtubule-targeting agents and their impact on cancer treatment. *Eur J Cell Biol* 99(4): 151075, 2020. DOI: 10.1016/j.ejcb.2020.151075
- 30 Dumontet C, Jordan MA: Microtubule-binding agents: a dynamic field of cancer therapeutics. *Nat Rev Drug Discov* 9(10): 790-803, 2010. DOI: 10.1038/nrd3253
- 31 Coulop SK, Georg GI: Revisiting microtubule targeting agents: α -Tubulin and the pironetin binding site as unexplored targets for cancer therapeutics. *Bioorg Med Chem Lett* 29(15): 1865-1873, 2019. DOI: 10.1016/j.bmcl.2019.05.042
- 32 Higa GM: The microtubule as a breast cancer target. *Breast Cancer* 18(2): 103-119, 2011. DOI: 10.1007/s12282-010-0224-7
- 33 Arnst KE, Wang Y, Hwang DJ, Xue Y, Costello T, Hamilton D, Chen Q, Yang J, Park F, Dalton JT, Miller DD, Li W: A potent, metabolically stable tubulin inhibitor targets the colchicine binding site and overcomes taxane resistance. *Cancer Res* 78(1): 265-277, 2018. DOI: 10.1158/0008-5472.CAN-17-0577
- 34 Jordan M: Mechanism of action of antitumor drugs that interact with microtubules and tubulin. *Curr Med Chem Anticancer Agents* 2(1): 1-17, 2012. DOI: 10.2174/1568011023354290
- 35 Mrkvová Z, Uldrijan S, Pombinho A, Bartůňek P, Slaninová I: Benzimidazoles downregulate Mdm2 and MdmX and activate p53 in MdmX overexpressing tumor cells. *Molecules* 24(11): 2152, 2019. DOI: 10.3390/molecules24112152
- 36 Wang L, Xu K, Wang N, Ding L, Zhao W, Wan R, Zhao W, Guo X, Pan X, Yang J, Rosas I, Yu G: Fenbendazole attenuates bleomycin-induced pulmonary fibrosis in mice *via* suppression of fibroblast-to-myofibroblast differentiation. *Int J Mol Sci* 23(22): 14088, 2022. DOI: 10.3390/ijms232214088
- 37 Peng Y, Pan J, Ou F, Wang W, Hu H, Chen L, Zeng S, Zeng K, Yu L: Fenbendazole and its synthetic analog interfere with HeLa cells' proliferation and energy metabolism *via* inducing oxidative stress and modulating MEK3/6-p38-MAPK pathway. *Chem Biol Interact* 361: 109983, 2022. DOI: 10.1016/j.cbi.2022.109983
- 38 Capece BP, Virkel GL, Lanusse CE: Enantiomeric behaviour of albendazole and fenbendazole sulfoxides in domestic animals: Pharmacological implications. *Vet J* 181(3): 241-250, 2009. DOI: 10.1016/j.tvjl.2008.11.010
- 39 Virkel G, Lifschitz A, Sallovitz J, Pis A, Lanusse C: Comparative hepatic and extrahepatic enantioselective sulfoxidation of albendazole and fenbendazole in sheep and cattle. *Drug Metab Dispos* 32(5): 536-544, 2004. DOI: 10.1124/dmd.32.5.536
- 40 Wu Z, Lee D, Joo J, Shin JH, Kang W, Oh S, Lee DY, Lee SJ, Yea SS, Lee HS, Lee T, Liu KH: CYP2J2 and CYP2C19 are the major enzymes responsible for metabolism of albendazole and fenbendazole in human liver microsomes and recombinant P450 assay systems. *Antimicrob Agents Chemother* 57(11): 5448-5456, 2013. DOI: 10.1128/AAC.00843-13
- 41 McKellar QA, Gokbulut C, Muzandu K, Benchaoui H: Fenbendazole pharmacokinetics, metabolism, and potentiation in horses. *Drug Metab Dispos* 30(11): 1230-1239, 2002. DOI: 10.1124/dmd.30.11.1230
- 42 Fenbendazole. Food and Agriculture Organization. Available at: https://www.fao.org/fileadmin/user_upload/vetdrug/docs/41-4-fenbendazole.pdf [Last accessed on June 29, 2024]
- 43 Bach T, Murry DJ, Stebounova LV, Deye G, Winokur P, An G: Population pharmacokinetic model of oxfendazole and metabolites in healthy adults following single ascending doses. *Antimicrob Agents Chemother* 65(4): e02129-20, 2021. DOI: 10.1128/AAC.02129-20
- 44 Gottschall DW, Theodorides VJ, Wang R: The metabolism of benzimidazole anthelmintics. *Parasitology today*, pp. 115-124, 1990.
- 45 Oxfendazole. Food and Agriculture Organization. Available at: https://www.fao.org/fileadmin/user_upload/vetdrug/docs/41-4-oxfendazole.pdf [Last accessed on June 29, 2024]
- 46 Short CR, Barker SA, Hsieh LC, Ou SP, McDowell T, Davis LE, Neff-Davis CA, Koritz G, Beville RF, Munsiff IJ: Disposition of fenbendazole in cattle. *Am J Vet Res* 48(6): 958-961, 1987.
- 47 Muser RK, Paul JW: Safety of fenbendazole use in cattle. *Mod Vet Pract* 65(5): 371-374, 1984.
- 48 Villar D, Cray C, Zaias J, Altman NH: Biologic effects of fenbendazole in rats and mice: A review. *J Am Assoc Lab Anim Sci* 46(6): 8-15, 2007.
- 49 An G, Murry DJ, Gajurel K, Bach T, Deye G, Stebounova LV, Codd EE, Horton J, Gonzalez AE, Garcia HH, Ince D, Hodgson-Zingman D, Nomicos EYH, Conrad T, Kennedy J, Jones W, Gilman RH, Winokur P: Pharmacokinetics, safety, and tolerability of oxfendazole in healthy volunteers: a randomized, placebo-controlled first-in-human single-dose escalation study. *Antimicrob Agents Chemother* 63(4): e02255-18, 2019. DOI: 10.1128/AAC.02255-18
- 50 Gokbulut C, Bilgili A, Hanedan B, McKellar QA: Comparative plasma disposition of fenbendazole, oxfendazole and albendazole in dogs. *Vet Parasitol* 148(3-4): 279-287, 2007. DOI: 10.1016/j.vetpar.2007.06.028
- 51 Hickman D, Wang JP, Wang Y, Unadkat JD: Evaluation of the selectivity of *in vitro* probes and suitability of organic solvents for the measurement of human cytochrome p450 monooxygenase activities. *Drug Metab Dispos* 26(3): 207-215, 1998.
- 52 Easterbrook J, Lu C, Sakai Y, Li AP: Effects of organic solvents on the activities of cytochrome p450 isoforms, udp-dependent glucuronyl transferase, and phenol sulfotransferase in human hepatocytes. *Drug Metab Dispos* 29(2): 141-144, 2001.
- 53 Chung I, Zhou K, Barrows C, Banyard J, Wilson A, Rummel N, Mizokami A, Basu S, Sengupta P, Shaikh B, Sengupta S, Bielenberg DR, Zetter BR: Unbiased phenotype-based screen identifies therapeutic agents selective for metastatic prostate cancer. *Front Oncol* 10: 594141, 2021. DOI: 10.3389/fonc.2020.594141

- 54 Abughanimeh O, Evans T, Kallam A: Fenbendazole as a treatment for diffuse large b-cell lymphoma. *Ann Hematol Oncol* 7(2): 1284, 2020.
- 55 Chiang RS, Syed AB, Wright JL, Montgomery B, Srinivas S: Fenbendazole enhancing anti-tumor effect: A case series. *Clin Oncol Case Rep* 4(2), 2021.
- 56 Yamaguchi T, Shimizu J, Oya Y, Horio Y, Hida T: Drug-induced liver injury in a patient with nonsmall cell lung cancer after the self-administration of fenbendazole based on social media information. *Case Rep Oncol* 14(2): 886-891, 2021. DOI: 10.1159/000516276
- 57 Thakurdesai A, Rivera-Matos L, Nagra N, Busch B, Mais DD, Cave MC: Severe drug-induced liver injury due to self-administration of the veterinary anthelmintic medication, fenbendazole. *ACG Case Rep J* 11(5): e01354, 2024. DOI: 10.14309/crj.000000000001354
- 58 Dogra N, Mukhopadhyay T: Impairment of the ubiquitin-proteasome pathway by methyl N-(6-phenylsulfanyl-1H-benzimidazol-2-yl)carbamate leads to a potent cytotoxic effect in tumor cells: a novel antiproliferative agent with a potential therapeutic implication. *J Biol Chem* 287(36): 30625-30640, 2012. DOI: 10.1074/jbc.M111.324228
- 59 Gao P, Dang CV, Watson J: Unexpected antitumorigenic effect of fenbendazole when combined with supplementary vitamins. *J Am Assoc Lab Anim Sci* 47(6): 37-40, 2008.
- 60 Jin IS, Jo MJ, Park CW, Chung YB, Kim JS, Shin DH: Physicochemical, pharmacokinetic, and toxicity evaluation of Soluplus® polymeric micelles encapsulating fenbendazole. *Pharmaceutics* 12(10): 1000, 2020. DOI: 10.3390/pharmaceutics12101000

Received July 9, 2024
Revised July 15, 2024
Accepted July 17, 2024

Fenbendazole and Diisopropylamine Dichloroacetate Exert Synergistic Anti-cancer Effects by Inducing Apoptosis and Arresting the Cell Cycle in A549 Lung Cancer Cells

THAI Q. NGUYEN^{1,2}, DANG H. NGUYEN¹, UYEN T. T. PHAN^{1,2}, PHUONG T. T. TRAN¹, HUONG T. LE¹, SON H. NGUYEN^{1,2}, JOLIE NGUYEN³, BO HAN⁴ and BA X. HOANG⁴

¹University of Science and Technology of Hanoi, Vietnam Academy of Science and Technology, Hanoi, Vietnam;

²ThaiMinh Pharmaceuticals, Hanoi, Vietnam;

³School of Pharmacy, University of Pittsburgh, Pittsburgh, PA, U.S.A.;

⁴Nimni-Cordoba Tissue Engineering and Drug Discovery Lab, Department of Surgery, Keck School of Medicine of University of Southern California, Los Angeles, CA, U.S.A.

Abstract. Background/Aim: Lung cancer is the leading cause of cancer-related mortality worldwide, accounting for approximately 2 million new cases and 1.8 million deaths annually. Standard treatment options include surgery, radiation therapy, chemotherapy, and targeted therapies. Despite advancements over the past 25 years, the prognosis of patients with lung cancer remains poor. This study evaluated the synergistic anticancer effects of fenbendazole (FZ) and diisopropylamine dichloroacetate (DADA) on A549 lung cancer cells. Materials and Methods: Fenbendazole (methyl N-(6-phenylsulfanyl-1H-benzimidazol-2-yl) carbamate) is a broad-spectrum benzimidazole anthelmintic commonly used in veterinary medicine. Diisopropylamine Dichloroacetate (DADA), an over-the-counter treatment for chronic liver disease, has demonstrated anti-tumor properties as an inhibitor of pyruvate dehydrogenase kinase. Results: The combination of FZ and DADA exhibited a synergistic effect on inhibiting the proliferation of A549 lung cancer cells. After 48 h of treatment, the FZ-DADA combination produced reactive oxygen species

(ROS) and promoted apoptosis by down-regulating Bcl2 and up-regulating BAX protein expression. The combination activated caspase-3, caspase-7, and PARP, further driving apoptosis in A549 cells. The FZ-DADA treatment also induced cell cycle arrest, as evidenced by the inhibition of Cyclin A and Cyclin E proteins. Conclusion: The synergistic anticancer effects of the FZ-DADA combination were confirmed at both cellular and protein levels in A549 lung cancer cells. The combination modulates key apoptotic proteins, induces cell cycle arrest, and increases mitochondrial ROS production, suggesting a promising approach for lung cancer treatment that warrants further investigation and development.

Lung cancer is the leading cause of cancer-associated mortality worldwide, accounting for an estimated 2 million diagnoses and 1.8 million deaths (1). Lung cancer is divided into two broad histologic classes, which grow and spread differently: small-cell lung carcinomas (SCLC) and non-small-cell lung carcinomas (NSCLC). Treatment options for lung cancer include surgery, radiation therapy, chemotherapy, immunotherapy, and targeted therapy. Despite the improvements in diagnosis and therapy made during the past 25 years, the prognosis for patients with lung cancer is still unsatisfactory (2). This research aimed to investigate the anti-cancer effect of Diisopropylamine Dichloroacetate and Fenbendazole in lung cancer models.

Fenbendazole [methyl N-(6-phenylsulfanyl-1H-benzimidazol-2-yl) carbamate] is a broad-spectrum benzimidazole anthelmintic approved for use in numerous animal species. Recent studies have shown that fenbendazole (FZ) exhibits cytotoxicity to human cancer cells at micromolar concentrations by inducing mitochondrial translocation of p53, inhibiting glucose uptake, and disrupting other cellular pathways (3). While most reported cases of FZ self-administration have noted reductions in tumor size (4, 5), in some cases, FZ has been found to cause liver injury (6, 7), in which patients promptly

Correspondence to: Ba X. Hoang, MD, Ph.D., Nimni-Cordoba Tissue Engineering and Drug Discovery Lab, Department of Surgery, Keck School of Medicine of University of Southern California, 1333 San Pablo Street, BMT-302, Los Angeles, CA, U.S.A. E-mail: baxuanho@usc.edu

Key Words: Diisopropylamine dichloroacetate, drug development, fenbendazole, lung cancer.

©2024 The Author(s). Published by the International Institute of Anticancer Research.



This article is an open access article distributed under the terms and conditions of the Creative Commons Attribution (CC BY-NC-ND) 4.0 international license (<https://creativecommons.org/licenses/by-nc-nd/4.0>).

recovered after discontinuing FZ. Combining FZ with another drug could mitigate this side effect and support the use of FZ in cancer treatment, enabling pilot clinical trials to be conducted. Therefore, identifying a safe, non-toxic drug synergistic with FZ, preferably a glycolysis inhibitor, is crucial for developing an effective anticancer combination therapy.

Diisopropylamine dichloroacetate (DADA), an over-the-counter drug for chronic liver disease, has demonstrated anti-tumor effects by inhibiting pyruvate dehydrogenase kinase (8). Additionally, DADA is a hepatoprotective pharmaceutical that would support the use of FZ in patients with liver cancer, bile duct cancer, or compromised liver function. FZ-DADA therapy could potentially reduce hepatotoxicity, enhance therapeutic efficacy, and improve tolerability within the framework of comprehensive metabolic therapy for proliferative disorders. This research investigated the effects of the FZ-DADA combination in A549 lung cancer cell line.

Materials and Methods

Cell culture. A549 cells were cultured in an 18 cm² petri dish with Roswell Park Memorial Institute (RPMI) medium (Thermo Fisher, Waltham, MA, USA) containing 10% fetal bovine serum (FBS) and incubated in a 5% CO₂ incubator at 37°C. The cells were frequently maintained, subcultured, and checked for contamination.

Cell cytotoxicity assay. A549 cells were cultured in 96-well plates (2.5×10⁴ cells/well) and incubated overnight in a 5% CO₂ incubator at 37°C. Cells were treated with various concentrations of FZ alone, DADA alone and FZ-DADA combination for 24, 48, and 72 h. The cell viability of A549 cells was measured using the MTT method. Violet crystals were dissolved in isopropanol, and the absorbance was measured with a spectrophotometer at 570nm using a SpectraMax ID5 microplate reader. The CI value was calculated using CompuSyn software.

ROS assay. A549 cells were seeded in 96-well plates (2.5×10⁴ cells/well) at 37°C, 5% CO₂ for 24 hours. Cells were then treated with various concentrations of FZ alone, DADA alone, and FZ-DADA combination for 48 h. ROS levels were measured with a Reactive Oxygen Species (ROS) Detection Assay Kit (ab287839) (Abcam, Cambridge, UK) at Ex/Em=495/529 nm in endpoint mode using SpectraMax ID5 microplate reader.

Hoechst staining. A549 cells were cultured in 6 cm plates (5×10⁵ cells/well) at 37°C, 5% CO₂ for 24 h. Cells were then treated with Paclitaxel 1 μM, FZ 1 μM, DADA 5 mM and FZ-DADA combination for 48 h at 37°C, 5% CO₂. After treatment, the supernatant was removed. Cells were washed 3 times with cold PBS.

Cells were incubated with the staining solution containing Hoechst 33342 (Thermo Fisher) for 15 min while protected from light. After 15 min, the staining solution was removed. Cells were washed three times with cold PBS before imaging with a fluorescent microscope.

Cell cycle arrest. A549 cells were seeded in 6-well plates for 24 h before being treated with or without FZ, DADA, or an FZ-DADA combination for 48 h. Cells adhering to the plate were collected and washed in PBS twice. After fixing with ice-cold 70% ethanol at -20°C

for 2 h, cells were washed with PBS and treated in PBS for 30 min with 1 mg/ml propidium iodide (PI) (Thermo Fisher) and 20 μg/ml RNase (Thermo Fisher). Cell cycle analysis was performed using a Novocyte 2000 flow cytometer (ACEA Biosciences Inc., San Diego, CA, USA) and NovoExpress software (ACEA Biosciences Inc.).

Apoptosis assay. A549 cells were seeded in 6-well plates for 24 h before being treated with FZ, DADA, or an FZ-DADA combination for 48 h in experiments. In time-dependent experiments, cells were treated with or without the FZ-DADA composition for 24, 48, and 72 h. The supernatant, cell death washes with PBS, and adhering cells were collected and washed twice with PBS. Apoptotic cells were stained with annexin-V (1 mg/ml) and PI (1 mg/ml) using an annexin-V/PI staining kit. Apoptosis analysis was performed using a Novocyte 2000 flow cytometer (ACEA Biosciences Inc.) and NovoExpress software (ACEA Biosciences Inc.).

Western blot. A549 cells were lysed using RIPA buffer containing protease inhibitor and then sonicated for complete cell disruption. The Bradford assay (SERVA Electrophoresis GmbH, Heidelberg, Baden-Württemberg, Germany) determined the total protein lysis concentration. SDS-PAGE was used to separate proteins, which were transferred to polyvinylidene fluoride membranes (PVDF, Millipore, Bedford, MA, USA) and blocked in TBS-T (50 mmol/l Tris-HCL pH 7.6), 150 mmol/l NaCl containing 0.1% Tween-20 (containing 5% BSA) for 1 h. Membranes were incubated with different antibodies (cell signaling) overnight at 4°C. Membranes were washed in TBST, labeled with an HRP-conjugated secondary antibody for 15 min (Thermo Fisher), washed thrice, and measured using an ECL luminescence enhancer (GE Healthcare, Chalfont St Giles, UK). Tubulin (Invitrogen, Waltham, MA, USA) was used as a loading control to ensure even protein distribution among the samples. Images of protein expression were captured by ImageQuant LAS 500.

Glucose uptake assay. Glucose uptake was conducted using 2-deoxyglucose (2-DG), which is structurally similar to glucose (glucose uptake kit, AB136955) (Abcam, Cambridge, UK). 2-DG is taken by glucose transporters and converted to 2-DG-6-phosphate (2-DG6P), which cannot be further metabolized and consequently accumulates inside cells. The accumulation of 2-DG6P is proportional to cells' absorption of 2-DG (or glucose). In this assay, 2-DG6P is oxidized to produce NADPH, the concentration of which is measured using an enzymatic recycling amplification reaction.

A549 cells were seeded in a 96-well plate (5×10⁴ cells/well) for 24 h. Cells were then starved overnight in high glucose DMEM without FBS. Next, cells were treated for 24 h with various FZ, DADA, and FZ-DADA combination concentrations. Cells were incubated with Krebs-Ringer Phosphate-Hepes (KRPH) buffer for 40 min and insulin 1 μM for 20 min. Then, 10 mM 2-DG was added and incubated for 20 min. Cells were lysed with an extraction buffer, frozen at -80°C for 10 min, and heated at 85°C for 40 min. The lysates were neutralized by adding a neutralization buffer and centrifuged to collect the NADPH supernatant samples. The products were amplified following the glucose uptake kit protocol. The absorbance was measured at 412 nm using the SpectraMax ID5 microplate reader.

Lactate assay. Lactate Colorimetric Assay kits (AB65331) (Abcam) were used to measure lactate in the medium and cell lysates according to the manufacturer's instructions. A549 cells were seeded in 96-well plates for 24 h, then treated with various concentrations of FZ, DADA

and FZ-DADA combination. At 48 h, the lactate concentration in the culture medium or cell lysates was measured at 450 nm using the SpectraMax ID5 microplate reader based on a standard curve generated with known concentrations of lactate solution.

Statistical analysis. Statistical analysis was performed using GraphPad Prism (GraphPad, Boston, MA, USA) and SPSS 22.0 (IBM, Chicago, IL, USA). Means \pm SD or % were calculated as appropriate. Experiments were performed at least in triplicate, and the average was calculated. The statistical significance of experimental observations was determined using ANOVA with a significance level of $p < 0.05$.

Results

Cytotoxic effects of FZ-DADA against A549 lung cancer cell lines. To evaluate the impact of FZ and DADA on cell viability, A549 lung cancer cells were treated with various concentrations of FZ and DADA for 48 h. IC₅₀ values of FZ and DADA were determined to be 1 μ M and 5 mM, respectively. The A549 cell death rate was determined to be dose-dependent, with approximately 30% of cells dying after treatment with the FZ, DADA, and FZ-DADA combination (Figure 1A). The results of combination doses were compared with single drug doses to determine the appropriate, effective combination ratio of FZ and DADA. Our results showed that the FZ-DADA significantly reduced cell cytotoxicity compared to FZ and DADA alone. Therefore, this combination ratio (1 μ M FZ and 5 mM DADA) was chosen for further cytotoxicity experiments. To investigate the synergistic effects of FZ-DADA, the combination index (CI) value was calculated (Figure 1B and C, and Table I). The results revealed that FZ-DADA had synergistic effects after 48 h, which improved when the combination dosage was increased. This was proved by the CI value of all test combination dosages being less than one, with the maximum number affected index (Fa) recorded being approximately 0.8. A previous study on combining FZ with the DADA-similar compound dichloroacetate (DCA) also showed synergistic effects consistent with this result (3).

FZ-DADA induced ROS in A549 cells. Reactive oxygen species (ROS) are chemically reactive chemicals containing oxygen (9). ROS are formed as a natural by-product of the normal metabolism of oxygen and have important roles in cell signaling and homeostasis (10). ROS and mitochondria play pivotal roles in the induction of apoptosis under physiological and pathological conditions. A high level of ROS may lead to increased cell damage through the oxidative process of DNA, carbohydrates, lipids, and proteins (11). To evaluate the effects of FZ and DADA on ROS productions, A549 cells were treated with various ratios of their combination. The level of ROS in the supernatant was then measured after 48 h. The results indicated that FZ-DADA increased ROS levels in A549 cells compared to the single treatment with FZ or DADA (Figure 2).

FZ-DADA combination induced apoptosis in A549 cells. Fluorescence-activated cell sorting (FACS) analysis employing Annexin-V-FITC and propidium iodide staining was used to investigate the effect of FZ, DADA, and their combination on apoptosis in A549 cells (Figure 3A and B). The flow cytometry results after 48 h treatments revealed that FZ and DADA alone substantially triggered apoptosis at their IC₅₀, with apoptosis occurring in 38.83% (14.62% early apoptosis and 24.01% late apoptosis) and 38.48% (16% early apoptosis and 22.48% late apoptosis), respectively. At the dose 1 μ M and 5 mM, FZ-DADA combination showed a dramatic percentage of 71.54% (13.1% early apoptosis and 58.44% late apoptosis) of apoptotic cells. This combination significantly increased the proportion of cells in the late apoptosis phase compared with the single-dose treatment with FZ or DADA.

The results of Hoechst staining confirmed the effects of FZ and DADA on A549 cells (Figure 3C). At the protein level, FZ-DADA increased approximately 17 times the expression of BAX and reduced 4 times the expression of Bcl2. The Bcl2 family proteins are key regulators of apoptotic cell death. High expression of Bcl2 in various human cancers mediates the resistance of cancers to a wide range of chemotherapeutic drugs and γ -irradiation, which act by inducing apoptosis in tumor cells. Therefore, the blocking of Bcl2 can restore the apoptotic process in tumor cells (12). In contrast, the expression of BAX in cancer cells activated cell death (13).

The morphological changes in apoptosis are primarily due to caspases, a family of cysteine proteases that act as effectors in the cell death pathway (14). As the most downstream enzyme in the apoptosis-inducing protease pathway, caspase 3 plays a pivotal role in cell death by cleaving key proteins in the cell repair process. Caspase 3 cleaves at an aspartate residue, producing p12 and p17 subunits, forming the active cleaved caspase 3. This enzyme is crucial for the morphological and biochemical changes characteristic of apoptosis (15-18). At the protein level, the combination of 1 μ M FZ and 5 mM DADA exhibited synergistic effects on cleaved caspase-3 protein, resulting in approximately 3.3 and 4 times increase in their levels compared with the treatment with 1 μ M FZ or 5 mM DADA alone, respectively. Similar to caspase 3, caspase-7 is universally activated during apoptosis. Interestingly, the combination of FZ-DADA with the dose 1 μ M and 5 mM increased the expression of cleaved caspase-7 by 12-fold, which is 3 times and 12 times higher than the levels induced by FZ and DADA alone, respectively. The caspase family, especially caspase-3 and caspase-7, cleave the 116 kDa form of PARP into 85 kDa and 24 kDa fragments (19, 20). PARP has been suggested to contribute to cell death by depleting the cells of NAD and ATP (21). PARP-1 cleavage is a switch point that directs death receptor signaling toward either apoptosis or necrosis (20). Our results indicated that the combination

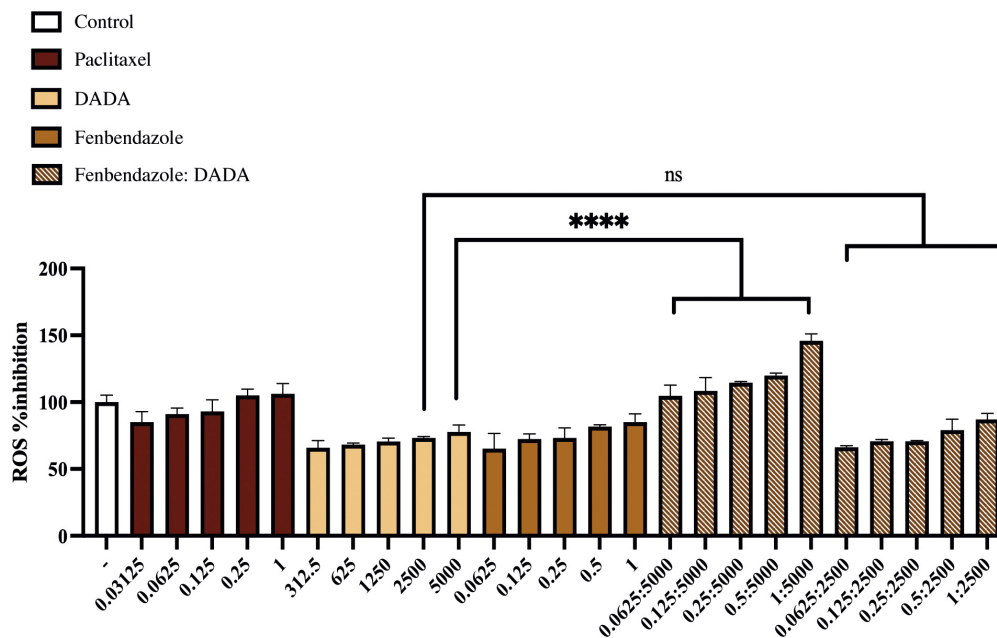


Figure 2. The combination of fenbendazole and diisopropylamine dichloroacetate (FZ-DADA) induced the production of reactive oxygen species (ROS) in A549 cells. A549 cells were treated with different concentrations of FZ, DADA, and the combination of FZ-DADA for 48 h in a 96-well plate. ROS levels were evaluated using the ROS Detection assay kit. Data was measured by mean±SD (**** $p < 0.0001$ compared with vehicle-treated control, $n=3$).

Table 1. The combination of fenbendazole and diisopropylamine dichloroacetate (FZ-DADA) showed a synergistic effect in A549 cell lines.

Total dose (µM)	Fa	CI value	Interpretation
625.125	0.16	0.88	Synergism
1250.25	0.34	0.74	Synergism
2500.5	0.51	0.8	Synergism
5001	0.66	0.93	Synergism
10002	0.82	0.88	Synergism

CI: Combination index.

influence of FZ and DADA was investigated to assess cell cycle regulation. At the protein level, the FZ-DADA combination decreased the expression of Cyclin A and Cyclin E about 3.5 times and 6.6 times compared to treatments with FZ and DADA alone, respectively (Figure 4E).

FZ-DADA combination inhibited glucose uptake and lactate production. In studies where A549 cells were treated with FZ alone, the anticancer effect of FZ was linked to the inhibition

of glucose uptake, resulting in changes in glucose metabolism and cell death (3). DADA was identified as a PDK-4 inhibitor, which reduces lactate generation (8, 23). As a result, the synergistic effects of the FZ-DADA combination, being a glucose uptake inhibitor and PDK-4 inhibitor, were chosen for the glucose metabolism study. Similar to earlier findings, FZ and high-dosage DADA alone dramatically inhibited glucose uptake in A549 cells after 24 h of treatment (Figure 5A). Compared to treatment with either agent alone, the combination treatment resulted in significantly less 2-DG absorption. As expected, FZ and DADA alone reduced lactate generation after 48 h, and the effect was further enhanced when these drugs were combined (Figure 5B). Thus, the FZ-DADA combination demonstrated a synergistic effect in inhibiting glucose uptake and lactate production.

Glucose uptake is a critical physiological process regulated by several mechanisms, with insulin playing the most prominent role. This powerful anabolic hormone facilitates glucose transport into cells, primarily in metabolically active tissues, such as skeletal muscles, adipose tissue, and the liver, via a specialized transporter known as GLUT4. The process involves a complex sequence of events, primarily mediated by

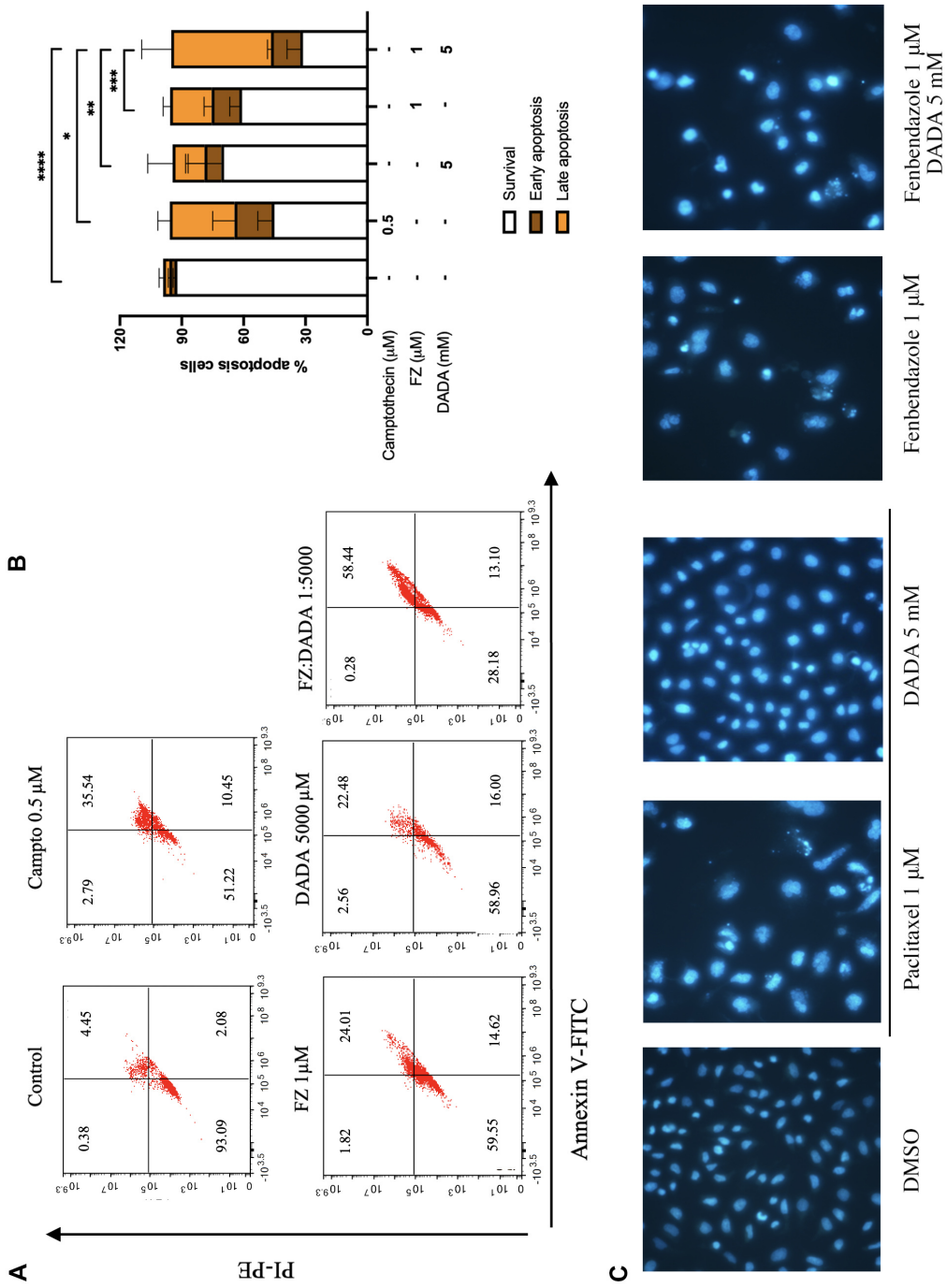


Figure 3. *Continued*

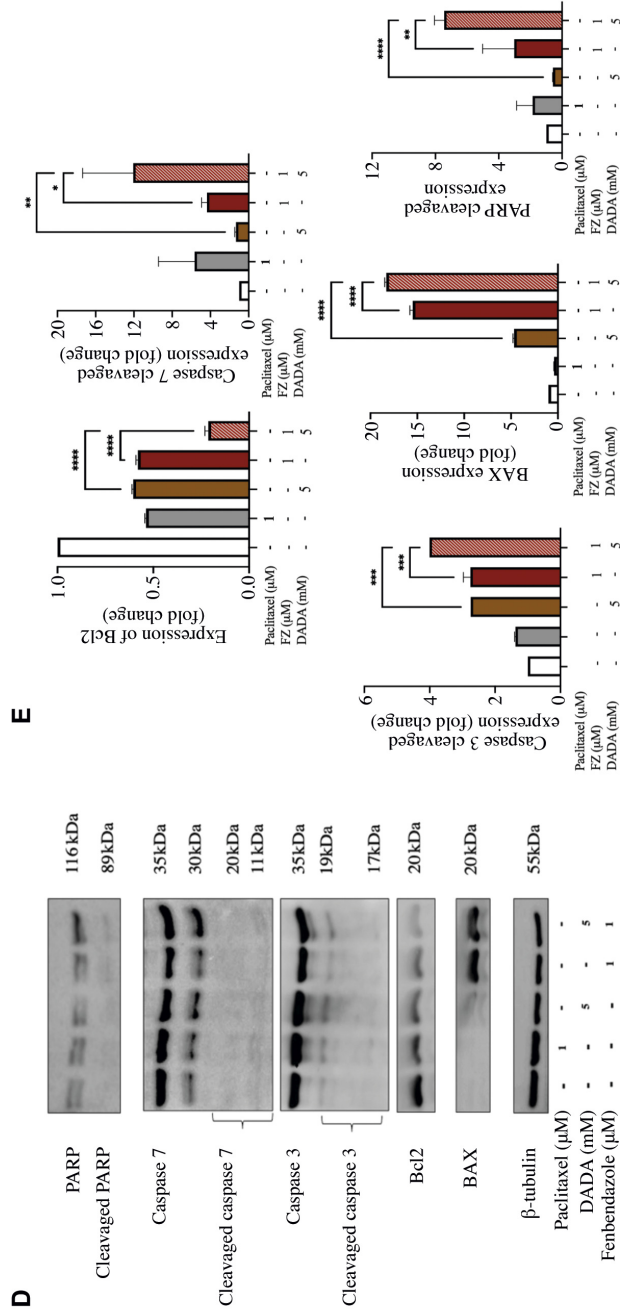


Figure 3. (A, B) The combination of fenbendazole and disopropylamine dichloroacetate (FZ-DADA) induced apoptosis in A549 cells. Cells were treated with fenbendazole (FZ), disopropylamine dichloroacetate (DADA), and their combinations for 48 h, then incubated with Annexin V and propidium iodine to detect the apoptotic stage. (C) Cells were treated with DADA alone, FZ alone, as well as the combination of DADA and FZ composition for 48 h. After removing the supernatant, cells were stained with a Hoechst staining solution for 15 min and observed under a fluorescent microscope (20 \times). (D) A549 cells were seeded in 6-cm plates for 24 h. Cells were treated with DADA alone, FZ alone, or FZ-DADA for 48 h. Cells were then harvested to extract proteins for western blot with the indicated antibodies. The expression of PARP, Bcl2 and BAX, caspase-3, and caspase-7 was normalized to the housekeeping α -tubulin; data are mean \pm SD (n=3), * p <0.05, ** p <0.001, **** p <0.0001 compared with the negative control.

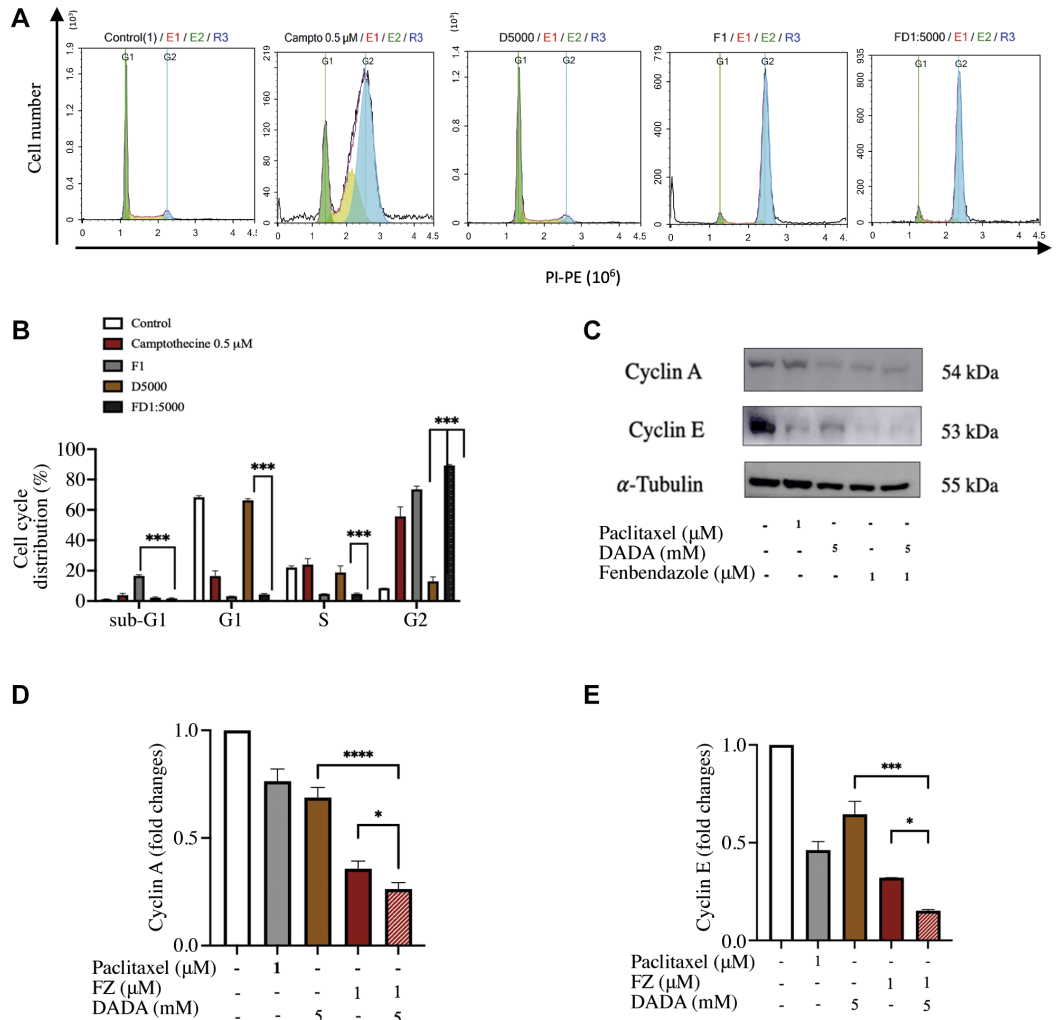


Figure 4. The combination of fenbendazole and diisopropylamine dichloroacetate (FZ-DADA) induced G₂/M cell cycle arrest in the A549 cell line when compared to the treatment with each component of the combination alone. Cells were treated with FZ, DADA, or FZ-DADA for 48 h, then incubated with RNase and propidium iodide to detect the apoptotic stage. (A) measurement of various cell cycle stages in untreated and treated A549 cells. (B) The bar graph represents the cell cycle results at the combination of FZ-DADA compared with each agent alone. The result was analyzed using ANOVA. **p*<0.05, ****p*<0.001. Error bars represent the standard deviation of three experiments. (C) A549 cells were treated with a single agent or the combination of DADA and FZ for 48 h. Total cells were harvested for the western blot experiment with indicating antibodies. The expression of cyclin A (D) and cyclin E (E) was normalized to the housekeeping α-tubulin; data are mean±SD (n=3), **p*<0.05, ***p*<0.01 ****p*<0.001, *****p*<0.0001 compared with negative control.

the PI3K/AKT signaling pathway (24). In time-dependent experiments, the FZ-DADA combination at a ratio of 1 μM and 5 mM reduced the levels of both pAKT and pPI3K (Figure 5C-F). The most significant inhibition of AKT and

PI3K phosphorylation occurred after 5 and 7 h of treatment with the FZ-DADA combination. For the concentration-dependent experiment, A549 cells were treated with FZ, DADA, or their combination for 7 h. The results showed

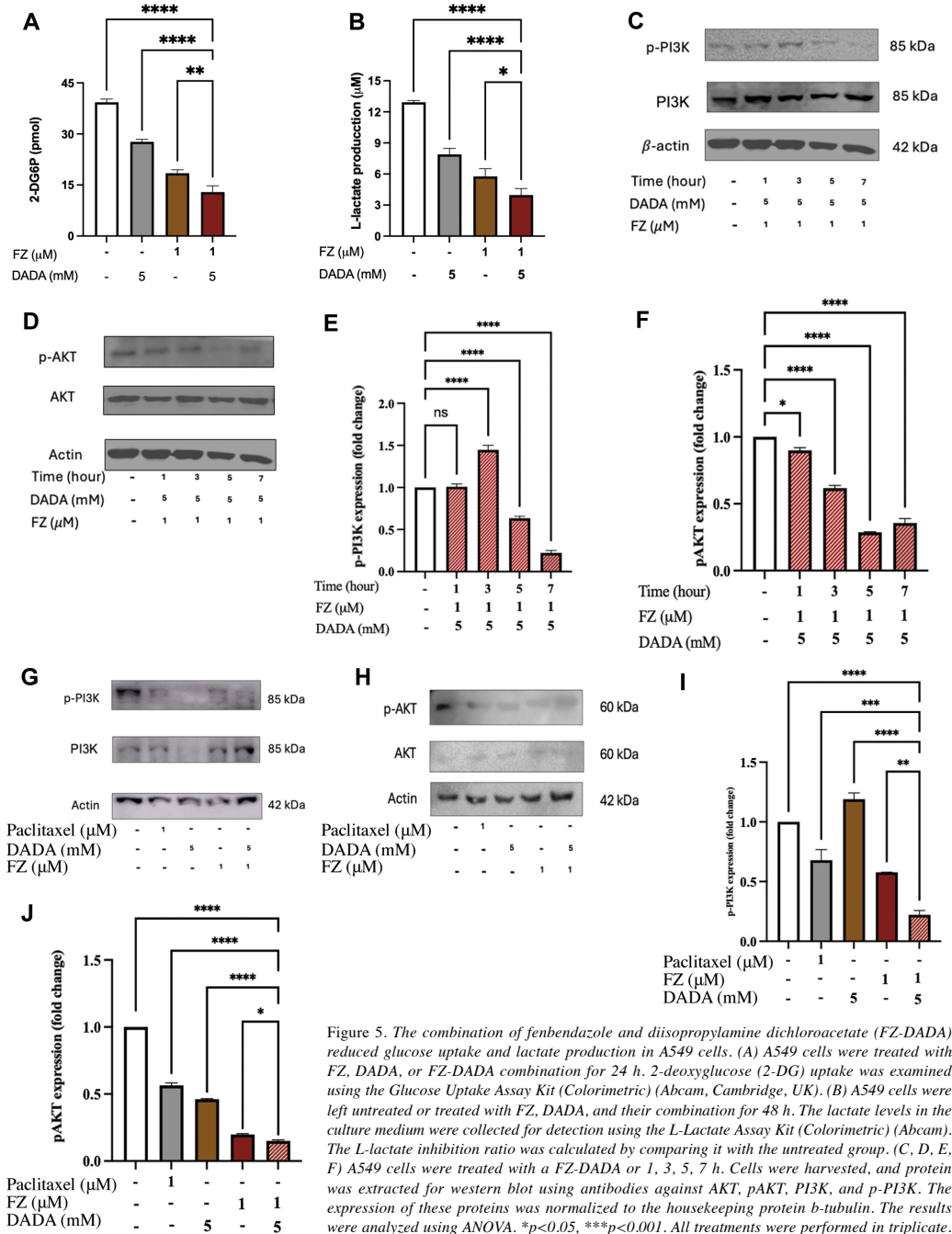


Figure 5. The combination of fenbendazole and diisopropylamine dichloroacetate (FZ-DADA) reduced glucose uptake and lactate production in A549 cells. (A) A549 cells were treated with FZ, DADA, or FZ-DADA combination for 24 h. 2-deoxyglucose (2-DG) uptake was examined using the Glucose Uptake Assay Kit (Colorimetric) (Abcam, Cambridge, UK). (B) A549 cells were left untreated or treated with FZ, DADA, and their combination for 48 h. The lactate levels in the culture medium were collected for detection using the L-Lactate Assay Kit (Colorimetric) (Abcam). The L-lactate inhibition ratio was calculated by comparing it with the untreated group. (C, D, E, F) A549 cells were treated with a FZ-DADA or 1, 3, 5, 7 h. Cells were harvested, and protein was extracted for western blot using antibodies against AKT, pAKT, PI3K, and p-PI3K. The expression of these proteins was normalized to the housekeeping protein b-tubulin. The results were analyzed using ANOVA. * $p < 0.05$, *** $p < 0.001$. All treatments were performed in triplicate.

inhibition of AKT and PI3K phosphorylation by FZ, DADA, and their combination (Figure 5G-K). These findings suggest that FZ and DADA inhibit glucose uptake and lactate production through the PI3K/AKT pathway.

Discussion

In the current study, the FZ and DADA combination exhibits a robust synergistic effect against A549 lung cancer cells. This combination enhances cytotoxicity, induces apoptosis, and disrupts cellular metabolism and cell cycle progression. Our study highlights the potential of the FZ-DADA combination as a therapeutic strategy for lung cancer treatment. These findings provide a solid foundation for further investigation in preclinical and clinical settings to optimize the usage of FZ and DADA in cancer therapy and determine the underlying molecular therapeutic mechanisms of the composition.

Our findings determined the potent synergy between FZ and DADA in inducing apoptosis in A549 cells. The significant modulation of key apoptotic markers, BAX and BCL2, underscores the mechanism through which this combination operates (12, 14, 26). The pro-apoptotic protein BAX promotes mitochondrial outer membrane permeabilization, facilitating the release of cytochrome c and the subsequent activation of the caspase cascade (12, 13). In contrast, Bcl2, an anti-apoptotic protein, prevents this permeabilization, thereby inhibiting apoptosis. The observed down-regulation of Bcl2 and up-regulation of BAX suggest a shift in balance towards apoptosis (12, 14, 27). Furthermore, our study showed up-regulation of the executioner caspases caspase-3 and caspase-7. Once activated, these caspases cleave various substrates, leading to the dismantling of the cell (14-18). This up-regulation indicates that the FZ-DADA combination effectively triggers the apoptotic machinery, reinforcing the mechanism of cell death.

Additionally, the combination treatment effectively arrested the cell cycle at the G₂/M phase. Cyclins and cyclin-dependent kinases (CDKs) are pivotal in cell cycle regulation. Cyclin A and Cyclin E are crucial for the G₁ to S phase transition and the G₂/M transition, respectively. The marked reduction in Cyclin A and Cyclin E levels upon treatment with the FZ-DADA combination aligns with the observed cell cycle arrest, reinforcing that disrupting these transitions is critical for inducing cell death (14, 22).

Another important aspect of this study is the role of mitochondrial ROS production in mediating apoptosis. Reactive oxygen species (ROS) are involved in various cellular processes, including apoptosis (9, 11). The mitochondrial pathway of apoptosis is particularly sensitive to changes in ROS levels. The increase in mitochondrial ROS production observed with a combination of 1 μ M and 5 mM FZ-DADA combination likely contributes to the disruption of mitochondrial function, further promoting apoptosis.

In the metabolic system, FZ and DADA demonstrated their capacity to inhibit glucose uptake and lactate synthesis by inhibiting the PI3K/AKT pathway. The FZ-DADA combination effectively prevented glucose uptake and lactate synthesis in A549 cells. Metabolic reprogramming is a hallmark of cancer, with glucose uptake and lactate production being key components of the altered metabolic pathways that support cancer cell proliferation and survival (28-31). The ability of FZ and DADA to inhibit glucose uptake and lactate synthesis highlights their potential to disrupt the metabolic flexibility of cancer cells, thereby impairing their growth and survival.

FZ-DADA's inhibition of the PI3K/AKT pathway is particularly noteworthy. The PI3K/AKT pathway is a critical regulator of cell metabolism, promoting glucose uptake and glycolysis while inhibiting apoptosis (32-35). By targeting this pathway, FZ-DADA effectively reduces glucose availability for energy production and biosynthesis, leading to decreased lactate production, a byproduct of aerobic glycolysis commonly known as the Warburg effect in cancer cells. This disruption of metabolic processes could sensitize cancer cells to apoptosis and reduce their proliferative capacity.

These findings provide valuable insights into the potential therapeutic applications of FZ and DADA. The ability to synergistically induce apoptosis through multiple mechanisms, including modulation of apoptotic proteins, cell cycle arrest, and ROS production, makes this combination a promising candidate for further investigation in lung cancer therapy. This combination warrants future studies exploring the detailed molecular pathways involved and assessing their efficacy in *in vivo* models.

Conclusion

The FZ-DADA combination therapy demonstrates a robust synergistic effect in inducing apoptosis in A549 cells, notably at the 1 μ M and 5 mM ratios. By modulating key apoptotic proteins, arresting the cell cycle, and increasing mitochondrial ROS production, this combination offers a promising approach to lung cancer treatment, warranting further exploration and development.

Conflicts of Interest

All Authors declare no conflicts of interest in writing and publishing the manuscript.

Authors' Contributions

TQN: Participated in research design, research, data analysis, and manuscript writing. DHN: Participated in research, data analysis, and manuscript writing. UTTP, PTTT, HTL, SHL: Participated in research design and execution. JN: conceptualization, writing, and editing. BH: conceptualization, writing, and editing. BXH: conceptualized and participated in research design, data analysis, and manuscript writing.

Funding

No external funding was received for this work.

References

- Thandra KC, Barsouk A, Saginala K, Aluru JS, Barsouk A: Epidemiology of lung cancer. *Contemp Oncol (Pozn)* 25(1): 45-52, 2021. DOI: 10.5114/wo.2021.103829
- Lemjabbar-Alaoui H, Hassan OU, Yang YW, Buchanan P: Lung cancer: Biology and treatment options. *Biochim Biophys Acta* 1856(2): 189-210, 2015. DOI: 10.1016/j.bbcan.2015.08.002
- Dogra N, Kumar A, Mukhopadhyay T: Fenbendazole acts as a moderate microtubule destabilizing agent and causes cancer cell death by modulating multiple cellular pathways. *Sci Rep* 8(1): 11926, 2018. DOI: 10.1038/s41598-018-30158-6
- Abughanimeh O, Evans T, Kallam A: Fenbendazole as a treatment for diffuse large b-cell lymphoma. *Ann Hematol Oncol* 7(2): 1284, 2020.
- Chiang RS, Syed AB, Wright JL, Montgomery B, Srinivas S: Fenbendazole enhancing anti-tumor effect: A case series. *Clin Oncol Case Rep* 4(2), 2021.
- Yamaguchi T, Shimizu J, Oya Y, Horio Y, Hida T: Drug-induced liver injury in a patient with nonsmall cell lung cancer after the self-administration of fenbendazole based on social media information. *Case Rep Oncol* 14(2): 886-891, 2021. DOI: 10.1159/000516276
- Thakurdesai A, Rivera-Matos L, Nagra N, Busch B, Mais DD, Cave MC: Severe drug-induced liver injury due to self-administration of the veterinary anthelmintic medication, fenbendazole. *ACG Case Rep J* 11(5): e01354, 2024. DOI: 10.14309/crj.0000000000001354
- Yamane K, Indalao IL, Chida J, Yamamoto Y, Hanawa M, Kido H: Diisopropylamine dichloroacetate, a novel pyruvate dehydrogenase kinase 4 inhibitor, as a potential therapeutic agent for metabolic disorders and multiorgan failure in severe influenza. *PLoS One* 9(5): e98032, 2014. DOI: 10.1371/journal.pone.0098032
- Bergamini C, Gambetti S, Dondi A, Cervellati C: Oxygen, reactive oxygen species and tissue damage. *Curr Pharm Des* 10(14): 1611-1626, 2004. DOI: 10.2174/1381612043384664
- Lennicke C, Cochemé HM: Redox metabolism: ROS as specific molecular regulators of cell signaling and function. *Mol Cell* 81(18): 3691-3707, 2021. DOI: 10.1016/j.molcel.2021.08.018
- Patel P, Chatterjee S: Chapter 1 - Innate and adaptive immunity: Barriers and receptor-based recognition. *In: Immunity and inflammation in health and disease*. Academic Press, pp. 3-13, 2018. DOI: 10.1016/B978-0-12-805417-8.00001-9
- Naseri MH, Mahdavi M, Davoodi J, Tackallou SH, Goudarzvand M, Neishabouri SH: Up regulation of Bax and down regulation of Bcl2 during 3-NC mediated apoptosis in human cancer cells. *Cancer Cell Int* 15: 55, 2015. DOI: 10.1186/s12935-015-0204-2
- Wei MC, Zong WX, Cheng EH, Lindsten T, Panoutsakopoulou V, Ross AJ, Roth KA, MacGregor GR, Thompson CB, Korsmeyer SJ: Proapoptotic BAX and BAK: a requisite gateway to mitochondrial dysfunction and death. *Science* 292(5517): 727-730, 2001. DOI: 10.1126/science.1059108
- Golstein P: Controlling cell death. *Science* 275(5303): 1081-1082, 1997. DOI: 10.1126/science.275.5303.1081
- Beroske L, Van den Wyngaert T, Stroobants S, Van der Veken P, Elvas F: Molecular imaging of apoptosis: the case of caspase-3 radiotracers. *Int J Mol Sci* 22(8): 3948, 2021. DOI: 10.3390/ijms22083948
- Huang JS, Yang CM, Wang JS, Liou HH, Hsieh IC, Li GC, Huang SJ, Shu CW, Fu TY, Lin YC, Ger LP, Liu PF: Caspase-3 expression in tumorigenesis and prognosis of buccal mucosa squamous cell carcinoma. *Oncotarget* 8(48): 84237-84247, 2017. DOI: 10.18632/oncotarget.20494
- Wang Y, Ye D: A caspase-3 activatable photoacoustic probe for *in vivo* imaging of tumor apoptosis. *Methods Enzymol* 657: 21-57, 2021. DOI: 10.1016/bs.mie.2021.06.021
- Wang Y, Yin B, Li D, Wang G, Han X, Sun X: GSDME mediates caspase-3-dependent pyroptosis in gastric cancer. *Biochem Biophys Res Commun* 495(1): 1418-1425, 2018. DOI: 10.1016/j.bbrc.2017.11.156
- Kaufmann SH, Desnoyers S, Ottaviano Y, Davidson NE, Poirier GG: Specific proteolytic cleavage of poly(adp-ribose) polymerase: An early marker of chemotherapy-induced apoptosis. *Cancer Res* 53(17): 3976-3985, 1993.
- Los M, Mozoluk M, Ferrari D, Stepczynska A, Stroh C, Renz A, Herceg Z, Wang ZQ, Schulze-Osthoff K: Activation and caspase-mediated inhibition of PARP: a molecular switch between fibroblast necrosis and apoptosis in death receptor signaling. *Mol Biol Cell* 13(3): 978-988, 2002. DOI: 10.1091/mbc.01-05-0272
- Grube K, Küpper JH, Bürkle A: Direct stimulation of poly(ADP ribose) polymerase in permeabilized cells by double-stranded DNA oligomers. *Anal Biochem* 193(2): 236-239, 1991. DOI: 10.1016/0003-2697(91)90015-1
- Pucci B, Kasten M, Giordano A: Cell cycle and apoptosis. *Neoplasia* 2(4): 291-299, 2000. DOI: 10.1038/sj.neo.7900101
- Su L, Zhang H, Yan C, Chen A, Meng G, Wei J, Yu D, Ding Y: Superior anti-tumor efficacy of diisopropylamine dichloroacetate compared with dichloroacetate in a subcutaneous transplantation breast tumor model. *Oncotarget* 7(40): 65721-65731, 2016. DOI: 10.18632/oncotarget.11609
- Świdwerska E, Strycharz J, Wróblewski A, Szmraj J, Drzewoski J, Śliwińska A: Role of PI3K/AKT pathway in insulin-mediated glucose uptake. *In: Blood glucose levels*. Szablewski L (ed.). IntechOpen, 2018.
- Manna P, Jain SK: PIP3 but not PIP2 increases GLUT4 surface expression and glucose metabolism mediated by AKT/PKC ζ / λ phosphorylation in 3T3L1 adipocytes. *Mol Cell Biochem* 381(1-2): 291-299, 2013. DOI: 10.1007/s11010-013-1714-7
- Raisova M, Hossini AM, Eberle J, Riebeling C, Wieder T, Sturm I, Daniel PT, Orfanos CE, Geilen CC: The Bax/Bcl-2 ratio determines the susceptibility of human melanoma cells to CD95/Fas-mediated apoptosis. *J Invest Dermatol* 117(2): 333-340, 2001. DOI: 10.1046/j.0022-202x.2001.01409.x
- Hussar P: Apoptosis regulators Bcl-2 and Caspase-3. *Encyclopedia* 2(4): 1624-1636, 2022. DOI: 10.3390/encyclopedia2040111
- Ward PS, Thompson CB: Metabolic reprogramming: a cancer hallmark even warburg did not anticipate. *Cancer Cell* 21(3): 297-308, 2012. DOI: 10.1016/j.ccr.2012.02.014
- Navarro C, Ortega Á, Santeliz R, Garrido B, Chacín M, Galban N, Vera I, De Sanctis JB, Bermúdez V: Metabolic reprogramming in cancer cells: emerging molecular mechanisms and novel therapeutic approaches. *Pharmaceutics* 14(6): 1303, 2022. DOI: 10.3390/pharmaceutics14061303

Synergistic anti-tumor effect of fenbendazole and diisopropylamine dichloroacetate in immunodeficient BALB/c nude mice transplanted with A549 lung cancer cells

Thai Q. Nguyen¹, Uyen T. T. Phan¹, Mao V. Can², Dang H. Nguyen¹, Bo Han³, Ba X. Hoang^{3^A}

¹University of Science and Technology of Hanoi, Vietnam Academy of Science and Technology, Hanoi, Vietnam; ²Department of Pathophysiology, Military Medical Academy, Hanoi, Vietnam; ³Nimni-Cordoba Tissue Engineering and Drug Discovery Lab, Department of Surgery, Keck School of Medicine of University of Southern California, Los Angeles, CA, USA

Contributions: (I) Conception and design: All authors; (II) Administrative support: TQ Nguyen, DH Nguyen; (III) Provision of study materials or patients: TQ Nguyen, DH Nguyen, UTT Phan, BX Hoang; (IV) Collection and assembly of data: All authors; (V) Data analysis and interpretation: All authors; (VI) Manuscript writing: All authors; (VII) Final approval of manuscript: All authors.

Correspondence to: Ba X. Hoang, MD, PhD, Nimni-Cordoba Tissue Engineering and Drug Discovery Lab, Department of Surgery, Keck School of Medicine of University of Southern California, 1333 San Pablo Street, BMT-302, Los Angeles, CA 90033, USA. Email: baxuanho@usc.edu.

Background: Lung cancer remains one of the leading causes of cancer-related deaths worldwide. Recent studies suggest that fenbendazole (FZ), even at micromolar doses, shows promising anticancer potential but can cause liver toxicity in some patients. Diisopropylamine dichloroacetate or vitamin B15 (DADA), known for its hepatoprotective properties, has also demonstrated antitumor properties and may reduce FZ-induced liver injury. Our research aimed to evaluate the synergistic anticancer effects of FZ and DADA *in vivo* lung cancer models.

Methods: Immunodeficient BALB/c nude mice (Foxn1nu) were utilized for *in vivo* assessment of anticancer activity. Human lung cancer cells (A549) were injected into the nude mice. When the tumor volume reached 50 mm³, the animals were randomized into eight groups, receiving either single or combined DADA and FZ treatments. The antitumor efficacy and toxicity were monitored over a 60-day period.

Results: DADA and FZ improved the safety profiles in BALB/c nude mice. In the animal model, combined treatment with 100 mg/kg DADA and 40 mg/kg FZ resulted in a 50% reduction in complete tumor regression, compared to 11.1% and 0% in the single-agent treatment groups, respectively. The combination therapy showed superior efficacy in reducing tumor size and inducing tumor loss compared to either treatment alone.

Conclusions: Combining oral treatment of 100 mg/kg DADA and 40 mg/kg FZ synergistically inhibited tumor growth in immunodeficient BALB/c nude mice transplanted with A549 lung cancer cells. A clinical study is warranted to prove the efficacy and safety of this well-characterized drug combination as a repurposing treatment for lung cancer.

Keywords: Anti-cancer; diisopropylamine dichloroacetate; fenbendazole (FZ); non-small cell lung cancer (NSCLC); lung cancer

Submitted Dec 28, 2024. Accepted for publication May 09, 2025. Published online Jul 25, 2025.

doi: 10.21037/tlcr-2024-1272

View this article at: <https://dx.doi.org/10.21037/tlcr-2024-1272>

^A ORCID: 0000-0003-2712-9747.

Introduction

According to GLOBOCAN 2020, lung cancer ranks among the highest cancer incidence and mortality rates worldwide. In 2020, 2.2 million new lung cancer cases and 1.8 million lung cancer-related deaths approximately represented approximately 11.4% and 18.0% of the total cancer cases and total cancer deaths, respectively (1). Lung cancer is broadly categorized into small cell lung cancer (SCLC) and non-small cell lung cancer (NSCLC), with NSCLC accounting for 85% of all cases (2,3). In recent years, many treatments for NSCLC patients have seen advancement, including surgical resection, chemotherapy, radiation therapy, targeted therapy, and immunotherapy (4-6). With the development of personalized, targeted therapies, NSCLC patients now benefit from individualized treatment options. However, despite progress in genetic understanding, diagnostics, and therapeutic strategies, the prognosis for lung cancer remains poor, with only about 20% of patients achieving an overall survival longer than 5 years post-diagnosis, and the figure has shown minimal improvement (7). This underscores the urgent need for new, effective therapeutic strategies for NSCLC patients.

Fenbendazole (FZ) or [5-(phenylthio)-1*H*-benzimidazol-2-yl] carbamic acid methyl ester is a benzimidazole commonly used as an antiparasitic agent in veterinary

medicine. Like several anticancer drugs, FZ inhibits the microtubules' formation and function by binding with tubulin (8,9). Recent studies have explored the anticancer activity of FZ. Han *et al.* improved the anti-cancer effect of FZ by inhibiting the reactive oxygen species (ROS) in HL-60 cells (10). In addition, previous investigations indicated that FZ can arrest the G2/M phase in the cell cycle of H4IIE hepatocellular cells (11) and SNU-C5 colorectal cancer cells (12). Peng *et al.* research demonstrated that FZ interferes with HeLa cervical cancer cell proliferation and glucose metabolism (13). Although most reported cases of FZ self-administration by oral treatment have shown their anti-cancer effects, FZ has been associated with drug-induced liver injury in some cases. However, patients generally recover after discontinuation of FZ (14,15). Furthermore, due to absorption limitation in the intestine, the systemic level of FZ and its metabolites in blood and tissue is lower than the administered dose (16,17). To optimize FZ's anticancer potential while minimizing this adverse effect, combining it with a synergistic, safe, and non-toxic agent may facilitate clinical translation. Specifically, identifying a partner compound that can act as a glycolysis inhibitor could be a key to developing an effective anticancer combination therapy.

By inhibiting pyruvate dehydrogenase kinase, diisopropylamine dichloroacetate (DADA), a therapeutic agent for chronic liver disease, has shown anti-tumor properties (18). DADA also acts as a hepatoprotective agent (19), which could support the use of FZ in patients with liver cancer, bile duct cancer, or compromised liver function. Combining FZ and DADA could potentially reduce liver toxicity, increase the effectiveness of the therapy, and improve patient tolerance within a comprehensive metabolic therapy framework for treating proliferative disorders. Thus, this study aimed to investigate the effects of the FZ-DADA combination in a mouse model of lung cancer. We present this article in accordance with the ARRIVE reporting checklist (available at <https://tclcr.amegroups.com/article/view/10.21037/tclcr-2024-1272/rc>).

Methods

Cells culture

A549 cells were purchased from ATCC (ATCC-CCL-185) and cultured in an 18 cm² culture dish with Roswell Park Memorial Institute (RPMI) medium (Sigma-Aldrich Solution, Merck, Germany) containing 10%

Highlight box

Key findings

- Demonstrated synergistic anticancer effects of fenbendazole (FZ) and diisopropylamine dichloroacetate (DADA) in immunodeficient BALB/c nude mice with A549 lung cancer cells.
- The treatment was safe, showing no adverse effects on body weight, blood sugar levels, or liver and kidney function.

What is known, and what is new?

- Previous studies indicated the anticancer effects of FZ and DADA but are associated with potential liver toxicity.
- This study is the first to show the synergistic efficacy of FZ and DADA in inhibiting tumor growth and improving safety profiles in lung cancer at the *in vivo* level.

What is the implication, and what should change now?

- This combination therapy represents a promising strategy for non-small cell lung cancer, especially for patients requiring long-term treatment or those with compromised liver function.
- Clinical studies are warranted to validate the efficacy and safety of this combination, paving the way for its development as a repurposed therapeutic option for lung cancer.

Table 1 Animals in treatment groups

Group	Treatment	N
1	Healthy control	6
2	Tumor control	9
3	Cisplatin 5 mg/kg	8
4	FZ 40 mg/kg	9
5	DADA 20 mg/kg	10
6	DADA 100 mg/kg	10
7	FZ 40 mg/kg + DADA 20 mg/kg	10
8	FZ 40 mg/kg + DADA 100 mg/kg	10

Group 1: six normal mice with no cancer cell implement stayed at healthy control. Sixty-six tumor beared nude mice were randomly divided into 7 groups, with different treatments: group 2: tumor control group with no treatment; group 3: positive control group with 5 mg/kg cisplatin daily injection; groups 4-8: daily administered orally treatment with different concentration and combination of FZ and DADA. DADA, diisopropylamine dichloroacetate; FZ, fenbendazole.

fetal bovine serum (FBS) (Gibco, Invitrogen, USA), 1% penicillin/streptomycin solution (penicillin 10,000 U/mL and streptomycin 10,000 µg/mL) (Gibco, Invitrogen, USA) and incubated at 37 °C with 5% CO₂. The cells were routinely maintained, subcultured, and checked for contamination. For animal injections, cells were washed twice with 1× phosphate buffer saline (PBS) solution and trypsinization with 1× Trypsin-EDTA solution. The numbers were evaluated using an Invitrogen Countess® II FL cell counter and analyzer. The study was conducted in accordance with the Declaration of Helsinki and its subsequent amendments.

Animal models

Immunodeficient BALB/c nude mice (Foxn1nu) were utilized for the *in vivo* assessment of anticancer activity. A total of 72 mice were imported from BioLASCO (Taiwan) for the study. The mice were housed in a sterile environment following the standard operating procedures for nude mouse care provided by the Center for Experimental Animal Research, Military Medical Academy. All animals were acclimated to the facility's conditions for one week before the initiation of the experiment, with ad libitum access to food and water. Room temperature and humidity were carefully controlled, and a 12-hour light/dark cycle was maintained. Human lung cancer cells (A549) were collected and diluted

in culture media to 2×10⁷/mL, and each immunodeficient mouse received 2×10⁶ cells/0.1 mL into the right flank's subcutaneous site. Tumor sizes were monitored. When the tumor reached 50 mm³, the mice were randomized into eight groups, as shown in *Table 1*.

Animals in treatment groups (groups 4, 5, 6, 7, 8) received a daily treatment administered orally, while mice in the positive control group received 5 mg/kg of cisplatin daily by injection directly around the tumor.

Evaluate the toxicity of FZ and DADA treatment

After 60 days of treatment, mice were anesthetized with isoflurane and euthanized by cervical dislocation. Serum, lung, and tumor samples were collected for assays. Post-tumor inoculation, the following parameters were monitored to assess overall health and treatment effects, including body weight, appearance, tumor growth, and survival time. Mice's health was evaluated based on the following criteria:

- ❖ Weight: recorded twice weekly using an electronic scale TE3102S Sartorius to track mice's weight changes before and after treatment;
- ❖ Movement: observations were made on movement patterns (normal, hyperactive, hypoactive, or immobile);
- ❖ Response to stimuli: response to tactile and environmental stimuli was categorized as normal, heightened, reduced, or absent;
- ❖ Skin color: evaluated for changes, including normal color, purple, and bleeding;
- ❖ Mice feces: monitored for consistency and appearance (normal, loose, bloody stool).

The safety assessment of FZ and DADA and their combination

The safety profile of FZ and DADA, individually and in combination, was evaluated through the following metrics:

- ❖ Mice's general condition and body weight: determine hematopoietic function by counting red blood cells, hemoglobin, and white blood cells;
- ❖ Determine the amount of liver cell damage by measuring enzyme activity in the blood [alanine aminotransferase (ALT), aspartate transaminase (AST), and histological pictures];
- ❖ Evaluate renal function using serum urea and creatinine levels and histopathological images.

Histopathological imaging

Immunodeficient BALB/c nude mice (Foxn1nu) were housed in a sterile environment following the standard operating procedures for nude mouse care. A549 were grown on cell culture flasks in RPMI 1640 culture media supplemented with 10% FBS, 1% penicillin and streptomycin at 37 °C and CO₂. After 1 week of housing, A549 cells were injected into mice with 2×10⁶ cells/0.1 mL/mice into the right flank's subcutaneous site. The manipulation is done in a sterile environment. When the tumor reached 50 mm³, the mice were randomized into eight groups: healthy control, tumor control, cisplatin, FZ 40 mg/kg, DADA 20 mg/kg, DADA 100 mg/kg, FZ 40 mg/kg + DADA 20 mg/kg, FZ 40 mg/kg + DADA 100 mg/kg. Animals were observed after 60 days. Hematoxylin and eosin staining were applied to liver and kidney tissues after harvesting.

Antitumor effect

The tumor volume was calculated using the following formula:

$$V = (D \times R^2) \times 0.5 \quad [1]$$

While: V: tumor volume (mm³); D: tumor length as measured (mm); R: tumor width as measured (mm).

The survival time of each mouse, the average survival time of the groups of mice, the cumulative survival of the treatment and control groups of mice, and the correlation comparison were all monitored until the end of the experiment.

Statistical analysis

Data were analyzed using SPSS version 22.0 (IBM Corp.) and GraphPad Prism 10 (GraphPad Software, USA). The Chi-square test (χ^2 test) was used to compare two observed proportions. For normally distributed data, a *t*-test is used to compare the means between two independent groups. In comparison, a one-way analysis of variance (ANOVA) is used to compare the means among three or more groups, with a Dunnett test used to determine which differences are significant. A two-way ANOVA compares the means among three or more groups at different time points. Comparison of medians between two independent groups was performed using the Mann-Whitney *U* test, with the significance determined based on the P value (P>0.05: no statistically significant difference and P<0.05: statistically significant

difference). The log-rank test was applied to compare the cumulative survival time between different treatment methods.

Ethical considerations

All experimental procedures involving animals followed institutional ethical guidelines for the laboratory animal use and care. The protocol was approved by the Dinh Tien Hoang Institute of Medicine's review board (operating code IRB-VN02010, approval No. IRB-A-2200) before the study. The protocol was prepared before the study without registration.

Results

Toxicity of FZ and DADA in BALB/c nude mice

After A549 cell transplantation, mice maintained normal behaviors, including consistent eating, weight gain, active movement, and responses to stimuli. There were no signs of loose stools, and the anal area remained dry. The mice's skin at the injection location was normal, with no bleeding or infection. The average weight of all 7 groups of mice was similar before treatment, and the difference was not statistically significant (P>0.05) (Table S1). After treatment, the body weights of the seven groups were measured twice a week. The body weight tended to increase compared to the baseline, except for group DADA, which was 20 mg/kg (Figure 1).

Hematological and kidney function analysis

To further evaluate the side effects of our treatment in mice, we continued to examine the hematological indices of the mice, which play a vital role in assessing the impact of FZ and DADA on BALB/c mice. Table 2 indicates that after 60 days of treatment, there was no statistically significant difference in hematopoietic function (red blood cell count, hemoglobin content, white blood cell count) among eight groups of mice (P>0.05). On the other hand, urea and creatinine levels in mice's blood were measured to confirm the effect of FZ and DADA on kidney function. After 60 days of therapy, kidney function tests in all 6 treatment groups (5 treatment groups, 1 positive control group) showed no statistically significant difference from the tumor non-treatment control group (P>0.05) (Table 3). Histological analysis of the kidney tissues again confirmed that FZ and

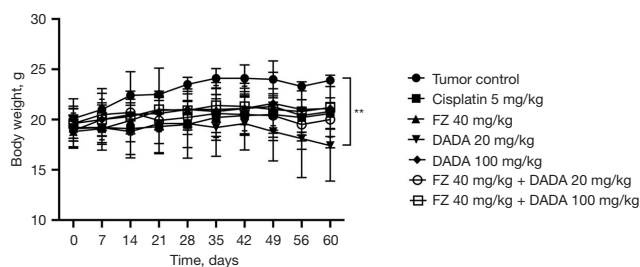


Figure 1 Mice's body weight after 60 days. Immunodeficient BALB/c nude mice (Foxn1nu) were housed in a sterile environment following the standard operating procedures for nude mouse care. A549 were grown on cell culture flasks in RPMI 1640 culture media supplemented with 10% FBS, 1% penicillin, and streptomycin at 37 °C and CO₂. After 1 week of housing, A549 cells were injected into mice with 2×10⁶ cells/0.1 mL/mice into the right flank's subcutaneous site. The manipulation is done in a sterile environment. When the tumor reached 50 mm³, the mice were randomized into eight groups: healthy control, tumor control, cisplatin, FZ 40 mg/kg—9 mice, DADA 20 mg/kg, DADA 100 mg/kg, FZ 40 mg/kg + DADA 20 mg/kg, FZ 40 mg/kg + DADA 100 mg/kg. The body weight of seven groups of mice was recorded twice a week by an electronic scale TE3102S Sartorius. Data are presented as mean ± SD. One-way ANOVA for the comparison of means among untreated and the other groups, **, P<0.01. ANOVA, analysis of variance; DADA, diisopropylamine dichloroacetate; FBS, fetal bovine serum; FZ, fenbendazole; SD, standard deviation; RPMI, Roswell Park Memorial Institute.

Table 2 Effect of FZ and DADA into the hematological indices' mice

Groups	n	Hematological indices		
		Red blood cell count (T/L)	Hemoglobin content (g/dL)	White blood cell count (G/L)
1	6	9.70±0.42	142.33±6.31	4.93±1.63
2	2	9.66±0.53	144.00±5.66	4.29±0.95
3	7	9.79±0.50	143.71±5.65	4.73±1.21
4	8	9.66±0.60	140.50±6.87	6.62±2.34
5	7	9.42±0.75	137.29±10.53	3.30±1.51
6	9	9.32±0.60	135.78±11.65	5.02±3.75
7	10	9.23±0.89	135.40±11.06	3.65±2.04
8	10	9.49±0.66	138.90±9.00	5.87±4.29
P		0.67	0.53	0.29

Data are presented as mean ± standard deviation. The hematological indices in eight groups was measured at day 60 after of the treatment. One-way ANOVA for the comparison of means among untreated and the other groups, Dunett's test was run after one-way ANOVA to determine which different are significant. Group 1: healthy control; group 2: untreated; group 3: positive control (cisplatin 5 mg/kg); group 4: FZ 40 mg/kg; group 5: DADA 20 mg/kg; group 6: DADA 100 mg/kg; group 7: FZ 40 mg/kg + DADA 20 mg/kg; group 8: FZ 40 mg/kg + DADA 100 mg/kg. ANOVA, analysis of variance; DADA, diisopropylamine dichloroacetate; FZ, fenbendazole.

DADA treatment did not adversely affect kidney function (Figure 2).

Liver function and metabolic assessment

ALT and AST levels were measured to elucidate the impact

of FZ and DADA in the liver, and liver tissue was analyzed histologically after 60 days of treatment (Figure 3). These evaluations showed no significant hepatocellular damage due to FZ and DADA treatment. Since cancer treatment can influence metabolic processes, glucose, and lactate were also measured in the blood samples, and our results showed

Table 3 Effects of drugs on the concentration of urea and creatinine in mice's blood

Groups	n	Urea (mg/dL)	Creatinine (mg/dL)
1	6	7.49±1.88	26.85±3.19
2	2	7.23±1.61	28.84±2.43
3	7	6.36±1.14	25.49±1.37
4	8	6.26±1.30	26.84±2.18
5	7	6.91±0.75	25.81±2.16
6	9	6.94±1.64	25.60±2.11
7	10	6.77±0.65	26.32±1.61
8	10	6.84±1.94	26.79±1.77
P		0.82	0.44

Data are presented as mean ± standard deviation. One-way ANOVA compares the means among the untreated and the other groups, Dunnett's test was run after one-way ANOVA to determine which different are significant. After the treatment, the eight groups' urea and creatinine levels were measured at day 60. Group 1: healthy control; group 2: untreated; group 3: positive control (cisplatin 5 mg/kg); group 4: FZ 40 mg/kg; group 5: DADA 20 mg/kg; group 6: DADA 100 mg/kg; group 7: FZ 40 mg/kg + DADA 20 mg/kg; group 8: FZ 40 mg/kg + DADA 100 mg/kg. ANOVA, analysis of variance; DADA, diisopropylamine dichloroacetate; FZ, fenbendazole.

nonsignificant differences in glucose and lactate levels in mice's blood among eight groups ($P>0.05$) (Figure 4).

Anti-tumor effect of FZ and DADA

At the start of treatment, there was no significant difference in the tumor volume across the groups ($P>0.05$) (Table S2). Tumor growth in the combination treatment group was slower than tumors in the single-treatment groups, with group 7 showing a smaller mean tumor volume than groups 4 and 5. However, this difference was not statistically significant ($P>0.05$). Interestingly, the combination of FZ and DADA in a ratio of 40:100 resulted in a greater reduction in tumor volume than in single-dose groups across all time points. From day 14, group 8 significantly decreased tumor volume compared with the tumor control group, while the others did not show any statistical difference. At day 60 of the experiment, the combination treatment in group 8 performed a greater anti-tumor effect than their single-dose treatment (Figure 5A), indicating the synergistic anti-tumor effect of FZ and DADA at 40:100 mg/kg ratio.

Tumor reduction rates of FZ and DADA in BALB/c nude mice

On day 7 following treatment, tumor reduction (tumor regression) began in the mice treated in groups 6, 7, and 8. The number of mice losing tumors in the therapy groups steadily rose. The tumor untreated group did not lose any tumor at any stage throughout the trial, whereas the number of dead mice progressively grew. Table 4 shows the number of mice that achieved tumor loss in treatment groups. From day 21 onward, the percentage of tumor-free mice in group 8 was significantly higher than that of the untreated group ($P<0.0001$). At the end of the experiment (day 60), the tumor reduction rate in the tumor control group, positive control, and group 6 was 0 (0%); groups 4, 5 was 1 (11.1%); group 7 was 2 (20%), group 8 was 5 (50%). The number of mice with tumor loss was 9, accounting for 15% of the total. Interestingly, from days 21 to 60, the proportion of tumor-losing mice in group 8 was significantly higher than that of groups 4 and 6 (Table 4, Figure 5B, 5C). Our results indicated the synergic effect of FZ and DADA at a ratio of 40:100 mg/kg in promoting tumor regression in BALB/c nude mice.

Effect of FZ and DADA on the survival duration and death rate of BALB/c nude mice

Survival time was used as a criterion to assess the effectiveness of FZ and DADA treatment in A549 lung cancer-bearing nude mice. As shown in Figure 6A, the average survival time in all treatment groups was significantly higher than in the control group. Survival rates were compared across groups to validate treatment efficacy further. In the tumor control group, the first death occurred on day 21, with mortality increasing steadily throughout the time. The number and death rates of mice in the tumor control group were higher than in the other six treatment groups at all research time points. However, the difference was only statistically significant between the control and treatment groups from day 49 to the completion of the experiment (day 60) (Figure 6B and Table 5).

Discussion

This study confirmed the safety profile of FZ (40 mg/kg) and DADA (100 mg/kg) in BALB/c mice. The treatment did not alter body weight, blood sugar levels, or liver and kidney function. Our findings demonstrate that combining

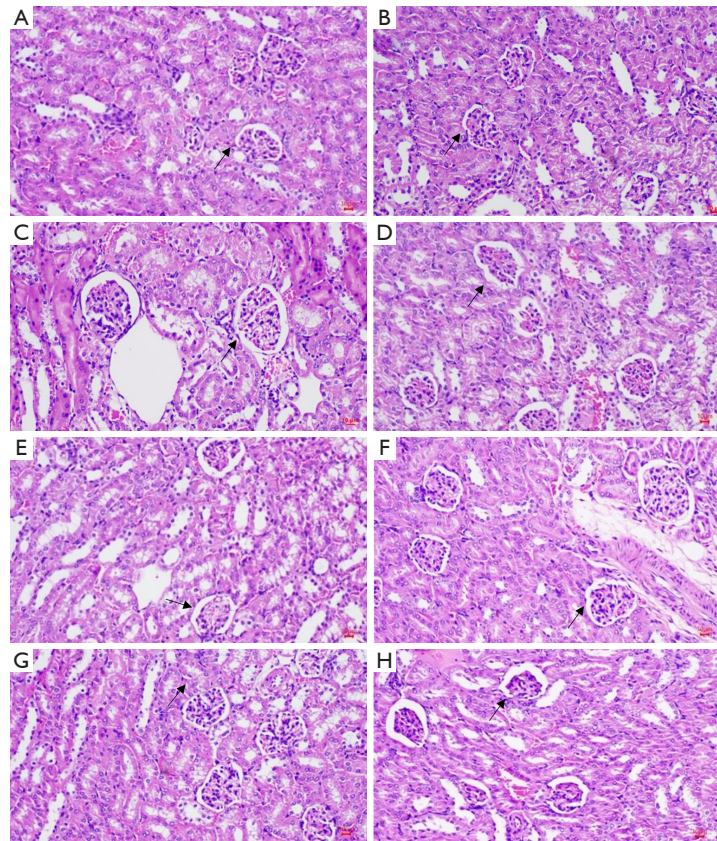


Figure 2 Histology sections of kidney in nude mice. Hematoxylin and eosin staining were applied to liver and kidney tissues after harvesting ($\times 40$). (A) Healthy control; (B) tumor control; (C) cisplatin 5 mg/kg; (D) FZ 40 mg/kg; (E) DADA 20 mg/kg; (F) DADA 100 mg/kg; (G) FZ 40 mg/kg + DADA 20 mg/kg; (H) FZ 40 mg/kg + DADA 100 mg/kg. The arrows represent the glomerulus. DADA, diisopropylamine dichloroacetate; FZ, fenbendazole.

FZ 40 mg/kg and DADA 100 mg/kg effectively inhibits tumor growth in BALB/c nude mice transfected with A549 NSCLC cells. The combination treatment group showed significantly reduced tumor volume and higher tumor regression rates than the single-treatment groups. Additionally, combination therapy markedly extended survival time in treated mice compared to controls. Previous studies have highlighted the anti-cancer effects of FZ in many cancer types (8-13,16,17,20). Similarly, DADA has shown promise in enhancing efficacy in cancer treatment

(21-24). Our findings suggested that the synergistic effects of oral treatment with FZ and DADA, a pyruvate dehydrogenase kinase inhibitor (18) and hepatoprotective compound (19,24,25), may represent a promising therapeutic strategy for NSCLC.

In our previous study, the combination of FZ and DADA showed a synergistic effect in inhibiting the proliferation of A549 lung cancer cells. The FZ-DADA combination induced ROS production and promoted apoptosis by downregulating B-cell lymphoma 2 (Bcl2) and

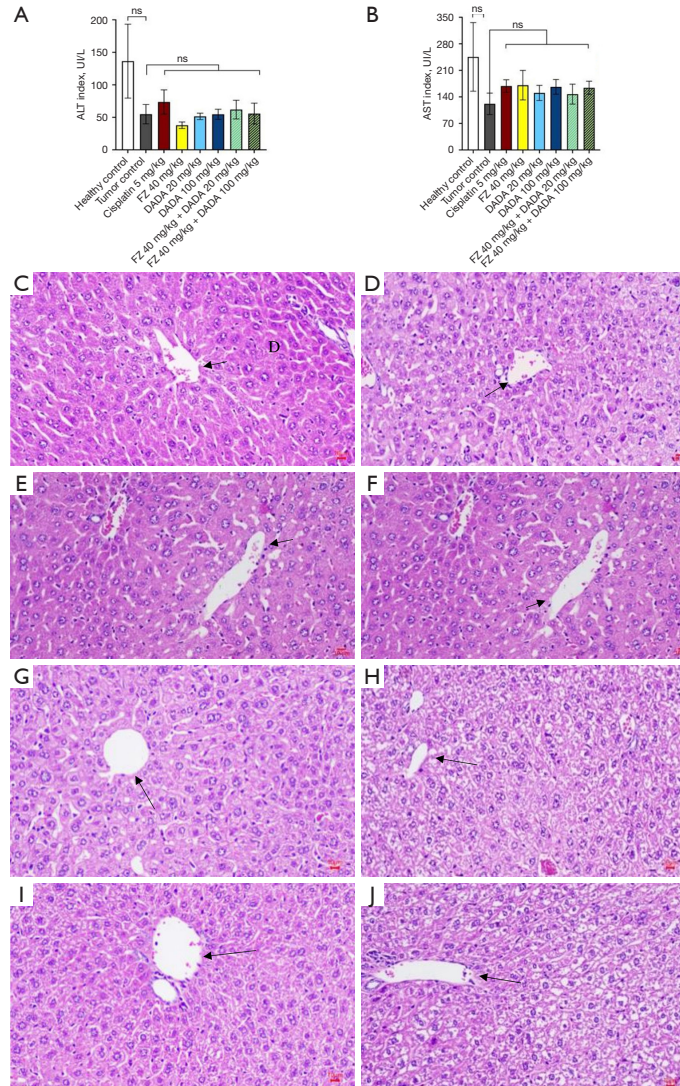


Figure 3 Effect of drug formulation on liver function. (A,B) The AST and ALT index in eight groups was measured at day 60 after the treatment. Data present mean \pm SD. One-way ANOVA for the comparison of means among untreated and the other groups. (C-J) Hematoxylin and eosin staining were applied to liver tissues after harvesting ($\times 40$): (C) healthy control; (D) tumor control; (E) cisplatin 5 mg/kg; (F) FZ 40 mg/kg; (G) DADA 20 mg/kg; (H) DADA 100 mg/kg; (I) FZ 40 mg/kg + DADA 20 mg/kg; (J) FZ 40 mg/kg + DADA 100 mg/kg. The arrows represent for the central lobule vein. ALT, alanine aminotransferase; ANOVA, analysis of variance; AST, aspartate transaminase; DADA, diisopropylamine dichloroacetate; ns, not significant; FZ, fenbendazole; SD, standard deviation.

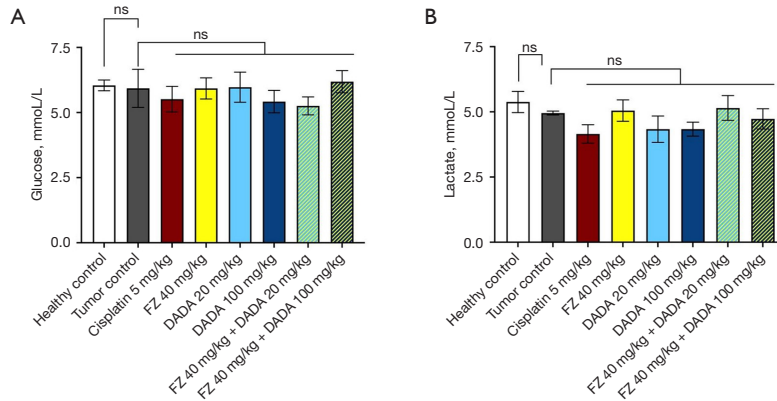


Figure 4 Effect of FZ and DADA on glucose metabolism. Glucose (A) and lactate levels (B) were determined in the blood of animals on day 60 of the experiment. Data presents mean \pm SD. One-way ANOVA for the comparison of means among untreated and the other groups, Dunett's test was run after one-way ANOVA to determine which different are significant. ANOVA, analysis of variance; DADA, diisopropylamine dichloroacetate; FZ, fenbendazole; ns, not significant; SD, standard deviation.

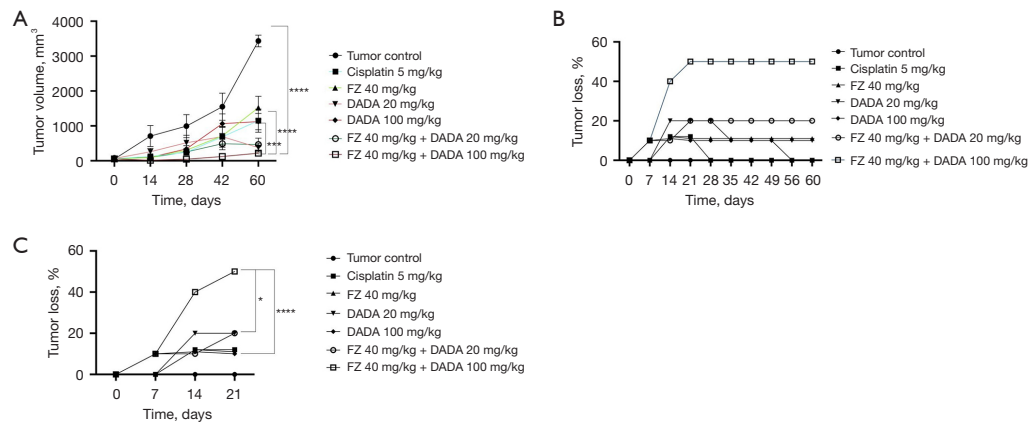


Figure 5 Tumor volume results in groups of mice during treatment. (A) The tumor volume was calculated using the following formula: $V = (D \times R^2) \times 0.5$ with V: tumor volume (mm³), D: tumor length as measured (mm), and R: tumor width as measured (mm). Data present mean \pm SEM, two-way ANOVA for the comparison of means among untreated and the other groups, *, $P < 0.05$; ***, $P < 0.001$; ****, $P < 0.0001$. (B,C) Tumor reduction rate in treated mice group. The number of tumor-loss mice in eight groups was recorded during 60 days. Chi-square test for comparison of two percentages. ANOVA, analysis of variance; DADA, diisopropylamine dichloroacetate; FZ, fenbendazole; SEM, standard error of the mean.

upregulating BAX protein expression. The combination activated caspase-3, caspase-7, and poly (ADP-ribose) polymerase (PARP), further driving apoptosis in A549 cells.

Additionally, FZ-DADA treatment also induced cell cycle arrest, as evidenced by the inhibition of Cyclin A and Cyclin E proteins. These findings provide valuable insights into

Table 4 Tumor reduction rate in treated mice group

Days	Tumor reduction rate, n (%)							P
	Group 2	Group 3	Group 4	Group 5	Group 6	Group 7	Group 8	
Day 7	0	0	0	0	1 (10.0)	1 (10.0)	1 (10.0)	$P_{2-6,7,8}=0.33$
Day 14	0	1 (12.5)	1 (12.5)	2 (20.0)	1 (11.1)	1 (10.0)	4 (40.0)	$P_{2-8}=0.054$
Day 21	0	1 (12.5)	1 (11.1)	2 (20.0)	1 (10.0)	2 (20.0)	5 (50.0)	$P_{2-8}<0.0001$; $P_{4-6}=0.01$; $P_{6-8}<0.0001$
Day 28	0	0	1 (11.1)	2 (20.0)	1 (10.0)	2 (20.0)	5 (50.0)	$P_{2-8}<0.0001$; $P_{4-6}=0.01$; $P_{6-8}<0.0001$
Day 35	0	0	1 (11.1)	1 (10.0)	1 (10.0)	2 (20.0)	5 (50.0)	$P_{2-8}<0.0001$; $P_{4-6}=0.01$; $P_{6-8}<0.0001$
Day 42	0	0	1 (11.1)	1 (10.0)	1 (10.0)	2 (20.0)	5 (50.0)	$P_{2-8}<0.0001$; $P_{4-6}=0.01$; $P_{6-8}<0.0001$
Day 49	0	0	1 (11.1)	1 (10.0)	1 (10.0)	2 (20.0)	5 (50.0)	$P_{2-8}<0.0001$; $P_{4-6}=0.01$; $P_{6-8}<0.0001$
Day 56	0	0	1 (11.1)	1 (10.0)	0	2 (20.0)	5 (50.0)	$P_{2-8}<0.0001$; $P_{4-6}=0.01$; $P_{6-8}<0.0001$
Day 60	0	0	1 (11.1)	1 (11.1)	0	2 (20.0)	5 (50.0)	$P_{2-8}<0.0001$; $P_{4-6}=0.01$; $P_{6-8}<0.0001$

The number of tumor loss mice in eight groups was recorded for 60 days. Chi-squared test was used to compare the difference between percentages. Group 2: untreated; group 3: positive control (cisplatin 5 mg/kg); group 4: FZ 40 mg/kg; group 5: DADA 20 mg/kg; group 6: DADA 100 mg/kg; group 7: FZ 40 mg/kg + DADA 20 mg/kg; group 8: FZ 40 mg/kg + DADA 100 mg/kg. DADA, diisopropylamine dichloroacetate; FZ, fenbendazole.

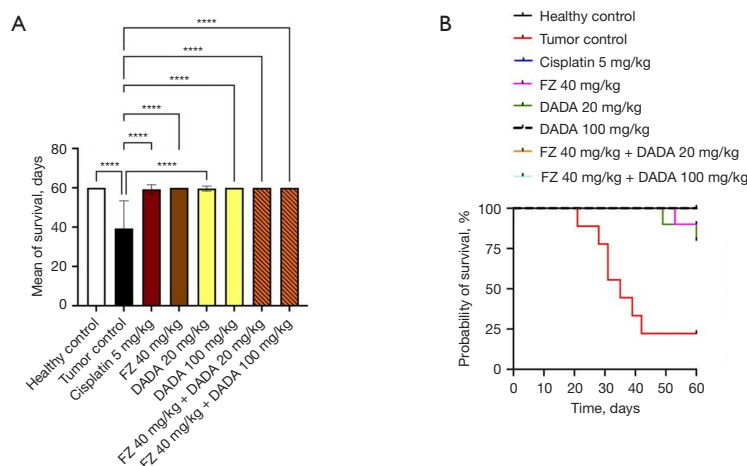


Figure 6 The survival duration and death rate death rate of nude mice. The number of survival mice in eight groups was recorded during 60 days of the experiment. (A) Mean of survival (day) data present mean \pm SD; one-way ANOVA was used to compare the mean of treatment groups and untreated group, ****, $P<0.0001$. (B) Survival rate (%), the log-rank test was applied to compare the cumulative survival time between different treatment methods. ANOVA, analysis of variance; DADA, diisopropylamine dichloroacetate; FZ, fenbendazole; SD, standard deviation.

the potential therapeutic applications of the FZ and DADA combination for lung cancer (25,26).

In the current study, we compared the therapeutic

efficacy of FZ-DADA with that of peritumoral cisplatin injection to evaluate its potential as a treatment for NSCLC. It is important to note, however, that this comparison may

Table 5 Survival rate in treatment groups

Groups	No. of mice	Survival rate, n [%]					
		Day 21	Day 28	Day 35	Day 39	Day 49	Day 60
2	9	7 [77.8]	5 [55.6]	4 [44.4]	3 [33.3]	2 [22.2]	2 [22.2]
3	8	8 [100]	8 [100]	8 [100]	8 [100]	7 [87.5]	7 [87.5]
4	9	9 [100]	9 [100]	9 [100]	9 [100]	9 [100]	8 [88.9]
5	10	10 [100]	10 [100]	10 [100]	10 [100]	10 [100]	7 [70]
6	10	10 [100]	10 [100]	10 [100]	10 [100]	10 [100]	9 [90]
7	10	10 [100]	10 [100]	10 [100]	10 [100]	10 [100]	10 [100]
8	10	10 [100]	10 [100]	10 [100]	10 [100]	10 [100]	10 [100]
P value		>0.05	P ₂₋₃ =0.031; P ₂₋₄ =0.023; P _{2-5,6,7,8} =0.018	P ₂₋₃ =0.012; P ₂₋₄ =0.009; P _{2-5,6,7,8} =0.006	P ₂₋₃ =0.004; P ₂₋₄ =0.003; P _{2-5,6,7,8} =0.002	P ₂₋₃ =0.007; P ₂₋₄ <0.001; P _{2-5,6,7,8} <0.001	P ₂₋₃ =0.007; P ₂₋₄ =0.004; P ₂₋₅ =0.037; P ₂₋₆ =0.003; P _{2-7,8} <0.001; P ₄₋₇ =0.28; P ₅₋₇ =0.06; P ₄₋₈ =0.89; P ₄₋₈ =0.30

Chi-square test was used to compare the difference between of two percentages. The number of survival mice in eight groups was recorded during 60 days of the experiment. Group 2: untreated; group 3: positive control (cisplatin 5 mg/kg); group 4: FZ 40 mg/kg; group 5: DADA 20 mg/kg; group 6: DADA 100 mg/kg; group 7: FZ 40 mg/kg + DADA 20 mg/kg; group 8: FZ 40 mg/kg + DADA 100 mg/kg. DADA, diisopropylamine dichloroacetate; FZ, fenbendazole.

not accurately reflect the true clinical advantage of FZ-DADA over cisplatin in human patients, as cisplatin is typically administered intravenously in clinical settings and is associated with severe adverse effects, including nephrotoxicity, bone marrow suppression, and increased susceptibility to infections—all of which can significantly impair quality of life and reduce overall survival. In contrast, FZ-DADA has demonstrated a favorable safety profile in both human preclinical and animal clinical studies.

Adding DADA to the potential therapeutic combination with FZ may thus serve a dual role in this combination therapy, enhancing FZ's anticancer efficacy while offering hepatoprotective benefits. This synergistic effect is particularly advantageous for patients with compromised liver function or those requiring long-term cancer treatment, as DADA could mitigate the risk of liver injury and potentially enhance systemic tolerability. Our findings in the current study underscore the potential clinical utility of combining FZ and DADA, supporting its translational research and development as a safe and effective therapeutic option for lung cancer.

Conclusions

Combining 100 mg/kg DADA and 40 mg/kg FZ

synergistically inhibited tumor growth in immunodeficient BALB/c nude mice transplanted with A549 lung cancer cells. A clinical study is warranted to prove the efficacy and safety of this well-characterized drug combination as a repurposing treatment for lung cancer.

Acknowledgments

The authors would like to thank Doctor Ngo Thi Thu Hang and the staff of the Center for Experimental Animal Research, Military Medical Academy, Hanoi, Vietnam, for all the assistance and technical help in animal experiments. We also express our gratitude to doctors Nguyen Khanh Hoa and Nguyen Thi Thanh Huong at the Dinh Tien Hoang Institute of Medicine for meaningful advice in experiment design.

Footnote

Reporting Checklist: The authors have completed the ARRIVE reporting checklist. Available at <https://tlcr.amegroups.com/article/view/10.21037/tlcr-2024-1272/rc>

Data Sharing Statement: Available at <https://tlcr.amegroups.com/article/view/10.21037/tlcr-2024-1272/dss>

Peer Review File: Available at <https://tclr.amegroups.com/article/view/10.21037/tclr-2024-1272/prf>

Funding: The project was funded by Thai Minh Pharmaceuticals JSC, Hanoi, Vietnam.

Conflicts of Interest: All authors have completed the ICMJE uniform disclosure form (available at <https://tclr.amegroups.com/article/view/10.21037/tclr-2024-1272/coif>). All authors report that the project was funded by Thai Minh Pharmaceuticals JSC, Hanoi, Vietnam. The authors have no other conflicts of interest to declare.

Ethical Statement: The authors are accountable for all aspects of the work in ensuring that questions related to the accuracy or integrity of any part of the work are appropriately investigated and resolved. All experimental procedures involving animals followed institutional ethical guidelines for the laboratory animal use and care. The protocol was approved by the Dinh Tien Hoang Institute of Medicine's review board (operating code IRB-VN02010, approval No. IRB-A-2200) before the study. The protocol was prepared before the study without registration. The study was conducted in accordance with the Declaration of Helsinki and its subsequent amendments.

Open Access Statement: This is an Open Access article distributed in accordance with the Creative Commons Attribution-NonCommercial-NoDerivs 4.0 International License (CC BY-NC-ND 4.0), which permits the non-commercial replication and distribution of the article with the strict proviso that no changes or edits are made and the original work is properly cited (including links to both the formal publication through the relevant DOI and the license). See: <https://creativecommons.org/licenses/by-nc-nd/4.0/>.

References

- Li C, Lei S, Ding L, et al. Global burden and trends of lung cancer incidence and mortality. *Chin Med J (Engl)* 2023;136:1583-90.
- Navada S, Lai P, Schwartz AG, et al. Temporal trends in small cell lung cancer: Analysis of the national Surveillance, Epidemiology, and End-Results (SEER) database. *J Clin Oncol* 2006;24:7082.
- Sher T, Dy GK, Adjei AA. Small cell lung cancer. *Mayo Clin Proc* 2008;83:355-67.
- Punekar SR, Shum E, Grello CM, et al. Immunotherapy in non-small cell lung cancer: Past, present, and future directions. *Front Oncol* 2022;12:877594.
- Mamdani H, Matosevic S, Khalid AB, et al. Immunotherapy in Lung Cancer: Current Landscape and Future Directions. *Front Immunol* 2022;13:823618.
- Molina JR, Yang P, Cassivi SD, et al. Non-small cell lung cancer: epidemiology, risk factors, treatment, and survivorship. *Mayo Clin Proc* 2008;83:584-94.
- Vicidomini G. Current Challenges and Future Advances in Lung Cancer: Genetics, Instrumental Diagnosis and Treatment. *Cancers (Basel)* 2023;15:3710.
- Duan Q, Liu Y, Rockwell S. Fenbendazole as a potential anticancer drug. *Anticancer Res* 2013;33:355-62.
- Dogra N, Kumar A, Mukhopadhyay T. Fenbendazole acts as a moderate microtubule destabilizing agent and causes cancer cell death by modulating multiple cellular pathways. *Sci Rep* 2018;8:11926.
- Han Y, Joo HG. Involvement of reactive oxygen species in the anti-cancer activity of fenbendazole, a benzimidazole anthelmintic. *Korean J Vet Res* 2020;60:79-83.
- Park D. Fenbendazole Suppresses Growth and Induces Apoptosis of Actively Growing H4IIE Hepatocellular Carcinoma Cells via p21-Mediated Cell-Cycle Arrest. *Biol Pharm Bull* 2022;45:184-93.
- Park D, Lee JH, Yoon SP. Anti-cancer effects of fenbendazole on 5-fluorouracil-resistant colorectal cancer cells. *Korean J Physiol Pharmacol* 2022;26:377-87.
- Peng Y, Pan J, Ou F, et al. Fenbendazole and its synthetic analog interfere with HeLa cells' proliferation and energy metabolism via inducing oxidative stress and modulating MEK3/6-p38-MAPK pathway. *Chem Biol Interact* 2022;361:109983.
- Thakurdesai A, Rivera-Matos L, Nagra N, et al. Severe Drug-Induced Liver Injury Due to Self-administration of the Veterinary Anthelmintic Medication, Fenbendazole. *ACG Case Rep J* 2024;11:e01354.
- Yamaguchi T, Shimizu J, Oya Y, et al. Drug-Induced Liver Injury in a Patient with Nonsmall Cell Lung Cancer after the Self-Administration of Fenbendazole Based on Social Media Information. *Case Rep Oncol* 2021;14:886-91.
- Düwel D. Fenbendazole. II. Biological properties and activity. *Pestic Sci* 1977;8:550-5.
- Prichard RK, Kelly JD, Bolin TD, et al. The effect of iron and protein deficiency on plasma levels and parasite uptake of [14C] fenbendazole in rats infected with *Nippostrongylus brasiliensis*. *Aust J Exp Biol Med Sci* 1981;59:567-73.

18. Yamane K, Indalao IL, Chida J, et al. Diisopropylamine dichloroacetate, a novel pyruvate dehydrogenase kinase 4 inhibitor, as a potential therapeutic agent for metabolic disorders and multiorgan failure in severe influenza. *PLoS One* 2014;9:e98032.
19. Hatano M, Katsu K, Ishihara M. Examination of toxicity of diisopropylammonium dichloroacetate (DADA), remedies for cardiac diseases, toward isolated rat hepatocytes. *Meikai Daigaku Shigaku Zasshi* 1990;19:137-44.
20. Sung JY, Joo HG. Anti-cancer effects of Fenbendazole and Paclitaxel combination on HL-60 cells. *Journal of the Preventive Veterinary Medicine* 2021;45:13-7.
21. Su L, Zhang H, Yan C, et al. Superior anti-tumor efficacy of diisopropylamine dichloroacetate compared with dichloroacetate in a subcutaneous transplantation breast tumor model. *Oncotarget* 2016;7:65721-31.
22. Wei M, Shen X, Liu Y, et al. The antitumor effect of diisopropylamine dichloroacetate on non-small cell lung cancer and its influence on the tumor immune microenvironment. *Front Oncol* 2024;14:1447828.
23. Dong G, Chen Q, Jiang F, et al. Diisopropylamine dichloroacetate enhances radiosensitization in esophageal squamous cell carcinoma by increasing mitochondria-derived reactive oxygen species levels. *Oncotarget* 2016;7:68170-8.
24. Liu D, Wang F, Yue J, et al. Metabolism targeting therapy of dichloroacetate-loaded electrospun mats on colorectal cancer. *Drug Deliv* 2015;22:136-43.
25. Nguyen TQ, Nguyen DH, Phan UTT, et al. Fenbendazole and Diisopropylamine Dichloroacetate Exert Synergistic Anti-cancer Effects by Inducing Apoptosis and Arresting the Cell Cycle in A549 Lung Cancer Cells. *Anticancer Res* 2024;44:4761-72.
26. Nguyen J, Nguyen TQ, Han BO, et al. Oral Fenbendazole for Cancer Therapy in Humans and Animals. *Anticancer Res* 2024;44:3725-35.

Cite this article as: Nguyen TQ, Phan UTT, Can MV, Nguyen DH, Han B, Hoang BX. Synergistic anti-tumor effect of fenbendazole and diisopropylamine dichloroacetate in immunodeficient BALB/c nude mice transplanted with A549 lung cancer cells. *Transl Lung Cancer Res* 2025. doi: 10.21037/tlcr-2024-1272

Supplementary

Table S1 The average weight of mice before treatment (g)

Groups	n	Weight, g	P
Non-treatment tumor control	9	20.10±1.97	0.65
Positive control	8	19.11±1.24	
FZ 40 mg/kg	9	18.80±1.65	
DADA 20 mg/kg	10	19.11±1.82	
DADA 100 mg/kg	10	18.81±1.68	
FZ 40 mg/kg + DADA 20 mg/kg	10	19.47±1.69	
FZ 40 mg/kg + DADA 100 mg/kg	10	19.48±1.45	

Data are presented as mean ± standard deviation. One-way ANOVA was used for the comparison of means among the untreated and other groups. Dunnett's test was then run after one-way ANOVA to determine which differences were significant.

Table S2 The average volume of mice tumors on the first day of treatment

Groups	n	Tumor volume (mm ³)		P
		Mean ± SD	Median (25%, 75%)	
Tumor control	9	50.67±14.69	48.00 (34.00, 60.88)	0.65
Positive control	8	58.04±17.02	50.40 (39.00, 75.00)	
FZ 40mg/kg	9	58.73±16.58	62.50 (44.00, 75.00)	
DADA 20 mg/kg	10	64.54±39.92	50.60 (45.60, 126.00)	
DADA 100 mg/kg	10	50.38±27.97	49.30 (34.00, 68.80)	
FZ 40 mg/kg + DADA 20 mg/kg	10	66.52±21.31	65.35 (44.20, 95.10)	
FZ 40 mg/kg + DADA 100mg/kg	10	54.35±12.30	50.60 (49.30, 75.00)	

One-way ANOVA was used for the comparison of means among the untreated and other groups. Dunnett's test was then run after one-way ANOVA to determine which differences were significant.

Số: 29 /QĐ-ĐHKHCN

Hà Nội, ngày 20 tháng 01 năm 2026

QUYẾT ĐỊNH

Về việc thành lập Hội đồng đánh giá luận án Tiến sĩ cấp trường
đối với nghiên cứu sinh Nguyễn Quang Thái

HIỆU TRƯỞNG

TRƯỜNG ĐẠI HỌC KHOA HỌC VÀ CÔNG NGHỆ HÀ NỘI

Căn cứ Quyết định số 2067/QĐ-TTg ngày 09/12/2009 của Thủ tướng Chính phủ về việc thành lập Trường Đại học Khoa học và Công nghệ Hà Nội (ĐHKHCNHN);

Căn cứ Quyết định số 2557/QĐ-TTg ngày 30/12/2016 của Thủ tướng Chính phủ về việc ban hành Quy chế tổ chức và hoạt động của Trường ĐHKHCNHN;

Căn cứ Quyết định số 140/QĐ-ĐHKHCN ngày 20/6/2017 của Hiệu trưởng Trường ĐHKHCNHN về việc ban hành Quy chế đào tạo trình độ tiến sĩ;

Căn cứ Quyết định số 353/QĐ-ĐHKHCN ngày 07/07/2020 của Hiệu trưởng Trường ĐHKHCNHN về việc sửa đổi, bổ sung Quy chế đào tạo trình độ tiến sĩ của Trường ĐHKHCNHN;

Căn cứ Quyết định số 463/QĐ-ĐHKHCN ngày 07/09/2020 của Hiệu trưởng Trường ĐHKHCNHN về việc công nhận nghiên cứu sinh Nguyễn Quang Thái, tên đề tài và người hướng dẫn luận án tiến sĩ;

Căn cứ các Quyết định số 599/QĐ-ĐHKHCN ngày 18/07/2023 và số 622/QĐ-ĐHKHCN ngày 15/7/2024 của Hiệu trưởng Trường ĐHKHCNHN về việc gia hạn thời gian thực hiện luận án tiến sĩ đối với nghiên cứu sinh Nguyễn Quang Thái;

Căn cứ Quyết định số 829/QĐ-ĐHKHCN ngày 05/9/2025 của Hiệu trưởng Trường ĐHKHCNHN về việc thành lập Hội đồng đánh giá luận án tiến sĩ cấp cơ sở đối với nghiên cứu sinh Nguyễn Quang Thái;

Căn cứ Biên bản họp Hội đồng đánh giá luận án tiến sĩ cấp cơ sở đối với nghiên cứu sinh Nguyễn Quang Thái ngày 09/09/2025;

Căn cứ Quyết định số 1147/QĐ-ĐHKHCN ngày 17/11/2025 của Hiệu trưởng Trường ĐHKHCNHN về việc công nhận thay đổi tên đề tài luận án tiến sĩ của nghiên cứu sinh Nguyễn Quang Thái;

Xét đề nghị của Trường phòng Quản lý đào tạo.

QUYẾT ĐỊNH:

Điều 1. Thành lập Hội đồng đánh giá luận án Tiến sĩ cấp trường đối với nghiên cứu sinh Nguyễn Quang Thái, mã số nghiên cứu sinh D20.PMAB.002, ngành Công nghệ Sinh học nông, y, dược.

Tên đề tài luận án: Investigation of synergistic effect of Diisopropylamine Dichloroacetate and Fenbendazole in lung cancer models.

Danh sách thành viên hội đồng tại Phụ lục kèm theo Quyết định này.

Điều 2. Hội đồng có trách nhiệm tổ chức đánh giá luận án Tiến sĩ của Nghiên cứu sinh theo quy chế đào tạo hiện hành và tự giải thể sau khi hoàn thành nhiệm vụ.



Điều 3. Trường phòng Quản lý đào tạo, Trường khoa Khoa học Sự sống, Chánh văn phòng, Trường phòng Bảo đảm chất lượng và Khảo thí, Trường phòng Kế toán – Tài chính và các thành viên có tên tại Điều 1 chịu trách nhiệm thi hành quyết định này./.

Nơi nhận:

- Như Điều 3;
- HT;
- Các PHT;
- Lưu: VT, KTTC, KHSS, QLĐT.L5.

HIỆU TRƯỞNG CHÍNH



Jean-Marc Lavest






**DANH SÁCH HỘI ĐỒNG ĐÁNH GIÁ LUẬN ÁN TIẾN SĨ CẤP TRƯỜNG
ĐỐI VỚI NGHIÊN CỨU SINH NGUYỄN QUANG THÁI**

(Kèm theo Quyết định số 29 /QĐ-ĐHKHCN ngày 20 /01/2026)

STT	Thành viên Hội đồng	Nơi công tác	Chức danh Hội đồng
1	PGS.TS. Nguyễn Trung Nam	Viện Sinh học, Viện Hàn lâm Khoa học và Công nghệ Việt Nam	Chủ tịch
2	GS.TS. Jeong- Hyung Lee	Trường Đại học Quốc Gia Kangwon, Hàn Quốc	Phản biện
3	TS. Trần Minh Ngọc	Viện dược liệu	Phản biện
4	PGS.TS. Phạm Thế Hải	Trường ĐHKHCNHN, Viện Hàn lâm Khoa học và Công nghệ Việt Nam	Phản biện
5	GS.TS. Đồng Văn Quyền	Viện Sinh học, Viện Hàn lâm Khoa học và Công nghệ Việt Nam	Ủy viên
6	TS. Nguyễn Phương Nhung	Trường ĐHKHCNHN, Viện Hàn lâm Khoa học và Công nghệ Việt Nam	Ủy viên
7	TS. Phạm Lê Minh	Trường ĐHKHCNHN, Viện Hàn lâm Khoa học và Công nghệ Việt Nam	Ủy viên, Thư ký

Danh sách gồm 07 thành viên. 

DECISION

**On establishing the Thesis Examination Jury to examine
the doctoral thesis of PhD student Nguyen Quang Thai**

**RECTOR OF
UNIVERSITY OF SCIENCE AND TECHNOLOGY OF HANOI**

Pursuant to Decision No. 2067/QĐ-TTg dated December 09, 2009 of the Prime Minister on the establishment of University of Science and Technology of Hanoi (USTH);

Pursuant to Decision No. 2557/QĐ-TTg dated December 30, 2016 of the Prime Minister on Regulations on organization and operation of USTH;

Pursuant to Decision No. 140/QĐ-ĐHKHCN dated June 20, 2017 of the Rector of USTH on issuing the Regulation of PhD training;

Pursuant to Decision No. 353/QĐ-ĐHKHCN dated July 07, 2020 of the Rector of USTH revising the Regulation of PhD training of USTH;

Pursuant to Decision No. 463/QĐ-ĐHKHCN dated September 07, 2020 of the Rector of USTH on recognizing doctoral student Nguyen Quang Thai, thesis topic and thesis supervisor;

Pursuant to Decision No. 599/QĐ-ĐHKHCN dated July 18, 2023 and Decision No 622/QĐ-ĐHKHCN dated July 15, 2024 of the Rector of USTH on approving the extension of the PhD program for PhD student Nguyen Quang Thai;

Pursuant to Decision No. 829/QĐ-ĐHKHCN dated September 05, 2025 of the Rector of USTH on the establishment of Internal Jury to examine the doctoral thesis of PhD student Nguyen Quang Thai;

Pursuant to Jury report of the Internal Jury for PhD thesis examination for PhD student Nguyen Quang Thai dated September 9, 2025;

Pursuant to Decision No. 1147/QĐ-ĐHKHCN dated November 17, 2025 of the Rector of USTH on the approval of the amendment to the thesis title of PhD student Nguyen Quang Thai;

At the proposal of Director of Department of Academic Affairs.

DECIDES:

Article 1. To establish the Thesis Examination Jury to examine the doctoral thesis of PhD student Nguyen Quang Thai, student ID D20.PMAB.002, program Pharmacological, Medical and Agronomical Biotechnology.

Thesis title: Investigation of synergistic effect of Diisopropylamine Dichloroacetate and Fenbendazole in lung cancer models

The list of members is in the Annex attached to this Decision.

Article 2. The Thesis Examination Jury shall be responsible for examining the doctoral thesis according to current training regulations and will be automatically dissolved after completing all tasks.

Article 3. Director of Academic Affairs, Director of Department of Life Sciences, Director of Administration, Director of Department of Quality Assurance and Examination, Head of Accounting and Finance Department and members mentioned in Article 1 shall be in charge of implementing this Decision./.

Recipients:

- As Article 3;
- Rector;
- Vice-Rectors;
- Archive: Admin, AF, LS, DAA.L5.

PRINCIPAL RECTOR

(Signed and sealed)

Jean-Marc Lavest

**LIST OF MEMBERS OF THE THESIS EXAMINATION JURY FOR
PHD STUDENT NGUYEN QUANG THAI**

(Attached with the Decision 29 /QĐ-ĐHKHCN dated 20/01/2026)

No.	Members	Institutions	Position in the jury
1	Assoc.Prof. Nguyen Trung Nam	Institute of Biology, Vietnam Academy of Science and Technology	Chairman
2	Prof. Jeong- Hyung Lee	Kangwon National University, Korea	Reviewer
3	Dr. Tran Minh Ngoc	National Institute of Medicinal Materials	Reviewer
4	Assoc.Prof. Pham The Hai	USTH, Vietnam Academy of Science and Technology	Reviewer
5	Prof. Dong Van Quyen	Institute of Biology, Vietnam Academy of Science and Technology	Member
6	Dr. Nguyen Phuong Nhung	USTH, Vietnam Academy of Science and Technology	Member
7	Dr. Pham Le Minh	USTH, Vietnam Academy of Science and Technology	Member, Secretary

The list includes 7 members.



UNIVERSITY OF SCIENCE & TECHNOLOGY OF HANOI
UNIVERSITE DES SCIENCES ET DES TECHNOLOGIES DE HANOI
TRƯỜNG ĐẠI HỌC KHOA HỌC & CÔNG NGHỆ HÀ NỘI

PhD Thesis Examination Jury Jury Report

Time: From 1:30 PM- 4:30 PM, March 19, 2026

Location: Meeting Room 402, USTH Building

I. JURY MEMBERS:

No.	Members	Institutions	Position in the jury
1	Assoc.Prof. Nguyen Trung Nam	Institute of Biology, Vietnam Academy of Science and Technology	Chairman
2	Prof. Jeong- Hyung Lee	Kangwon National University, Korea	Reviewer
3	Dr. Tran Minh Ngoc	National Institute of Medicinal Materials	Reviewer
4	Assoc.Prof. Pham The Hai	USTH, Vietnam Academy of Science and Technology	Reviewer
5	Prof. Dong Van Quyen	Institute of Biology, Vietnam Academy of Science and Technology	Member
6	Dr. Nguyen Phuong Nhung	USTH, Vietnam Academy of Science and Technology	Member
7	Dr. Pham Le Minh	USTH, Vietnam Academy of Science and Technology	Member, Secretary

II. PHD STUDENT:

Full name	Nguyen Quang Thai
Student ID	D20.PMAB.002
Program	Pharmacological, Medical and Agronomical Biotechnology
Thesis title	Investigation of synergistic effect of Diisopropylamine Dichloroacetate and Fenbendazole in lung cancer models/ <i>Nghiên cứu tác dụng hiệp đồng của Diisopropylamine Dichloroacetate và Fenbendazole trên các mô hình ung thư phổi..</i>
Supervisor	Assoc. Prof. Nguyen Hai Dang, USTH
Co-supervisor	Dr. Hoang Xuan Ba, University of Southern California

III. JURY COMMENTS:

- **Assoc.Prof. Pham The Hai:** This thesis presents a comprehensive and scientifically sound study with a scope and level of complexity comparable to doctoral research. The topic is highly relevant, particularly in the context of drug repurposing strategies aimed at reducing the time and cost of developing new anticancer therapies. The study demonstrates several strengths. The experimental design is well-structured, integrating both in vitro and in vivo approaches. A range of advanced techniques has been applied, reflecting strong technical competence. The investigation of multiple biomarkers and underlying mechanisms provides a valuable contribution to understanding therapeutic effects in lung cancer models. Overall, the work is well designed, and the scientific approach is appropriate. However, several aspects should be improved. The discussion section is relatively limited and does not sufficiently explore the underlying mechanisms or compare findings with current literature. Some conclusions appear to be overstated in relation to the presented data, particularly regarding potential clinical applications. In addition, the study is mainly focused on lung cancer cell lines; expanding to other models could enhance the robustness and generalizability of the results. The consistency between in vitro and in vivo findings should also be clarified in more detail.

There are also minor issues related to presentation, including inconsistencies in figures, tables, units, and formatting. Some references are outdated and should be updated with more recent studies.

Questions for the candidate:

- Is a Combination Index (CI) < 1 sufficient to confirm a synergistic effect, or are additional validation methods required?

- How do you explain the consistency between in vitro and in vivo results, particularly in terms of experimental conditions?

Conclusion:

Overall, this is an impressive and well-executed study with clear scientific merit. The thesis is recommended for acceptance after minor revisions.

Mr Nguyen Quang Thai:

Point 1: A Combination Index (CI) < 1 indicates a synergistic effect between the tested agents.

Point 2: In in vitro conditions, drugs can directly interact with cells, whereas in vivo systems involve complex three-dimensional biological environments. Therefore, differences between in vitro and in vivo results can arise due to variations in drug distribution, microenvironment, and biological complexity

- **Prof. Jeong- Hyung Lee:**

Point 1: The conclusions show some discrepancies between in vitro and in vivo results. While the in vivo data demonstrate strong therapeutic effects, the in vitro findings appear less pronounced. This difference may be explained by the complexity of the in vivo tumor microenvironment, including factors such as three-dimensional tumor architecture, immune interactions, drug metabolism, and pharmacokinetics, which cannot be fully replicated in vitro.

Point 2: Western blot analysis indicates that although a synergistic effect is observed in vitro, the in vivo results show a more pronounced therapeutic response. However, the expression of caspase-3 does not significantly change in the combination treatment group. This suggests that the enhanced in vivo efficacy may not primarily rely on caspase-3-mediated apoptosis, but could involve alternative mechanisms such as metabolic reprogramming, cell cycle arrest, or modulation of the tumor microenvironment.

Mr Nguyen Quang Thai:

Point 1: I observed that many promising results were obtained in vitro; however, when translated to in vivo models, some differences emerged. These discrepancies may be attributed to factors such as drug bioavailability, differences in effective drug concentrations, and the inherent challenges in translating in vitro conditions to in vivo systems. For example, both fenbendazole and DADA require dose adjustments when moving from in vitro to in vivo settings, which can lead to variations in observed outcomes.

Point 2: For the Western blot results, the expression of caspase-3 does not show a clear difference by visual inspection. However, quantitative analysis using image processing software may reveal subtle differences. In addition, tumor size was selected as the primary parameter for monitoring treatment effects rather than tumor weight, as it allows continuous and non-invasive assessment in animal studies. Further clarification on this point will be added in the revised version.

- Dr. Tran Minh Ngoc

The study presents a substantial amount of therapeutic data, with extensive use of Western blot analysis and multiple biomarkers. The in vitro and in vivo results are well illustrated and provide strong evidence supporting the proposed anticancer effects. Overall, the thesis contains a large volume of valuable data with potential applications.

However, several issues need to be addressed. Some conclusions appear too extensive and should be carefully revised to better align with the presented data. The first table should be rechecked and corrected, and font sizes should be standardized throughout the thesis. The literature review requires further refinement and more detailed description. In addition, the use of multiple positive controls is excessive and should be reconsidered.

Specific points for revision include:

- Table 2 should be reviewed and reformatted.
- Cancer cell lines and related figures (e.g., Figure 8, Figure S3) should be carefully checked.
- Figure 21 contains several errors and needs correction.
- The reference list shows multiple formatting inconsistencies and should be standardized.
- Figures S1 and S2 use colors but lack proper explanation.

Despite these minor issues in presentation and formatting, the thesis provides comprehensive data and meaningful scientific contributions. After careful revision, it can be considered for the doctoral degree.

Mr Nguyen Quang Thai:

Responses to Questions

Point 1 (Positive controls):

There are indeed multiple positive controls used in this study. After determining the optimal dose, paclitaxel was selected as the primary positive control for subsequent experiments.

Point 2 (Dose ratio in vitro vs in vivo):

The dose ratio between fenbendazole and DADA differs between in vitro and in vivo experiments. This is mainly due to differences in bioavailability and solubility, particularly for fenbendazole. Therefore, we referred to available literature to select appropriate dosing ratios for in vivo studies. However, it remains challenging to establish a direct correlation between in vitro and in vivo conditions.

Revision statement:

All identified issues will be carefully reviewed and corrected in the revised version.

- **Prof. Dong Van Quyen:** The candidate has obtained very promising results overall. However, several points should be considered:

- From a technical perspective, although the thesis presents strong results, it would benefit from the inclusion of additional cancer cell lines to strengthen the robustness of the findings.
- The dose ratio used in in vivo experiments appears to be influenced by time limitations; therefore, this ratio should be considered as a preliminary suggestion rather than a definitive conclusion.
- The study suggests increased ROS production and induction of apoptosis in cancer cell lines; however, more direct experimental evidence is needed to support these claims.
- The limitations of the mouse model, particularly regarding the immune system, should be acknowledged and discussed more clearly.
- Improving the solubility of the compounds would enhance the translational potential of the study.

Mr Nguyen Quang Thai:

- These limitations are acknowledged, and further studies are needed to address them.
- Additional cancer cell lines should indeed be included. However, in our current study, although we used nude mice models, we were not able to successfully establish tumor models in some cases.
- At present, we have mainly developed lung and liver models, while other tumor models have not yet been established. These will be further explored and developed in future work.

- **Dr. Nguyen Phuong Nhung:**

Overall good thesis, well presented

Questions

- In the in vitro experiments, how were replicates handled, and how were cell numbers quantified?
- In the in vivo experiments, how were the drug solutions prepared, and what is the potential effect of DMSO on drug activity?

Mr Nguyen Quang Thai:

- Cell numbers were determined by direct counting under a microscope. Replicates and counting procedures will be further clarified and standardized in future work.



UNIVERSITY OF SCIENCE & TECHNOLOGY OF HANOI
UNIVERSITE DES SCIENCES ET DES TECHNOLOGIES DE HANOI
TRƯỜNG ĐẠI HỌC KHOA HỌC & CÔNG NGHỆ HÀ NỘI

- DMSO was used at a low concentration, which is generally considered to have minimal impact on drug activity. However, this potential effect will be further evaluated and controlled in future studies

- Dr. Pham Le Minh

Overall good thesis, well presented

Questions

Why did you not consider intratumoral administration for fenbendazole and DADA in your study?

Mr Nguyen Quang Thai:

The history of fenbendazole has motivated us to further explore its potential and discover new applications

Assoc.Prof. Nguyen Trung Nam:

The thesis presents several novel contributions and provides a comprehensive demonstration of the research findings. However, the introduction section is relatively brief and should be expanded to improve the overall balance of the thesis.

Some figures are missing and need to be carefully checked. In addition, Figures 15, 16, and 17 contain issues in their descriptions and should be revised for clarity and accuracy.

Overall, the conclusions are appropriate, and the thesis is suitable for the award of a doctoral degree.

IV. CONCLUSION:

- The title of the thesis is appropriate for the program of Pharmacological, Medical and Agronomical Biotechnology (Code: 9420201).
- The thesis does not overlap with any previously published works or theses.
- The main scientific conclusions, new findings, and contributions of the thesis are as follows:



UNIVERSITY OF SCIENCE & TECHNOLOGY OF HANOI
UNIVERSITE DES SCIENCES ET DES TECHNOLOGIES DE HANOI
TRƯỜNG ĐẠI HỌC KHOA HỌC & CÔNG NGHỆ HÀ NỘI

-
-
- Agree to award the PhD diploma to the candidate.
 Agree to award the PhD diploma to the candidate after revision.
 The thesis is not qualified for the PhD diploma. A second jury could be considered.

V. SIGNATURES:

Chairman

A handwritten signature in blue ink, appearing to read 'MOW' with a long horizontal stroke extending to the right.

Assoc.Prof. Nguyen Trung Nam

Secretary

A handwritten signature in blue ink, appearing to read 'Minh' with a horizontal line underneath.

Dr. Pham Le Minh

**PhD Thesis Examination Jury
Final Assessment**

Time : March 19, 2026
Location : Meeting Room 402, USTH Building

I. PHD STUDENT:

Full name	Nguyen Quang Thai
Student ID	D20.PMAB.002
Program	Pharmacological, Medical and Agronomical Biotechnology
Thesis title	Investigation of synergistic effect of Diisopropylamine Dichloroacetate and Fenbendazole in lung cancer models/ <i>Nghiên cứu tác dụng hiệp đồng của Diisopropylamine Dichloroacetate và Fenbendazole trên các mô hình ung thư phổi.</i>
Supervisor	Assoc. Prof. Nguyen Hai Dang, USTH
Co-supervisor	Dr. Hoang Xuan Ba, University of Southern California

II. COMMENTS (if any):

III. FINAL ASSESSMENT:

- Agree to award the PhD diploma to the candidate.
 Agree to award the PhD diploma to the candidate after revision.
 The thesis is not qualified for the PhD diploma. A second jury could be considered.

Jury member
(Signature & full name)


Nguyen Trung Nhan

PhD Thesis Examination Jury Final Assessment

Time : March 19, 2026

Location : Meeting Room 402, USTH Building

I. PHD STUDENT:


Full name	Nguyen Quang Thai
Student ID	D20.PMAB.002
Program	Pharmacological, Medical and Agronomical Biotechnology
Thesis title	Investigation of synergistic effect of Diisopropylamine Dichloroacetate and Fenbendazole in lung cancer models/ <i>Nghiên cứu tác dụng hiệp đồng của Diisopropylamine Dichloroacetate và Fenbendazole trên các mô hình ung thư phổi.</i>
Supervisor	Assoc. Prof. Nguyen Hai Dang, USTH
Co-supervisor	Dr. Hoang Xuan Ba, University of Southern California

II. COMMENTS (if any):

None

III. FINAL ASSESSMENT:

- Agree to award the PhD diploma to the candidate.
- Agree to award the PhD diploma to the candidate after revision.
- The thesis is not qualified for the PhD diploma. A second jury could be considered.

Jury member
(Signature & full name)
Lee Jeong-Hyung 

PhD Thesis Examination Jury Final Assessment

Time : March 19, 2026

Location : Meeting Room 402, USTH Building

I. PHD STUDENT:

Full name	Nguyen Quang Thai
Student ID	D20.PMAB.002
Program	Pharmacological, Medical and Agronomical Biotechnology
Thesis title	Investigation of synergistic effect of Diisopropylamine Dichloroacetate and Fenbendazole in lung cancer models/ <i>Nghiên cứu tác dụng hiệp đồng của Diisopropylamine Dichloroacetate và Fenbendazole trên các mô hình ung thư phổi.</i>
Supervisor	Assoc. Prof. Nguyen Hai Dang, USTH
Co-supervisor	Dr. Hoang Xuan Ba, University of Southern California

II. COMMENTS (if any):

(Handwritten mark)

III. FINAL ASSESSMENT:

- Agree to award the PhD diploma to the candidate.
- Agree to award the PhD diploma to the candidate after revision.
- The thesis is not qualified for the PhD diploma. A second jury could be considered.

Jury member

(Signature & full name)

(Handwritten signature)
Dong Van Bui

PhD Thesis Examination Jury Final Assessment

Time : March 19, 2026

Location : Meeting Room 402, USTH Building

I. PHD STUDENT:

Full name	Nguyen Quang Thai
Student ID	D20.PMAB.002
Program	Pharmacological, Medical and Agronomical Biotechnology
Thesis title	Investigation of synergistic effect of Diisopropylamine Dichloroacetate and Fenbendazole in lung cancer models/ <i>Nghiên cứu tác dụng hiệp đồng của Diisopropylamine Dichloroacetate và Fenbendazole trên các mô hình ung thư phổi.</i>
Supervisor	Assoc. Prof. Nguyen Hai Dang, USTH
Co-supervisor	Dr. Hoang Xuan Ba, University of Southern California


II. COMMENTS (if any):

III. FINAL ASSESSMENT:

- Agree to award the PhD diploma to the candidate.
- Agree to award the PhD diploma to the candidate after revision.
- The thesis is not qualified for the PhD diploma. A second jury could be considered.

Jury member

(Signature & full name)


Phạm Thế Hải

PhD Thesis Examination Jury Final Assessment

Time : March 19, 2026

Location : Meeting Room 402, USTH Building

I. PHD STUDENT:

Full name	Nguyen Quang Thai
Student ID	D20.PMAB.002
Program	Pharmacological, Medical and Agronomical Biotechnology
Thesis title	Investigation of synergistic effect of Diisopropylamine Dichloroacetate and Fenbendazole in lung cancer models/ <i>Nghiên cứu tác dụng hiệp đồng của Diisopropylamine Dichloroacetate và Fenbendazole trên các mô hình ung thư phổi.</i>
Supervisor	Assoc. Prof. Nguyen Hai Dang, USTH
Co-supervisor	Dr. Hoang Xuan Ba, University of Southern California

II. COMMENTS (if any):


PhD candidate should ~~revison~~ revise the manuscript as per comments of Jury members

III. FINAL ASSESSMENT:

- Agree to award the PhD diploma to the candidate.
- Agree to award the PhD diploma to the candidate after revision.
- The thesis is not qualified for the PhD diploma. A second jury could be considered.

Jury member

(Signature & full name)


Nguyen Phuong Nhung



UNIVERSITY OF SCIENCE & TECHNOLOGY OF HANOI
UNIVERSITE DES SCIENCES ET DES TECHNOLOGIES DE HANOI
TRƯỜNG ĐẠI HỌC KHOA HỌC & CÔNG NGHỆ HÀ NỘI

PhD Thesis Examination Jury Final Assessment

Time : March 19, 2026
Location : Meeting Room 402, USTH Building

I. PHD STUDENT:

Full name	Nguyen Quang Thai
Student ID	D20.PMAB.002
Program	Pharmacological, Medical and Agronomical Biotechnology
Thesis title	Investigation of synergistic effect of Diisopropylamine Dichloroacetate and Fenbendazole in lung cancer models/ <i>Nghiên cứu tác dụng hiệp đồng của Diisopropylamine Dichloroacetate và Fenbendazole trên các mô hình ung thư phổi.</i>
Supervisor	Assoc. Prof. Nguyen Hai Dang, USTH
Co-supervisor	Dr. Hoang Xuan Ba, University of Southern California

II. COMMENTS (if any):

III. FINAL ASSESSMENT:

- Agree to award the PhD diploma to the candidate.
 Agree to award the PhD diploma to the candidate after revision.
 The thesis is not qualified for the PhD diploma. A second jury could be considered.

Jury member
(Signature & full name)


Trần Minh Ngọc

PhD Thesis Examination Jury Final Assessment

Time : March 19, 2026

Location : Meeting Room 402, USTH Building

I. PHD STUDENT:

Full name	Nguyen Quang Thai
Student ID	D20.PMAB.002
Program	Pharmacological, Medical and Agronomical Biotechnology
Thesis title	Investigation of synergistic effect of Diisopropylamine Dichloroacetate and Fenbendazole in lung cancer models/ <i>Nghiên cứu tác dụng hiệp đồng của Diisopropylamine Dichloroacetate và Fenbendazole trên các mô hình ung thư phổi.</i>
Supervisor	Assoc. Prof. Nguyen Hai Dang, USTH
Co-supervisor	Dr. Hoang Xuan Ba, University of Southern California

II. COMMENTS (if any):

III. FINAL ASSESSMENT:

- Agree to award the PhD diploma to the candidate.
 Agree to award the PhD diploma to the candidate after revision.
 The thesis is not qualified for the PhD diploma. A second jury could be considered.

Jury member

(Signature & full name)

Phạm @ Minh



UNIVERSITY OF SCIENCE & TECHNOLOGY OF HANOI
UNIVERSITE DES SCIENCES ET DES TECHNOLOGIES DE HANOI
TRƯỜNG ĐẠI HỌC KHOA HỌC & CÔNG NGHỆ HÀ NỘI

Examination Jury for PhD thesis Reviewer's Report

PhD Student	
Full name	Nguyen Quang Thai
Program/ Department	PMAB/ Life Sciences
Student ID number	D20.PMAB.002
PhD thesis	
Title	Investigation of synergistic effect of Diisopropylamine Dichloroacetate and Fenbendazole in lung cancer models
Supervisor	Assoc. Prof. Nguyen Hai Dang, USTH
Co-supervisor	Dr. Hoang Xuan Ba, University of Southern California
Reviewer	
Full name	Lee Jeong-Hyung
Title	Professor
Institution	Kangwon National University
Contact (Email/SMS)	Jhlee36@kangwon.ac.kr
Technical comments (e.g. on the research topic, methodology, finding, discussion, thesis structure, wording, references etc)	

Overall, this manuscript is written well. The strengths and weaknesses of this thesis are follows;

Novelty in Drug Repurposing: Combining Fenbendazole (a veterinary anthelmintic) with DADA (a liver metabolism drug) is an innovative approach. Drug repurposing is a high-interest area because it reduces the time and cost of drug development.

Comprehensive Methodology: The study spans from in vitro (cell lines) to in vivo (animal models), providing a solid foundation for claiming therapeutic potential.

Clear Mechanistic Markers: This study was identified specific molecular pathways for apoptosis (Bcl-2/BAX, Caspase-3/7, PARP) and cell cycle arrest (Cyclin A/E), which adds scientific weight to your observations.

Safety Assessment: Including liver and kidney function tests in the animal model addresses a major concern regarding the toxicity of non-traditional cancer treatments.

High Efficacy: The mention of "complete tumor loss" suggests a potent synergistic effect that, if reproducible, could be a significant breakthrough.

Questions/ Suggestions/ Request of Revisions

Criticisms:

- 1) What are the synergistic effects of FZ and DADA at ratios other than 1:5000?
- 2) Discrepancy between in vitro and in vivo ratios: It is necessary to clarify why the synergistic ratio observed in the cellular models (1:5000) was not translated to the animal models (1:2.5). Please include these additional results in the "Results" section or provide a detailed justification in the "Discussion" section on the revised manuscript.
- 3) In chemistry, a "complex" implies a new molecular structure formed by chemical bonding. If you simply mixed two drugs together, you should use the term "combination" or "co-administration." Using "complex" incorrectly can lead to questions about the chemical characterization of your formula.
- 4) The term "Complete Loss" is inaccurate. It is safer to use "Significant tumor regression."

Conclusions (whether the work is suitable/ could be suitable after revisions for presenting to obtain the USTH PhD degree?)

This manuscript has a Novelty in Drug Repurposing. Therefore, this manuscript may be accepted with minor revisions and that the candidate will be eligible for the USTH PhD degree.

- Recommended for defense at the PhD Thesis Examination Jury in the current form.
- Recommend for defense at the PhD Thesis Examination Jury with minor revisions.
- Not recommended for defense at the PhD Thesis Examination Jury.

March 9, 2026

Reviewer's signature

Lee Jeong-Hyung





UNIVERSITY OF SCIENCE & TECHNOLOGY OF HANOI
UNIVERSITE DES SCIENCES ET DES TECHNOLOGIES DE HANOI
TRƯỜNG ĐẠI HỌC KHOA HỌC & CÔNG NGHỆ HÀ NỘI

Examination Jury for PhD thesis Reviewer's Report

PhD Student	
Full name	Nguyen Quang Thai
Program/ Department	PMAB/ Life Sciences
Student ID number	D20.PMAB.002
PhD thesis	
Title	Investigation of synergistic effect of Diisopropylamine Dichloroacetate and Fenbendazole in lung cancer models
Supervisor	Assoc. Prof. Nguyen Hai Dang, USTH
Co-supervisor	Dr. Hoang Xuan Ba, University of Southern California
Reviewer	
Full name	Dr. Tran Minh Ngoc
Title	Investigation of synergistic effect of Diisopropylamine Dichloroacetate and Fenbendazole in lung cancer models
Institution	National Institute of Medicinal Materials
Contact (Email/SMS)	tmngoc@nimm.org.vn
Technical comments (e.g. on the research topic, methodology, finding, discussion, thesis structure, wording, references etc)	
<p>The thesis addressed a timely research topic in the field of cancer biology, namely, "Investigation of synergistic effect of Diisopropylamine Dichloroacetate and Fenbendazole in lung cancer models". Focusing on a drug combination strategy to achieve a synergistic effect is scientifically reasonable, as recent studies have shown that agents targeting cellular metabolism and microtubule dynamics may enhance therapeutic efficacy when used together. In addition, the use of both in vitro models (A549 cell line) and in vivo models (BALB/c nude mice</p>	

bearing xenograft tumors) increases the reliability and comprehensiveness of the study, allowing the therapeutic effects to be evaluated from the cellular level to the physiological level of tumor growth.

Regarding the research methodology, the thesis employed a range of molecular and cellular biology techniques that are appropriate for the research objectives. These included cell viability assays, apoptosis assays, cell cycle analysis, reactive oxygen species (ROS) measurement, glucose uptake assays, lactate assays, Western blot analysis, and experiments using an animal model. The analysis of apoptosis-related proteins (Bcl-2, Bax, caspase-3, caspase-7, and PARP) as well as cell cycle regulatory proteins (Cyclin A and Cyclin E) is appropriate for elucidating the potential mechanisms underlying the effects of the FZ–DADA combination. However, the study utilized only a single lung cancer cell line (A549), which may limit the generalizability of the findings to other subtypes of non-small cell lung cancer.

Regarding the findings, the data indicated that the combination of FZ and DADA effectively inhibited lung cancer cell proliferation, induced apoptosis, caused cell cycle arrest, and increased ROS production. Results from the mouse model also demonstrated a reduction in tumor size following combination treatment, while no significant adverse effects on liver or kidney function were observed. These findings supported the hypothesis that the combination of these two compounds may produce stronger anticancer effects than single-agent treatment.

In terms of thesis structure, the organization of the chapters is generally appropriate, including sections on literature review, materials and methods, results, discussion, and conclusions. The literature review summarizes the mechanisms of action of FZ and DADA as well as previous studies on combination therapy in lung cancer.

Regarding references, the dissertation cites relevant scientific publications, including several recent studies in the field.

In summary, the thesis presents a meaningful investigation into the potential of the FZ and DADA combination therapy for lung cancer treatment. The research design is relatively comprehensive, and the results demonstrated the promising anticancer potential of this therapeutic strategy.

Questions/ Suggestions/ Request of Revisions

Several issues should be revised or clarified in the thesis:

- + The font formatting in the Table of Contents should be checked and standardized.
- + Table 1 (page 7): The font size should be reduced, or the table should be rotated to landscape format so that the text (e.g., “publication”, “experimental”) is not truncated.
- + The literature review section should be clearly separated from the methodology section to improve the structure of the thesis.
- + Section 3.1: Additional chemicals used in the experiments, such as camptothecin, paclitaxel, and cisplatin, should be listed and described.
- + The author should clarify why multiple positive controls were used in the experiments.
- + The presentation of “cells/well” in the “Density” column in Table 2 should be reviewed and formatted consistently.
- + Section 4.1: The sentence “Camptothecin was used as a positive control to validate the reliability of the results” should be reconsidered. According to the appendix, cisplatin was used as the positive control for HepG2 cells. In addition, the abbreviation for camptothecin should be used consistently (e.g., CPT in Fig. 8 vs. Campto in Fig. 10A and Figure S3).
- + The thesis does not include experiments on normal (non-cancerous) cells, which would be useful for evaluating the selectivity and safety of the treatment.

- + Attention should be paid to the spelling of "paclitaxel" throughout the thesis. In Figure 9 (page 39), it should be verified whether the compound used is cisplatin or paclitaxel.
- + Page 40: The text alignment and formatting should be corrected.
- + Figure 11: The font size is too small and should be enlarged. The figure labels should also be standardized (e.g., paclitaxel, Bcl-2, FZ, caspase-3, caspase-7). Similar issues should be checked in Figures 13 and 14.
- + Figure 12: The *** statistical annotation should be clearly indicated in Fig. B (G2).
- + The author should explain why different numbers of mice were used in different experimental groups (page 53).
- + Figure 21: The labels "Fen" and "Dada" should be standardized to match the terminology used in the *in vitro* figures. A similar issue appears in Figure 26A.
- + For figures presenting experimental results, it would be helpful to include corresponding numerical data tables in the appendix for easier verification and interpretation.
- + The reference list should be formatted consistently according to a single citation style.
- + Supplementary Information: Figures S1 and S2 lack color legends, and the concentration units are not specified.

Conclusions (whether the work is suitable/ could be suitable after revisions for presenting to obtain the USTH PhD degree?)

In conclusion, the thesis presents a meaningful investigation into the potential anticancer effects of the combination of fenbendazole and diisopropylamine dichloroacetate in lung cancer models. The research design is generally appropriate and the results provide useful insights into the potential synergistic mechanisms of these compounds. However, several minor issues related to formatting, presentation, and clarification of experimental details should be revised. After addressing these comments, the thesis could be considered suitable for the award of the PhD degree at USTH.

- Recommended for defense at the PhD Thesis Examination Jury in the current form.
- Recommended for defense at the PhD Thesis Examination Jury with minor revisions.
- Not recommended for defense at the PhD Thesis Examination Jury.

Hanoi, March 5, 2026

Reviewer's signature



Tran Minh Ngoc



UNIVERSITY OF SCIENCE & TECHNOLOGY OF HANOI
UNIVERSITE DES SCIENCES ET DES TECHNOLOGIES DE HANOI
TRƯỜNG ĐẠI HỌC KHOA HỌC & CÔNG NGHỆ HÀ NỘI

Examination Jury for PhD thesis Reviewer's Report

PhD Student	
Full name	Nguyen Quang Thai
Program/ Department	PMAB/ Life Sciences
Student ID number	D20.PMAB.002
PhD thesis	
Title	Investigation of synergistic effect of Diisopropylamine Dichloroacetate and Fenbendazole in lung cancer models
Supervisor	Assoc. Prof. Nguyen Hai Dang, USTH
Co-supervisor	Dr. Hoang Xuan Ba, University of Southern California
Reviewer	
Full name	Pham The Hai
Title	Assoc. Prof.
Institution	USTH
Contact (Email/SMS)	Pham-the.hai@usth.edu.vn

Technical comments (e.g. on the research topic, methodology, finding, discussion, thesis structure, wording, references etc)

1.1 Research topic and scientific relevance

The thesis investigates the synergistic anti-cancer effects of fenbendazole (FZ) and diisopropylamine dichloroacetate (DADA) in lung cancer models, particularly using the A549 non-small cell lung cancer cell line and a xenograft mouse model. The topic is relevant because lung cancer remains a major cause of cancer mortality worldwide and drug repurposing represents a promising strategy for identifying new therapeutic options.

The rationale for combining FZ and DADA is also presented in the literature review, including the metabolic effects of DADA and previously reported anticancer activities of fenbendazole. The thesis further discusses the potential benefit of DADA in mitigating possible liver toxicity associated with fenbendazole.

Overall, the research topic is timely and scientifically relevant.

1.2 Methodology and experimental design

The thesis combines *in vitro* experiments and *in vivo* animal studies, which is appropriate for evaluating potential anticancer activity. The use of apoptosis markers, cell cycle analysis, and xenograft models represents a standard approach in experimental oncology.

In vitro experiments

The thesis employs several complementary assays to evaluate anticancer activity, including:

- Cell viability assay
- Hoechst staining
- Apoptosis assay
- Cell cycle analysis
- ROS detection
- Glucose uptake and lactate assays
- Western blot analysis of signaling proteins

These methods are appropriate for evaluating cellular responses to drug treatment. The study also examines key molecular markers related to apoptosis and signaling pathways, including BAX, BCL-2, caspase-3, caspase-7, PARP, Cyclin A, Cyclin E, and PI3K/AKT signaling.

The inclusion of metabolic assays such as glucose uptake and lactate production is a positive aspect because it supports the hypothesis that the combination may influence cancer metabolism.

However, the *in vitro* experiments rely mainly on one lung cancer cell line (A549). Considering the heterogeneity of non-small cell lung cancer, including additional cell lines would strengthen the generalizability of the findings.

Analysis of synergistic effects

The thesis includes a dedicated section (2.3 Investigation of synergistic effects) describing theoretical approaches used to evaluate drug interactions. The author explains different models including Loewe additivity, Bliss independence, and the Combination Index approach.

The study ultimately adopts the Chou-Talalay Combination Index (CI) method to evaluate synergy. The thesis also provides the mathematical formulation of the median-effect equation and defines the interpretation of CI values (CI < 1 indicating synergy, CI = 1 additive effect, CI > 1 antagonism).

This methodological framework is appropriate and widely used in pharmacological studies of drug combinations.

Nevertheless, the description of the synergy analysis could be improved by presenting more detailed information regarding:

- the dose-response curves used to calculate median-effect parameters
- the full range of CI values obtained across different dose combinations
- graphical representations such as isobologram or CI-fraction affected plots.

Providing these details would improve transparency and reproducibility of the synergy evaluation.

In vivo experiments

The in vivo study uses BALB/c nude mice transplanted with A549 lung cancer cells to evaluate the anticancer effect of FZ and DADA.

Thesis Thai Dec 1- Sau HDCS

When tumors reached approximately 50 mm³, mice were randomized into multiple experimental groups including:

- Healthy control
- Tumor control
- Cisplatin positive control
- FZ treatment
- Two DADA treatment groups
- Two combination therapy groups.

Tumor volume, survival time, body weight, and toxicity indicators were monitored during the experiment. Tumor volume was calculated using standard formulas based on tumor length and width measurements.

The inclusion of a positive control group (cisplatin) is an important strength of the experimental design.

The thesis also evaluates safety parameters such as body weight changes, hematological indicators, and kidney function markers.

However, additional details on randomization procedures, blinding during measurement, and statistical power calculations would further strengthen the methodological rigor.

3. Findings

The results suggest that the FZ-DADA combination inhibits proliferation of A549 lung cancer cells and induces multiple anticancer responses.

The study reports that the combination treatment:

- increases ROS production
- induces apoptosis through regulation of BAX/BCL-2 balance
- activates caspase-3 and caspase-7
- increases PARP cleavage

- induces G2/M cell-cycle arrest
- suppresses Cyclin A and Cyclin E expression.

The results also indicate that the combination influences metabolic activity and may inhibit the PI3K/AKT signaling pathway.

In the animal model, combination treatment appears to reduce tumor growth and extend survival time compared with untreated tumor-bearing mice.

Overall, the findings are internally consistent and supported by multiple experimental approaches.

Variability between different experimental models is not fully addressed

The thesis presents results obtained from multiple experimental systems, including in vitro cytotoxicity assays and in vivo experiments. While these results provide useful data, the differences between experimental models are not always thoroughly analyzed.

For instance, the degree of cytotoxicity observed in cell culture experiments does not always directly correspond to the magnitude of tumor inhibition observed in vivo. Such discrepancies are common in biomedical research due to differences in drug bioavailability, metabolism of fenbendazole in vivo, or tumor microenvironment effects.

Some conclusions appear stronger than the data directly support:

In several places, the thesis suggests that the tested drug combination shows promising anticancer potential. While the experimental results indeed indicate cytotoxic and possibly synergistic effects in cell models, the available data remain preliminary and limited to preclinical experiments. Therefore, the conclusions should be carefully drawn to reflect that the findings mainly demonstrate in vitro and early in vivo effects, rather than implying direct clinical relevance.

4. Discussion

The discussion relates the findings to current literature on cancer metabolism, apoptosis signaling, and drug repurposing strategies.

The thesis provides a reasonable interpretation of how the combination treatment might enhance anticancer effects through:

- increased oxidative stress
- modulation of apoptotic signaling
- disruption of metabolic pathways.

However, the discussion could be strengthened by including a more critical evaluation of:

- potential limitations of the study
- differences between the experimental model and clinical lung cancer
- future research directions needed before clinical translation.

5. Thesis structure and organization

The thesis follows a conventional structure:

- Introduction (3 pages)
- Literature review (20 pages)
- Materials and methods (13 pages)
- Experimental results (31 pages)
- Discussion (4 pages)

There should be an imbalance in chapter organization. The Literature Review is relatively concise compared with the large number of references cited (153). The Results section is comparatively extensive, while the Discussion is relatively brief, limiting deeper interpretation of the findings. Some methodological explanations (for example, the rationale behind synergy analysis methods) could have been better contextualized earlier in the thesis.

This imbalance may give the impression that experimental results are emphasized more than critical scientific interpretation, whereas a doctoral thesis should demonstrate not only technical work but also strong analytical and conceptual discussion of the findings.

There are 27 Figures, but Figures 15-17 are lacking. The corresponding pages in the List of Figures are not corrected. The caption format is not homogeneous (Figure 1. And Figure 3:), grammatical error: Figure 20. concentration-dependance -> it should be concentration-dependent. Lacking information in caption of Figure 12: The FZ-DADA combination induced cell cycle arrest in A549 cells. Figure 1 must include reference.

The thesis contains 9 tables summarizing experimental data and methodological information. In general, the tables present useful quantitative results. However, several issues in table presentation should be improved. In particular, the use of units is not always consistent (e.g., μM vs uM), and some table captions do not provide sufficient methodological details such as treatment duration, number of replicates, or statistical representation (mean \pm SD/SEM). In addition, abbreviations used in tables are not always explained in footnotes, which may reduce the clarity of the data presentation.

Several minor but noticeable spelling and language inconsistencies are present throughout the thesis. For example, incorrect spellings such as "dependance" and "time dependant" appear in figure captions and methodological descriptions. In addition, there is inconsistent use of British and American English (e.g., "analysed" vs "tumor"). Some terms are also not consistently formatted (e.g., "micro-environment" vs "microenvironment"). Although these issues do not affect the scientific content, careful proofreading would improve the overall quality and professionalism of the thesis.

6. Language and presentation

The thesis is generally understandable, although some sections contain grammatical errors or awkward phrasing. Careful language editing would improve clarity and readability.

Figures and tables are useful for illustrating experimental findings, but some figure captions could provide more detailed explanations of experimental conditions.

7. References

The thesis cites a broad range of literature related to lung cancer biology, drug repurposing, and metabolic targeting in cancer therapy with 153 references.

- 2020-2024: 65 (42%)
- 2015-2019: 55 (36%)
- 2010-2014: 22 (14%)
- <2010: 11 (7%)

The thesis includes a relatively comprehensive list of 153 references, of which approximately 40–45% were published within the last five years (2020–2024). This indicates that the candidate has considered a reasonably up-to-date body of literature in the field.

The formatting of references is not fully consistent throughout the list. For example, journal names are sometimes written in full and sometimes abbreviated, page ranges use both hyphen and en dash, and the number of authors listed before using “et al.” is not always consistent. In addition, a few references appear to lack complete bibliographic details (e.g., volume or page numbers). Careful editing of the reference list according to a single citation style (e.g., Vancouver) would improve the overall consistency and professionalism of the thesis.

Questions/ Suggestions/ Request of Revisions

Before the thesis can be considered for final acceptance, the following revisions are recommended:

- Clarify the experimental design and statistical analysis, including the number of replicates, statistical methods used, and representation of variability in all quantitative results.
- Improve the presentation of figures and tables, ensuring that captions contain sufficient methodological information and that units and abbreviations are consistently defined.
- Revise the language and correct minor spelling and formatting errors, including inconsistencies in scientific terminology and punctuation.
- Standardize the reference formatting according to a single citation style (e.g., Vancouver style), ensuring that all bibliographic details are complete and consistent.
- Strengthen the discussion section by providing deeper interpretation of the results, particularly regarding the biological mechanisms underlying the observed drug interactions and the limitations of the study.

Questions

1. The results show that the combination treatment produced stronger effects than single compounds in some experiments. Could the candidate explain how the drug combination ratios were determined in the study?
2. Several experiments report IC₅₀ values for fenbendazole and its combinations in different cancer cell lines. Could the candidate clarify how many independent experiments were performed and whether the reported IC₅₀ values represent mean values with standard deviation or standard error?
3. The thesis presents both in vitro cytotoxicity results and in vivo tumor inhibition data. How does the candidate explain the potential differences between the magnitude of effects observed in cell culture experiments and those obtained in animal models?
4. Some CI values suggest synergistic interactions (CI < 1). Could the candidate elaborate on whether this synergistic effect is consistent across different concentration ranges and different levels of fraction affected (Fa)?
5. The thesis suggests that the investigated drug combination may have potential therapeutic implications. Considering that the experiments were performed mainly in preclinical models, how does

the candidate evaluate the limitations and challenges in translating these findings to clinical applications?

Conclusions (whether the work is suitable/ could be suitable after revisions for presenting to obtain the USTH PhD degree?)

Overall, the thesis addresses a relevant research topic related to the potential anticancer effects of fenbendazole and its combination with other compounds. The study presents experimental data obtained from both in vitro assays and in vivo models, and applies quantitative approaches such as the Chou-Talalay method to evaluate drug interactions. Despite these limitations, the thesis demonstrates that the candidate has conducted a substantial amount of experimental work and has acquired relevant research skills in biomedical experimentation and data analysis. The scientific content is generally sound and contributes incremental knowledge to the field.

Therefore, in my opinion, the thesis could be suitable for presenting in defense for the USTH PhD degree after appropriate revisions addressing the comments above. The candidate should carefully revise the manuscript to improve clarity, consistency, and scientific interpretation before the final submission.

- Recommended for defense at the PhD Thesis Examination Jury in the current form.**
- Recommend for defense at the PhD Thesis Examination Jury with minor revisions.**
- Not recommended for defense at the PhD Thesis Examination Jury.**

Hanoi March 6th, 2026

Reviewer's signature



Pham The Hai

Examination Jury for PhD thesis Jury Member's Assessment Form

PhD Student	
Full name	Nguyen Quang Thai
Program	Pharmacological, Medical and Agronomical Biotechnology
PhD ID	D20.PMAB.002
PhD thesis	
Title	Investigation of synergistic effect of Diisopropylamine Dichloroacetate and Fenbendazole in lung cancer models/ <i>Nghiên cứu tác dụng hiệp đồng của Diisopropylamine Dichloroacetate và Fenbendazole trên các mô hình ung thư phổi.</i>
Supervisor	Assoc. Prof. Nguyen Hai Dang, USTH
Co-supervisor	Dr. Hoang Xuan Ba, University of Southern California
Jury Member	
Full name	Nguyen Trung Nam
Title	A. Prof. Dr.
Institution	Institute of Biology, Vietnam Academy of Science and Technology
Contact (Email/SMS)	nam@ib.ac.vn
Role (Chairman/ Reviewer/ Member)	Chairman
Technical comments (e.g. on the thesis topic, research methodology, finding, discussion, thesis structure, wording, references, etc). Please note that the reviewers can fill this part as "please refer to my review report" and/or with additional comments on the revised manuscript and/or on the presentation made by the candidate	
<p>The thesis addresses a timely and significant area of oncology by exploring drug repurposing, specifically the combination of Fenbendazole (an anthelmintic) and Diisopropylamine Dichloroacetate (DADA). The combination is recognized as an innovative approach with the potential to reduce the time and cost associated with traditional drug development. The study effectively utilizes the metabolic effects of DADA to potentially mitigate liver toxicity associated with Fenbendazole while enhancing anti-cancer activity.</p>	

The study employs a comprehensive framework spanning from *in vitro* (A549 cell lines) to *in vivo* (xenograft mouse models). The use of standard oncology markers (apoptosis, cell cycle analysis) and the inclusion of a positive control group (Cisplatin) provide a solid foundation for the results. The candidate correctly adopted the Chou-Talalay Combination Index (CI) method.

PhD. candidate should provide more detailed synergy data, including dose-response curves, and the full range of CI values.

The results demonstrate that the FZ-DADA combination inhibits A549 cell proliferation by increasing ROS production, inducing G2/M cell-cycle arrest, and activating apoptotic pathways (Bcl-2/BAX, Caspase-3/7, PARP)

The Discussion section is currently too brief. It needs to be strengthened with a more critical evaluation of the biological mechanisms, study limitations, and the challenges of translating preclinical data to clinical application

There is a noted imbalance in the chapter lengths; the Results section is extensive (31 pages), while the Literature Review and Discussion are relatively concise. Figures 15, 16, and 17 are currently missing from the manuscript, and the List of Figures must be updated accordingly.

Comment on the candidate ability (e.g. general scientific background, understanding on the research field and research topic, presentation skill, English level, etc)

The candidate, Nguyen Quang Thai, demonstrates a strong foundational knowledge in experimental oncology and pharmacology. He has acquired and successfully applied a wide range of research skills, from *in vitro* cellular assays (viability, apoptosis, cell cycle, ROS detection, and metabolic assays) to *in vivo* animal modeling. The candidate shows a high level of engagement with the current state of drug repurposing and lung cancer research. He effectively connected the metabolic effects of DADA with the anti-cancer properties of Fenbendazole, showing an ability to synthesize different scientific concepts into a coherent research plan. The candidate's ability to organize a large-scale project is evident. Overall, the manuscript is written well. The candidate's English level is generally good and understandable, sufficient for high-level academic defense.



UNIVERSITY OF SCIENCE & TECHNOLOGY OF HANOI
UNIVERSITE DES SCIENCES ET DES TECHNOLOGIES DE HANOI
TRƯỜNG ĐẠI HỌC KHOA HỌC & CÔNG NGHỆ HÀ NỘI

Conclusions (indicates whether the manuscript is accepted in the current form or accepted after minor/ major revisions; and whether the candidate deserves the USTH PhD degree)

The thesis is clear enough to communicate complex pharmacological interactions and molecular pathways. Candidate has good scientific background and understanding on the research field and research topic. The candidate Nguyen Quang Thai deserves the USTH PhD degree.

- Accept the manuscript in the current form.
- Accept the manuscript with minor revisions.
- The manuscript is not qualified to for the PhD degree.

March 8th, 2026

Jury Member's signature

Nguyen Trung Nam

End of the document



with lung cancer worldwide, the development of novel therapeutic approaches based on existing compounds is of both scientific and practical interest.

The objective of the thesis is to evaluate the synergistic anticancer effects of Diisopropylamine Dichloroacetate (DADA) and Fenbendazole (FZ) in lung cancer models and to investigate the potential molecular mechanisms underlying this interaction. The candidate conducted a series of in vitro experiments using lung cancer cells and in vivo studies in xenograft mouse models. The experimental approaches include cell viability assays, apoptosis and cell-cycle analyses, ROS measurement, and Western blotting for key regulatory proteins. Drug interaction was evaluated using the Combination Index (CI) method.

The results demonstrate that the combination of DADA and FZ exerts a synergistic inhibitory effect on lung cancer cell proliferation, accompanied by increased ROS production, induction of apoptosis, and modulation of apoptosis-related proteins. In the xenograft model, the combined treatment significantly reduced tumor growth compared with single-agent treatments. These findings suggest that the combination of these two compounds may represent a potential strategy for lung cancer therapy.

The thesis is generally well structured, and the experimental results are presented clearly. The discussion appropriately relates the findings to current literature on metabolic targeting and repurposed drugs in cancer therapy.

Comment on the candidate ability (e.g. general scientific background, understanding on the research field and research topic, presentation skill, English level, etc)

The candidate demonstrates a good scientific background and adequate experimental skills in the field of biomedical research. The work shows the candidate's ability to conduct laboratory experiments, analyze data, and interpret the results in the context of existing literature. The thesis is clearly written and logically organized, and the candidate shows a good understanding of the research topic. The overall level of English is satisfactory.

Examination Jury for PhD thesis Jury Member's Assessment Form

PhD Student	
Full name	Nguyen Quang Thai
Program	Pharmacological, Medical and Agronomical Biotechnology
PhD ID	D20.PMAB.002
PhD thesis	
Title	Investigation of synergistic effect of Diisopropylamine Dichloroacetate and Fenbendazole in lung cancer models/ <i>Nghiên cứu tác dụng hiệp đồng của Diisopropylamine Dichloroacetate và Fenbendazole trên các mô hình ung thư phổi.</i>
Supervisor	Assoc. Prof. Nguyen Hai Dang, USTH
Co-supervisor	Dr. Hoang Xuan Ba, University of Southern California
Jury Member	
Full name	Dong Van Quynh
Title	Prof
Institution	Institute of Biology
Contact (Email/SMS)	lvquynh@ib.ac.vn
Role (Chairman/ Reviewer/ Member)	Member
Technical comments (e.g. on the thesis topic, research methodology, finding, discussion, thesis structure, wording, references, etc). Please note that the reviewers can fill this part as "please refer to my review report" and/or with additional comments on the revised manuscript and/or on the presentation made by the candidate	
This thesis addresses a relevant topic in cancer pharmacology, particularly the exploration of drug repurposing strategies for the treatment of lung cancer. Considering the high mortality associated	

Conclusions (indicates whether the manuscript is accepted in the current form or accepted after minor/ major revisions; and whether the candidate deserves the USTH PhD degree)

The thesis presents original research results and makes a meaningful contribution to the field of cancer pharmacology. Although some limitations exist, they do not significantly affect the scientific value of the work.

The thesis satisfies the requirements for the PhD degree at the University of Science and Technology of Hanoi (USTH), and the candidate deserves to be awarded the PhD degree, subject to minor revisions.

However, several limitations should be noted:

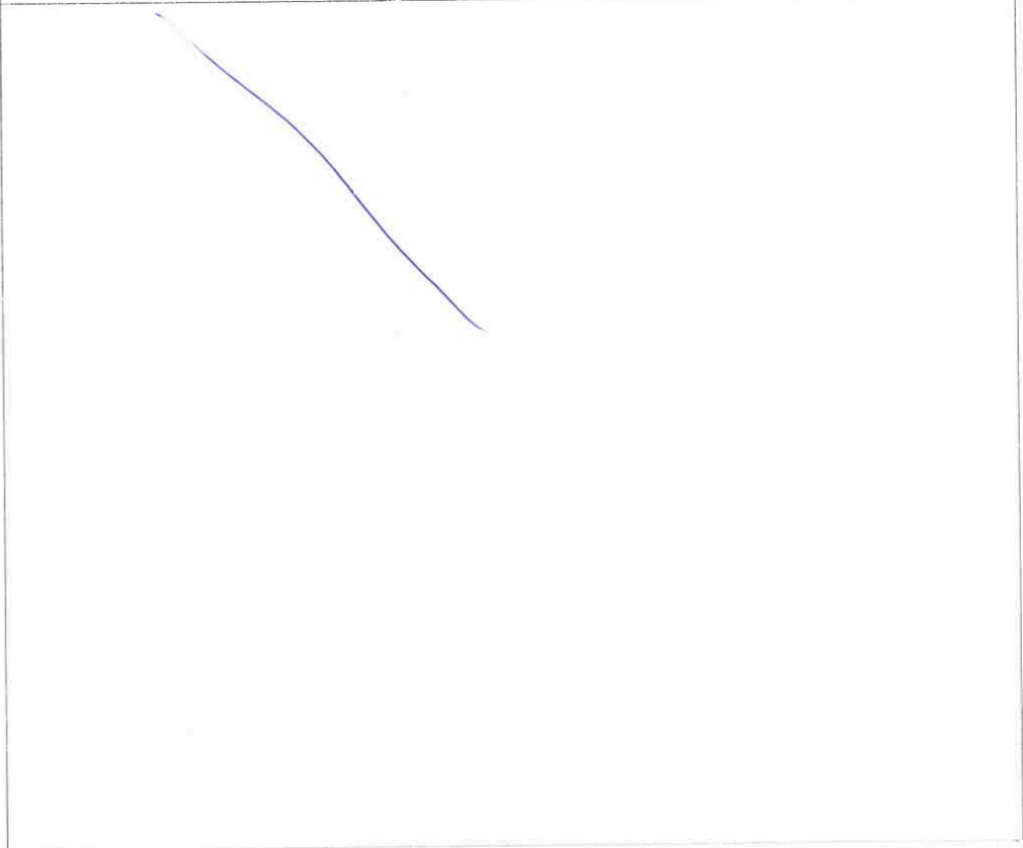
1. The study mainly relies on a single lung cancer cell line, which limits the generalizability of the conclusions. Validation in additional lung cancer cell lines with different genetic backgrounds would strengthen the findings.

2. The molecular mechanism underlying the synergistic interaction between DADA and FZ is only partially explored, and further studies on metabolic pathways and signaling networks would provide deeper insights.

3. The animal model used is relatively simple, and the absence of an intact immune system in xenograft models may limit the interpretation of the antitumor effects.

4. Additional studies on pharmacokinetics, long-term toxicity, and translational relevance would be necessary before considering clinical applications.

Despite these limitations, the thesis provides valuable preliminary evidence supporting the potential of combining DADA and Fenbendazole as a repurposed therapeutic strategy for lung cancer.





UNIVERSITY OF SCIENCE & TECHNOLOGY OF HANOI
UNIVERSITE DES SCIENCES ET DES TECHNOLOGIES DE HANOI
TRƯỜNG ĐẠI HỌC KHOA HỌC & CÔNG NGHỆ HÀ NỘI

- Accept the manuscript in the current form.
- Accept the manuscript with minor/ major revisions.
- The manuscript is not qualified to for the PhD degree.

Henry... 19... Mar 2026

Jury Member's signature

End of the document

Examination Jury for PhD thesis Jury Member's Assessment Form

PhD Student	
Full name	Nguyen Quang Thai
Program	Pharmacological, Medical and Agronomical Biotechnology
PhD ID	D20.PMAB.002
PhD thesis	
Title	Investigation of synergistic effect of Diisopropylamine Dichloroacetate and Fenbendazole in lung cancer models/ <i>Nghiên cứu tác dụng hiệp đồng của Diisopropylamine Dichloroacetate và Fenbendazole trên các mô hình ung thư phổi..</i>
Supervisor	Assoc. Prof. Nguyen Hai Dang, USTH
Co-supervisor	Dr. Hoang Xuan Ba, University of Southern California
Jury Member	
Full name	Nguyen Phuong Nhung
Title	Dr
Institution	USTH
Contact (Email/SMS)	
Role (Chairman/ Reviewer/ Member)	Member
Technical comments (e.g. on the thesis topic, research methodology, finding, discussion, thesis structure, wording, references, etc). Please note that the reviewers can fill this part as “please refer to my review report” and/or with additional comments on the revised manuscript and/or on the presentation made by the candidate	
The thesis explore the drug repurposing of two well known compounds diisopropylamine dichloroacetate and fenbendazole targeting anticancer activity against lung cancer model especially A549 cell line. The research has diverse results from <i>in vitro</i> and <i>in vivo</i> novel findings and demonstrates an original combination of two compounds in anticancer activity. Manuscripts well	

comply the regulation of USTH PhD thesis representing results with chronological order with adequate discussion.

However, there are many points which PhD candidate should revise for better manuscript. Specifically:

- Revise grammar, many references were not cited adequately

1. Abstract

- Two first paragraphs can be discarded, it looks like an introduction, too long. Results should be clarified with the extent of each effect.

2. Introduction

- Clarify the drawbacks of available therapeutic strategies.

- page 2: check further whether ref. no. 13 is correct as it only stated results about fenbendazole but the text refers to both substances.

3. Literature review

- page 17: please explain the principle of Combination index model.

- In vitro study: reference should be cited.

- Abbreviation should be defined clearly before first usage (page 19)

- A549 cell line introduction is not necessary.

- Rationale for combining two drugs should be moved to the introduction to 2 drugs.

4. Materials and methods (cite the method)

- Many chemical reagents were not described.

- Cell seeding: please describe culture conditions for other cell lines.

- Cell viability assay: please rationalize the formula to calculate CS

- **Hoechst staining: how many replicates? (Results have SD?). Could you please explain how you count the number of apoptosis cells? (manually?)**

- Apoptosis assay: the explanation about caspase pathway is not necessary. **Again, how many replicates?**

Figure 7: please explain the color of different symbols in the image. Page 28: correct the cross reference (it should be figure 7, but you mentioned figure 8).

- Western blot, Cell cycle arrest: **Again, how many replicates?** Please clarify the version of software.

- Animal experiments:

+ Fix the typo error.

+ **How do you prepare the drug solution (FZ and DADA) solution?**

+ **You inject the cancer cell line into the mice, wait for growth until 50 mm³ → how do you measure it? Do tumors in all groups of mice reach the same volume at the same moment?**

What is the difference between healthy control and tumor control groups? As healthy control groups, they also contain tumors?

Number of injection per day for group?

+ What is the basis to select the dosage? Why the combination ratio of 5000:1 was not tested despite its promising *in vitro* results?

- Statistical analysis: **do you check the normality of the data before ANOVA test?**

5. Results

In general, in many results, the combination effect is not really synergistic, it is smaller than sum of individual effects.

5.1. Cytotoxic effect: **why you tested other cell lines? As the title of subsection only refers A549 cell line.**

- **You used a computational model to investigate the synergistic effect of 2 drugs. What is the model? Can you describe it?**

- You can comment IC50 of two drugs compared previous literature.

- **Can you justify why you selected 1:5000 as 1: 4000 ratio also exhibit good result.**

- **Do you calculate CI in triplicate? DO you calculate the confidence interval of CI? Whether it is statistically smaller than 1?**

5.2 Hoechst staining

- The positive control in image and graph is different from each other (palitaxel or cisplatin?)

- % cell apoptotic cell: **How you calculate this?**

Comment on the candidate ability (e.g. general scientific background, understanding on the research field and research topic, presentation skill, English level, etc)

The PhD candidate shows deep knowledge on the research topic. He exhibits a good and professional presentation skill. He can well rationalize the research design and obtained results with good English communication skill.



UNIVERSITY OF SCIENCE & TECHNOLOGY OF HANOI
UNIVERSITE DES SCIENCES ET DES TECHNOLOGIES DE HANOI
TRƯỜNG ĐẠI HỌC KHOA HỌC & CÔNG NGHỆ HÀ NỘI

Conclusions (indicates whether the manuscript is accepted in the current form or accepted after minor/ major revisions; and whether the candidate deserves the USTH PhD degree)



UNIVERSITY OF SCIENCE & TECHNOLOGY OF HANOI
UNIVERSITE DES SCIENCES ET DES TECHNOLOGIES DE HANOI
TRƯỜNG ĐẠI HỌC KHOA HỌC & CÔNG NGHỆ HÀ NỘI

- Accept the manuscript in the current form.
- Accept the manuscript with minor/ major revisions.
- The manuscript is not qualified to for the PhD degree.

March 19, 2026

Jury Member's signature

Nguyen Phuong Nhung

Examination Jury for PhD thesis Jury Member's Assessment Form

PhD Student	
Full name	Nguyen Quang Thai
Program	Pharmacological, Medical and Agronomical Biotechnology
PhD ID	D20.PMAB.002
PhD thesis	
Title	Investigation of synergistic effect of Diisopropylamine Dichloroacetate and Fenbendazole in lung cancer models/ <i>Nghiên cứu tác dụng hiệp đồng của Diisopropylamine Dichloroacetate và Fenbendazole trên các mô hình ung thư phổi..</i>
Supervisor	Assoc. Prof. Nguyen Hai Dang, USTH
Co-supervisor	Dr. Hoang Xuan Ba, University of Southern California
Jury Member	
Full name	Phạm Lê Minh
Title	Dr.
Institution	Life sciences
Contact (Email/SMS)	Pham-le.minh@usth.edu.vn
Role (Chairman/ Reviewer/ Member)	Member
Technical comments (e.g. on the thesis topic, research methodology, finding, discussion, thesis structure, wording, references, etc). Please note that the reviewers can fill this part as "please refer to my review report" and/or with additional comments on the revised manuscript and/ or on the presentation made by the candidate	
- The thesis topic is relevant and addresses an important issue in cancer research, particularly the potential synergistic effects of repurposed drugs for lung cancer treatment. The research objectives	

are clearly defined and the experimental approach, including both *in vitro* and *in vivo* models, is appropriate for the research question.

- The methodology is generally well described, and the results are presented in a logical structure. The findings provide useful insights into the potential synergistic effects between the investigated compounds and their possible mechanisms of action. The discussion adequately relates the results to existing literature.

- The thesis is generally well organized and follows a standard scientific structure. Some minor improvements could be made regarding wording, language polishing, and consistency in formatting and references.

Comment on the candidate ability (e.g. general scientific background, understanding on the research field and research topic, presentation skill, English level, etc)

- The candidate demonstrates a good scientific background and a solid understanding of the research topic. The work indicates that the candidate is capable of conducting independent research, analyzing experimental data, and interpreting scientific results.

- The candidate's presentation during the defense was clear and structured, and the candidate was able to answer questions from the committee satisfactorily. The overall English level and scientific communication are adequate for doctoral work.

Conclusions (indicates whether the manuscript is accepted in the current form or accepted after minor/ major revisions; and whether the candidate deserves the USTH PhD degree)

- The manuscript is accepted after minor revisions.
- Based on the quality of the thesis and the candidate's performance during the defense, the candidate deserves to be awarded the PhD degree of the University of Science and Technology of Hanoi (USTH).



UNIVERSITY OF SCIENCE & TECHNOLOGY OF HANOI
UNIVERSITE DES SCIENCES ET DES TECHNOLOGIES DE HANOI
TRƯỜNG ĐẠI HỌC KHOA HỌC & CÔNG NGHỆ HÀ NỘI

[Empty box for comments or additional information]

- Accept the manuscript in the current form.
- Accept the manuscript with minor/ major revisions.
- The manuscript is not qualified to for the PhD degree.

..... *March 19*, 2026

Jury Member's signature

Minh
Phạm Lê Minh

End of the document

**GIẤY XÁC NHẬN HOÀN THÀNH BẢO VỆ LUẬN ÁN TIẾN SĨ
CERTIFICATION ON SUCCESSFUL COMPLETION OF PHD DEFENSE**

**HIỆU TRƯỞNG
RECTOR OF**

**TRƯỜNG ĐẠI HỌC KHOA HỌC VÀ CÔNG NGHỆ HÀ NỘI
UNIVERSITY OF SCIENCE AND TECHNOLOGY OF HANOI**

Xác nhận/ Certifies that:

Nghiên cứu sinh/ Student: **Nguyễn Quang Thái/ Nguyen Quang Thai**
Sinh ngày/ Date of birth: **15/09/1983**
Giới tính/ Gender: **Nam/ Male**
Mã nghiên cứu sinh/ Student ID: **D20.PMAB.002**
Ngành học/ Major: **Công nghệ Sinh học nông, y, dược/ Pharmacological,
Medical and Agronomical Biotechnology**
Ngôn ngữ/ Language: **Tiếng Anh/ English**
Quyết định công nhận NCS số/
Recognition Decision No: **463/QĐ-ĐHKHCN ngày/ dated 07/09/2020**

Đã bảo vệ thành công luận án tiến sĩ cấp trường với đề tài/ *has successfully defended the PhD thesis at the Institutional level with the thesis title:* **Nghiên cứu tác dụng hiệp đồng của Diisopropylamine Dichloroacetate và Fenbendazole trên các mô hình ung thư phổi/ Investigation of synergistic effect of Diisopropylamine Dichloroacetate and Fenbendazole in lung cancer models.**

Theo Quyết định thành lập Hội đồng
số/ According to the Decision No: **29/QĐ-ĐHKHCN ngày/ dated 20/01/2026**

Thời gian bảo vệ/ Date of defense: **19/03/2026**

Kết quả/ Result: **Đạt/ Passed**

Nghiên cứu sinh đã hoàn thành chương trình đào tạo trình độ tiến sĩ và bảo vệ luận án tiến sĩ theo quy định hiện hành của Trường/ The PhD student has fully completed the PhD program and successfully completed the PhD thesis defense in accordance with the current regulations of the University.

Giấy xác nhận này được cấp để sử dụng trong thời gian chờ hoàn tất các thủ tục xét và cấp bằng tiến sĩ/ This certification is issued for use during the period pending the completion of procedures for the award of the PhD Degree.

Hà Nội, ngày **30** tháng **3** năm 2026

Hanoi, **March 30**, 2026

HIỆU TRƯỞNG CHÍNH/ PRINCIPAL RECTOR



Jean-Marc Lavest